# DEVELOPMENT OF OVERMOLDED ALL-BIODEGRADABLE FUNCTIONAL POLY(LACTIC ACID)/JUTE ECO-COMPOSITE MATERIALS

**A THESIS SUBMITTED TO**

**GRADUATE SCHOOL OF NATURAL AND APPLIED SCIENCES**

**OF**

**KOCAELI UNIVERSITY**

**BY**

**ABDULMOUNEM ALCHEKH WIS**

**IN PARTIAL FULFILLMENT OF THE REQUIREMENTS**

**FOR**

**THE DEGREE OF DOCTOR OF PHILOSOPHY**

**IN**

**CHEMICAL ENGINEERING**

**KOCAELI 2020**

# DEVELOPMENT OF OVERMOLDED ALL-BIODEGRADABLE FUNCTIONAL POLY(LACTIC ACID)/JUTE ECO-COMPOSITE MATERIALS

**A THESIS SUBMITTED TO**
**GRADUATE SCHOOL OF NATURAL AND APPLIED SCIENCES**
**OF**
**KOCAELI UNIVERSITY**

**BY**

**ABDULMOUNEM ALCHEKH WIS**

**IN PARTIAL FULFILLMENT OF THE REQUIREMENTS**
**FOR**
**THE DEGREE OF DOCTOR OF PHILOSOPHY**
**IN**
**CHEMICAL ENGINEERING**

| | | |
|---|---|---|
| **Prof. Dr. Güralp ÖZKOÇ** | | |
| **Supervisor,** | **Kocaeli University** | **.....** |
| **Assoc. Dr. Bağdagül KARAAĞAÇ** | | |
| **Jury member,** | **Kocaeli University** | **.....** |
| **Assoc. Dr. Olcay MERT** | | |
| **Jury member,** | **Kocaeli University** | **.....** |
| **Assoc. Dr. Mehmet DOĞAN** | | |
| **Jury member,** | **Erciyes University** | **.....** |
| **Assist. Prof. Dr. Ali Sinan DİKE** | | |
| **Jury member,** | **Adana Bil. ve Tekn. University** | **.....** |

**Thesis Defense Date: 09.07.2020**

## PREFFACE AND ACKNOWLEDGEMENTS

All praise be to Allah for His blessing in completing this dissertation.
All the work couldn't be accomplished without the assistance of a number of people and the financial support of the Turkey scholarships (Turkiye Burslari). I would like to express my sincere appreciation of their generous help and support.
First and foremost, I would like to thank my supervisor, Prof. Dr. Güralp Özkoç, who, since the first day I came to Kocaeli, has supported me not only by providing research aids during my studying years, but also academically and emotionally through this rough and colorful road until today. He has tirelessly guided me in the experiments and the analysis of the results.
Special thanks to my committee, Assoc. Dr. Bağdagül Karaağaç and Assoc. Dr. Olcay Mert for their valuable comments on this research. And I would like to thank the members of the jury, Assoc.Dr. Mehmet DOĞAN and (Dr.Öğr.Üyesi Ali Sinan DİKE, for their attendance in my defense.
I am so grateful to Prof. Dr. Oktay Baykara for his support financially and morally through TUBİTAK 1001 project (231M500), a novel radiation absorbing materials: Nano- BN/polymer composites.
I am so grateful to TOFAŞ Company for its support financially through TUBİTAK Teydeb 1501 project, new generation door-liners for automobiles, Ravago Standart Profil TOFAŞ.
I am so grateful to Prof. Dr. Ufuk Yildiz and Dr. Leyla Şenol for helping me and giving me a lot of support at the beginning of my Ph.D. life.
I am so thankful to Dr. Mehmet Kodal who was, is, and will remain my close friend (dostum) for his full support and high morals. The same gratitude should be also given to my colleagues who helped me during my thesis. I appreciate Dr. Humeyra Şirin, Dr.Nilay Tüccar and Buse Nur Can who have helping me to conduct the Experiments. I would also express my sincere gratitude to my PhD colleague Serkan Akpınar and the other colleagues at polymer lab. They have accompanied me all the way during my four-year life of working.
I am grateful to my family for all that they have given me throughout my lifetime. I want to send special thanks to my parents, who have always supported me in what I've done, and who have given me the opportunities that have led me to where I am today. Thanks a dozen to my sister Asma'a and my brothers, Omer, Mouhammed, Abdulwahab, Hamza and Youseef. This thesis would not have been written without the support and love of my wife Maryam who have been a great source of strength through this work during the time far from home.

Words can’t even express my thanks to the Department of Chemical Engineering who provided the technical assistance for my research and for my University (Kocaeli University) which I lived one of the happiest days of my life.

I want to dedicate this work to my father (Abdulah Omer Alchekh wis), who is my first teacher, that it is my honour to carry his name.

To my mother (Felek kamel Alchekh wis), the world of tenderness, who I yearn to meet.

To my sister (Asmaa) and brothers (Omer, Mohammed, Abdulwhab, Hamza and Yoseff) the source of my strength.

To my wife (Maryam Alsaid), the love of my heart.

July - 2020 Abdulmounem Alchekh Wis

**CONTENTS**

## LIST OF FIGURES

## LIST OF TABLES

## LIST OF SYMBOLS AND ABBREVIATIONS

| | |
|---|---|
| E ' | : Elastic / Storage module, (MPa) |
| E " | : Viscose / Loss module, (MPa) |
| ΔH | : Enthalpy change (J) |
| Tc | : Crystallization temperature (oC) |
| Tg | : Glass transition temperature (oC) |
| Tm | : Melting temperature (oC) |
| Tonset | : Melting start temperature (oC) |
| tan δ | : Tangent delta |
| Xc% | : Degree of crystallization |

### Abbreviations

| | |
|---|---|
| APS | : Ammoniumpolyphosphate with Synergists |
| CF | : Carbon Fiber |
| CFRP | : Carbon Fiber Reinforced Plastic |
| CFRT | : Continuous Fiber Reinforced Thermoplastic |
| DMA | : Dynamic Mechanical Testing |
| DSC | : Differential Scanning Calorimetry |
| FRP | : Fiber reinforced polymer |
| FR | : Flame Retardant |
| FTIR | : Fourier transform infrared spectroscopy |
| FWHM | : Full Width at Half Maximum |
| GF | : Glass Fiber |
| JF | : Jute Fiber |
| LOI | : limiting oxygen index |
| NF | : Natural fibers |
| ADS | : Aluminum diethylphosphinate |
| MPZ | : Melamine polyphosphate and Zinc borate |
| PLA | : Poly (lactic acid ) |
| SEM | : Scanning Electron Microscope (Scanning Electron Microscope) |
| SMC | : Sheet Molding Composite (Ready Molding Textile) |
| TGA | : Thermal Gravimetric Analysis |
| TP | : Thermoplastic (Thermoplastic) |
| TS | : Thermoset (Thermoset) |
| UL-94 | : Underwriters Laboratories |
| WJF | : Woven Jute Fiber |

**ÜZERİNE KALIPLAMA YÖNTEMİ İLE ÜRETİLMİŞ TAMAMIYLA BİYOBOZUNUR FONKSİYONEL POLİ(LAKTİK ASİT)/JÜT EKO-KOMPOZİT MALZEMELERİN GELİŞTİRİLMESİ**

## ÖZET

Bu çalışmada, poli(laktik asit) (PLA) polimeri, üzerine enjeksiyon yöntemi kullanılarak PLA/jüt elyaf kompozitlerin üzerine kalıplanmış ve "ekotabaka (ecosheet)" olarak da adlandırılan biyobozunur kompozitler hazırlanmıştır. Sıcak pres kullanarak ekotabakaları hazırlamak için tabaka istifleme yöntemi kullanılmıştır. Elyaf oryantasyonu −45 ° / + 45 ° ve 0 ° / 0 ° olarak ayarlanmıştır. −45 ° / + 45 ° yönü, eko-tabakalar için 0 ° / 0 ° ile karşılaştırıldığında daha iyi özellikler sergilemiştir; bu nedenle bu yapı, üzerine kalıplanmış kompozitler (OMC'ler) üretmek için kullanılmıştır. Mekanik testler, OMC'lerin bükülme modülünün ve mukavemetinin saf PLA'ya kıyasla arttığını göstermiştir. Çalışmanın ikinci aşamasında, jüt liflerinin yüzeyi, alkali muamele ve ardından silan modifikasyonu uygulanması gibi iki yöntem kullanılarak muamele edilmiştir. Alkali işlemi ve ardından silan modifikasyonu yöntemi, jüt ve PLA arasındaki iyileşen arayüzey etkileşimi nedeniyle daha yüksek mekanik özellikler ile sonuçlanmıştır. Üçüncü aşamada, farklı amonyum polifosfat, melamin polifosfat, çinko borat ve alüminyum dietilfosfinat kombinasyonları kullanılarak kompozitlerin alev geciktiriciliğini iyileştirmeye odaklanılmıştır. Sonuçlar, melamin polifosfat ve çinko borat birlikte kullanıldığında alevlenme direncinde büyük bir iyileşme elde edildiğini göstermiştir. Bu yeni tekniğin en büyük avantajlarından birinin, yoğunluğu değiştirmeden PLA'nın mekanik özelliklerinin iyileştirilebilmesi olduğu sonucuna varılmıştır.

**Anahtar Kelimeler:** Alev Geciktiricilik, Biyobozunabilir Kompozitler, Jüt Elyaf, PLA, Üzerine Kalıplama.

**DEVELOPMENT OF OVERMOLDED ALL-BIODEGRADABLE FUNCTIONAL POLY (LACTIC ACID)/JUTE ECO-COMPOSITE MATERIALS**

## ABSTRACT

Environmentally friendly, biodegradable composites were prepared via overmolding of poly (lactic acid) (PLA) onto PLA/jute-mat composites, named as "ecosheets". Film stacking procedure was used to prepare ecosheets using a hot-press. The fiber orientation was changed as −45°/+45° and 0°/0°. The −45°/+45° orientation exhibited higher properties as compared to 0°/0° for ecosheets; therefore, this construction was used to produce overmolded composites (OMCs). The mechanical tests showed that flexural modulus and strength of OMCs were improved in comparison to neat PLA. In the second step of the study, surface of jute fibers was treated using two methods, such as alkaline treatment and alkaline treatment followed by silane modification. Alkaline treatment followed by silane modification resulted in higher mechanical properties due to improved interfacial interaction between jute and PLA. In the third stage, it was focused to improve the flame retardancy of the composites using different combinations of ammonium polyphosphate, melamine polyphosphate, zinc borate and aluminum diethylphosphinate. The results of showed that a great improvement in flame resistance was obtained when melamine polyphosphate and zinc borate were used together. It was concluded that one of the biggest advantages of this novel technique was the increase of mechanical properties of PLA without altering the density.

**Keywords:** Flame Retardance, Biodegradable Composites, Jute Fiber, PLA, Overmoulding.

## INTRODUCTION

During the past few decades, significant environmental damage has been caused by the use of huge amounts of synthetic plastics which is the main cause of global warming [1]. Therefore, these issues have triggered an increased interest to replace the Traditional polymers with more environmentally friendly alternative or to develop a new composite material with addition of more than one reinforcement that are biodegradable resources [2]. Traditional composite materials are multifunctional materials which consist of two or more materials in which the individual components retain their separate identities [3]. A fiber reinforced polymer (FRP) is a composite material consisting of a polymer matrix imbedded with high-strength fibers such as glass, aramid and carbon [2]. The result of combining two different types of material (reinforcement and matrix) into one composition is a composite with hybrid properties. There are usually two types of reinforcement the discontinuous phase which is more rigid and stronger than the second type the continuous phase. For the matrix material, it can be classified into several types such as ceramic, polymeric (thermoplastics and thermosetting) and metallic. The main advantage of this type of composite is that the strength of one fiber overshadows the weakness of the other [4]. Recently, polymer as matrix composites have been widely used for many applications such as construction materials, military, space craft, packaging [5], civil use, industry, automotive parts [6], and airplanes interior parts [7] because of their excellent thermo-mechanical properties. But with the increasing awareness of environmental concerns and limited availability of petroleum resources in recent years, it has pushed the researchers to investigate the properties of renewable resources which are biodegradable and abundantly available in nature, due to their lower cost and easier availability [8]. We can reduce the amount of artificial plastic by inserting natural fibers into them. Natural fibers are one of the natural forms of materials which are increasingly used as alternative fillers in polymer composites and had been used as potential reinforcements in polymer matrix in place of synthetic fibers. Synthetic fibers is made from chemicals. Examples of this type are aramid,

Boron, glass, carbon, etc. These fibers are usually produced by chemical retting, mechanical decorticator [9], water retting [10] etc. due to the advantages such as its adequate specific properties, low cost, less tool wear during processing, acceptable biodegradability, and low density [11]. Unlike other reinforcing fibers, they can allow a high volume of filling in composites and are readily available [12]. Because of that, natural fibers such as jute, flax, bamboo, and kenaf [13] have recently received much attention from scientists and technologists. Hemp, flax and other kinds of natural fibers are investigated to be used in plastics. Jute fibers (Corchorus capsularis) have a high worldwide annual production at about 103 ton [14]. Jute is eco-friendly fiber extracted from the stem of jute plant. It has high tensile strength, modulus, light weight, high strength to weight ratio which replaced several synthetic fibers in development of many composite materials. The composites that replace steel can save a 60-80% of the total weight, while in the case of aluminum is 20-50%. Since jute has higher strength and modulus than plastic [15], jute was used to produce composite materials with different matrices such as PP [16], polybutylene succinate, [17] polycarbonate, polyethylene, and polycaprolactone etc. [18]. These composites have already been adopted as automobile parts. In addition, for achieving more thorough biodegradability of composites, biodegradable polymers receive attention as alternatives to petroleum-based polymers. Among many kinds of Biodegradable/ biobased polymers such as poly (lactic acid) (PLA), aliphatic, cellulose esters, poly(vinyl alcohol), starch plastic has the potential to be manufactured from renewable and synthesized resources which make it the new generation of bio-based polymers. Poly (lactic acid) is the most popular for use as the matrix of green composites. Poly (lactic acid) is a kind of linear aliphatic bio-based polymer that is produced from renewable resources. The synthesis of high molecular weight Poly (lactic acid) was carried out in 1932 by Carothers et al [19]. PLA possesses good mechanical properties, (high tensile strength and Young's modulus, good flexural strength) [20], which are even higher than those of PS, PP, PE, or other polymers. We can compare the tensile strength of PLA with PET, and so do the elastic modulus, but unfortunately PLA is very brittle, with less than 10% elongation at break and low toughness, which limits its use in applications that need plastic deformation under high stress [21]. However, many researches on PLA-based composites reinforced with NF, such as jute, kenaf and hemp, have been carried out

in expectation of enhancing the mechanical and thermal properties of PLA [22]. The combination of thermoplastics and renewable natural fiber such as jute as reinforcement in composite will answer the demand for environmentally friendly composite [23]. However, there is a limited number of studies focusing on reduction of weight while maintaining or improving other desirable attributes [24]. As far as we know, there is no reports about the Over-molding Technology with natural polymers. Over-molding Technology is the injection molding process to apply one material [Over-Mold] onto another material [Substrate] [25]. The over-molded material should form a bond with the substrate that endures the end-use environment and offers functional performance. Over-molding eliminates the need for adhesives and primers to bond TPEs to rigid substrates. Over-molding technology offers design flexibility, lower manufacturing costs coupled with ease of manufacture [26] which is a well-founded method for producing lightweight structures. The concept is to combine the advantages of injection molding and Continuous Fiber Reinforced Thermoplastic (CFRT) properties to produce strong lightweight structures that have higher mechanical properties than molding compounds, but they can be integrated directly in the molding process. Potential applications for over-molded CFRT inserts are in seat structures, airbag housings, front end modules, crash beams and other structural applications [27]. The combination of interesting mechanical and physical properties of 'all-biodegradable green-composites' together with over-molding technology is the primary goal in our study .The present work study the preparation and characterization of woven Jute fiber reinforced PLA composites. In order to improve adhesion, modification of PLA with Talc is performed. The mechanical and thermal properties of jute/PLA composites are investigated to see the effect of this modification. The mechanical and thermal properties of composites are investigated in detail. Also by SEM microscopy and FTIR. This study is characterized not only as an academic research but also as an industrial development to produce new green and more environmentally friendlier materials and their applications in automotive.

# 1. BACKGROUND INFORMATION

This thesis is concerned with developing Jute fiber reinforced PLA biodegradable composite material using hot film-stacking molding method and Over-molding technique. The work is based on a combination of textile and composite technologies. This chapter includes a short introduction to composites and woven technologies followed by a literature survey to give a brief overview of areas relevant to this project.

## 1.1. Composite Materials

Composite materials consist of mixing two different materials to produce a composite that combines the best properties of the two materials and avoids their defects [21]. Usually one of the materials used in the composite is fibers, flakes, or particles and is called the reinforcing phase. The other material is called the matrix which is serves as a medium (in continuous form) [23]. Reinforcements are dipped in the matrix to produce composite and improve properties. Reinforcement fiber is often of high strength, stiffer and orthotropic. The responsibility of the reinforced fibers is to control the mechanical properties of the compound because it is considered the strong part, while the matrix or resin consists of synthetic polymers whose task is to preserve and contain fibers in a specific form. The matrix material is ordinarily of a high-performance type. Moreover, both fibers and matrix may be organic or inorganic in nature [24].

Composite materials are increasingly replacing conventional metallic materials because of its light weight, high strength, easy manufacturing methods and high design flexibility. The term ‘Textile Composite’ can be produced from any textile processes such as spinning, weaving, knitting, braiding or nonwoven [25]. This technique has opened the door to endless possibilities to produce composites with different type of reinforced fibers and matrix.

### 1.1.1. Classification of composites

Usually the composite materials are classified into two. The first classification is according to the matrix and the second classification is according to the reinforced material structure. [29].

For classification by matrix we can classified the composite into three classes:

- Metal Matrix Composites (MMC)
- Ceramic Matrix Composites (CMC)
- Polymer Matrix Composites (PMC)

For this project the interest is in the field of polymer matrix composites where Poly (lactic acid) (PLA) are used as polymer matrices. On the basis of polymer used, composites can be classified into two categories, such as thermoset composites and thermoplastic composites. To manufacture thermoset composites the thermoset polymers are used as a matrix material and thermoplastic polymers are used to produce thermoplastic composites. Polymer matrix composites are also formed by mixing thermoplastic polymer with reinforcing fibers and then the blend is subjected to a high temperature and pressure so that the thermoplastic polymer melt and act as a matrix material [36]. This system of manufacturing thermoplastic composite enhances the delamination resistance of composite materials. Thermoplastic composites are characterized by the possibility of recycling and molding, but after several times of recycling, it loses its strength and sent for disposal. Unfortunately most of the time, some materials such as inorganic materials or fiberglass remain and cannot be disposed of and this makes this type of composites an environmental problem and urgent solution to it must be found. We can solve this problem by the use of biodegradable reinforcements (jute or hemp) and biodegradable matrix (PLA) so that we can complete the recycling cycle of composites. Thus the carbon dioxide resulted from manufacturing is the same as that consumed in the growing step of the plant [31].

On the basis of the reinforcing material and the structure, composite materials can be classified into three categories [33]:

- Fiber Reinforced Composites.

- Particle Reinforced Composites.
- Dispersion Strengthened Composites.

Synthetic and natural fibers are used to give the composites strength and improve its mechanical properties. The study will focus on the type of fiber reinforced composites, especially the textile fibers. The fiber element performs the main load-bearing component in fiber reinforced composites. These types of composites create lightweight yet durable and rigid materials. Fiber reinforced composites can be classified according to the form in which the reinforcement fiber material is used. These are short discontinuous, long discontinuous and continuous fiber reinforced composites. It can be further classified according to the structure of the reinforcement such as woven, nonwoven, braided, knitted etc.

The parameters of fibers i.e. length, orientation and volume content dominate the engineering properties of the composite. Among them, the length of the fiber is very important, and the continuous and long discontinuous fiber composites are better in terms of engineering properties [39]. Short or long staple fiber composite pre-pregs are discontinuous in nature. The chopped fibers (long or short) are distributed in random direction or straight direction. The fibers orientation has two types: unidirectional like yarns and bidirectional like woven fabrics. According to their structure, composites may be classified as laminates and sandwich panels. According to their structure, composites may be classified as laminates (by applying multiple layers we control the thickness of the composites) and sandwich panels. In order to get a specific properties or pattern, we place the layers of reinforcement precisely to create a laminar composites [31]. There are several types of Laminates such as non-woven, reinforced fiber, woven and matt, and 2D woven or unidirectional fibers. Advantages of laminated composites are relatively well defined position of fibers in final composite piece, higher strength, higher fiber to volume ratio; their disadvantages are relatively poor through-the-thickness properties [34] and problems of process induced deformations.

The fiber reinforced composite, where fibers are distributed in order and based on woven fabric principle is called woven fiber reinforced composite. Woven fiber (Fig.2.2.) are made by weaving two sets of yarns at perpendicular angle to each

other. The terms warp and weft (Fig. 1.1.) are used to distinguish between the two different directions of yarns.

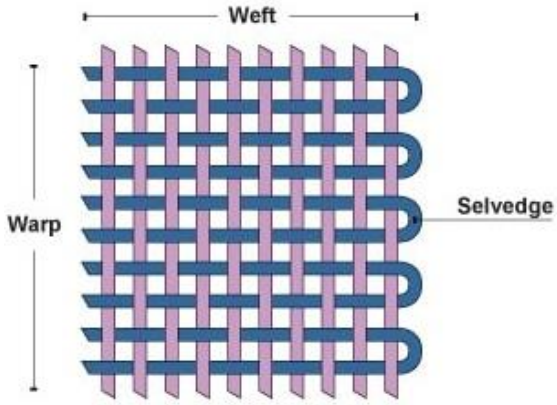


Figure 1. 1. Pattern of weft and warp yarns in a woven jute fiber [15]

Warp defines the longitudinal yarn, i.e., the direction in which production proceeds (also called machine direction or MD). Weft defines the transverse direction, i.e. running width-wise (also known as cross machine direction or CD). Figure 1.2. Show surface texture of a typical woven jute fiber.

Figure 1. 2. Woven jute fiber

Woven fiber composites are mainly used in structural applications. Because of their fiber orientation and the use of mostly continuous yarns in this type of material, the mechanical properties such as strength and stiffness of these composites are superior as compared to short and random fiber composites. Due to their handle ability,

isotropy, process ability, and especially low cost, this type of composite is widely used [38].

### 1.2. Biodegradable and Sustainable Materials

Biodegradable materials can be defined as materials that are able to be broken down into simple elements and compounds such as carbon dioxide and water by microorganisms under natural environment without generating any harmful substances [7, 40]. The biodegradation process, in other words chemical decomposition, usually occur through enzymatic action of microorganisms (bacteria, fungi, etc.), and abiotic reactions including mineralization, photo degradation, oxidation and hydrolysis [41. 42]. There are three main classification for the Biodegradable polymers:

Biopolymers and polysaccharides like (chitin, chitosan, cellulose, silk and wool). The second main section is synthetic polymer such as aliphatic polyester (e.g. Poly (lactic acid) and polybutylene succinate) and polyester produced by microorganisms (e.g. poly (hydroxyl alkanoate) [7, 43]. Recently, due to the rapid growth in the consumption of composite material, biodegradable composite is being developed for more extensive applications. Biodegradable composites (biocomposites) are commonly known as the composites materials consisted of biodegradable natural or synthetic fibers as reinforcement and biodegradable or non-biodegradable polymers as matrix [46].

Sustainable materials are usually produced from completely renewable resource, and there is no fossil fuel derived energy in their production processes [47]. Moreover, the definition of sustainability from Cargill Dow LLC, which built the commercialization of PLA polymers under the trade mark Nature Works TM, is based on three aspects: economic sustainability, social sustainability and environmental sustainability [49]. The specifications of the sustainable material have been defined by three basic qualities. First, the sustainable material is capable of performing the tasks performed by the substitute material. Second, it should be available at a reasonable price. Third, its negative impact on the environment should be in the minimum level. Sustainable materials are also known as “green” materials. An idealized life cycle of green materials is presented in Figure 1.3. [50]. The

requirements of innovative green materials include: the improvement of material from biodegradable or renewable polymers, the minimization of using fossil based materials, the diminution of fossil fuels used during material production, the reduction of carbon dioxide released, the reduction of the quantity of wastes, and the minimization of hazards from non-ecofriendly chemistry at every stage of the green material life cycle [53].


Figure 1. 3. Life cycle of green materials [65]

Figure 2.4. Indicates a pyramid diagram of the whole-life energy of plastics after service. Waste reduction is most desirable and can be achieved by re-designing the products to improve their durability. Reuse requires less energy than recycling of the plastic after service, but it normally needs inspection, cleaning and repair for the plastic used for other purposes. Despite many commercial thermoplastic polymers such as PET and PE having good recyclability, most of their raw materials are generated from fossil-fuel and natural gas. Besides, the recycling rates of these recyclable materials are not as high as they could be. Biodegradable plastics, such as PLA, can slowly decompose to harmless components in soil. Composting can reduce the amount of plastic waste going to incineration and landfill, which are the most undesirable methods for waste management. In a study by Themelis et al. in 2011 [30], only about 6.5% of the used plastics are recycled, 7.7% are burned for energy in the U.S., the remaining 85.8% went to landfill [66]. These plastics will bring environmental pollution at their end-of-life cycle. Moreover, the fast growth of the demand of composites and the limited amount of these natural resources are leading

to increasing in the polymers' price. Therefore, biodegradable and/or sustainable polymers may replace traditional polymers gradually for plastics, textiles and composites.

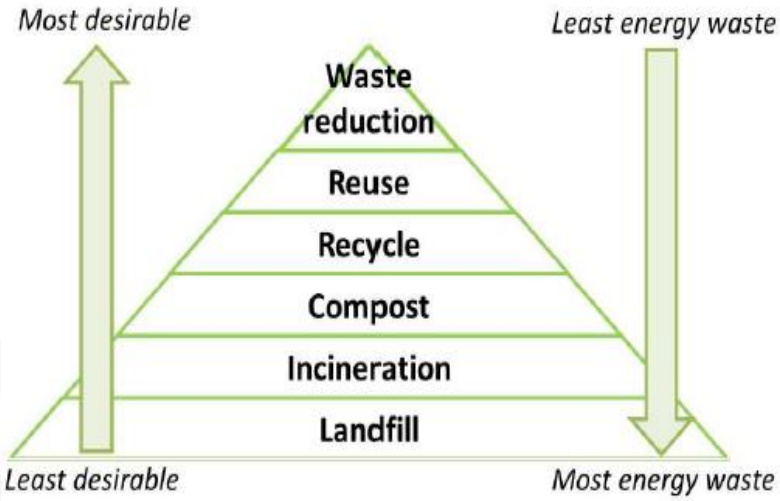


Figure 1. 4. Whole-life energy of plastics after service [66]

Poly (lactic acid) (PLA) is a very popular biodegradable polymer and has been commercially manufactured in many countries. It belongs to aliphatic polyester and has outstanding biodegradability and sustainability. Hence, research of novel "green" materials made up of the biodegradable polymer has become a new trend. In the next part we will focus on the physical properties and chemical structure.

### 1.3. Poly (lactic acid)

Poly (lactic acid) was first manufactured in 1932 by Wallace Carothers. PLA belongs to an aliphatic polyesters family which is characterized by being derived from 100% nature renewable sources like sugar cane and corn. PLA is a thermoplastic polymer made from α-hydroxyl acids with high efficacy for biodegradability and for composability. PLA has excellent strength and modulus. However, due to the high price of manufacturing applications, it was limited to medical fields like suture implants [67]. For example, the PLA fibers can be made into a 2D or 3D textile scaffold as an implant, where different human organs can be cultured [68]. In the recent years, it has been widely developed and manufactured on a large-scale by Nature Works LLC, USA, who markets the fiber form of the PLA polymer under the

"INGEOTM" brand. Now there are many applications for PLA such as food packaging, biodegradable composites, apparel and wipes.

Compared with synthetic polymers which is made from decreasing fossil fuels, Poly (lactic acid) (C3H4O2)n is important because it is manufactured naturally from sustainable and available sources, with 100% biodegradable capability [60]. The process of synthesis of PLA polymer is shown in Figure 2.5. In the production of PLA, the carbohydrates (starch or sugar) are extracted from plants cells and converted to fermentable sugars by enzyme hydrolysis with water [68]. After the enzyme hydrolysis, the fermentation of dextrose occurs to make the lactic acid. Then, PLA can be formed by either polycondensation or ring-opening polymerization of lactic acid [68, 70]. The direct polycondensation of lactic acid is based on esterification of monomers. In order to eliminate the water, this process needs to be operated under high temperature and progressive vacuum [71]. The ring-opening polymerisation occurs via lactide as a cyclic intermediate dimer [68, 69]. The ring-opening polymerization usually gives longer molecules (higher molecular weight) than the direct polycondensation, because it is difficult to remove the water and impurities in the polycondensation [68, 70, 72].

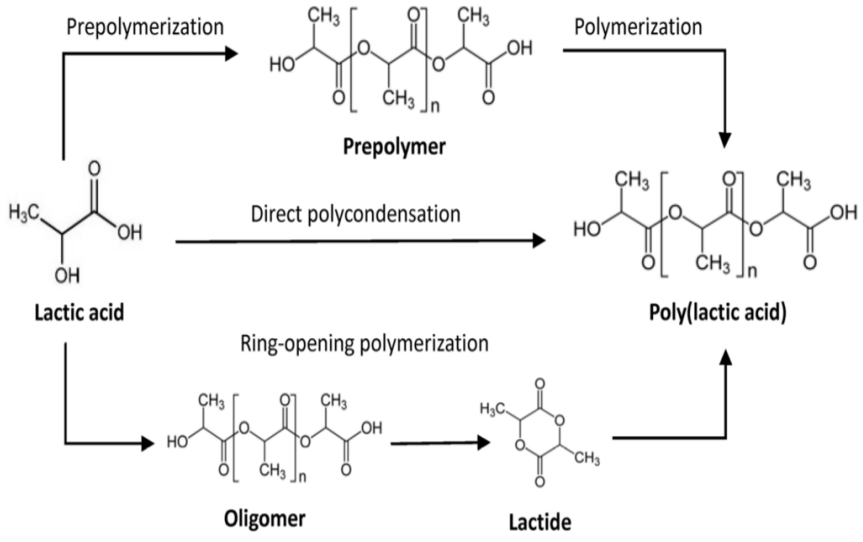


Figure 1. 5. The synthesis of PLA polymer [68]

Due to the chirality of lactic acid, the fermentation of sugar produces the lactic acid which exists as two stereoisomers (L- or D-lactic acid). Before ring-opening polymerization occurs, lactic acid produces the cyclic lactide dimer under milder

condition by eliminating water. Three potential forms of lactide can be created. These are L-lactide, D-lactide, and Meso-lactide. The crystalline PLA polymer usually contains high proportion of poly L-lactic acid (PLLA), while the amorphous PLA polymer is produced by a higher proportion of poly D-lactic acid (PDLA) (more than 15%) in the polymer chain [68]. The characteristics of PLA, such as molecular weight, crystallinity, the thermal properties of PLA vary with the difference of the quantity and the sequence of L- and D-lactic acid units [68]. There is no specific point for melting point of the PLA, but a range from 130 to 230°C because of the different sequence and quantity L- and D-lactic acid units. [68, 73].

PLA is similar to most thermoplastic polymers, in which the mechanical properties highly depend on the molecular weight, crystallinity and orientation. The unique characteristic that makes Semi-crystalline PLA distinctive from others is the different mechanical properties depending on the distribution and quantity L- and D- lactic acid units such as flexural strength of 50-120 MPa, tensile strength of 50-70 MPa and elongation at break of 2-10%. For example, amorphous PLA usually has tensile strength between 50 and 70 MPa, while that of poly DL-lactic acid (PDLLA) is from 40 to 53 MPa [74, 75].

The improvement of PLA mechanical properties can be done by making highly oriented fiber. This technique is affected by roll speed, draw ratio and other spinning parameters. The tensile strength, elastic modulus and elongation at break of PLA fiber can be developed up to 450 MPa (about 36 cN/tex, based on bulk density of 1.25 g/cm3), 5.7 GPa (draw ratio of 4) and 160% (spinning speed of 1000 m/min) [68, 76, 77]. Figure 2.6. Shows a comparison of tensile properties between natural fibers, common synthetic fibers and PLA fiber [68]. It is clear from this figure that the initial modulus of the PLA fiber is similar to the other textile fibers, while the yield after elastic tensile is very obvious and similar to wool. PLA fiber is also very extendable, even its strain at break is higher than wool, which is the most extendable natural fiber. However, the tensile strength of PLA fiber is lower than common synthetic fibers such as Lyocell and high-density polyester, but it is higher than viscose and close to cotton fiber.

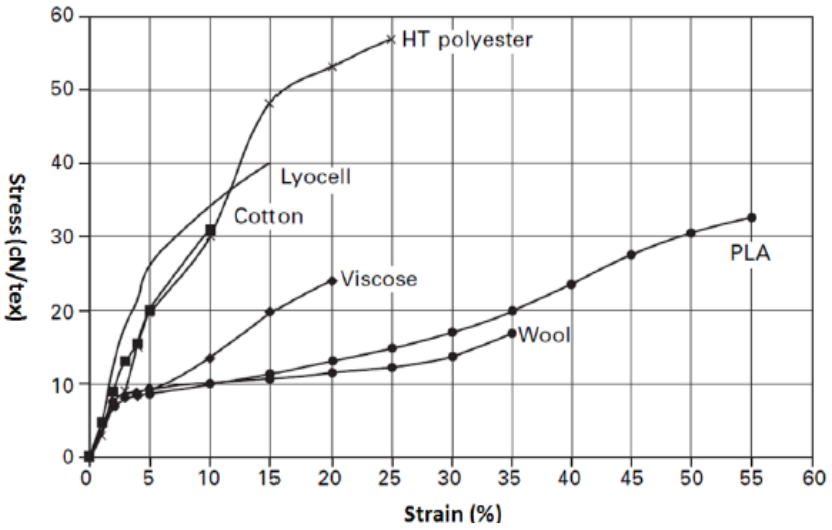


Figure 1. 6. Tensile stress-strain curves for PLA and other common textile fibers [68]

The reason why PLA is stiff and brittle at room temperature is that the glass transition temperature is between 50°C and 70°C and the melting point is from 130°C to 230°C depending on the ratio of L- and D- in PLA backbone [68]. For pure PLLA or PDLA, the melting point is between 170°C and 190°C [68, 73]. Ikada et al. [78] found that the highest melting point of 230°C of PLA polymer can be achieved by blending PLLA and PDLA to create a stereocomplex polymer. In addition, the crystallization temperature of amorphous PLA polymer is typically between 110°C 130°C, based on the molecular weight [73].

As a large number of biodegradable products based on the PLA polymer have been produced every year and the processing conditions and final properties are highly related to the crystallization of amorphous and melting behavior, a lot of studies [79] concentrated on the crystallization and melting behavior of PLA polymer. A double melting behavior has been found in the PLA material and reported by a number of authors [79, 80, 83].

In general, the phenomenon of multiple melting endothermal peaks commonly appears in the DSC plots of synthetic macromolecules, and has been observed for many semi crystalline polyesters containing flexible or semi-stiff polymers such as PE, PP, PET and poly (butylene terephthalate) etc. [79, 84]. This phenomenon in principle can be attributed to many factors such as the presence of two or more crystal forms, molecular weight segregation, varying crystal orientation, and

different crystal size and morphologies [79, 85]. The appearance of multiple melting peaks also can be brought about by the original crystals with different stability [85]. The double melting behavior of PLA is attributed to a low temperature melting that happened because of the melting of the original crystals with a low thermal stability, then the crystals go through a recrystallization, and finally to a prefect crystals which refers to high temperature melting in the DSC heating scan. [79, 80].

PLA, despite being a synthetic polymer, is fully biodegradable and compostable polymer, as it is derived from renewable resource. The PLA degradation done by ester bond hydrolysis without an enzyme to catalyze this hydrolysis or by various microorganisms under controlled conditions [69, 86]. The degradation rate is influenced by ordered molecular structure (crystallinity), molecular weight, and surface area, hydrophilic and hydrophobic properties [86]. Because the crystalline structure is more resistant to degradation then the amorphous, the higher the crystallinity the less the degradation. The PLA degradation depends on the degrading environment such as temperature and humidity. Under the natural environment, PLA has a degradation time from six months to two years, which is much shorter than that of polyethylene, 500-1000 years [69]. However, the degradation time of PLA can be shortened to 3-4 weeks when PLA is composted with microorganisms in an appropriate environment [87].

### 1.4. Biocomposites

Biocomposites have a broad classification and can be partially or completely biodegradable [62, 88]. The classification of biocomposites is shown in Figure 2.7. Partial biodegradable composites are based on biofibers as reinforcement and non-biodegradable thermoplastic (polypropylene/polyethylene) or thermoset (epoxy/unsaturated polyester) polymers as matrix. If the matrices are biodegradable polymers, which can be derived from renewable or petro-based resource, the biocomposites are completely biodegradable. The renewable polymers include starch plastics, soy plastics, cellulosic acetate and PLA. The petro-based synthetic polymers include aliphatic polyester, aliphatic-aromatic polyester, polyester amides, and polyvinyl alcohols [61, 62, 88].

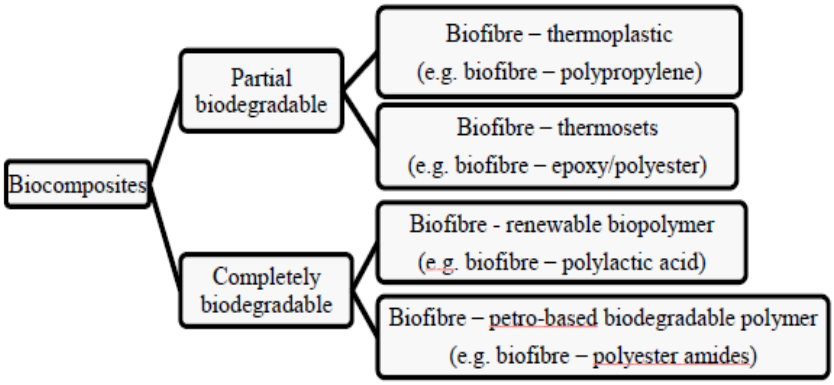


Figure 1. 7. Classification of biocomposites [62]

In the biocomposites, biofibers are mainly natural fibers, which can be grouped into bast, strew, leaf, or wood fibers [61]. Because of their low density, low cost and good mechanical properties that is near to glass fiber, natural fibers have been considered as feasible alternatives to the expensive glass, aramid carbon fibers in a composite, especially in automobile and construction industries [61, 62, 88, 89].

An all-composite-made automobile is more than 50% lighter than a similar sized steel automobile. Because of the low density of the natural fibers in the reinforced composites, they can become lighter [89]. Table 2.1. Shows the comparison of mechanical properties for synthetic fibers and natural fibers. The stiffness of jute and hemp are higher than glass fiber, also the specific modulus of natural fibers is close to glass fiber. However, the mechanical properties of synthetic fibers are higher than natural fibers [61, 89, 90].

Furthermore, it has been reported in several studies that 10-11 million vehicles in the United States need to be disposed annually after their end-use, and approximately 25% by weight of the vehicles are discarded as wastes, including plastics, composites, rubber and foams [61, 88]. Thus, the other advantage of using biocomposites to replace glass fiber composite is that the biocomposites have good biodegradability; they can be simply consumed by landfill. In the last decades, natural fiber reinforced composites have been used widely as interior and exterior material with multiple functions. They have been used as door panels, door trim panels, floor mats and spare tyre covers for automobiles to reduce the weight for higher fuel efficiency and to enhance sustainability [88, 89].

Table 1. 1. Properties of natural fibers and high-performance fibers [90]

| Fiber | Density ($g/cm^3$) | Tensile strength (MPa) | Young's mod(GPa) | Elongation at break (%) |
|---|---|---|---|---|
| Jute | 1.3-1.49 | 393-800 | 13-26.5 | 1.16-1.5 |
| Flax | 1.5 | 345-1500 | 27-39 | 2.7-3.2 |
| Hemp | 1.47 | 550-900 | 38-70 | 1.6-4 |
| Kenaf | 1.5-1.6 | 350-930 | 40-53 | 1.6 |
| Ramie | 1.5-1.6 | 400-938 | 6.4-128 | 1.2-3.8 |
| Sisal | 1.45 | 468-700 | 9.4-22 | 3-7 |
| Coir | 1.15-1.46 | 131-220 | 4-6 | 15.40 |
| E-glass | 2.5 | 2000-3500 | 70-73 | 2.5 |
| S-glass | 2.5 | 4570 | 86 | 2.8 |
| Aramid | 1.4 | 3000-3150 | 60-67 | 2.5-3.7 |
| Carbon | 1.78 | 4000-4800 | 230-425 | 1.4-1.8 |

Compared to synthetic fibers, bast fibers have lower density and higher biodegradability. Since they also have relatively high Young's modulus and tensile strength, bast fiber reinforced PLA composites have attracted significant attention. The bast fibers that are usually used for biodegradable composites are hemp [91-93], jute [16, 94], flax [95-98] and kenaf [99-103].

There are more than one way to produce these composites. Injection molding is one of them. This method supplies a very well fiber wetting because of the well mixing of PLA matrix and jute fiber in the extruder [93, 97, 102-104]. On the other hand, the disadvantage is the limited of reinforcement structure in the composite like chopped short fibers. Here comes the importance of compression molding as it can use more than one form of reinforced structures like chopped short fiber [91, 94, 98], short fiber mat and textile fabric. [99, 101]. The degree of fiber wetting is highly depending on the processing temperature, pressure and time.

Oksman et al. has found that the flax fiber (30-40 wt %) reinforced PLA composite has 44-53 MPa tensile strength and 7.38.3 GPa E-modulus, which are higher than or equivalent to those of PP composites [104]. The mechanical properties of flax-PLA composites with higher fiber content (4060 wt %) have been reported in Alimuzzaman et al.'s study [98]. By changing the molding temperature and time during heat compression, the highest tensile properties (tensile strength= 80.3 MPa, tensile modulus = 9.9 GPa) flexural (flexural strength = 138.5 MPa, flexural modulus= 9.9 GPa) are achieved by the 50 wt% flax composite at 180°C molding temperature and 5 min molding time. Ochi developed the unidirectional kenaf-PLA

composite with 70% fiber content. The tensile and flexural strengths can reach 223 MPa and 254 MPa respectively [99].The tensile modulus and strength of a short kenaf fiber –PLA with 30% fiber content can reach about 5.5 GPa and 52 MPa, and the flexure modulus and strength are 6 GPa and 85 MPa, respectively [103]. Kenaf-PLA composites also have high heat resistance and strength. Thus, they can be used in the housing of electronic products [102]. The mechanical properties of PLA are improved by the addition of jute fibers to it. It turns out that with increasing fiber volume, the tensile strength and modulus increase but bending strength and modulus decrease. [116] The mechanical properties of jute-PLA composites depend on the manufacturing temperature. The degree of fiber wetting is very poor at low temperature because of the high melt viscosity of PLA matrix [94].

Hu and Lim found the mechanical properties of hemp-PLA composites peak at the fiber volume fraction by about 50% [92]. As fiber content increases, the tensile strength, elastic modulus and flexural strength decrease. A possible explanation for this is that the fiber wetting became poor at the high fiber content, which is due to the insufficient penetration of resin fraction to wet all the fiber surfaces. Sawpan et al. successfully evaluated the fracture toughness of hemp-PLA composite by single-edge-notched-bending test. The fracture toughness of the composite is lower than the neat PLA and is decreased with the increase of fiber content. This could be caused by the increased stress concentration and PLA matrix crystallinity [106].

The poor interfacial bonding is a well-known problem in natural fiber reinforced synthetic composites. Many studies have worked on the improvement of interfacial bonding by fiber surface treatment, the addition of plasticizer and coupling agent. Three types of fiber treatments are used in Huda el al's study including aqueous alkaline solution, Silane coupling agent, and a combination of both [100]. The flexural properties are improved by these treatments of kenaf-PLA composite compared to untreated fiber. As a result, interfacial bonding is increased due to the coupling agent which increased the cross linking degree in the fiber surface area and its interface [100]. This treatment allows the removal of wax and pectin from the fiber surface [107]. However, it has been reported that the impact properties of PLA-flax significantly is decreased by the surface treatment [104].

### 1.5. Natural Fibers

Natural fibers are classified by their origins such as plants and animals. The most commonly used species in reinforcement is plant fibers which include (cotton, kapok) as hairs, (jute, hemp and flax) as bast and (sisal, henequen) as hard-fibers. India and Bangladesh are the largest producers of jute. The good quality of fibers provides a basic requirement to maintain a good level of mechanical properties and the lack of this quality is currently one of the biggest drawbacks. Some properties must be presented in the reinforcement fibers so they are considered to be of high quality such as:

• Good adhesion between fiber and matrix.
• Degrees of polymerization and crystallization.
• Moisture repellence, and Flame retardant properties.

#### 1.5.1. Natural fibers and their chemical compositions

Table 1.2. Presents the chemical composition of plant-fibers that vary depending on the natural conditions and age. In general, natural fibers contain cellulose, lignin and hemi-cellulose as the fundamental components. These components are responsible for the physical properties of the fibers.

Table 1. 2. Composition of different cellulose based natural fibers

| | Cotton | Jute | Flax | Ramie | Sisal |
|---|---|---|---|---|---|
| Cellulose | 82.7 | 64.4 | 64.1 | 68.6 | 65.8 |
| Hemi-cellulose | 5.7 | 12.0 | 16.7 | 13.1 | 12.0 |
| Pektin | 5.7 | 0.2 | 1.8 | 1.9 | 0.8 |
| Lignin | - | 11.8 | 2.0 | 0.6 | 9.9 |
| Water soluble | 1.0 | 1.1 | 3.9 | 5.5 | 1.2 |
| Wax | 0.6 | 0.5 | 1.5 | 0.3 | 0.3 |
| Water | 10.0 | 10.0 | 10.0 | 10.0 | 10.0 |

The name of cellulose was given by Anselme Payen In 1838 who discovered that all plants consist mainly of this substance. Cellulose consists of units called glucose, which are originally anhydroglucose joined by β-1, 4-glycosidic bonds. These rings are within 4C1 conformation which refer to multiple -OH and –CH2OH groups on the edge of the ring. The molecular structure of cellulose is responsible for its supramolecular structure of cellulose determines most of its physical and chemical properties. We can see the molecular structure (The Haworth projection) in fig. 2.8.

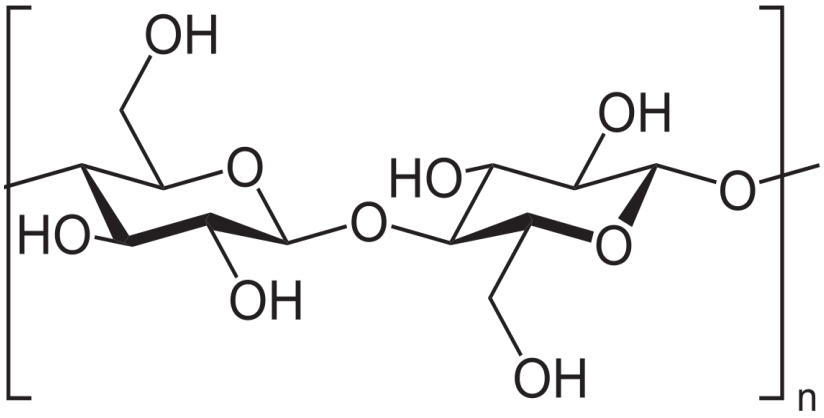


Figure 1. 8. The Chemical Structure of Cellulose [16]

The repeating units in cellulose are linked to the 180° angle of the main planes site and the ratio of these units to the molecule is half the DP. However, there is a decrease in this ratio after the purification process, where the original number is approximately 14000 and the number after the operation is approximately 2500. Because of the unique geometry of each cellulose cell, the degree of polymerization varies with cellulose type and this affects the mechanical properties of the natural fibers, and that determines the length of the polymer. The molecular structure of cellulose is similar to that of a polymer in terms of solid regions (high order, crystalline form) and another disorder area called amorphous. Natural cellulose is a single orientated chain which crystallizes in monoclinic sphenoid structures.

Unlike cellulose, hemicellulose is not a derivative or close to cellulose. Hemicellulose is a polysaccharide which is derived from the rest of the cellulose bonding after the removal of the lignin. There are 3 fundamental differences between cellulose and hemicellulose: First, hemicellulose consists of several types of sugar units, while cellulose consists of only 1.4-β- -glucopyranose type. Second, cellulose is a linear polymer while Hemicellulose is a branched polymer. Third, the degree of polymerization of cellulose is much higher than that of hemicellulose (higher from 10 to 100). The chemical composition of hemicellulose varies depending on the source or type of plant.

These materials are complex because of their different ring-to-linear structure and because of their difference by source.

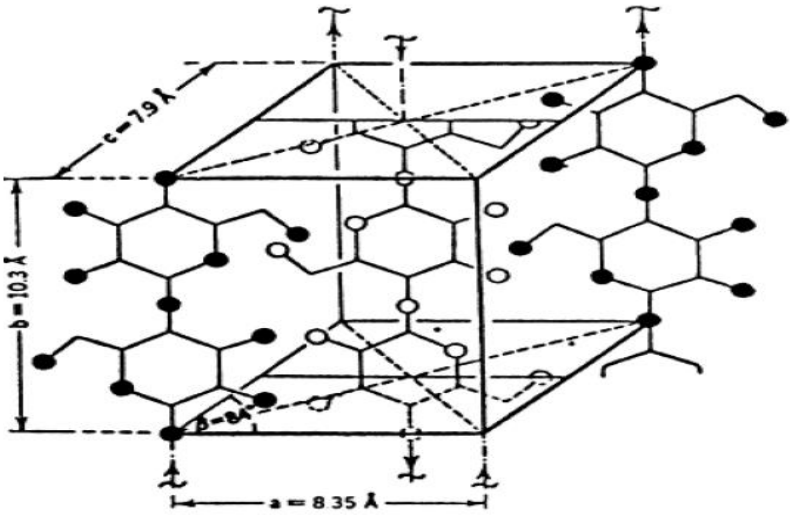


Figure 1. 9. The Cell geometry of Cellulose [106]

The mechanical properties of Lignins are generally lower than cellulose. Pectin is a variety of polygalacturonic acid types which called heteropolysaccharides. Pectin is not soluble in water but after the alkali or ammonium hydroxide treatment it became soluble in water. Wax is a component of natural fibers and is insoluble in water and is usually consist of (stearic acid, palmitic acid, oleaginous acid).

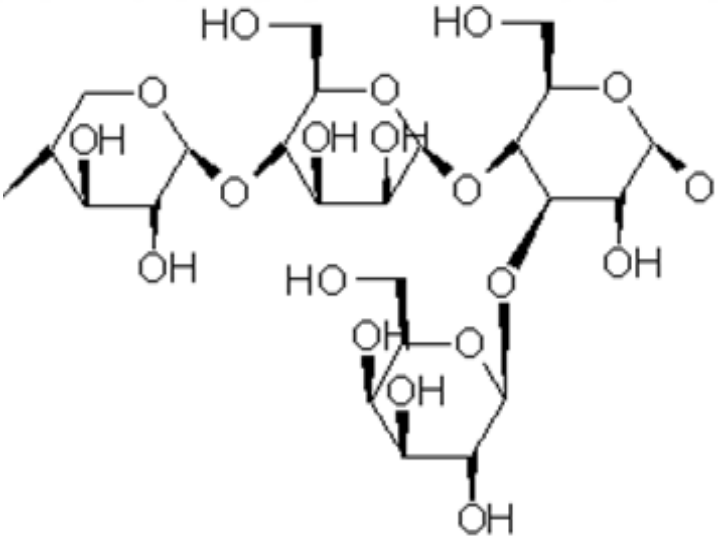


Figure 1. 10. The Chemical Structure of Hemicellulose [106]

Because of its special strength, low density and stiffness, natural fibers can be used to reinforce plastics (thermoplastics or thermosets) (Table 1.3.). The distinctive values of jute and soft wood fibers are the same as those of glass-fibers, types E.

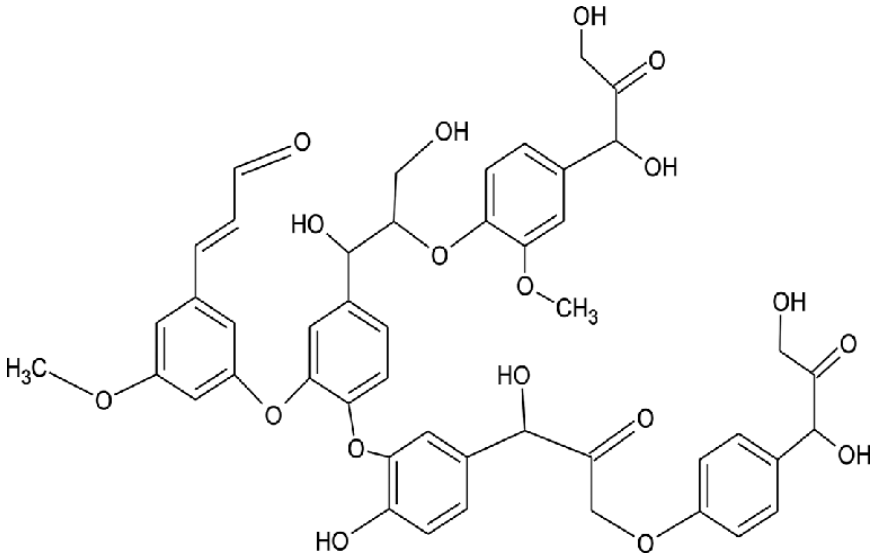


Figure 1. 11. The Chemical Structure of Lignin structure [25]

It is clear from the table (2.3) that the most significant defects of natural fibers is the large range of properties due to the different chemical composition by source and natural conditions during growth. This problem can be solved using many methods of treatment of natural fibers and producing fibers with stable properties. In general, the elastic modulus of natural fibers is 10 GPa but for cellulose after treatment is up to 40 GPa and it can reach to 70 GPa after several methods of chemical and mechanical treatment. Theoretical calculations put the elastic moduli of cellulose up to 250 GPa, but the separation problem makes these values unattainable at the moment.

Table 1. 3. Mechanical properties of natural fibers as compared to conventional reinforcing fibers

| Fiber | Density ($g/cm^3$) | Elongation at break (%) | Tensile strength (MPa) | Young's mod(GPa) |
|---|---|---|---|---|
| Cotton | 1.5-1.6 | 7.0-8.0 | 287-597 | 5.5-12.6 |
| Jute | 1.3 | 1.5-1.8 | 393-773 | 26.5 |
| Flax | 1.5 | 2.7-3.2 | 345-1035 | 27.6 |
| Hemp | - | 1.6 | 690 | - |
| Ramie | - | 3.6-3.8 | 400-938 | 61.4-128 |
| Sisal | 1.5 | 2.0-2.5 | 511-635 | 9.4-22.0 |
| Coir | 1.2 | 30.0 | 175 | 4.0-6.0 |
| Viscose(cord) | - | 11.4 | 593 | 11.0 |
| Soft wood kraft | 1.5 | - | 1000 | 40.0 |
| E-glass | 2.5 | 2.5 | 2000-3500 | 70.0 |
| S-glass | 2.5 | 2.8 | 4570 | 86.0 |
| Aramide(normal) | 1.4 | 3.3-3.7 | 3000-3500 | 63.0-67.0 |
| Carbon(standard) | 1.4 | 1.4-1.8 | 4000 | 230.0-240.0 |

The tensile strength of Natural fibers, such as glass fibers, depends on the length of the sample. The tensile strength of glass fibers is measured by single fiber test, while for jute fibers it is based on the length of the fibers and not the length of the cross section. This relationship between test length and strength can be considered as a general measure of the degree of homogeneity or the total defects in the fibers. One of the most important disadvantages of natural fibers is Hydrophilic, especially if we want to use these fibers as a reinforcement for plastic. Water absorption in fibers depends on the number of amorphous (non-crystalline) areas and this increases the presence of gaps and reduces the strength of fibers and generally weakens the mechanical properties of fibers.

### 1.6. Jute Fibers

Jute fibers have several unique properties compared to glass fibers such as: high specific modulus (40 GPa) (for glass fibers 30 GPa), Lower specific gravity (1.29), high tensile strength, 100% bio-degradable, and good insulating properties. All these features make jute fibers an excellent alternative to glass fibers to be used as reinforcement in composites.

One of the most important advantages of jute fiber is that it is not only environmentally friendly, recyclable, can be used more than once, but also the energy requirement is only 2% of the energy required for fiberglass production.

Nowadays, there are great uses for jute fibers in many industries, including: composites, paper, nonwoven textiles and geotextiles for car industries, celluloid products (films), helmets, grain storage silos, paperweights, biogas containers, prefabricated buildings, covers of pipes, electrical appliances, and many other everyday applications.

Jute growth conditions and fiber processing technique are considered to be the major influences on the mechanical and physical properties of fibers and it affects the sample test-length. As mentioned earlier, jute fibers are affected not only by cellulose but also by hemicellulose and lignin which have a clear effect on the properties and are greatly influenced by the chemical treatment method using caustic soda. The existence of hydroxyl and polar groups in jute fibers is one of the major

drawbacks because it helps to increase the moisture uptake (approx. 12.5% for dry fiber and 14.6% for wet fiber at 20 C, 65% relative humidity) and this increases the spacing between the fibers, increases the weak interfacial bonding between the fibers and hydrophobic polymer and makes the jute fiber have low wettability with resin. The environmental performance of jute composites is at its best up to 70% of humidity, but the properties begin to decrease after that. Here comes the importance of chemical treatment of fibers so that the absorption of moisture is reducing and wettability of the resin is increasing. Alkaline treatment removes lignin and hemicellulose and this makes the fibers more resilient, easier to be rearranged (especially in the direction of tensile deformation), less rigid and makes the interfibrillar region of the fibers less dense. These changes help jute fibers when they are stretched as they facilitate and speed up the rearrangement process and this produces fibers with better load sharing and higher stress upgrade in Jute fibers. But this process negatively affects the stress transfer between polymer and jute fibers, and that why the total stress becomes higher on the fibers tensile when it is deformed. In addition, NaOH treatment causes a molecular orientation increasing and a spiral angle decreasing. The removal of non-cellulosic substances adds randomness in the orientation of crystallites. This important factors affect the crystallite length, degree of polymerization and degree of crystallinity, and these have a significant impact on mechanical properties.

### 1.7. Methods for Surface Modification of Natural Fibers

The quality of the fiber surface (fiber–matrix interface) is one of the most important factors that affect the reinforcement between the fibers and the polymer. Therefore, many chemical and physical methods have been used to optimize this interface. These treatment methods have different efficiency for matrix-fiber adhesion.

#### 1.7.1. Physical methods

There are many examples of physical treatment of fibers such as calendaring, thermal treatment, stretching, the activation of surface oxidation by cold plasma and hybrid yarns production. These techniques alter the structure and surface of the fibers, which changes the bonding properties between the polymer and the fibers. The effects of cold plasma treatment on the fibers change the surface energy and increase

the aldehyde groups' amount. Surface crosslinking could be insert or free radicals reactivation could be produced.

### 1.7.2. Chemical methods

The difficulty of adhesion of fibers and polymer is due to that fibers have a strong polarity characteristic and polymers have hydrophobic characteristic. Therefore, the chemical treatment requires the addition of a third material that helps to bond and has intermediate properties between polymer and fibers. There are several ways to cause coupling like:

- By removing the weak boundary layers.
- By making more flexible and tough layer form the deformable layers.
- By improving a highly crosslinked interphase region between the fiber and the polymer.
- By improving the wettability between polymer and fibers.
- By adding coupling agents to form a covalent bonds between the polymer and the fibers.
- By acid–base treatment where coupling agents change the acidity of the treated surface.

The difficulty of knowing the mechanism of coupling agents bonding in composites lies in the fact that there is no complete theory in this field and that the chemical bonding theory is not enough. So the consideration of interphase morphology, surface energy, the wetting phenomena and the acid–based interface reactions becomes a necessity.

The hydrophilic is very close to surface energy of jute fibers. For that, many researchers investigate the effect of decreasing the fibers hydrophilicity. It had been noted that processing of jute fibers by polyvinyl acetate increases moisture repellent and mechanical properties. On the other hand, the use of silane coupling agents adds a hydrophilic characteristic to the interface, especially amino-functional silanes like (urethanes and epoxies silanes) which acts as a primer with polymers and this allows it to add much more amine functionality than the normal interphase with resin. Silane is also used by combining two types of silane, one is hydrophilic and the other is

hydrophobic like pheniltrimethoxysilane. This gives thermal stability and improves the mechanical properties of the composite.

By using the impregnation method a good degree of combination is achieved between the polymer and the fibers. Polymer solutions or low-viscosity polymers are used for this purpose, but the lack of solvents for some polymers limits the possibility of using this technique. For example, when using butyl benzyl phthalate plasticized polyvinyl chloride (PVC), it significantly decreases the viscosity of the polymer and it can be used as co-solvent for PVC and polystyrene (PS).

This method which has been explained previously has a very important characteristic by adding chemical bridges and increasing the interfacial adhesion between the matrix and fiber.

Graft copolymerization is one of the most important chemical methods to improve natural fibers. The first step of this process is the interaction of free radicals with cellulose molecules, then the fibers are dipped with a special ion solution and the fibers are exposed to high energy radiation. After their exposure to radiation cracks and roots produced in the cellulose fibers, these roots are treated with a suitable solution convenient with the polymer (such as silane, acrylonitrile and polystyrene). The output of this process is a marked improvement of the fiber's properties convergence of polymer properties. Fibers become better and have higher matrix tolerance, which improves the adhesion and increases the internal bonding. This method is effective but complex.

### 1.7.3. Alkaline treatment of natural fibers

The method of alkaline fiber treatment is characterized by its highly targeting non-cellulose components in fibers such as hemicellulose and lignin which are components affecting the mechanical and thermal properties of fibers. Hemicellulose is sensitive to reaction with caustic soda. There are many studies on the effect of alkaline treatment on jute fibers which often leads to the removal of hemicellulose with lignin which increases the tensile properties in fibers. After the removal of hemicelluloses and lignin, there are gaps in the fibers and the density of fibers becomes less and less stiff which makes the fibers have a greater and faster ability to

be rearranged, especially in the direction of tensile deformation. Rearranging makes the fibers better in carrying and distributing the load and produces higher stress in the fibers. On the other hand, the softening in the interfibrillar matrix negatively affects the transfer of stress among the fibers which make the total stress development of the fiber in the deformed tensile. After the removal of the lignin, the middle layers of the fibers become directly attached to the matrix which increase the homogeneity of the composite. The effect of alkaline treatment on crystallinity in fibers has been reported. The alkalis removes the interstitials in the crystal, increases the percentage crystallinity index of the treated fiber and makes the crystal more compact. The treated fibers are also subject to a decrease in the spiral angle near the fiber axis which increases the possibility of the rotation of the chains. Having easy rotation gives the fibers a higher Young's modulus, especially rotatable fibers such as jute which are better than limited-spinning fibers such as cotton. Alkaline treatment also contributes to unifying the direction of the fibers and increases the strength of the weak points.

### 1.7.4. Silane treatment

Silane is one of the common coupling agents that has been widely used to modify the surface characteristics of a substrate [77]. The chemical structure of silane has a bi-functional group, Figure 1.12. Which could interact with two different phases, of which the surface characteristics are different.

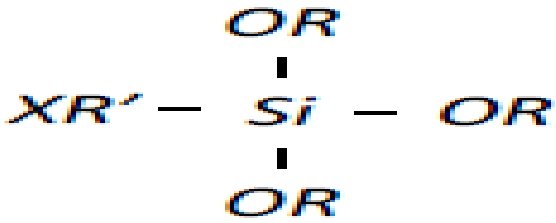


Figure 1. 12. The general chemical structure of silane

The bi-functional structure of silane is interesting as it is applied to the cellulosic fibers to modify their surface characteristic, and improve the compatibility with a polymeric matrix. With the rich hydroxyl groups on the surfaces of cellulosic fibers, the alkoxy groups (R) in silane structure can chemically react with these reactive hydroxyl groups through hydrogen bonding in the presence of water, and leave the

group of organofunctionality (X) on the outer surface of treated fibers, Figure 1.13. [77,91].

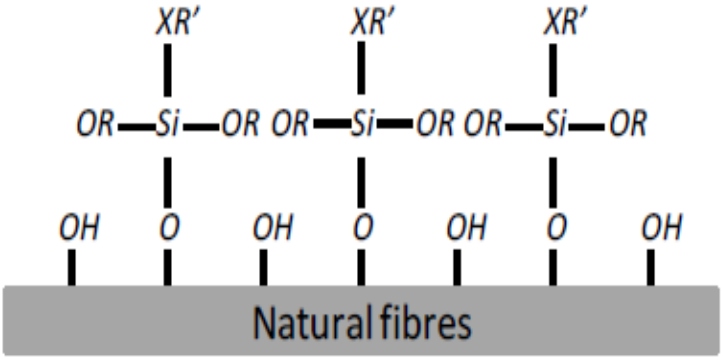


Figure 1. 13. The hydrogen bonding between silane and natural fibers

The organofunctionality on the surface of treated fibers affects the surface of the fibers and changes several properties. Interfacial adhesion increases because of the physical or chemical interaction between the fibers and the polymer matrix [77, 80,81]. Selection of silane is important because it will affect the adhesion strength between the functional group and the polymer matrix. The selection of silane depends on the type of target polymer and the possibility of interaction between the functional group and the polymer.

Table 1. 4. Examples of potential Silane chemicals for natural fiber Composites, and their targeted polymer matrices [77]

| Chemical structure | Functionality | Target polymer matrix |
|---|---|---|
| $(OR)_3$-Si-R'-NH2 | Amino | Polyethylene<br>Polypropylene<br>Polyacrylate<br>Polyvinyl chloride<br>Epoxy |
| $(OR)_3$-Si-CH=CH2 | Vinyl | Polyethylene<br>Polypropylene<br>Polyacrylate |
| $(OR)_3$-Si-R'-CH3 | Alkyl | Polyethylene<br>Polypropylene<br>Natural rubber |
| $(OR)_3$-Si-R'OC(CH3)C=CH2 | Methacryl | Polymethyl methacrylate<br>Polyacrylate<br>Polyester |
| $(OR)_3$-Si-C6H4-SO2-N3 | Azide | Polyethylene<br>Polypropylene<br>Polystyrene |

The greater the compatibility and interaction between the silane and the polymer the greater the adhesion between the silane and the polymer matrix. Table 1.4. Shows some examples of silane agent's types and the suitable polymer groups.

Polyester is reinforced with jute fabrics treated with γ-methacryloxypropyl trimethoxysilane (MPS) solutions. The mechanical properties of the composite had been investigated by Sever et al [93]. The results showed that flexural and tensile properties increased for the treated jute with MPS. The concentrations of the applied MPS solution also affected the properties as the improvement in mechanical properties of jute reinforced polyester was further increased when treating jute fabrics with higher concentration of MPS solution.

### 1.8. Fire Performance

Since the materials used for the reinforcement of the polymer matrix and the natural fiber composites are flammable, flame retardants can be introduced in either one or both components to retard the burning in the composites and to laminate the preparation process. Flame retardants are a group of chemicals, which, when incorporated in a material, reduce its flammability at the exposure to fire. In general, flame retardants function in vapor and/or condensed phases, depending on the functional groups in the chemicals to slow down or stop the combustion process in material. In the vapor phase, flame retardants can work chemically to interfere with the combustion process by quenching the free radicals generated from a burning material, or physically by diluting the flammable volatiles with production of inert gas from decomposition of flame retardants [43]. Examples of first type are halogen based flame retardants, and of the second type are alumina hydrate, magnesium hydroxide, etc. The importance of reacting the condensed phase between the polymer and the flame retardants material is that the flame retardant materials change the way the polymer decomposes during the fire, which produces more char than volatile and flammable materials. All phosphorus based flame retardants function in this manner. During burning, some condensed phase flame retardants absorb energy to decompose their selves, which results in the cooling effect to lower the temperature of the decomposing material, hence, further decomposition and burning is stopped. [43]. in

the following section different flame retardant methods used for different components of the composite are discussed.

### 1.8.1. Flame retardant treatments of natural fibers

The flame retardant treatments for natural fibers, typically cellulosic fibers such as cotton, have been well established for many years. Flame retardants can be simply applied to natural fibers by using textile finishing processes. The process of Pad/dry-cure is one of the most important processes used in the treatment of fibers where the fibers are dipped with a solution of flame retardants, then the excess solution is eliminated. The fibers/fabrics are then placed in an oven to get rid of the solvent [5]. Flame retardants in this treatment are usually water soluble, such as inorganic acid salts. Also durable flame retardants can be used such as tetrakis (hydroxymethyl) phosphonium and N-methylol dialkyl phosphonopropionamides which are useful for cotton fabrics [101,102]. The most commonly used commercial products of these are Pyrovatex CP and Proban CC respectively [8,102].

In general, the chemicals of this type of flame retardants are phosphoric acid salt of organic and inorganic nitrogen-containing compounds such as ammonia, guanidine and guanylurea [104]. The well-known example of flame retardants in this group are mono- and di-ammonium phosphate (MAP and DAP respectively). These phosphorus (P)-containing and nitrogen (N)-containing flame retardants mainly work in condensed phase. When these P-N flame retardants are presented in cellulosic fibers, they produce phosphoric acid on heating to esterify the cellulose through phosphorylation and form phosphorus ester cellulose [101,102]. The phosphorus ester in cellulose influences the decomposition pathway of cellulose to favor dehydration decomposition (as discussed in Section 2.1.1), and hence, promoting more char formation and less flammable volatiles as compared to untreated cellulose. With the presence of nitrogen, a synergistic action can occur allowing the P-based flame retardant to form the crosslinked P-N intermediates which are more reactive phosphorylating agents, and hence, providing the better flame retardant efficiency than the related P-based flame retardant without the nitrogen [104-106].

Ammonium sulfamate and sulfates are flame retardant chemicals, which work in the condensed phase. Ammonium sulfamate and sulfates release Sulfuric acid upon

decomposition, which reacts with hydroxyl groups of cellulosic fibers through a sulfation reaction, thereby, changing the decomposition pathway of cellulose. In sulfation, Sulfuric acid works as a Lewis acid to esterify cellulose and form the sulfate ester cellulose. This sulfate ester works in a similar way as the discussed-above phosphate ester, to influence decomposition of cellulose to yield less flammable products and promote better char formation [103,107].

In practice, the use of this technique introducing the flame retardants to natural fiber composites through the reinforcing component has hardly been explored. Only a few works have been published in the literature [108,109]. Matko et al have studied the flammability of flame retarded cellulosic fillers reinforced polyurethane (PU) prepared from wood flakes and corn shell treated with di-ammonium phosphate (DAP) [108]. The fillers are immersed in aqueous solution of DAP, followed by drying under infrared lamp. The ratio between fillers and DAP is kept 1:1 by weight. The flammability of the composites containing 20 wt-% of untreated and DAP treated cellulosic fillers are evaluated by using UL-94 and Limiting Oxygen Index (LOI) tests. In UL-94, the addition of DAP in cellulosic fibers significantly improved the fire performance of the composites from HB (failed to rank in UL-94 vertical classification) to V-0 rating, whereas the LOI results showed that DAP dramatically increased the LOI values of the composites from 20 - 23% of non-flame retarded cellulosic reinforced PU to 30% of the flame retarded ones. The flame retardancy of epoxy composites reinforced with coir fibers treated with halogenated flame retardant system, saturated bromine and stannous chloride has been investigated by Misra et al by using LOI. [109]. With the halogenated treatment, the LOI value of coir fibers reinforced epoxy composites was increased from 36% to 39%.

### 1.8.2 The Flame retardant additives of polymer materials

The polymer can be made flame retardant by one of the following methods, by adding a flame retardant additives where this technique used in the thermoplastic and thermoset polymers or chemical modification on the polymer chains where this technique used in the thermoset resin or both. [5]. Common example of modified thermoset resin is the use of halogenated thermoset resin, and the replacement of ordinary curing agents/hardeners with halogenated compounds such as using

dichlorostyrene and bromostyrene instead of styrene in unsaturated polyester [1,5,43,110]. Flame retardant additives can be introduced to thermoplastic and thermoset polymer systems by using various techniques. The common process used for mixing flame retardants with thermoplastic polymers is compounding where flame retardant additives and polymer are mixed together in the polymer molten stage by using a twin-screw extruder, similar to the process described in 2.11. Flame retardants are often introduced to thermoset resin by mixing with the liquid mixture of resin and curing agent by using a mechanical stirrer prior to casting to solid polymers. There are a number of flame retardants reported in literature for polymers of natural fiber composites fabrication. The examples are ammonium polyphosphate (APP), aluminum hydroxide (ATH), and magnesium hydroxide, and expandable graphite [82, 84, 86, 108, 111-116].

Ammonium polyphosphate (APP) has been widely used to flame-retard many polymers. The mechanism of APP is similar to that of water soluble P-N flame retardants explained in Section 2.8.1. While heating, APP is being decomposed and is forming polyphosphoric acid. In the condensed phase of combusted polymers, the acid is acting as a catalyst to the dehydration process and is increasing the crosslinking to promote more char formation [25,117]. The efficiency of APP varies in different polymers. With the oxygen containing polymers, the efficiency of APP is higher than polyolefin [5,28]. This is due to the reason that polyolefins, i.e. polyethylene (PE) and polypropylene (PP) mostly decompose with no char residue, therefore, APP which is a condensed phase flame retardant is less effective [5].

Ammonium polyphosphate can be classified into two main groups: Crystal phase I and Crystal phase II.

This group is characterized by the length of the linear chain, which reduces the decomposition temperature (around 150°C) and makes it more soluble in water. Usually the number of phosphate units in this group is less than 100.

This group is characterized by being more branched and crosslinked than the first group and has a high molecular weight where the number of phosphate units is more than 1000.

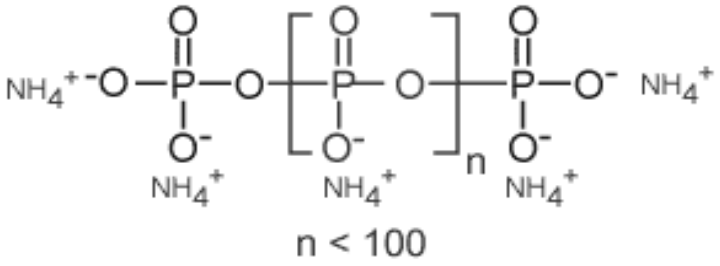


Figure 1. 14. The Crystal Phase I Ammonium Polyphosphate [106]

These properties make this group less soluble in water and more thermal stability where the decomposition is about 300°C.

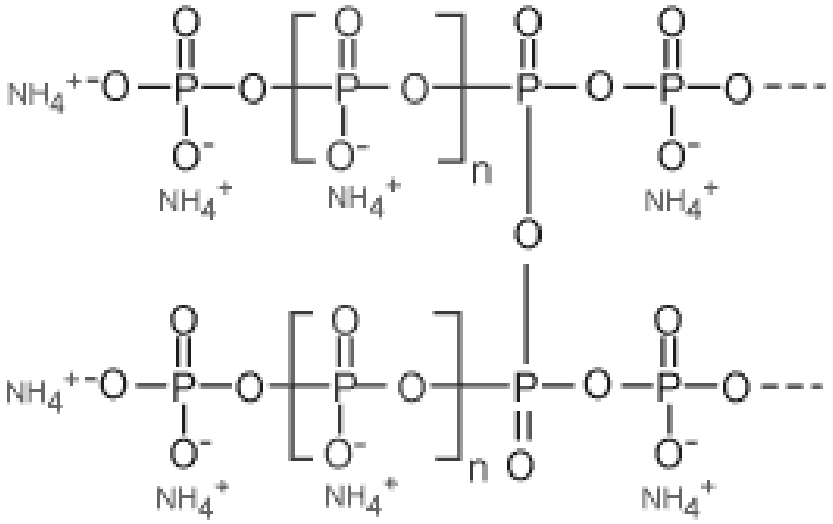

Figure 1. 15. Crystal Phase II Ammonium Polyphosphate [106]

The efficiency of APP to flame retarding the natural fiber composites has been investigated by many researchers [82, 84,108,111-114]. Le bras et al report the use of APP in flax reinforced PP (Flax/PP) composites [82]. The results showed a significant improvement in flax fibers and less flammability. They have investigated the flammability of flax reinforced polypropylene (30/70 by weight) with and without addition of 25 wt-% of APP in the polymer matrix. The cone calorimetric results showed that APP significantly reduced the PHRR and THR of flax reinforced polypropylene composites by about 40 - 50%, and noticeably increased the charred residue from 11% to 29%. The efficiency of APP has also been studied by Arao et al [111]. When comparing the cone calorimetric results of wood flour/polypropylene composites containing 30% by weight APP and the non-flame retarded composites,

the results have showed that the addition of APP decreased PHRR and THR of the composites by about 45% and 20% respectively. The effect of the APP content has been studied by Matko et al [108]. They have produced a corn starch based thermoplastic biopolymer containing APP at 10, 20, and 30% by weight, and characterized the flammability by using limiting oxygen index (LOI). The results have showed that the flame retardant efficiency of APP is greater at higher APP content; an increase of the LOI from 33% to 60% has been reported when the APP content in the samples has been increased from 10% to 30% by weight.

### 1.9. Metal Hydroxides

Metal oxides, such as aluminum and magnesium hydroxide, work by physical mechanism to reduce the flammability of polymers. On heating, aluminum and magnesium hydroxide undergo endothermic decomposition at temperature between 180 - 240oC and 330 - 460oC respectively, and release water vapor as shown in Equation 1.1 [128].

$$2Al(OH)_3 \rightarrow Al_2O_3 + 3H_2O \quad (1.1)$$

$$Mg(OH)_2 \rightarrow MgO + 2H_2O \quad (1.2)$$

Equation 1.1. Decomposition of (a) aluminum hydroxide and (b) magnesium hydroxide [28].

The released water vapor helps to reduce the temperature of the burning polymers as well as diluting the flammable volatiles produced from the pyrolysis of polymers [128]. They can provide effective flame retardant effective only when used at high loading of about 50 - 60% in the polymer matrix [5].

Aluminum hydroxide (ATH) has been used at 40 wt-% addition in the hemp reinforced unsaturated polyester composite by Hapuarachchi et al [86]. They have investigated the flammability of the composites with and without ATH by using cone calorimeter at 50 kW/m2 external heat flux. The results have showed that ATH is able to delay the ignition time of unsaturated polyester reinforced hemp by about 45% and to reduce the heat release rate to 180 kW/m2. The effect of the treatment of rice husk and sawdust with magnesium hydroxide and the use of these fibers to reinforced polypropylene was studied by using (ASTM D 635) and limiting oxygen

index (LOI) by Sain et al. [115]. The results have showed that by replacing 50% of cellulosic fillers with magnesium hydroxide, the LOI values of the composites was increased from 26% to 35%, and the horizontal rate of burning was significantly reduced from 35 mm/min to 15 mm/min.

On heating, expandable graphite undergoes endothermic decomposition, and expands up to 300 times of its initial volume [25]. The expanded graphite works as an insulating layer for underlying materials [115,125]. Schartel et al have compared the flammability of flax/polypropylene composites flame retarded with APP and expandable graphite [84]. The cone calorimetric results at 40 kW/m2 heat flux showed that at the same solid content expandable graphite showed greater flame retardant efficiency by 70% reduction of PHRR, while 50% reduction in PHRR was observed in APP flame retarded composites. The greater efficiency of expandable graphite was further supported by UL-94 result where composites containing expandable graphite could pass V-1 rating, but those containing APP failed the test.

Surface coating is another effective methodology to render materials' flame retardant. A coating layer is applied on the surface of composites to protect the composites from the heat source during burning and slow down or stop the combustion process. One of well-known example of coating used for flame retards of materials is intumescent coating. The performance of the swollen coating depends on the thickness of the coated layer and how much it foamed carbonaceous char layer, because this layer act as insulation barrier for heat and flame [118]. Another coating that can be used to fire-resistant composites is flame retardant coating. Flame retardant coating generally contains flame retardant chemicals, such as halogenated or phosphorus based compounds, dispersed in a binder. In most cases, flame retardant coating is used to inhibit a flame spread of burning materials by the action of flame retardants contained in the coating [119-121]. These flame retardants function in a similar manner as discussed in above sections. Flame retardant coatings are not as effective as intumescent coatings.

At present, there are a number of tests and standards available to assess flammability and to evaluate the level of fire performance of materials. The testing conditions of these techniques vary depending on the application where materials are used. Examples of fire testing specified for different applications are surface flame spread

test as specified in BS 476 Part 7 for materials used in British railways; room/corner test (ISO 9705) for marine applications; single burning item test (EN 138230), and ignitibility and flame spread test (EN ISO 11925-2) for construction. Some of these tests have already been discussed in Chapter 1. As initial assessment for research purposes limiting oxygen index and cone calorimeter are used to access flammability of materials. Limiting oxygen index (LOI) is a technique used to determine the ignitibility of materials in term of minimum oxygen concentration materials required to sustain candle-like burning behavior. Cone calorimeter is used mainly to measure heat release of materials when it burns under force flaming condition. The principle and testing protocols of LOI and cone calorimeter tests will be discussed in more details in Chapter 3.

### 1.10. Polymer Processes

Injection molding technology is one of the best techniques used in the manufacture of natural fiber composites (NFCs). This technique is characterized by the ease of production of composites with complex shapes and a large amount of production, but it has limitations on the length and quantity of the used fiber. The longer the length of the fiber, the more difficult molding and more internal friction of the fibers [172].

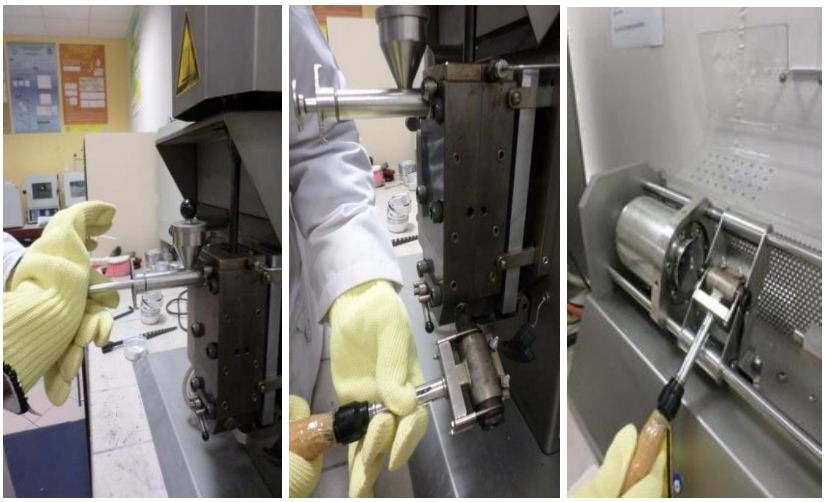

Figure 2. 16. The Extruder and Injection molded Process

There must be an extruder before the injection molded, because the injection molding is characterized by short screws and this makes it excellent for composite production but makes it impractical to mixing the composite or to make the mixture homogenous. Therefore, extruder is needed before the injection molding so that we

control the homogeneity and mixing of the composite, then the composite transferred to the injector which is in an equal temperature to the extruder so that the composite does not burn or be solidified before the molding. This allows continuous production of composite parts to be manufactured by using the appropriate mold (die) [191].

Nowadays, there is a growing interest in NFCs especially using the injection molding technique. Injection molding makes it easier to produce complex shaped panels that are difficult to be produced by a single press-molded technique. Natural fiber composites (NFCs) are manufactured by press molded technology and this is suitable for thermoset and thermoplastic polymers. The growing interest in thermoplastic can be noticed because it is easy to be processed and recycled.

### 1.10.1. Compression molding

One of the methods used in plastic molding is pressure molding. This process is done by placing the plastic directly on a hot surface, which is controlled by electric heaters, with the plastic reaching the appropriate temperature (soften). Then the soften plastic is pressed by a hydraulic press in a specific mold and then the mold closes and cools [196]. The contact of the plastic with the hot surface makes it soften and then begins to fill the spaces in the mold. The pressure and cooling stage affect the curing of the plastic and the thickness of the curing layer. Several factors control this method like mold thickness, polymer type and temperature. This technology is characterized by the weight of materials before manufacturing to minimize the possibility of an excess flash.

There are many uses for this technology, especially in the field of thermoplastics and reinforcements in thermoplastics composite where you can use many types and forms of fiber (woven fabrics, chopped, unidirectional and randomly oriented fiber) [175]. Many forms of thermoplastic can be used (such as sheet, film, paste, pellets, solution or fiber) [194]. The thermoplastic is heated over their melting point. In general, the better the polymer distribution on the surface of the mold, the better the output.

This technique is suitable for making high-strength parts or large size parts. This technique is characterized by a short cycle time with a large production rate. Complete production lines are possible for this technique, especially production lines

for scoops, hoods, spoilers, fenders and lift gates. This technology is characterized by the possibility of producing strong, thin, large and stiff parts. It is also ideal for making light-weight fiber reinforced composites [147]. It can also be used to produce a thin structural part like sheet molding compound (SMC) [209]. One of the most important advantages of this technique is that it does not cause damage in the used fibers which make the physical properties in the minimum level. It is noted that there are damages and problems in the used fibers during injection molding technique due to the rotation of the screw [215]. The two most important factors affecting this technique are pressure and molding temperature, especially in biocomposites. Increased heat can lead to damage in the natural fiber, but it makes thermoplastics less viscous and more able to wetting the fibers whereas molding pressure plays an important role in removing the trapped air in the composites which is responsible for the presence of voids in the composites [189].

The film stacking process is one of the most used methods for the manufacture of composites. Polymer is used in the form of films in this method. By heating and compressing the polymer pellets, we can prepare the polymer film. Several layers of the matrix and natural fibers (similar dimensions) are stacked together, then it is heated and compressed for some time. When the polymer melts, it presses with the fiber in the desired order, then the mold is allowed to cool under constant pressure. The fiber volume in the composite is calculated by the ratio between the thermoplastic mass and the fiber mass. By controlling pressure, temperature and time, the melting temperature and viscosity of the polymer is adjusted (which varies depending on the type of polymer) and the same is calculated for the fibers [199]. This technique is used by [205] to produce reinforced thermoplastic composites with flax fibers. Flax fibers are evenly distributed along the mold. Figure 1.18. Shows a schematic diagram for this process. By heating and compressing the polymer pellets, we can prepare the polymer film. Several layers of the matrix and natural fibers (similar dimensions) are stacked together, then it is heated and compressed for some time. When the polymer melts, it presses with the fiber in the desired order, then the mold is allowed to cool under constant pressure. The fiber volume in the composite is calculated by the ratio between the thermoplastic mass and the fiber mass.

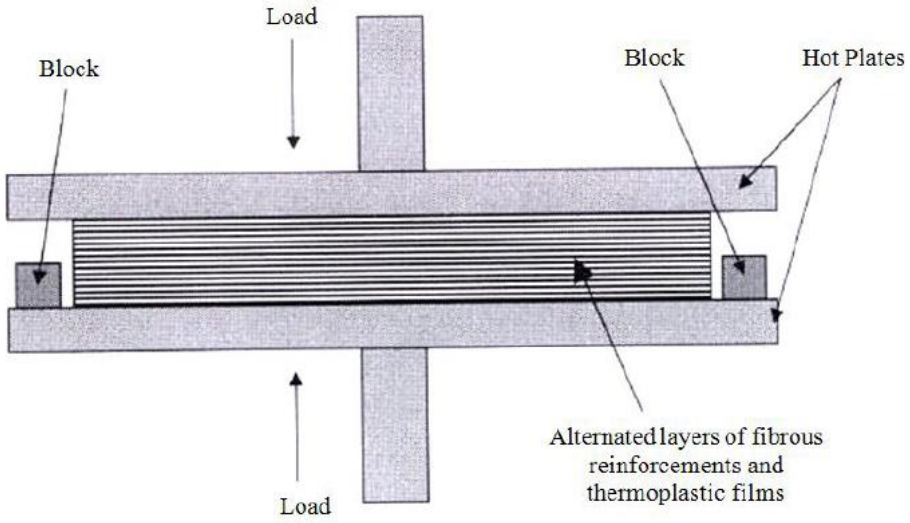


Figure 1. 17. Schematic diagram of the film stacking process [45]

This technique has been used to produce flax fiber reinforced PLA biocomposites [147]. The thickness of PLA film is approximately 0.2 mm. The surface of flax fiber is treated by silane addition in different percentage. Factors such as temperature, pressure, time, flax addition, and silane addition are also studied

The details are shown in Table 1.5.

Table 1. 5. Variable factors and levels of the test [147]

| Levels | Factors | | | |
|---|---|---|---|---|
| | Flax Addition (%) | Silane Addition (%) | Hot-press Temperature(℃) | Hot-press Time (min) |
| 1 | 30 | 1 | 190 | 3 |
| 2 | 40 | 3 | 200 | 5 |
| 3 | 50 | 5 | 210 | 7 |

The compression molding has also been used for the production of composites of PLA fibers as reinforcement in PLA [185]. In this case flax fibers are used in nonwoven web form with a density of 200 ± 10 g/m2, prepared by needle punching technique and PLA was used in the solution form. PLA pellets are dissolved in chloroform to make the solution equivalent to 0.9, 0.8 and 0.7 weight fractions of the web. Then the PLA solution is poured over the nonwoven web inside a mold. Finally the composite material is made by hot pressing at 190 °C temperature and 50 bar pressure for 15 minute. The typical process is shown in Figure 2.19.


Figure 1. 18. Procedures for preparation of nonwoven PLA composites [185]

The matrix fibers and reinforcing fibers are mixed, then the mixture is evenly combed (carding) and distributed. A set of needles make a set of holes in the composite then a hot-pressing makes the final composite. Figure 1.19. Shows a schematic diagram of making the composite by carding process.

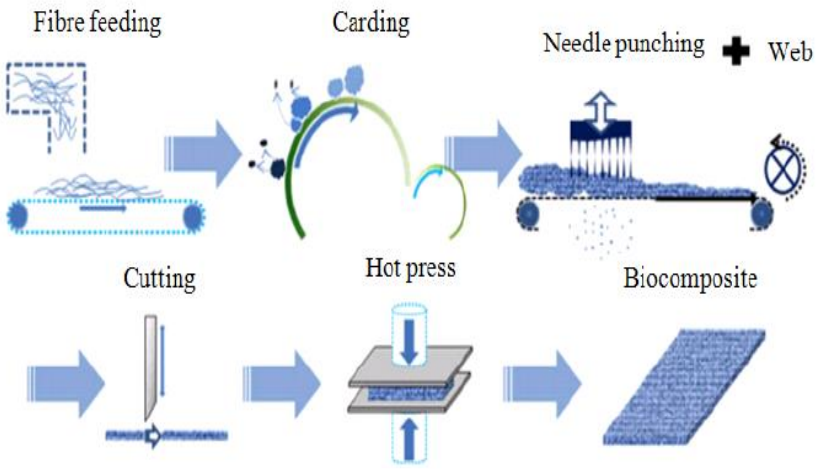


Figure 1. 19. Carding process for manufacturing biocomposites [193]

Lee et al. used this technique to produce kenaf fiber reinforced PLA biocomposites. They converted the pre-pressed mat into composite by using hot pressing for 5 minutes at 200 °C temperature under 7 MPa pressure. The compositions of various PLA/Kenaf biocomposites investigated by them are listed in Table 1.6.

Table 1. 6. Composition of biocomposites [203]

| Fiber | Percentage of composition (%) | | | | |
|---|---|---|---|---|---|
| PLA fiber | 100 | 90 | 70 | 50 | 30 |
| Kenaf fiber | 0 | 10 | 30 | 50 | 70 |

### 1.10.2 Overmolding Technology

Over-molding Technology is an injection molding process in which a single part is molded using two different materials to form one part. Mostly the first material, (the substrate), is covered (partially or fully) by different materials (overmold materials) during the production process which is a valid method for producing structures with reduced weight. The concept is to combine the advantages of injection molding and Continuous Fiber Reinforced Thermoplastic (CFRT) properties to produce strong lightweight structures that have higher mechanical properties than molding compounds, but they can be integrated directly in the molding process. Potential applications for over-molded CFRT inserts are in seat structures, airbag housings, front end modules, crash beams and other structural applications [207].

The substrate can be any material such as a piece of plastic, a metal or an existing product (screws and electrical connectors). This substrate is the main piece to which another material will be added until it finally becomes one continuous part chemically or mechanically connected. The plastic comes in many forms, the most important of which is pellet and film. The pellet is mixed with other additives such as fillers, colorants and foaming agents. The mixture is heated to the melting point and injected as a liquid. Not all polymers are valid for this technique. If the substrate is metal, you can overmold it with any type of plastic or other materials. But for Overmolding a plastic substrate with another plastic or any other material it has limitation and compatibility issues.

There are many advantages that can be utilized by using Overmolding technique:

- Reduced operation and labor costs due to reducing the number of steps needed to work to only one step (one molded step).
- The bonding step in manufacturing is eliminated due to the strength of bonding, which leads to increased reliability in the component.

- Plastic parts in this technique are lightweight, suitable for the compound and has the possibility to be reinforced with a shock-resistant resin.
- Increases the bonding and coherence of the pieces and gives them consistent structure.
- Allows greater freedom at designing and multiple compounds can be used in the process (provides the ability to form a product of several thermoplastic materials).

There are two injection molding processes that currently control the overmolded technique:

- Multi-shot injection molding.
- Insert molding.

This method is the most popular process where a previously pre-molded piece is put in the mold and then directly polymer is injected above it.

This method is characterized by the fact that the old machines in factories do not need to be replaced and it is enough to introduce a simple adjustment to enable them to absorb the modern technology, and that’s what makes this process easier and faster than multi-shot process.

This process is called of several names, such as two-step injection, multi-injection, or multiple materials. Manufacturers choose this process to reduce injection time, produce superior parts with mechanical properties and reduce production price

## 2. EXPERIMENTAL

This chapter discusses the materials and experimental methodologies used for the development of high-performing and biodegradable overmolded eco-composites by using the combination of jute fibers and PLA. Firstly, materials used for the development of ecosheet composites in this PhD are discussed in details. They include jute fibers and bio/synthetic PLA polymer to identify them and to choose suitable components for overmolded eco-composites, beside the chemicals and flame retardant used for surface modification treatments to improve the flame retardant specifications and mechanical performances of ecosheet composites. The methods applied on flame retardants and the fibers' surface modification treatments on the identified composite components are explained.

### 2.1. Materials

The quality and properties of a product mainly depend on the raw material. Raw material selection is an important and primary part of any research. The reinforcing fibers and the matrix materials are the main raw materials of this project work.

The best parts from which jute fibers are extracted are bast. The bast fibers are preferred for use as reinforcement in biodegradable composites. The advantages of this bast fibers over other cellulose based fibers are explained in Section 2.5.1. Among the bast fibers, jute is one of the lightest, and it has high mechanical properties which are distinctive from its counterparts like (tensile strength, elongation and modulus). [191].

Matrix materials are usually used in liquid or film form to produce composite materials. There are many naturally occurring polymers that can be used in biodegradable compounds such as PLA, thermoplastic starch, cellulose, PHAs, etc. which are used as matrix materials to produce fully biodegradable composites. To minimize delamination and achieve better blend effect with jute fiber for thermoplastic composite, PLA is selected for this study because it is the only natural

Polymer that is artificially manufactured and can be used for melt-process for many times. The properties of PLA are described in Section 1.3. [189].

Table 2. 1. The properties of Jute

| Material | Source and key properties | Abbreviation |
|---|---|---|
| Jute Woven Fabric | Izmir, Turkey, Local producer<br>Areal weight: 220 g/m2<br>500 warp tows and 400 weft tows per meter<br>Linear weights of warp and weft tows are equal | Jute |

Jute and PLA fibers are both inexpensive and easily available commercially in Turkey. A woven jute fabric is used for the ecosheet and overmolded study of composites. Their properties are given in Table 2.1.

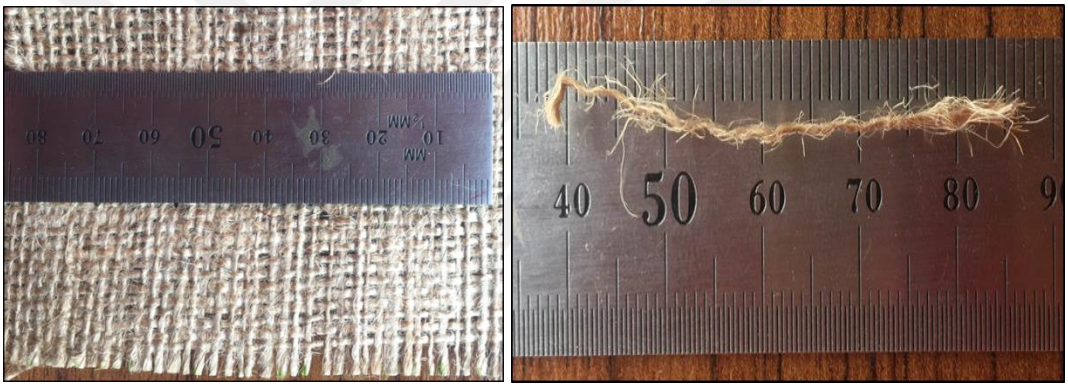


Figure 2. 1. Jute Woven Fabric

All chemicals, listed below, are reagent grade with at least 98% purity, and supplied by Sigma-Aldrich Corporation -USA.

- Sodium hydroxide (NaOH), 98% purity.
- 3-aminopropyltriethoxysilane (3-APTS) ( $C_9H_{23}NO_3Si$), 98% purity.
- Acetic acid (CH3COOH), 99.7% purity.

Jute and PLA fibers are both inexpensive and easily available commercially in Turkey. A woven jute fabric is used for the ecosheet and overmolded study of composites. Jute and PLA fibers are both inexpensive and easily available commercially in Turkey. A woven jute fabric is used for the ecosheet and overmolded study of composites. Their properties are given in Table 2.1.

Table 2. 2. The PLA polymer used in this study

| Material | Source and key properties | Abbreviation |
|---|---|---|
| Poly (lactic acid) used in ecosheets | Natureworks, USA 2100 D<br>Density: 1.30 g/cm3<br>MFI: 5-15 g/10 min (190$^{o}$C/2.16 kg)<br>Crystallizable, Opaque<br>High heat resistant PLA | ecosheet-PLA |
| Poly (lactic acid) used for over-molding | Natureplast, France<br>PLI003 Injection molding grade<br>Amorphous, Transparent<br>MFI: 20 g/min (190$^{o}$C/2.16 kg) | Overmold-PLA |

All the flame retardant chemicals listed below, are supplied by Clariant -Switzerland

- Ammoniumpolyphosphate with Synergists (APS) 98% purity.
- Melamine polyphosphate and Zinc borate (MPZ) 98% purity.
- Aluminum diethylphosphinate (ADS) 99.7% purity.

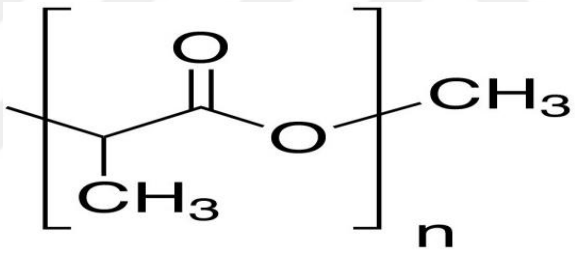


Figure 2. 2. The Chemical Structure of Poly (lactic acid)

**2.3. Samples Preparation**

In order to develop the composite material, there is a need of ecosheet. From the literature survey it is found that around 70% to 60% matrix materials are generally present in thermoplastic composite materials to achieve good fiber/matrix bonding. Voids are formed during the composite fabrication. Jute itself has voids due to the lumen. Fiber and matrix blend ratio by weight is selected by limiting the void content from 5% to 10% by volume [142, 193, 126, 117, and 175]. The jute fiber content by weight is considered to examine the effect of different fiber content on the performance of composite material. The nominal jute fiber content is designed to be 40, 30, and 20%. According to the blend ratios by weight, the ecosheet is divided into the following three types:

- Type A (60P/40j): 60% PLA + 40% jute
- Type B (70P/30j): 70% PLA + 30% jute
- Type C (80P/20j): 80% PLA + 20% jute

As stated in Section 2.10., ecosheet can be made by using different techniques. Woven technique is used in this research for making ecosheet from PLA/jute fiber blend. This woven technique consists of two steps: hot press and overmolding.

### 2.3.1. Hot pressing

The hot pressing stage is made as showing (plates dimension: 15 cm×25 cm), see Figure 2.3. Although the hot press has a computer controlled system, it lacks temperature accuracy, which is confirmed by comparing the temperatures that are detected by the thermocouple and the temperature sensors inside the hot press plate. The thermocouple detected temperature is regarded as the real composite processing temperature instead of the temperature showing on the hot press monitor. From the literature survey it is found that around 70% to 60% matrix materials are generally present in thermoplastic composite materials to achieve good fiber/matrix bonding. Voids are formed during the composite fabrication. Jute itself has voids due to the lumen.

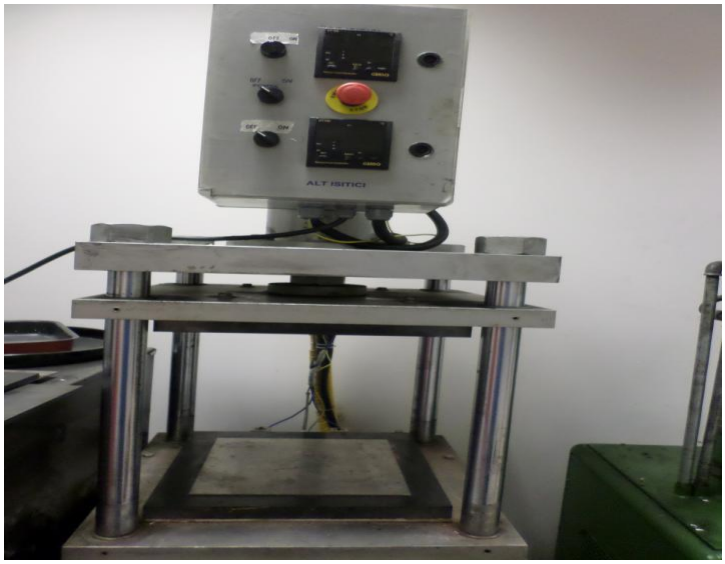

Figure 2. 3. Hot Pre

### 2.3.2. The Ecosheet samples preparation

Three different concentrations of jute, 20%, 30% and 40% are selected for use in the ecosheet samples. The hydraulic press is used to increase the bonding between the fibers and the polymer in the ecosheet. The sizes used to make the ecosheet are 300 mm by 200 mm. Jute fibers and PLA film are cut according to these measurements. See Fig. 2.3. Two to three layers of jute are laid in turn with 6 to 7 layers of PLA film. These layers are confined between two iron plates and then placed in the mold inside the hot press. The temperature is set to 190 °C and pressure is 8 MPa. The layers are pressed for 5 to 7 minutes, as shown in Figs. 3.4. After being pressed for a full five minutes, the temperature is reduced while keeping the same pressure until it reached room temperature 25 °C. After the temperature reaches 25 °C, the ecosheets are extracted from the mold. 5 ecosheets are made for each sample. The layers of jute are laid in a specific direction of 0°, 90° and 45° /−45°. These angles are selected to study the effect of fibers direction on the mechanical properties of ecosheet as well as the ability of the polymer to penetrate and adhere to the fibers and the angle effect on it. See table 2.3. For full details of the ecosheet Specifications.

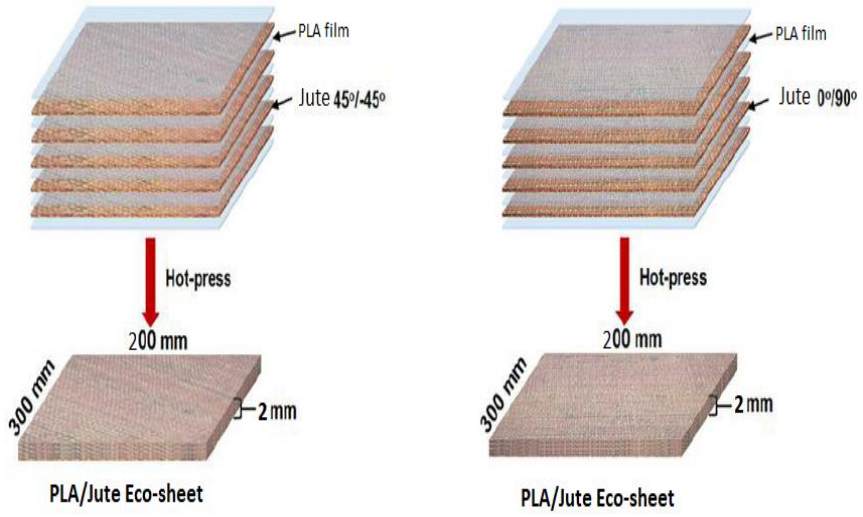


Figure 2. 4. The Ecosheet samples preparation

These angles are selected to study the effect of fibers direction on the mechanical properties of ecosheet as well as the ability of the polymer to penetrate and adhere to the fibers and the angle effect on it. See table 2.3. For full details of the ecosheet Specifications.

Table 2. 3. Compositions of different materials

| Materials | Matrix (wt. %) | Flax fibers (wt. %) | Orientation |
|---|---|---|---|
| PLA/Jute | 80 | 20 | 0,90,45° |
| PLA/Jute | 70 | 30 | 0,90,45° |
| PLA/Jute | 60 | 40 | 0,90,45° |
| OM-PLA/Jute | 80 | 20 | 45° |
| OM-PLA/Jute | 70 | 30 | 45° |
| OM-PLA/Jute | 60 | 40 | 45° |
| OM(PLA70%-TPU30%)/jute | 80 | 20 | 45° |
| OM(PLA50%-TPU50%)/jute | 80 | 20 | 45° |
| OM(PLA70%-TPU30%)/jute | 70 | 30 | 45° |
| OM(PLA50%-TPU50%)/jute | 70 | 30 | 45° |
| PLA100% | | | |

## 2.4. Jute Fibers Surface Treatment

In order to treat the surface of jute fibers, the fibers are washed with water to remove dust and impurities. The washing is done at room temperature and then the fiber is left for 48 hours to dry in the air. After the initial drying phase, jute fibers are placed in the oven to remove the rest of the moisture for 73 hours at 80 ° C. The surface of the jute fiber is treated in two different ways: 1- Alkaline treatment using (NaOH) material. 2- Alkaline treatment + Silane treatment (separately). The fibers are classified into 3 sections: 1- Untreated fibers, 2- Alkali treated fibers and 3- Alkali + Silane treated fibers.

### 2.4.1. Alkaline treatment

The first step for the alkaline treatment of jute fibers is to soak the fiber in aqueous solution of NaOH .The solution ratio 1:20 (w/w). Three different concentrations of solution 1%, 5 %and10% (w/v) are selected. The soaking time is 2h, 4 h, 6h and 8h at room temperature. The Jute fibers is weighed before the operation (W1). After the treatment time was finished, it is washed with distilled water several times until all the NaOH residue is removed from the jute surface. The fibers are neutralized by adding citric acid until the pH reaches 7. The treated Jute fibers (JFNA) is placed in an oven and vacuum dried for 72 hours at 80 ° C. The fibers are once again weighed (W2) Weight loss is calculated

$$\% \text{ Weight loss} = [(W1 - W2) / W1] \times 100 \quad (2.1)$$

The reaction of alkali with jute fibers is shown in Figure 2.5. [11,15].

The Reaction mechanism of jute fibers with NaOH solution can be explained in two steps:

The first stage is that the hydrogen ion (H+) of the hydroxyl group in jute fiber is replaced by sodium ion (Na+). The second stage in which the sodium ion(Na+) of the fiber surface is replaced by the hydrogen ion(H+) of acetic acid. This method is characterized by dissolving impurities and secondary materials in fibers such as wax, hemicellulose and oily substances.

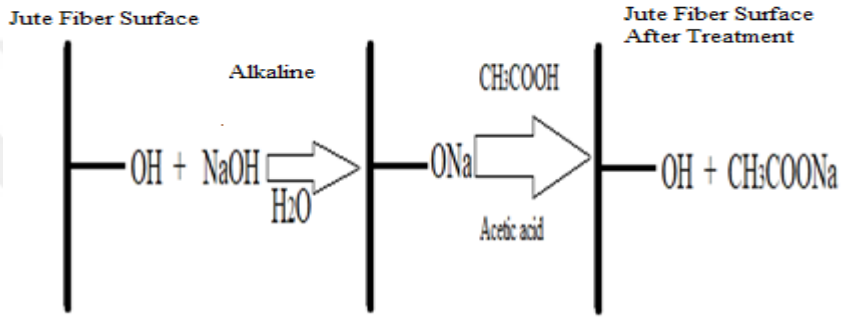


Figure 2. 5. Reaction of alkali with jute fibers

### 2.4.2. Alkali and silane treatment

After the alkaline treatment is completed, treatment is carried out with silane. Three different concentrations are selected, taking into account the weight of jute fiber: 1%, 1.5 and 3% wt%. 3-aminopropyltriethoxysilane (3-APTS) is used in this treatment. The solution is prepared by dissolving silane in a mixture of water and ethanol by (60/40 w/w) for hydrolysis. The pH is maintained constant by glacial acetic acid at 3.5-4.0. Until the silane is completely dissolved, it is continuously stirred for two hours. Jute fibers are immersed in a silane solution for 6 hours at 65 ° C. After finishing the treatment, the fibers are washed several times until all impurities and residues of the silane are removed. The fibers is dried in vacuum oven at 80 ° C for 72 hours. The reaction mechanism is explained in the picture Figure 2.6. [206,207]. The pH is maintained constant by glacial acetic acid at 3.5-4.0. Until the silane is completely dissolved, it is continuously stirred for two hours. Jute fibers are immersed in a silane solution for 6 hours at 65 ° C.

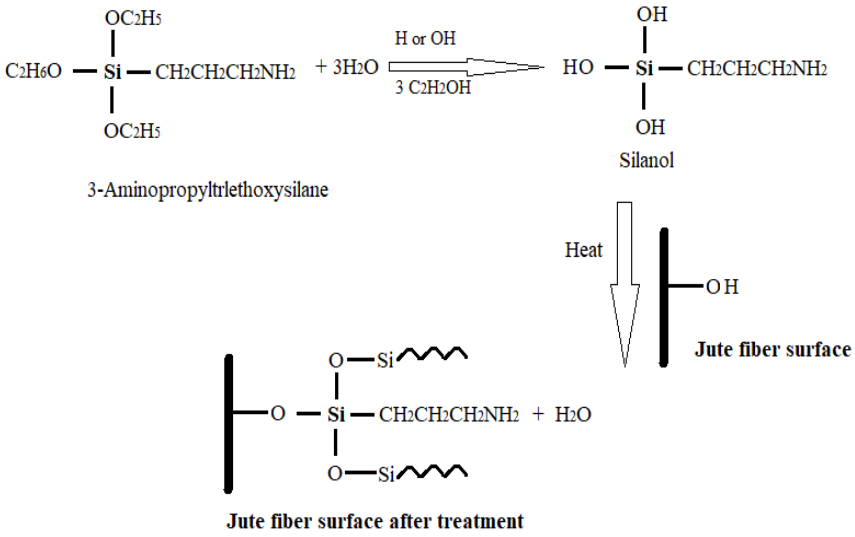


Figure 2. 6. Hydrolysis process of silane and reaction of silanol with jute fibers [102]

The fibers is dried in vacuum oven at 80 ° C for 72 hours. The reaction mechanism is explained in the picture Figure 2.6. [206,207].

Table 2. 4. Compositions of different materials

| N | Materials | Orientation | NaOH % | NaOH + Silane% |
|---|---|---|---|---|
| 1 | PLA100% | - | - | - |
| 2 | PLA/Jute 70%-30% | 45 | 1% | - |
| 3 | PLA/Jute 70%-30% | 45 | 5% | - |
| 4 | PLA/Jute 70%-30% | 45 | 10% | - |
| 5 | PLA/Jute 70%-30% | 45 | 10% | 1% |
| 6 | PLA/Jute 70%-30% | 45 | 10% | 1.5% |
| 7 | PLA/Jute 70%-30% | 45 | 10% | 3% |
| 8 | PLA/Jute 60%-40% | 45 | 1% | - |
| 9 | PLA/Jute 60%-40% | 45 | 5% | - |
| 10 | PLA/Jute 60%-40% | 45 | 10% | - |
| 11 | PLA/Jute 60%-40% | 45 | 10% | 1% |
| 12 | PLA/Jute 60%-40% | 45 | 10% | 1.5% |
| 13 | PLA/Jute 60%-40% | 45 | 10% | 3% |

## 2.5. Preparation of Overmolding Samples

We cut the samples according to the size of the mold and then the sample is placed inside the mold. Then the sample is exposed to hot air through the heat gun until the temperature of the sample Surface reached 100 $c^{o}$. The mold containing the cut ecosheet sample (according to the required sizes) is placed in the injection molding and then the molten PLA polymer is injected onto the ecosheet. After the sample is

cooled it is extracted. A single cohesive piece of ecosheet and PLA polymer is created and it is called an overmold sample composite.

Figure 2. 7. Preparation of the PLA/JUTE in photos

The mold containing the cut ecosheet sample (according to the required sizes) is placed in the injection molding and then the molten PLA polymer is injected onto the ecosheet.

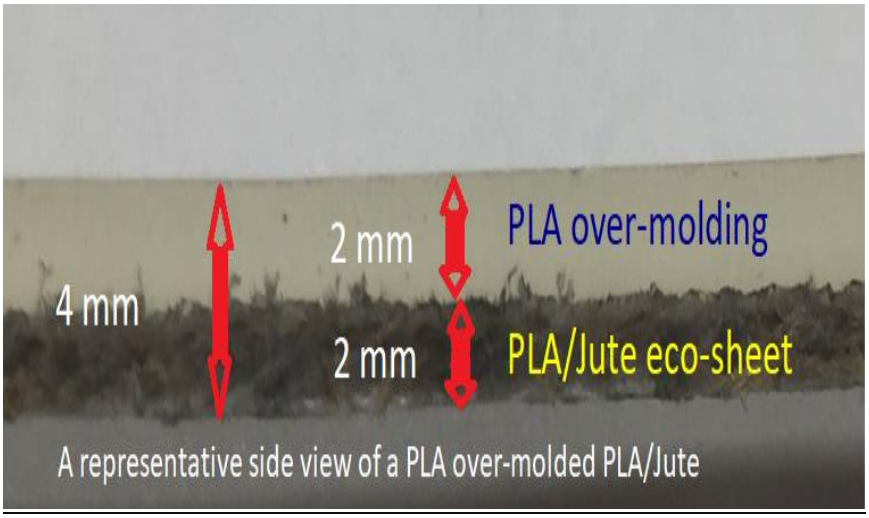


Figure 2. 8. PLA Overmolding

**2.6. Preparation of Flame Retardant Samples**

The PLA is mixed with flame retardant in extruder device of 20/80% and 10/90%, then it is extracted in the form of granules, then it is injected again on the ecosheet

until the plate is covered with the mixture. The ratio is 50/50% between the ecosheet and the mixture.

Table 2. 5. Compositions of different materials

| Materials | Flame retardant (wt. %) | Jute-PLA (wt. %) | Orientation |
|---|---|---|---|
| 10(ADS)-90%PLA | 100% (90/10) | 0% | - |
| 10(ADS)-90%PLA+jute | 50% (90/10) | 50% (60/40) | 45 |
| 20(ADS)-80%PLA | 100% (80/20) | 0% | - |
| 20(ADS)-80%PLA-jute | 50% (80/20) | 50% (60/40) | 45 |
| 10(APS)-90%PLA | 100% (90/10) | 0% | - |
| 10(APS)-90%PLA-jute | 50% (90/10) | 50% (60/40) | 45 |
| 20(APS)-80%PLA | 100% (80/20) | 0% | - |
| 20(APS)-80%PLA jute | 50% (80/20) | 50% (60/40) | 45 |
| 10(MPZ)-90%PLA | 100% (90/10) | 0% | - |
| 10(MPZ)-90%PLA-jute | 50% (90/10) | 50% (60/40) | 45 |
| 20(MPZ)-80%PLA | 100% (80/20) | 0% | - |
| 20(MPZ)-80%PLA-jute | 50% (80/20) | 50% (60/40) | 45 |

## 2.7 Samples Characterization

The objectives of this research are to develop completely biodegradable woven composite materials and to establish the optimum processing parameters by evaluating the properties of the composites. This chapter summarizes the general approach to the study and provides detailed information on how the overall objectives of the research will be achieved. The composite materials are evaluated by analyzing the physical, mechanical and thermal properties.

Properties of the raw materials play an important role in the final product. End-uses of the product depend also on the properties of raw materials. As reinforcing material, jute fiber plays an active role in the composite material. Fiber length, fiber diameter, fiber linear density, and fiber strength are all important material parameters. In order to select the appropriate processing temperature in composite manufacture, the melting point of PLA is also tested.

Fiber diameter is important for the measurement of fiber volume fraction to determine the fiber and polymer content. The average value of fiber diameter is calculated because, as natural fiber, jute fiber diameter differs along individual fiber axis and also between fibers.

The melting point of PLA is determined to select the processing i.e. molding temperature for the composite manufacture because the molding temperature

depends on the melting temperature of PLA fiber. The melting point of the matrix is the reference for determining the consolidation temperature of the composite manufacture (sometimes slightly higher than the melting point of the matrix) and should be lower than the melting point of the fiber. The differential scanning calorimeter (DSC) determines the melting behavior of the polymer by identifying several points such as the glass transition temperature (Tg), the crystallinity of the polymer and its melting temperature(Tm).

### 2.7.3. Evaluation of ecosheet

The area density (g/m2), thickness and tensile strength of the ecosheet are tested for evaluating the ecosheet and are discussed in Section 5.1. Area density of the ecosheet is determined to analysis the web variation. The tensile strength of the ecosheet is measured according to ISO 15100: 2000 by a METTLER Density determination machine.

From the literature review, the hot press method is found to be beneficial over the other method such as injection molding, resin transfer molding, etc. for making the ecosheet, as discussed in Section 2.10. Moreover, hot press is commonly used in industry and it is easy to be handled.

The following processing parameters are considered in the manufacturing of PLA/jute composite panels using the hot press method. Different settings are used for each variable in order to optimize the process. The settings are discussed below:

The molding temperature mainly depends on the melting point of matrix material. From the previous studies we can determine the melting point of PLA and the appropriate degree of operation (usually higher than the melting degree of 10 °C to 20 °C). The melting point of PLA is estimated to 165°C to 170°C [206, 217, 225]. To examine the effect of different temperature on the performance of composite material, two molding temperatures 180 and 190 °C are considered for this work. It is found that thermal degradation of jute fiber is not really significant in the first few minutes and between 180 to 200°C temperatures i.e. jute is not affected by these molding temperatures [229, 222].

From the literature survey it is found that the molding or consolidation time for manufacturing thermoplastic composite material is around 5 minutes [24 and 46] to 15 minutes [25]. It is found that the molding time depends on the molding temperature and pressure. Three molding times are selected in this study to study the effect of time change on composite performance. The three molding times are 3, 5 and 7 minutes. It is important to control the parameters in the process, especially temperature and time, because jute fibers are sensitive to these changes. Therefore, when adjusting these parameters, we can ensure that a significant portion of the strength or stiffness of these fibers is not lost and that makes the composite more stable and stronger [102].

From the literature survey it is found that a wide range of pressure could be used. For example, [117] has used a fixed pressure of 30 bar, Kumar et al. [815] has used a fixed pressure of 50 bar, Bos et al. [102] has used a fixed pressure of 40 bar, and Patel et al. [148] has used a fixed pressure of 100 bar. It is also found that the selection of pressure depended on the molding temperature, time and thickness of the material. For this research, a pressure of 100 bar are selected to manufacture ecosheet composite. The tensile properties are tested to determine the optimal pressure for the highest composite performance. This is reported in Section 3.1. The highest tensile strength is found to be from the composite material manufactured by using 100 bar molding pressure. Thus, molding pressure is fixed at 100 bar for subsequent work in this research.

The ecosheet composite panels are manufactured by using hot press molding. The standard method is followed to manufacture the composite material and the manufacturing system is discussed in Section 3.3.2.

One of the main distinguishing features of natural fiber-based composites is that they are an excellent alternative to glass fiber reinforced composites. The proposed areas of the end use of the product manufactured by this project include automotive industry- car interiors, interior floor panel, door panels, automotive structural beam, vehicle body panel, beside exterior engine components, building industry-ceiling tiles, windows, doors, hard boards, particle board, low cost buildings ceilings, house-hold products, furniture, cupboard, lamp shade, luggage, computer cases, electric fan blades, cover of electrical appliances, biogas containers, railway coaches, food

container, industrial packaging material. The composites need to have satisfactory mechanical properties for these applications.

The density of the composite is one of its important physical properties and is dependent on the amount of reinforcement presented in the structure. The density is calculated by using the immersion method, ISO 15100: 2000 which is discussed in Section 5.1. Fiber is often used as reinforce in composite. Therefore, it is preferably used in a larger volume fraction to obtain the best properties of the matrix. It is preferable to reduce the spaces between the fibers (voids) as much as possible because the increase of these voids leads to weak mechanical properties of the composites.

For the tensile properties, the Instrumental 3345 model universal testing machine is selected and the method used to test the composite samples is ISO 178. See the results in Section 4.1. For the flexural properties, the three-point flexure reference scale system is selected. The method is described in ISO 527(5a). See the results in Section 4.1. The impact test is selected to study the behavior of samples under extreme conditions because one of the most important applications of these composite is to use them in the door panels or instrument panels and therefore must ensure the safety of passengers. Method ISO 180 -1 is selected for Izod impact tests by using notched samples in an Avery pendulum impact tester. See the results in section 4.1. Differential scanning calorimetry (DSC) technique determines the quantity of heat either absorbed or released when a substance undergoes a physical or chemical change. Several parameters can be estimated by performing a DSC scan. Among these parameters are melting enthalpy ($\Delta Hm$), glass transition temperature (Tg) and melting temperature (Tm). In this study, a calibrated DSC 3 - Differential Scanning Calorimeter from Mettler-Toledo device is used to perform these tests. For the study of Thermal degradation changes of biocomposites, a thermogravimetric analysis (TGA) device (METTLER instrument, TGA2 device) is used. See the details in Section 4.1.

Water absorption behavior indicates the stability of the composite and is an important property of the biocomposites. The water absorption of the composite samples is measured following the ASTM D570 and the results are discussed in Section 4.1.

## 2.8. The Characterisation Experiments of Composites

Since the mechanical properties of the biocomposites depend on their real fiber volume fraction and void content, the density of the biocomposites is important to calculate the void content. Thus, the density of the composite materials are considered as physical properties for this research work.

### 2.8.1 Physical properties of the composites

Density is an important property for composite. The structure of the composite depends on the amount of reinforcements in the composite and consequently on the density of the composite. To calculate the density the ISO 15100: 2000 methods are used in this study. Laminates are cut into 1 cm × 1 cm size. Specimens are cut from each panel from different places. Then specimens are oven dried to remove moisture from them. Using density measuring machine (Figure 3-9), density is measured directly. This machine is composed of an electric balance which can measure the weight of a specimen in air and in water; from these data's, machine can automatically calculate the density of any specimen. For each type of laminates, three specimens are tested and an average is taken.

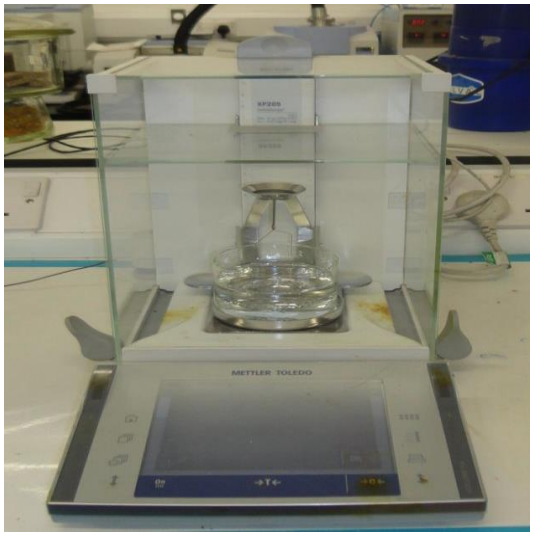


Figure 2. 9. Density measuring machine

The composite pieces and its weight in air ($m^3$) and water ($m^3$) are measured. The weight in air of the specimens ($m^3$) is measured by hanging them through a balance hook by means of the wire. Also the weight of the specimens in water ($m^3$) is determined by immersing them in water in a 100 ml beaker while they are suspended steadily by the wire. Care is taken to avoid any air bubbles adhering to the specimen or found in the beaker, otherwise the bubbles are removed by means of a fine wire.

The density of the specimen is calculated using the Equation 2.2.

$$\rho s = \frac{ms,A \times \rho IL}{ms,A - msIL} \quad (2.2)$$

Where,

$\rho s$ is the density, in $g/cm^3$, of the specimen;

$ms,A$ is the apparent mass, in grams, of the specimen in air, ($m^3$ - $m^3$);

$ms,IL$ is the apparent mass, in grams, of the specimen in the immersion liquid,

($m^3$ - $m^3$);

$\rho IL$ is the density, in $g/cm^3$, of the immersion liquid (water).

### 2.8.2. Mechanical property testing

Due to the high oil prices, the increasing global interest by the environment, and the problems of global warming, Biocomposites are attracting more researchers' attention. These composite are lighter in weight and more economical in production than glass and carbon fibers composites. These composites have become the replacement of synthetic composite in various fields such as building industries and automotive. They are widely used in high performance applications also. Satisfactory mechanical properties are vital in these types of applications. The tensile, flexural, DMA and impact properties are considered for this research work to evaluate the mechanical performance of the composite materials.

There are many variables affecting the mechanical properties of composites. Some of these variables partially affect the composite such as the degree of adhesion between

the matrix and fibers, the quality of the final product, and other variables in the processing stage. Some of them affect mainly the mechanical properties which are:

- The fiber properties.
- The matrix properties.
- The fiber surface properties.

### 2.8.2.1. Tensile properties

Composite strength depends on the strength and stiffness of the fibers used in reinforcing the matrix. The composite is subjected to a tensile load until the strength of the composite is measured. When tensile force applied to composite, the force transformed from the matrix to the fibers and this is the main objective of the use of tensile test which is to measure the strength and modulus of the composite. Additional information can be obtained by careful observation of the sample under the applied load. A composite may split or delaminate; the nature of the failure may be brittle with no warning; or it may start with visible or audible signs. All this information is useful and knowledge of the failure mode is vital to establish the end use of the material [186].

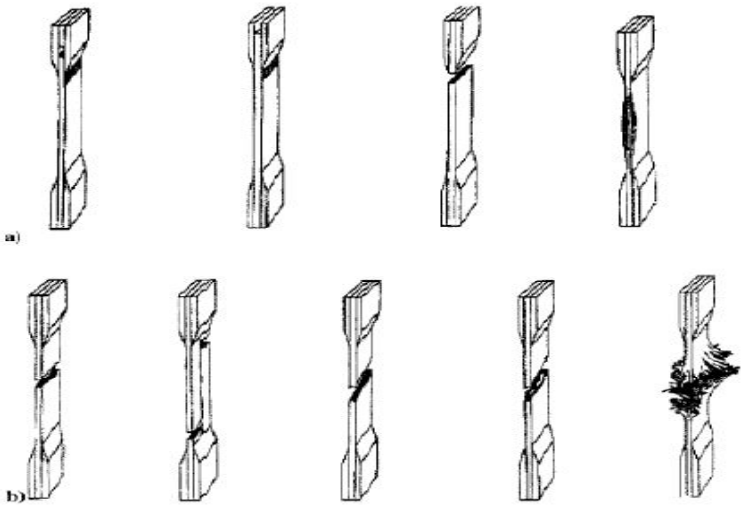

Figure 2. 10. Unacceptable failures (a) and Acceptable failures (b) [186]

During a tensile test, a rectangular strip which is cut from a panel having a longer length compared to its width is subjected to the tensile load or stressed in the length

direction by holding one end of the strip and stretching the other end. Both the ends of the strip are held with the help of grips and if breakage occurs near the grip, the sample is rejected. An example of acceptable and unacceptable failure under tensile load is shown in the Figure 2.10.

The basic purpose of tensile testing is to determine the tensile strength and modulus of the material. There are varieties of specimen sizes, test piece specifications, and testing procedures described in a number of published standards to measure the tensile stress and strain at breaking point and the Young's modulus. The standard followed for the determination of tensile properties in this study is ISO 178.


Figure 2. 11. Bench Circular Saw

The tests are conducted on a universal Instron which is a universal testing machine model 3345; with a 10 kN load cell; the crosshead speed is 10 mm/min. Five specimens of each type are cut in the machine directions using a vertical band saw (Figure 2.11) and the dimensions of all the specimens are measured before the test. A rectangular specimen of 67 by 10 mm is cut from the ecosheet composite sample and the initial distance between grips is fixed at 10 mm.

Extensometer is attached to the composite specimens during the testing, as shown in Figure 2.12. To acquire data for establishing the values of the modulus of elasticity in mega Pascal. The stresses and strains are calculated at all the points from the load and displacement curve.


Figure 2. 12. Composite specimen tensile testing

The tensile stress at the breaking load is calculated by using the Equation 2.3.

$$\sigma t = \frac{F}{Acs} \tag{2.3}$$

Where,

σt is the tensile stress at break in mega Pascal (MPa);

F is the force or load at break in Newton (N);

Acs is the initial cross-sectional area of the specimen in square millimeters (mm2).

The tensile strain at the breaking load was calculated by using the Equation 2.4.

$$\varepsilon t\ (\%) = 100 \times \frac{\Delta L^{\circ}}{L^{\circ}} \tag{2.4}$$

Where,

εt is the tensile strain at break expressed in percentage (%);

Lo is the gauge length of the test specimen expressed in millimeters (mm);

ΔLo is the increase in the specimen length between the gauge marks, expressed in millimeters (mm).

The stresses and strains are calculated at all the points from the load and displacement curve.

The tensile modulus or Young's modulus of the specimen is calculated by using the Equation 2.5.

$$Et = \frac{\sigma 2 - \sigma 1}{\varepsilon 2 - \varepsilon 1} \quad (2.5)$$

Where,

Et is the Young's modulus of elasticity, expressed in megapascal (MPa);

$\sigma 1$ is the stress, in megapascal, measured at the strain value = 0.05%;

$\sigma 2$ is the stress, in megapascal, measured at the strain value = 0.25%.

### 2.8.2.2. Flexural properties

Like tensile strength, the bending force when applied to a composite sample, the applied force transferred from the matrix to the fibers. From here we can measure the capacity of the sample resistance when exposed to the bending load by measuring the flexural properties. There are two simultaneous events that occur when a composite sample is exposed to bending condition. The first event is compression which occurs at the point of the bending force. The second event occurs at the same time on the other side of the sample, which is tension or stretch. Due to the ease of operation of the flexural test and the availability of tools for testing, the flexural test is widely used in the industry for fiber reinforced polymer composites and resins. Flexural test is carried out to measure several things including flexural strain at break, stress at break and modulus which is the purpose objective of this test.

The ISO 527(5a) standard method is used to determine the flexural properties like strain at break, flexural stress at break and modulus. The method usually used in this standard for the determination of flexural properties is called method A. The three-point flexure system is used in method A. Three-point bending is the method in which a bar of rectangular cross-section is loaded from the top while resting on the two supports as shown in Figure 2.13. The geometry of three-point bending offers the application of the stress concentrations to occur at the loading point; so it is easier to perform the three-point bending test [213].

To reduce the impact of shear deformation and interlaminar shear failure, method A is selected for testing. The three-point system is used in this study. Dog bone samples are equipped for this work. See (Figure 2.13).

F-is the applied load; L-is the span length; l-is the specimen length; and h-is the thickness of the specimen

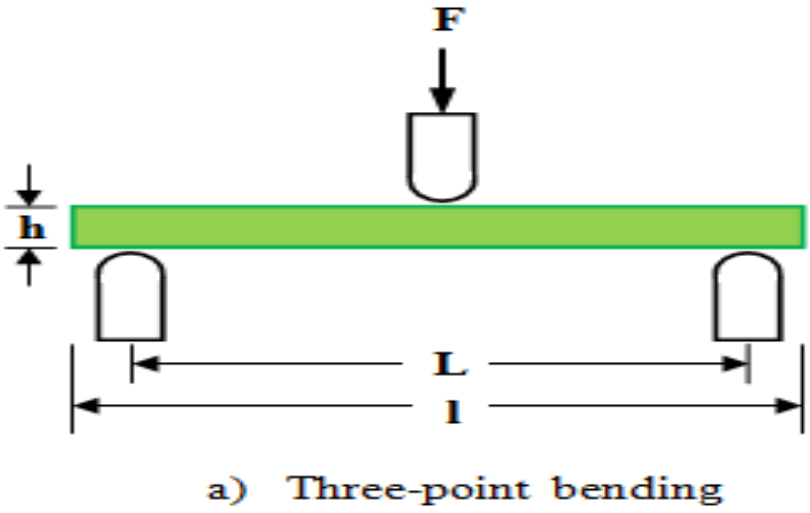


Figure 2. 13. Flexure testing assembly [ISO 527(5a)] [213]

The flexure testing can result in a wide range of failure modes depending on the chosen method, type, and lay-up of the materials being tested. The potential failure modes are tensile fracture, compressive fracture, tensile and compressive fracture accompanied by interlaminar shear and interlaminar shear fracture as shown in Figure 2.14. All failure modes are not acceptable especially those initiated by interlaminar shear.

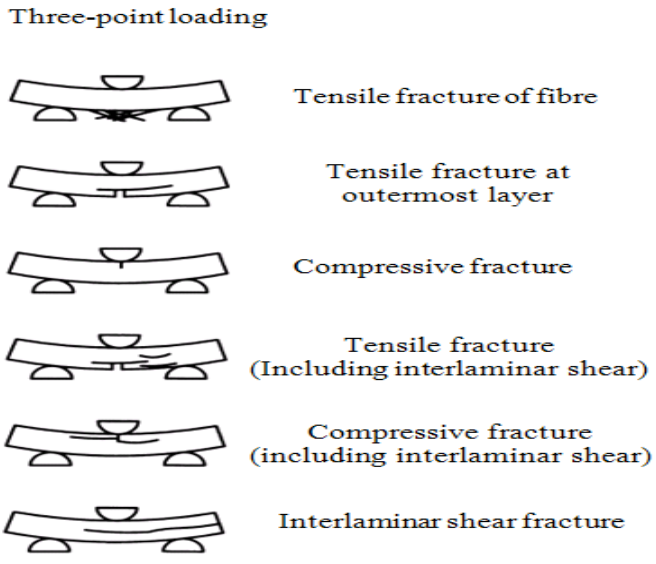


Figure 2. 14. Failure of composite samples in different modes under bending load [ISO 527(5a)] [213]

This test method is not appropriate for the determination of design parameters, but used as a quality-control test. That's because the specimen is subjected to a combined stress state, and the flexure strength and modulus are combinations of the subsequent tensile and compressive properties of the material ISO 527(5a) [213].

The specimen length and span length of the sample depends on the thickness of the sample. Five specimens of each type are cut using a vertical band saw. The thickness of the specimen is 4mm. Thus, the dimensions of the specimens are 67 mm × 10 mm × 4 mm, and the span length is 57 mm. The testing is conducted on an Instron 3345 model universal testing machine with 5 kN load cell at a constant crosshead speed of 10 mm/min (Figure 2.15). The radii of loading nose and the supports are selected as 5.0 mm and 2.0 mm respectively. All tests are performed at 23 ± 2 °C temperature and RH 50 ± 5%.

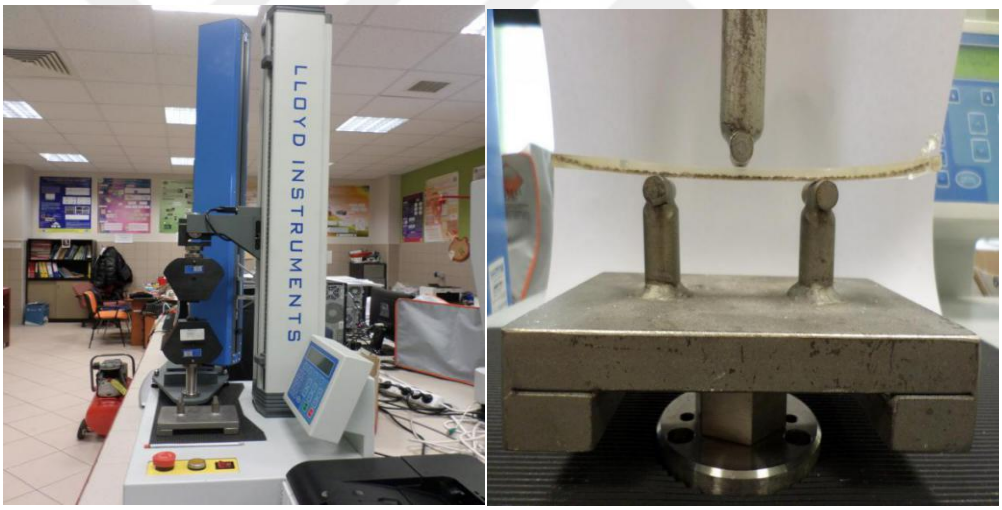


Figure 2. 15. Composite specimen undergoing flexure testing

Flexural stress is defined as a material's ability to resist deformation under load. The flexural stress is calculated by using the Equation 2.6.

$$\sigma f = \frac{3FL}{2bh^2} \tag{2.6}$$

Where,

σf is the flexural stress at break, in megapascal (MPa);

F is the load at break, in Newton (N);

L is the span length, in millimeters (mm);
b is the width of the specimen, in millimeters (mm);
h is the thickness of the specimen, in millimeters (mm).
Flexural strain is calculated by using the Equation 2.7

$$\varepsilon = \frac{6sh}{L^2} \tag{2.7}$$

Where,

ε is the flexural strain at break;
S is the beam mid-point deflection at break in millimeters (mm);
h is the thickness of the specimen, in millimeters (mm);
L is the span length, in millimeters (mm).
After obtaining the load displacement curve, the slope of the curve is determined in the region where it is linear and the flexural modulus is determined using the Equation 2.8.

$$Ef = \frac{L^3}{4bh^3} \tag{2.8}$$

Where,

Ef is the flexural modulus of elasticity, in megapascal (MPa);
L is the span length, in millimeters (mm);
b is the width of the specimen, in millimeters (mm);
h is the thickness of the specimen, in millimeters (mm).

**2.8.2.3. Impact Properties**

The property of impact resistance is one of the most important properties that give an excellent idea for composite strength and its ability to withstand the impact or the limits of the composite ability to resist the impact without damage (resilience). There are many factors that can be studied in this area such as: Maximum force required to break the sample (the impact strength); the amount of energy absorbed by the standard shape sample before the crash (the crush resistance); and the level of damage to the sample under certain conditions (damage tolerance) [213]. Impact testing is usually performed to study the toughness of composite. During plastic

deformation, the toughness of the composite is the superior force at this stage. Therefore, the toughness is tested by measuring the energy absorbed in the plastic deformation phase of the composite. Due to the poor resistance of the plastic deformation phase of the Brittle material, its toughness level is small. By measuring the absorbed energy of composite at impact test, we can measure the toughness of the composite, the strength of the composite, and its carrying capacity.

There are two methods of measuring the energy absorbed and the strength of the sample at impact: the Izod and Izod test. In our current study, we can use the two methods because both are suitable for reinforced composite [213]. The sample is placed in the Izod method by fixing the sample prominently from one side and hit it with a hammer hanging in the form of a pendulum. For the Izod method, the sample is fixed in two ends and hit in the middle by a pendulum. Complete or notched samples can be used in both methods (Figure 2.16.). In this study, a complete sample (unnotched) of the composite is selected for the Izod impact test.

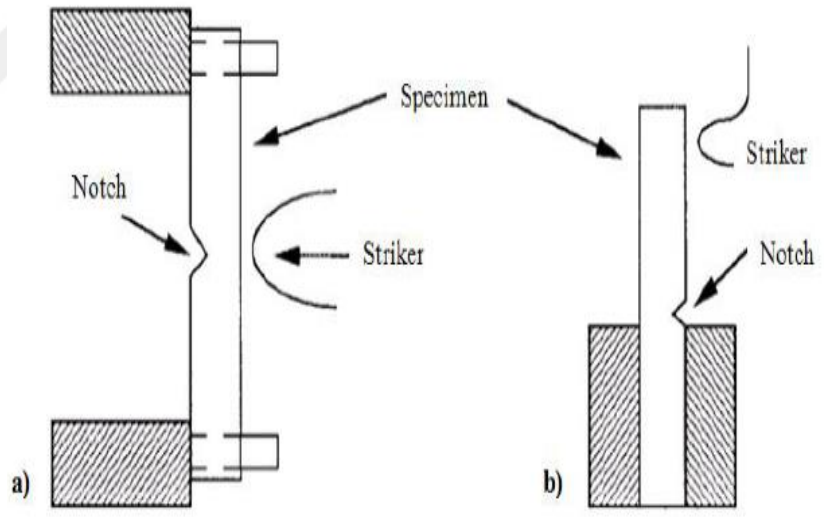


Figure 2. 16. Schematic representation of the Izod (a) and Izod (b) impact equipment [213]

The Izod test consists of three main pieces: a hammer hanging in a pendulum shape called the striker; the sample container (in the base of the machine); the container in which the sample is fixed vertically; the lever (movable vice jaw) that releases the pendulum to attack the sample. The test is performed by releasing the horizontally hanging pendulum above the device; the moving pendulum strikes the sample at the base of the device. Then the absorbed energy

and sample strength are calculated. There are varieties of specimen sizes, test piece specifications, and testing procedures described in a number of published standards to measure the impact strength. The standard followed for the determination of impact strength in this study is ISO 180.

(Figure 2.17.) Shows the impact machine. Five specimens of each sample are used for the measurement of the impact properties and the average results have been reported. The test specimens are cut to the required dimension according to the standard using a vertical band saw. For the unnotched sample dimensions 57 mm × 10 mm × 4 mm, see Figure 2.18.

The Izod impact strength of unnotched specimens is calculated and 5 samples was tested by using the Equation 2.9.

Figure 2. 17. Composite specimen undergoing impact testing

The Izod impact strength of notched specimens is calculated by using the Equation 2.9. Five specimens of each sample are used for the measurement of the impact properties and the average results have been reported. Shows the impact machine. Five specimens of each sample are used for the measurement of the impact properties and the average results have been reported.

Figure 2. 18. The Izod Impact Test Samples

$$\text{aiu}\,\frac{\text{Ec}}{\text{h}\times\text{b}} \times 10^{3} \qquad (2.9)$$

Where,

aiu is the unnotched Izod impact strength (KJ/m²);
Ec is the corrected energy, in joules, absorbed by breaking the test specimen;
h is the thickness, in millimeters, of the test specimen;
b is the width, in millimeters, of the test specimen.

### 2.8.3. The thermal properties of composites

The manufacturing process of fiber-reinforced biocomposites is adjusted by of adjusting the temperature of the matrix. The reason for choosing the melting temperature of the matrix is because this is the point that determines the properties of the matrix and the compound. To understand the change in the polymer at different temperatures, there are three main factors that will enable us to understand the thermal nature of the polymer. The most important factor is the glass transition temperature (Tg) factor because the polymer behaves much differently before and after this point. Before (Tg), the polymer is more fragile (more brittle) and at higher temperatures the polymer is softer (more rubbery). The second factor is the crystallization temperature (Tc) and the third factor is the melting temperature (Tm). These factors have a significant impact on the study of polymers and its application. So when choosing a particular polymer, you should have an idea about how it will behave under the applied heat flow. To determine the above mentioned temperatures, Differential Scanning Calorimetry (DSC) analysis is the most famous device used in

thermal analysis of polymers and composite. For the study of thermal degradation characteristics of polymers, Thermogravimetric analysis (TGA) device is used.

### 2.8.3.1. Differential scanning calorimetry (DSC)

The Differential Scanning Calorimetry technique is the best way to find out what are called “thermal transitions” of a polymer such as: glass transitions (Tg), and melting point and crystallization. Generally, the Differential Scanning Calorimetry (DSC) system consists of two pans. This device works on the principle of comparison between two pans in thermal properties; one pan is empty and (reference) and the other contains the sample. We place the empty pan so that the effect of the pan containing the sample is eliminated so that we only have the sample behaved with temperature difference. The reference pan is held empty. Small holders contain either the sample or the reference material. The holders are placed in an adiabatic environment as shown in Figure 2.19. The temperatures of the holders are monitored using thermocouples, while the electrically supplied heat keeps the temperature of the two holders equal. The computer plots the difference in heat output of the two heaters against the average temperature. By using this graph, one can find the thermal transition temperature such as (Tg) and the melting point of the composite. The enthalpies which correspond to the crystallization and melting peak can also be calculated.

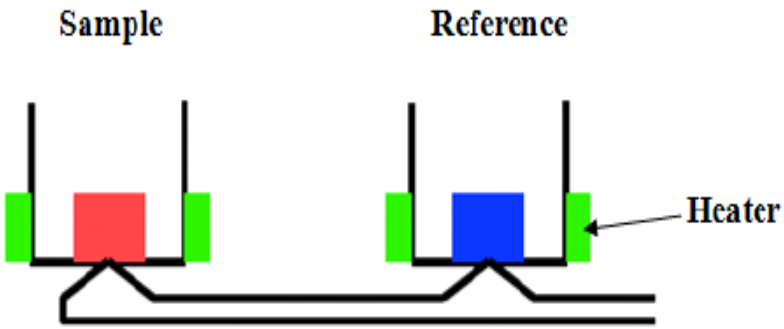


Figure 2. 19. Schematic of Differential Scanning Calorimetry

The DSC measurements are able to provide information on exothermic or endothermic reactions of polymers. This information can be quantitative or qualitative. The DSC curve provides many information that can be seen in the Figure 2.20. The melting points of the polymer can be observed in the DSC curve because

the melting polymer absorbs heat. The degradation of the polymer can be observed because the polymer releases heat. An area can be observed in the DSC curve called crystallization temperature (Tc), which comes after the glass transition due to the polymer's acquisition of sufficient energy capable of displaying or destroying the crystal form. Since the polymer melting process is an endothermic process, we can observe the area beyond the melting temperature (Tm) in the DSC curve as an endothermic peak. The area before the melting point is the area where the polymer releases heat (exothermic peak) in order to transform from amorphous solid to a crystalline solid.

Three pieces are taken from different locations of each sample to take an accurate look at the changes that occurred during the temperature change. The experiment is conducted in the presence of nitrogen and is initially from room temperature to 220 degrees at a rate of 10 °C/min. The sample weight is approximately 3-8 mg. A METTLER Instrument 2 DSC type device is used for testing the Differential Scanning Calorimetry (DSC). See Figure 2.21.

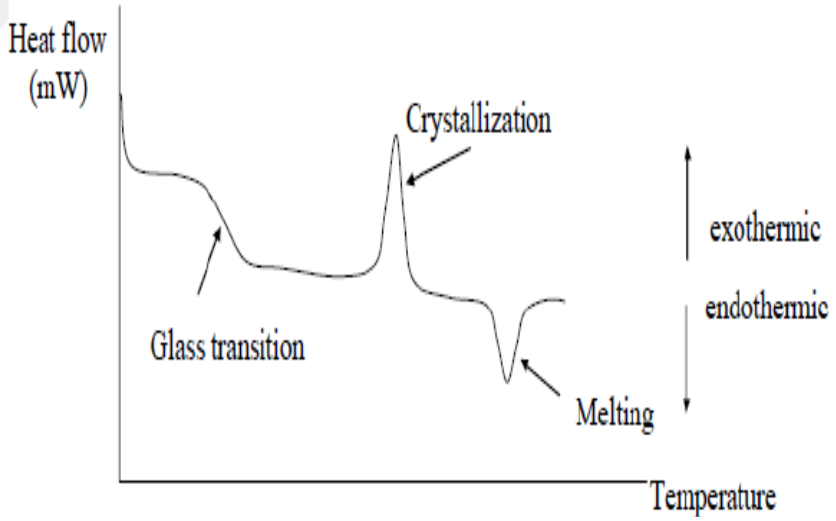


Figure 2. 20. Schematic DSC curve demonstrating the appearance of several common features [44]

The Glass transition (Tg) from heating data for the first cycle is determined. The melting temperatures (Tm) and crystallinity is also determined from the same heating data. See Figure 2.22.


Figure 2. 21. Differential scanning calorimetry – METTLER 2 DSC used in measuring thermal characteristics of sample

The percent crystallinity (%XC) is calculated according to Equation 2.10. by using the DSC curve of the first heating cycle:

$$\%Xc = \frac{\Delta Hm - \Delta Hc}{\Delta Hm * \phi} \times 100 \quad (2.10)$$

Where:

ΔHm is the melting enthalpy (J/g) ;

ΔHc is the cold crystallization enthalpy (J/g) ;

ΔHm* is the melting enthalpy of 100% crystalline PLA (93 J/g) [213] ;

ϕ is the fraction of PLA in the composites.

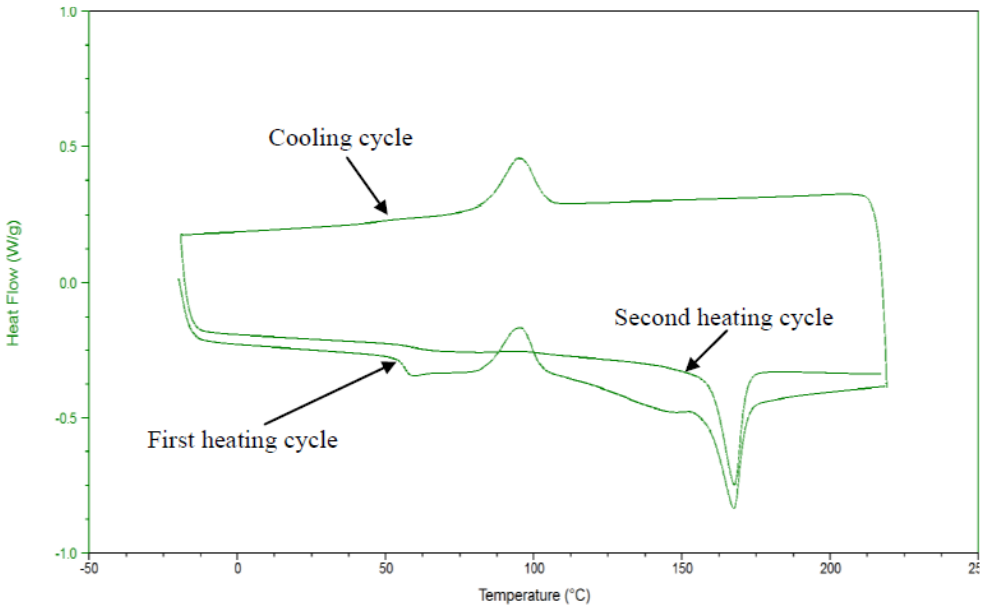


Figure 2. 22. A typical DSC curve of first heating, cooling and second heating cycle [44]

### 2.8.3.2 Thermogravimetric analysis (TGA)

A METTLER instrument, 3-TGA type device, is selected to analyze the Thermal degradation characteristics of the composites. The weight of the measured sample is between 3-8 mg.


Figure 2. 23. Thermogravimetric analysis 3-TGA used in measuring thermal characteristics of sample

The experiment is conducted in the presence of nitrogen and the starting temperature is 30 to 900°C at a rate of 20°C/ min. See Figure 3.23. Which shows a TA instrument for TGA analysis of the materials. Thermogravimetric (TG) curves of the material are obtained from the TGA testing. The TG curves indicate the thermal stability of the materials.

### 2.8.4. Water absorption testing

To determine the amount of water absorbed by the composites, ASTM D570 water absorption test is selected. The cut samples to the required dimensions (100 mm × 100 mm × 40 mm) are placed in a vacuum oven for drying. The drying time is 24 hours at 70 ± 2 °C. Samples are weighed immediately after drying and are considered as the initial weight ($m_1$). The samples are submerged in distilled water containers for 45 days at 23 ± 2 °C. The amount of distilled water in each container is calculated as 300 ml to prevent the concentrated of any material in the container. See Figure 2.24.

Figure 2. 24. Water absorption measurements

During the immersion period, the samples are weighed every 5 days to calculate the amount of water absorbed. Samples are removed from the containers and then dried with tissue to remove excess water and weighed as ($m_2$). The weight is calculated as an average value of three weights for every sample. The amount of water absorbed is calculated according to the following Equation 2.11.

$$C = \frac{m2-m1}{m1} \times 100\% \quad (2.11)$$

Where:

C is the percentage by mass of water absorbed;
$m_1$ is the mass of the test specimen after initial drying and before immersion (mg);
$m_2$ is the mass of the test specimen after immersion (mg).
Fiber volume fraction can be defined as,

$$Vf = vf / vc \quad (2.12)$$

Where

vf = volume of fiber;
vc = volume of composite.
Now that

vf = volume of fiber; vc = volume of composite; vm = volume of matrix;

Vf = Fiber volume fraction; Vm = Matrix volume fraction.

Fiber volume fraction of laminates is measured from fiber mass, fiber density, composite mass, and composite density. Fiber weight is measured after drying; composite weight is measured after Cooling to room temperature. Fiber density is known from literature and composite density is measured.

### 2.8.5. Fourier transformed infrared (FTIR) spectroscopy

The chemical characteristics on the surfaces of jute/PLA ecosheet before and after treatments are studied by using FTIR spectroscopy analysis in the attenuated total reflectance (ATR) mode by using Perkin Elmer spectrum 100 FTIR spectrometer coupled with the smart ATR accessory. The range of IR wavelength in which the samples are measured is from 650 to 4000 cm-1.

### 2.8.6. Surface morphology testing

After the flexural, tensile, and impact tests, the tested samples are taken and their surface and fracture surface are examined by a Scanning electron microscope (SEM) device. SEM device gives us an accurate analysis of the morphology of the sample surface; the impact of the tests on the matrix and fibers; and the effect of chemical treatment on the sample.

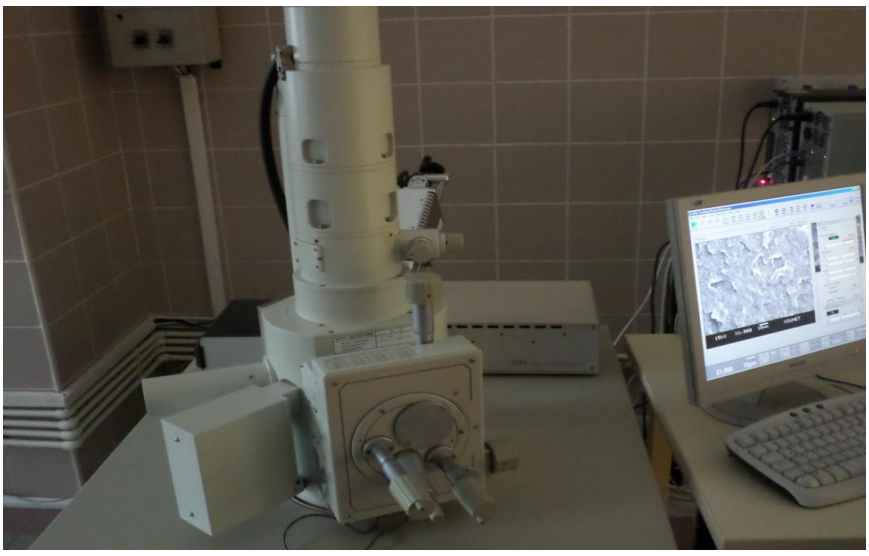

Figure 2. 25. Edwards coating system, E306A, USA (a), Scanning Electron Microscope, Philips XL30 (b)

A JEOL JSM 6060 model, scanning electron microscope SEM, microscope device is used to inspect the composite samples. Figure 3.25. Shows the SEM equipment used in this work. The samples are coated with a thin layer of carbon by using an Edwards E306A sputter coater device. The coating take place to increase the conductivity of the sample surface.

The operation condition of the microscope is set at an accelerating voltage of 5.00 kV. For each specimen, images with 4 different magnifications of 50, 100, 200 and 500× are used. Smaller magnifications are more useful to understand the dispersion of the plant fibers into the polymer matrix, while increasing the magnification helps to observe the interface of fiber and matrix.

### 2.8.7. Flammability testing

#### 2.8.7.1 Limiting oxygen index (LOI)

To measure the flammability of the composites, a Limiting oxygen index test is selected. LOI test works by measuring the minimum amount of oxygen sufficient to create a flame such as that of a candle in the composites. The amount of oxygen is determined by a mixture of oxygen and nitrogen gas. The percentage of oxygen volume is calculated and from it the LOI [13,14].

As described in ISO 4589-2, a bar shaped specimen, sized 57 mm x 10 mm with the thickness of 4 mm, is ignited at the top of specimen by using an ignition gas flame which is withdrawn from the specimen once the ignition of specimen occurs. The burning time of the ignited specimen at different oxygen concentrations is recorded in order to determine the minimum oxygen concentration that the specimen requires to sustain burning for at least 3 min. after the removal of the ignition flame [14].

According to the above method, the samples are cut to the required standards ISO 4589. The dimensions are 10 mm width and 57 mm long.

#### 2.8.7.3. UL-94 test

UL-94 is one of the most commonly used flammability test, especially in industrial applications, for determination of the burning behavior of materials in terms of ignitibility of materials when exposed to a 20 mm height small flame by giving

classification of V-0, V-1 and V-2 by using UL94 vertical burning test (details are discussed below).

### 2.8.7.4. Vertical burning test

The Vertical burning test is prepared by placing the cut sample (57 mm x 10 mm x 4 mm) vertically and marking the sample to determine the amount burned and the burning speed (five marks are selected at every 10 mm in the sample). A Bunsen flame is placed 10 mm away from the sample and a layer of cotton is placed 300 mm away from the sample to study whether the burned, fallen parts (drops ) is burning the cotton or not. See Figure 2.27.

The experiment is carried out in two phases. In the first stage, the flame is shed from the bottom of the sample for 10 s and then the flame is removed and the time noted (t1). If there is no burn or if the sample does not burn completely, we continue to the second stage. The second stage is to shed the flame for 10 seconds from the bottom of the sample and then removed it (t2).

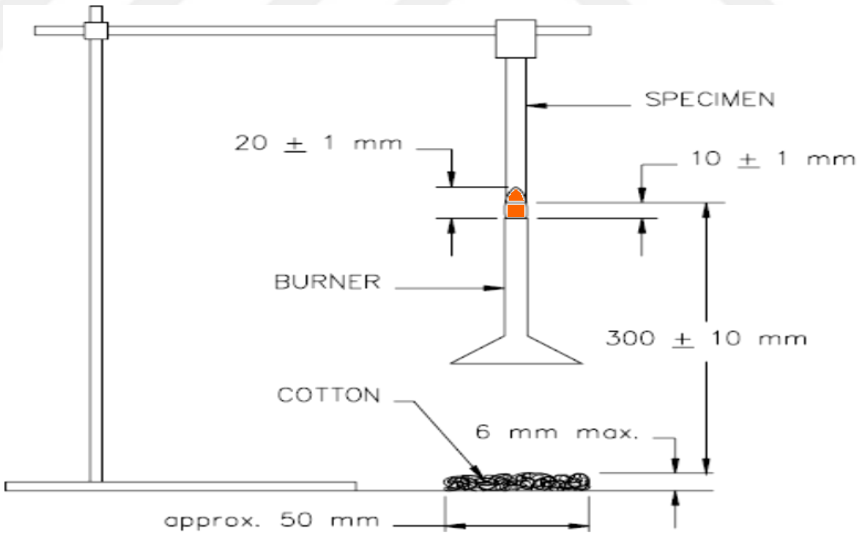


Figure 2. 26. The schematic of UL-94 vertical burning test [15]

If there is burnt residue, then it will be taken into consideration whether the cotton is ignited or not. If the sample is completely burned or if the burns continues for more than 30 seconds, the sample is considered to be a failure. If ignition is less than 30 seconds, the sample is classified according to the table below. See table 2.6.

Table 2. 6. Criteria of UL-94 vertical rating classifications [15]

| Classification | Vo | V1 | V2 |
|---|---|---|---|
| T1 | <10 | <30 | <30 |
| T2 | <10 | <30 | <30 |
| T1+ T2 | <50 | <250 | <250 |
| T2+T3 | <30 | <60 | <60 |
| Cotton ignited by burning drips | No | No | Yes |
| Afterglow or afterflame up to the holding clamp | No | No | No |

In this work, the burning times when the flame reaches each timing mark of the specimen are also recorded. Since the length of the burnt sample is known, the vertical rate of burning of the materials can be calculated.

### 2.8.8. Dynamic mechanical analysis (DMA)

The Dynamic mechanical analysis (DMA) device is one of the most important instruments for measuring the viscoelastic and morphology properties of polymers. The device is capable of analyzing many properties in crystalline polymers which are important properties such as storage modulus, dynamic fragility [215], crosslinking density [214], stress–relaxation modulus and storage/loss compliance. The dynamic modulus (storage modulus (E′)) is closely related to Young's modulus. These characteristics express the stiffness of the material and show whether the material is stiff and brittle, how much energy is applied to the polymer, or how much energy the polymer can store. The characteristic of the Loss modulus (E″) expresses many transformations that can occur within the sample such as the molecular motions, morphology, relaxation process, internal friction and other types of sensitive changes. The Loss modulus (E″) is a measure of viscous response of internal materials and the ability of the material to distribute the energy applied on it [127]. Thermomechanical properties of the samples are analyzed by dynamic mechanical analysis (DMA) (Metravib 01 Db DMA50 instrument). The frequency was 1 Hz, heating rate is 3 _C/min, and the scanned temperature range is 25–150 °C in flexural mode. Storage modulus and tangent delta curves are obtained from the DMA analysis.

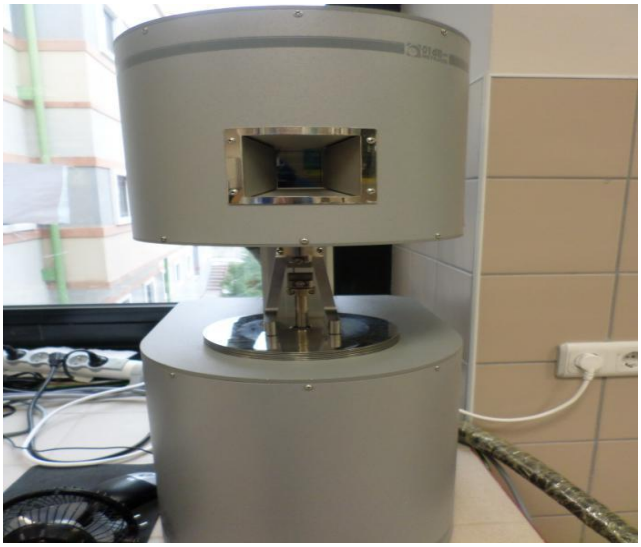

Figure 2. 27. Dynamic mechanical analysis DMA

There is also an important feature that can be obtained from the DMA which is the tan δ. Tan δ expresses how elastic the composite is; in other words, the tan is the ratio between loss and storage modulus (Tan δ = E″/E′). The mechanical damping factor is a dimensionless number. See Fig. 3.29. In Fig. 3.30. You can see in DMA graph the relationship between Tan δ, storage and loss modulus. When tan δ is high, this means that the composite has non-elastic strain component.

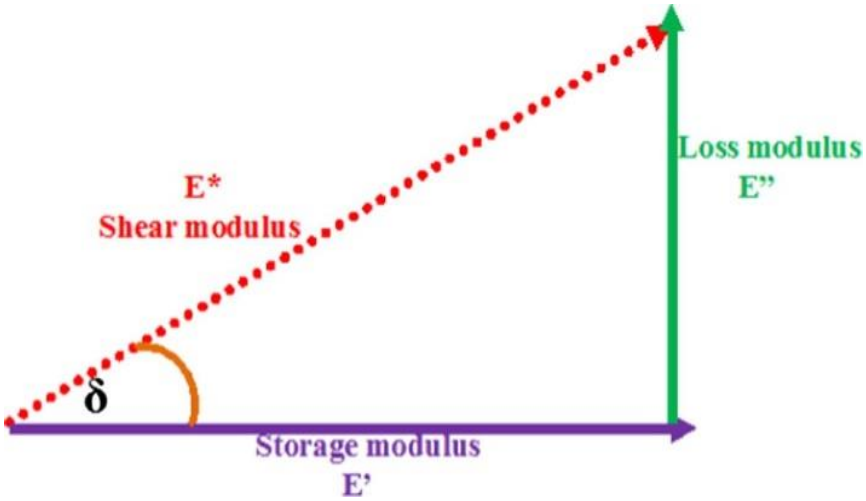


Figure 2. 28. The mechanical damping factor defined as the ratio of loss and storage modulus [203]

The second case, if tan δ is low, it means that the composite is elastic. In the case of increasing the percentage of fibers inside the composite, it will lead to a reduction in the interface bonding of the fiber/matrix. This decrease leads to a decrease in the value of energy loss according to the storage capacity because of the lack of mobility

in interface bonding between the fibers/ matrix which make Tan δ (E″/E′) value greater in the system. There are many factors affecting the damping factor, including the molecular movements of the composite, the presence of defects, cracks and phase boundaries [118].

Some researchers have been conducted on the dynamic mechanical properties of natural polymers reinforced by natural fibers. A table of these studies has been made below (see Table 2.7.). All these studies show an increase in storage modulus as the percentage of fiber in the composites increased.

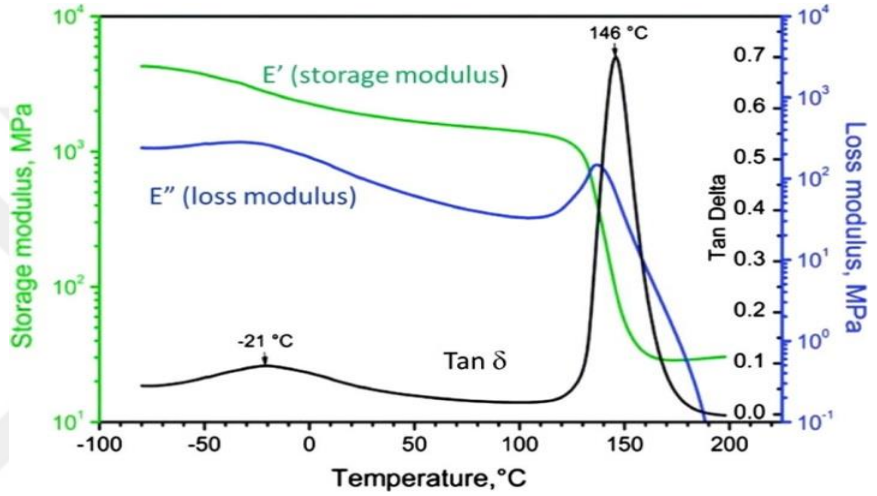


Figure 2. 29. The relationship between loss, storage modulus and Tan δ in the DMA graph versus temperature [203]

This increase is likely to be due to improving in the interfacial adhesion, which acts as a plasticizing agent for the composite, facilitating the transfer of energy applied to the composite. It is also observed that twill woven fibers have a higher storage modulus than plain woven fibers.

Table 2. 7. The reported work on the study of dynamic mechanical analysis of natural fibers based reinforced bio-polymer composites

| Reinforcement | Matrix | Refs. |
|---|---|---|
| Modified jute fiber | Biopol | [59] |
| Kenaf fiber | Poly (lactic acid)/Thymol | [60] |
| Woven hemp fiber | Poly (lactic acid) | [61] |
| Short ramie fiber | Poly (lactic acid) | [62] |
| Wood-fiber | Poly (lactic acid) | [63] |
| Cotton stalk bast fiber | Poly (butylene succinate) | [64] |
| Mercerised kenaf fiber | Poly (lactic acid) | [21] |
| UD* and twill 2/2 Flax fiber | Poly (lactic acid) | [20] |

* Unidirectional (UD)

### 2.8.9. Heat deflection temperature (HDT)

Heat distortion temperature' (HDT) is one way to study the bear ability of polymer at elevated temperatures to a given load. Usually there are two weights used in this test: 0.46 MPa and 1.8 MPa. The ASTM D 648 standard method that corresponds to the ISO 75 Method B standard method is used in this study. The figure below shows the test geometry.

ASTM D648: The deflection temperature is the temperature at which a test bar, loaded to the specified bending stress, deflects by 0.010 inch (0.25 mm).

The value that obtained from the experiment depends on two important factors. The origin of the polymer or matrix, the presence of fibers in the sample and the amount of these fibers. The presence of synthetic or natural fibers leads to raise in the deflection temperature of the composite and it can approach the melting point of the matrix.

This test is a short-term test and should not be relied upon only in the design of the composite, because there are other factors affecting the composite such as the time of exposure to temperature, the geometry of the composite and the rate of temperature increase.

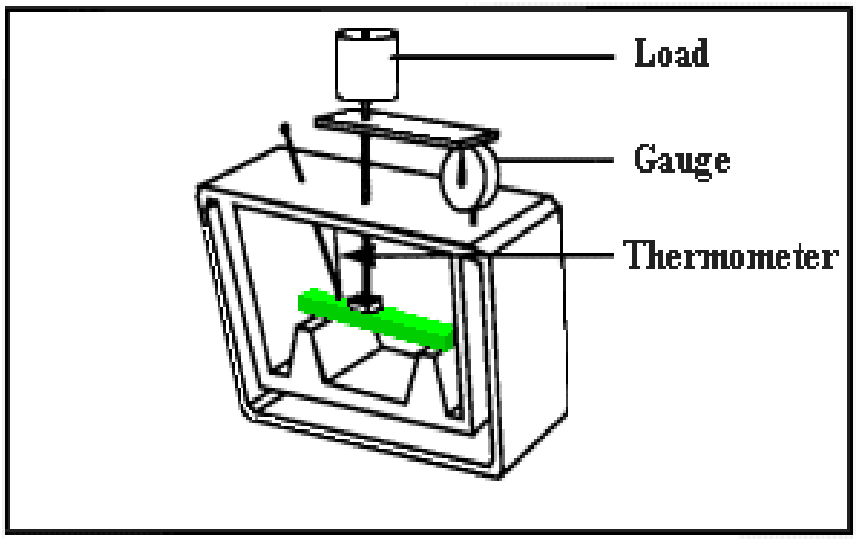


Figure 2.30. Heat Distortion Temperature (HDT)

On the other hand, this test is suitable to determine the appropriate temperature tolerated by the polymer under a certain load especially in load-bearing parts.

## 3. RESULTS AND DISCUSSIONS

This chapter is related to physical, mechanical and thermal properties of PLA, jute fiber, eco-sheets, and overmolded composite materials.

Table 3. 1. The Physical and Mechanical Properties of Jute [131]

| Fiber type | Physical properties | Mechanical properties | | |
|---|---|---|---|---|
| | Density (g/cm3) | Tensile strength (MPa) | Elongation at break (%) | Young's Modulus (GPa) |
| Jute1 | 1.46 | 393-800 | 1.5–1.8 | 55 |
| Jute2 | 1.44 | 393–773 | 1.5–1.8 | 10–30 |

The mechanical properties of jute are measured, including the tensile strength where two types of jute are measured: single jute thread (Jute 1) and woven jute (Jute2). The results show that the tensile strength of the Jute 1 is less than the tensile strength of the Jute 2 due to the presence of many defects in the single jute yarn compared to the woven jute as expected. There are three main factors that control jute strength: the diameter, number and size of defects, and the angle of twisting in the thread [131]. Bonding in jute fibers is usually due to the presence of weak pectin. Therefore, the larger the gauge length, the more likely to failure at the interface under at lower stress.

### 3.1. Properties of Ecosheets

The density of the ecosheet is measured using British standard, the inundation method. Figure 4.1. Shows the density (mass per unit area) in g/cm³ for all measured samples. It can be observed that the greater the amount of fibers in the ecosheet increased the density. It may be because of an increasing of jute fiber weight percentage. The fiber densities of PLA and jute are 1.48 g/cm$^3$ and 1.32 g/cm$^3$ [131], respectively. It can be seen that the density variations among the samples having different orientations are very small.

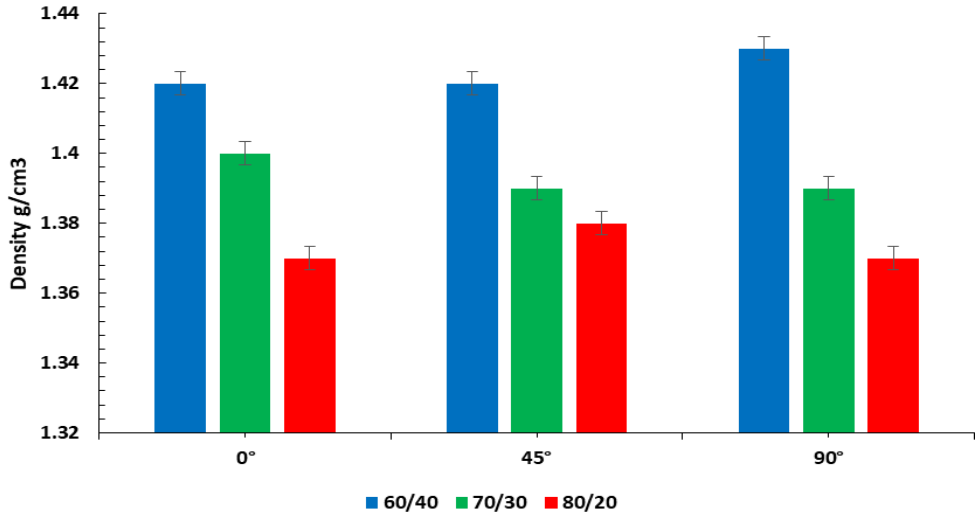


Figure 3. 1. The Density of Ecosheet

For the flexural (bending) properties of the ecosheets samples compared to the neat PLA, the flexural strength and flexural modulus are tested. The flexural modulus is the measure of the ecosheets resistance to deformation in bending. Figure 3.2. Shows the results of the flexural strength of ecosheets samples compared to the neat PLA. The results indicate a 4 times higher bending strength in the ecosheets than neat PLA (363 ± 26/90 ± 5 MPa). As for the bending coefficient, the results in Fig. 3.3. Show that the bending coefficient is 7 times higher in ecosheets than the neat PLA (26 ± 2.2/3.4 ± 0.27 GPa).

The flexural test relies on the focusing on the outer layer of the composite rather than the middle layers. PLA film's surface is subjected to more tension because it is farther from the neutral axis of sample. These conclusions mean that the thicker the polymer layer, the greater the tension on the sample; in other words, the closer the jute fibers to the surface, the less tension in the sample. That is because the thickness of the PLA layer increases, small defects increase, and any small deformation can grow under stress until it reaches a sudden collapse of the layer. PLA film's surface is subjected to more tension because it is farther from the neutral axis of sample. These conclusions mean that the thicker the polymer layer, the greater the tension on the sample; in other words, the closer the jute fibers to the surface, the less tension in the sample.

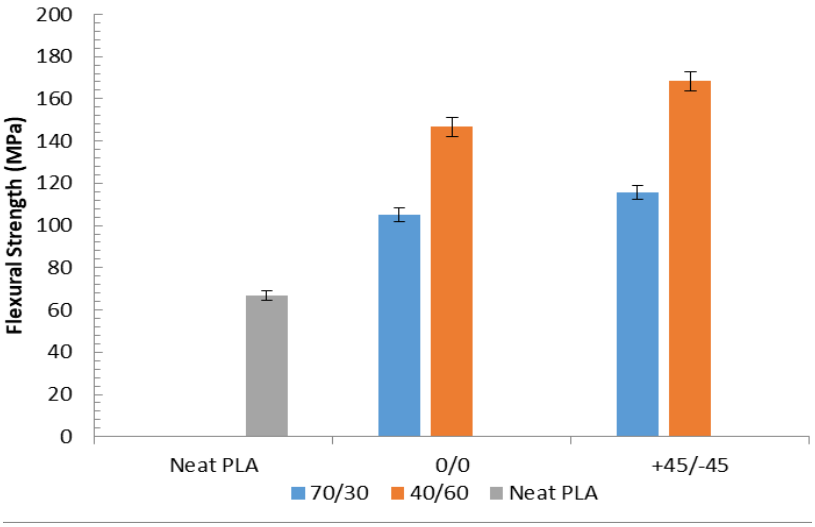


Figure 3. 2. The Flexural Strength of PLA/Jute Ecosheets

This explains the variability resulting at this stage. Ecosheets with 80/20 % have a greater amount of PLA, and therefore, are more likely to be more stressful and consequently, lower tensile strength. On the other hand, we can notes that ecosheets with 70/30 and 60/40% have more tensile strength; see fig 3.2. The flexural strength and flexural modulus are controlled by controlling the extreme layers of reinforcement. The ecosheet is compressive on the upper surface side and under tensile mode on the bottom side during the flexural test [71].

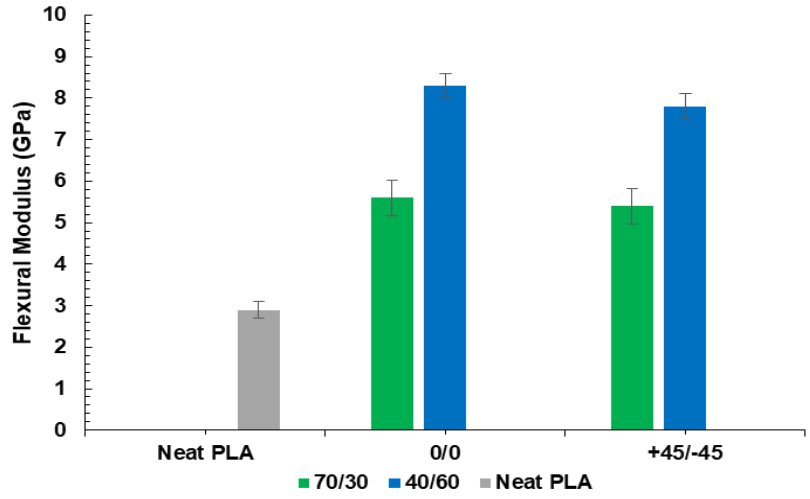


Figure 3. 3. The Flexural Modulus of PLA/Jute 45˚ Ecosheets

The average flexural strength and flexural modulus of untreated ecosheet in 45$^{o}$ direction are found to be 95.2% and 42.4% higher than the 0$^{o}$ direction. Fibers look shorter in this direction because these fibers are monolithic in the same direction. Another reason is that there is not enough length or fiber compensation as in 45$^{o}$

direction, and therefore, the short yarns in 0° direction of composite limit their tensile stress dispersion. Therefore, as the tensile stress tries to propagate upwards, delamination failure occurs, thus, reduces its flexural strength [72]. It is also seen that the flexural properties of 45° ecosheet are higher than those of 0° and 90° ecosheet because of the angle; this 45° direction of the sample makes the fibers look longer and this gives them more freedom in movement and supports the matrix which is exposed to pressure and make it stronger. Under tensile loading, these crimped fibers tend to be straighten out, which create high stresses in the matrix. As a result, the strength of the 45° is greater than the strength in 0° and 90° composite. In addition, in the 45°, it is very difficult to displace this layers, but in 0° and 90°, the dislocation or slip is easier, which explains the increase in flexural properties of 45° ecosheet compared to 0° and 90° composite; see figs 3.2. And 3.3.

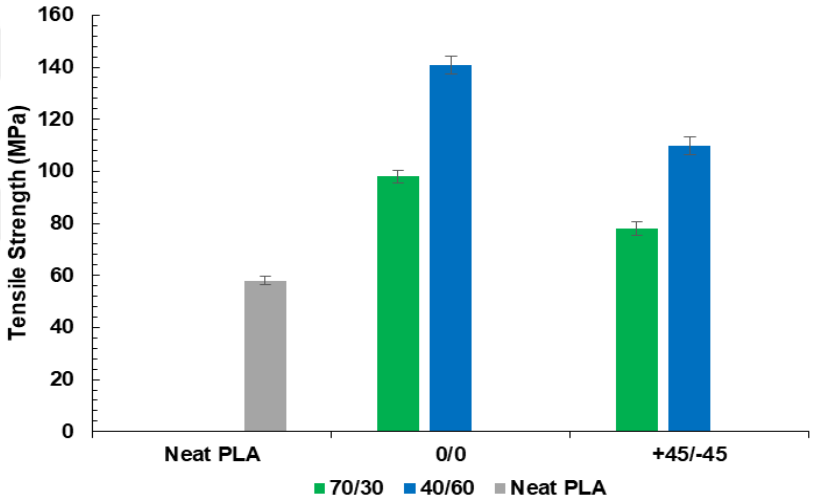


Figure 3. 4. The Tensile Strength of PLA/Jute Ecosheets

The tensile modulus value is determined by calculating the slope of the initial portion of the stress–strain curve. Significant increases and improvement in tensile strength and tensile modulus are observed for the PLA enhanced by untreated woven jute fiber. The results for 0° direction show that they increase by 102.5% and 211.1% respectively. For samples with a 45° direction, they increase by 77.5% for tensile strength and by 105.6% for tensile modulus higher than neat PLA samples. For untreated WJF/PLA composite samples in 0° direction, the strains at maximum tensile stress is 3.8%; for 45° direction it is 4.1%. It has been noticed that tensile strength and tensile modulus of untreated WJF/PLA composite are higher in 60/40 than 70/30. This is not the case for the elongation at break. Due to the overlap

sections of crimped fibers in woven fabric composite, when applying tensile stress to the sample, this overlap reduces the speed of energy transfer in the composite and obstruct the fiber attempt to be straightened. This affects the strength of composite in long-term or under creep rupture performance [29]. These differences depend on the density of fibers in the composite. The reason for the difference in WJF is that there are more fibers in the warp direction more than the weft direction. These fibers in the warp direction cause increased performance in the composite exposed to stress in the weft direction. It is noted that the tensile stain is higher in the warp direction. The reason for this is that in a single layer warp woven composites, the yarn can significantly elongate during the tensile test. The difference of yarns orientation causes a difference in tensile stain values (see Fig 3.4).

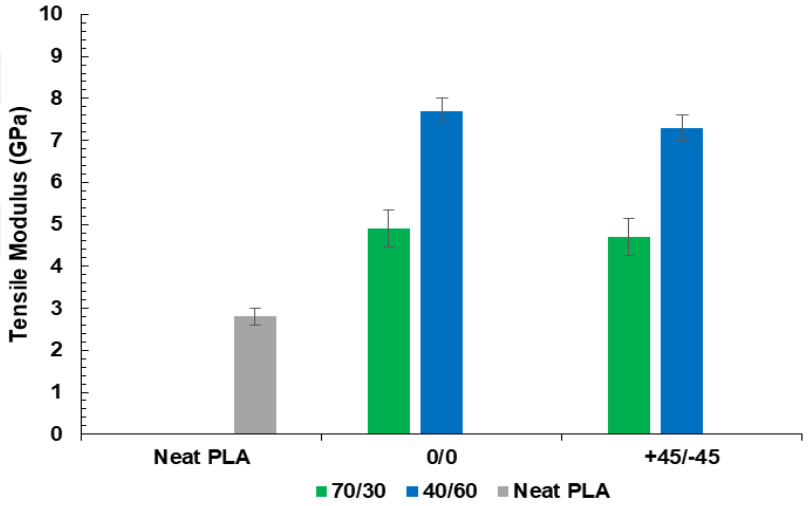


Figure 3. 5. The Tensile Modulus of PLA/Jute Ecosheets

From Figure 3.5. It has been observed that the ecosheet is affected as the fiber orientation increases. In jute fibers, the more defects and cracks, the weaker the fibers during tension test and strain rate. For woven jute, stacking and cohesion in jute fibers reduce these defects and make the fabric strengthen each other, which is a positive feature. But the presence of voids and non-cellulosic materials directly affect the strength of the fibers and this will be treated in the next stage, the stage of chemical treatment of jute fibers. In the case of composites, the presence of PLA polymer interfering with the fibers enhances the consistency and adhesion of jute fibers. This is the principle of the composites where the presence of different

materials changes the properties of these composites. The decreased tensile strength value can be explained by defects presence in both the matrix and the fibers.

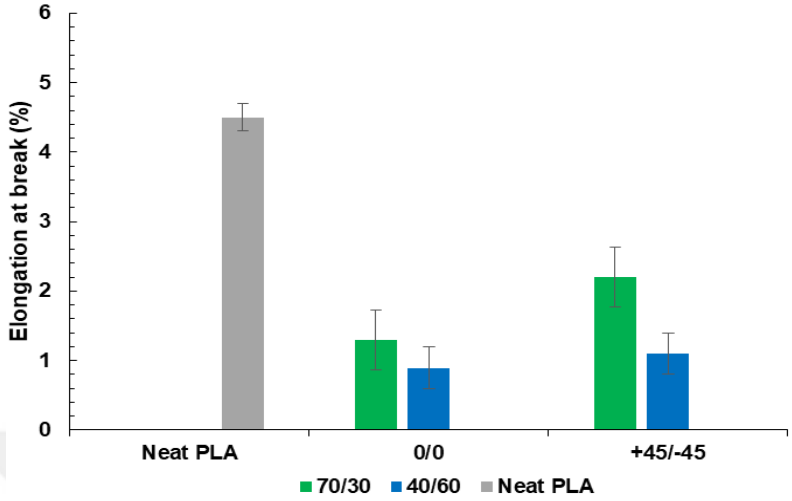


Figure 3. 6. The Elongation at Break of PLA/Jute Ecosheets

The tensile strength of the 45° angle samples is similar to the 90° angle samples, both of which are significantly lower than the tensile strength of the 0° angle samples. The lower tensile strength of the ecosheet (45° and 90°), can be explained by the fact that at these angles, the greatest influence on the sample is the homogeneity of fibers and matrix in this angle. The presence of defects and voids will lead to a greater impact in the angles (45° and 90°) than in the angle 0° because the different angle of fibers leads to weak strength of composite [18, 19]. These defects usually occur in the manufacturing stage and are concentrated in the fusion areas between the matrix and the fibers [20, 21]. We can summarize the result as: the tensile strength experiments of the 90° direction and 45° direction composites samples are significantly lower than the 0° direction samples. This made the maximum fiber strength efficiency inaccessible [22, 23]. The increase in tensile strength of 0° direction samples can be explained because the two main factors are the strength of jute fibers and the weakness of the PLA matrix strength which control the tensile strength, and this can be clearly seen in the fracture morphology. For +45/-45° composites, the biggest factor which controls the tensile strength is longitudinal of the fiber in the composite. For the case of +45/-45° composite, the strongest control over the strength of the composite is the strength of the area where the fibers join together with the matrix. As mentioned earlier, these areas have many defects which make the tensile strengths

in longitudinal directions weak. For the elongation at break of the +45/-45° composite, it is higher than those of 0° composite. For the composite with 0° direction, the defects in the fiber matrix interface become large and their resistance disappears due to the absence of fibers in another direction. For +45/-45° direction composite, these fibers act as resistors (source of resistance) and allow better energy distribution, which makes the elongation at break value higher than 0° direction (see Fig 3.6.).

The Dynamical mechanical analysis (DMA) test is performed to verify the hypothesis that the addition of jute fibers will improve the thermo mechanical properties of the ecosheet such as the maximum use of PLA temperature and the possibility of interaction between the matrix and jute fibers. The PLA is usually an amorphous but it can be considered as semi-crystalline. A DMA test is placed on the 3-point bending mode to study the internal changes of the composites.

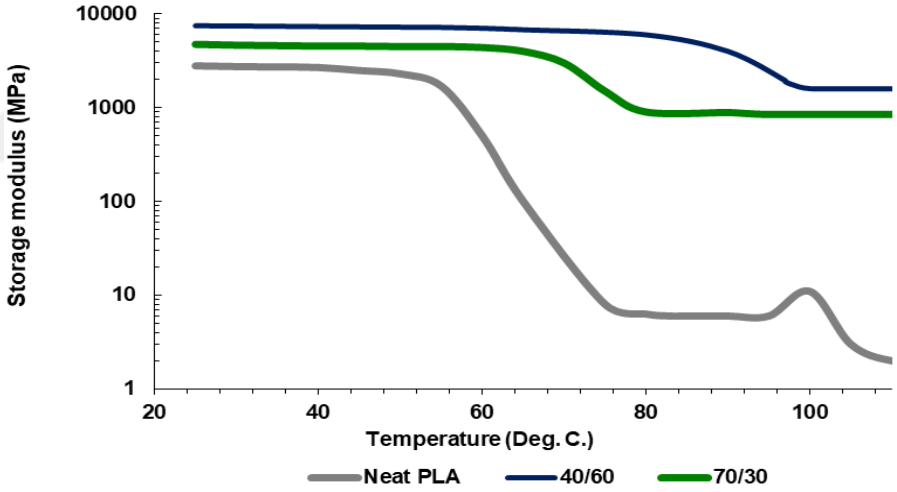


Figure 3. 7. Storage Modulus of PLA/Jute 45˚ Ecosheets

Crystallization usually occurs at a temperature between 80–100°C. Fig 3.7. Shows the storage modulus and Fig 3.8. Shows the tan delta curves of the PLA/jute ecosheet composites. We can clearly observe in Figure 3.7. That the thermal properties of PLA increase with increasing the percentage of jute fiber. The pure PLA begins to soften at 55°C degrees, but with the addition of jute, it rises to 60°C and it continue to increase if the composite is crystallized. The composite begins to soften at 68°C but we observe an increase at 80°C in modulus. This can be explained by the cold crystallization effect [15]. The curve of the ecosheet sample 70/30% shows very

good thermal properties but the 60/40% samples are much better. Fig.3.8. shows tan delta for PLA as well as 70/30% and 60/40% composites. The tan delta peak is changed due to the addition of jute and it is very much affected by the crystallization. The peak of 70/30% is slightly changing, broadened, and is also very low compared to neat PLA sample. The thermal properties of 60/40% are increased which is even expected because of the quantity of fiber. The addition of fibers and crystallization increases the softening temperature. In tan delta curves, the addition of fiber decreases the tan delta peak high but it changes it to a higher temperature from 63°C to 55°C for 60/40. The addition of fiber results in increased tan delta temperature for all ecosheet composites compared to neat PLA. Tan delta increases from 55°C to 70°C which indicates some kind of interaction effect between the fibers and PLA due to the cohesion. Further, the peak moves to higher temperatures and is also broadened for cold crystallized sample. Higher values for the damping factor tan are obtained for the 60/40 % composites tested at direction 45° intermediate values for 70/30 % at 45°, and minimum values for neat PLA.

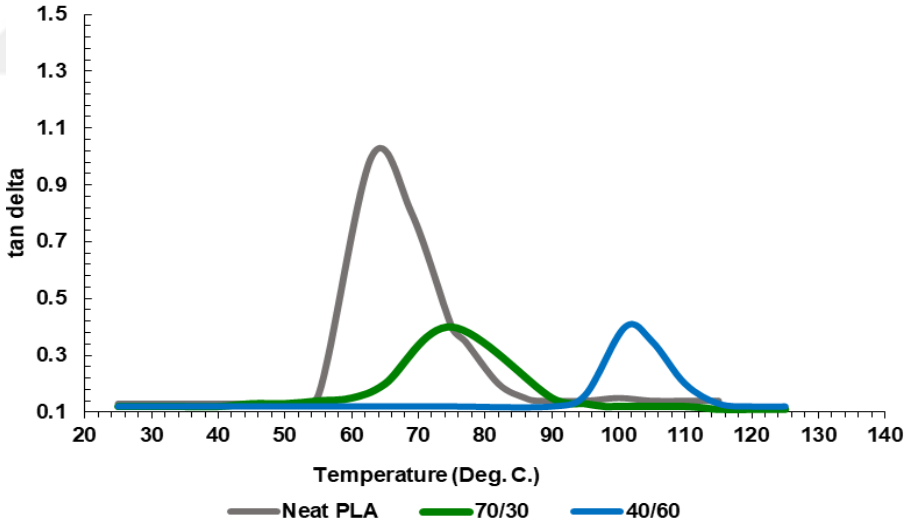


Figure 3. 8. Tan Delta of PLA/Jute 45˚ Ecosheets

Fig. 3.9. Shows the fracture surface of the PLA/jute 45° composite. It is possible to see the good polymer penetration through the fibrils but with poor adhesion to the interface. Further, Fig. 3.9 shows that the fracture surfaces of the composites showed fake ductile behavior due to the shearing effect of the 45° laminate. The Jute fiber and the PLA matrix share the stress together but because the fiber is stronger than the PLA, thus, the fiber is pulled out.

SEM of PLA/jute tensile specimen fracture surfaces are shown in Figs. 3.10. The brittle nature of the jute fiber fracture is clearly seen and is quite different in appearance from cases where, for example, jute is embedded in PLA, and much more fiber pull-out generally occurs. As with the tensile test results, this is suggestive of a better interface between fiber and polymer; but Figs. 3.9. And 3.10. In particular also show that gaps in the fiber/polymer interface can arise either as a result of manufacturing or during the process of tensile testing. The brittle nature of PLA and its manner of breakage, leaving plate-like areas on the fracture surface, is shown in Figs. 3.10 (right). The typical surface zone of these composites, largely consisting of polymer in the first 50 to 100 microns, is also shown at the top of Figs. 3.10. (Left); as a result, it can be noted that the tensile-fracture surface has good polymer penetration through the fibrils but with poor adhesion at the interface.

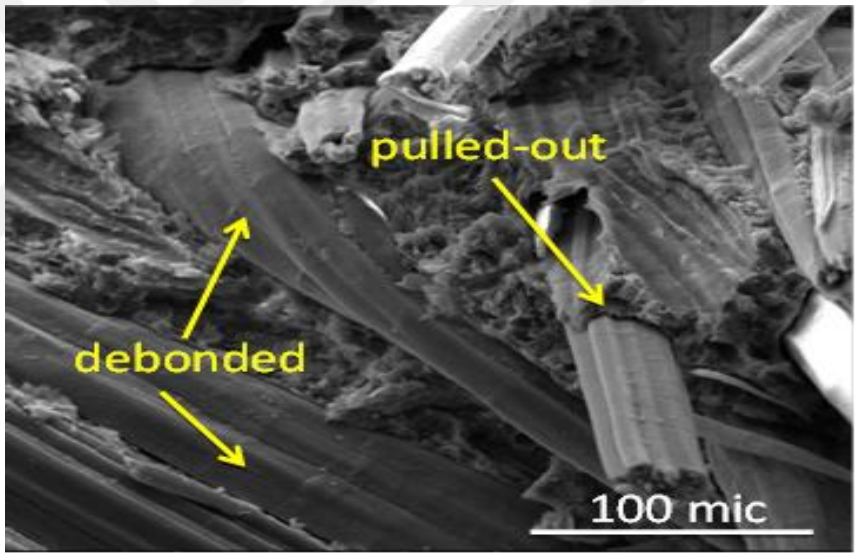


Figure 3. 9. The Flexural-Fractured Surface of PLA/Jute

For 60/40% composites, two-step type of fracture morphology has been observed. At first, deboning at the matrix/fiber interfaces is taken place. Then matrix is broken because of its relatively lower tensile strength. At last, jute fiber having relatively higher tensile strength value is broken. This phenomenon is shown in Fig. 3.10. (Right). As the jute fiber has a high tensile strength, the composite show higher tensile strength in the $0^{o}$ direction.

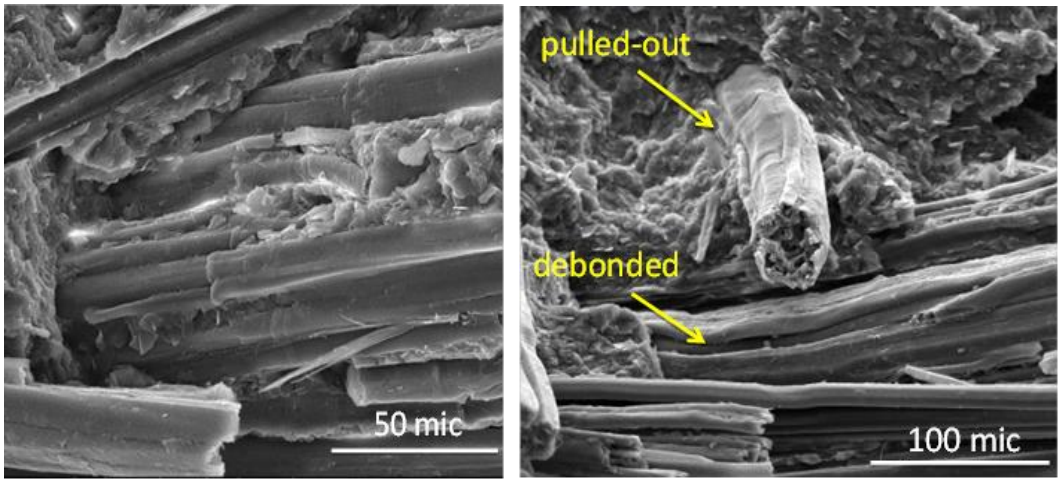


a) b)

Figure 3. 10. Tensile-Fractured Surface of PLA/Jute (a) deboned (b) pulled out

### 3.2. Properties of Overmolded PLA Composites

Depending on the ASTM D1348 standard, moisture absorption is measured by determining the extra weight from the dry weight. We can calculate the weight of the absorbed water (MC, %) using the following equation:

$$\mathrm{WC}(\%) = \frac{Wm-Wd}{Wd} \times 100 \qquad (3.1)$$

Where: WC (%) is the Water absorption; Wm is the moist weight; and Wd is the dry weight. Five samples are tested and calculated. The average is taken for each sample. In general, the phenomenon of water absorption in fibers is affected by the process of fiber extraction; the quality of the soil planted in it; how old the plant is and its maturity; etc. [32]. But the good thing is that it is easy to solve this problem. The result of the treatment process is that the fibers are stronger, more cohesive and have a high porosity. Here the advantage of using these fibers lies in reinforcement of the composites as it adds strength to the composites and yet it is lightweight, biodegradable and sustainable. Various concentrations of untreated jute fibers are added to PLA and then submerged in water and the water absorption behavior is calculated for the composites which presented in Fig. 3.11.

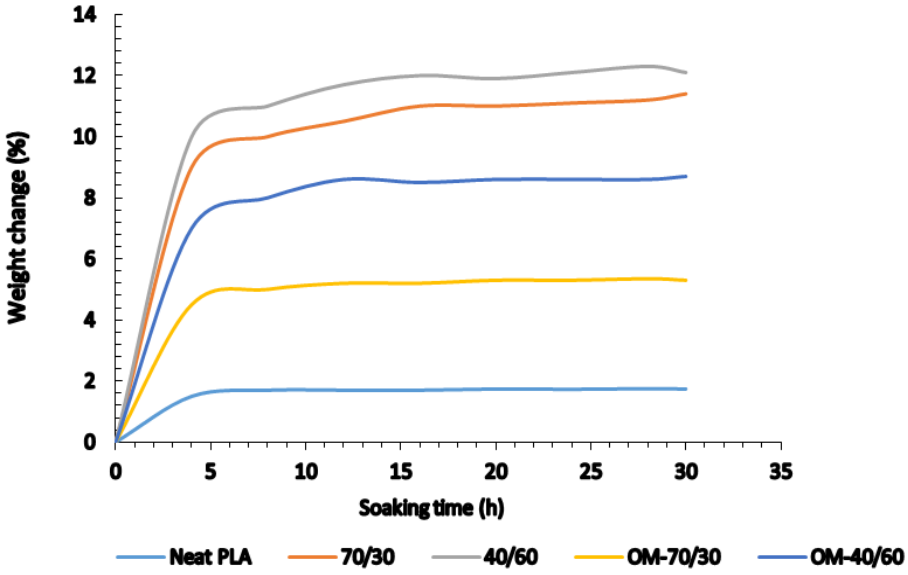


Figure 3. 11. The Water Uptake Of +45/-45 Ecosheets and Over-molded PLA/Ecosheet Composites

The water absorption is measured for pure PLA which is 0.88% after 48 h. This proves the hydrophobic nature of PLA. As for jute fibers, they are hydrophilic because they contain hydroxyl groups, so an increase in water absorption is measured for jute fibers. Because of the different nature of Polymer PLA (hydrophobic) and jute fiber (hydrophilic), the composites are tested and the results show an increase in water absorption during the first 24 hours and then stabilized.

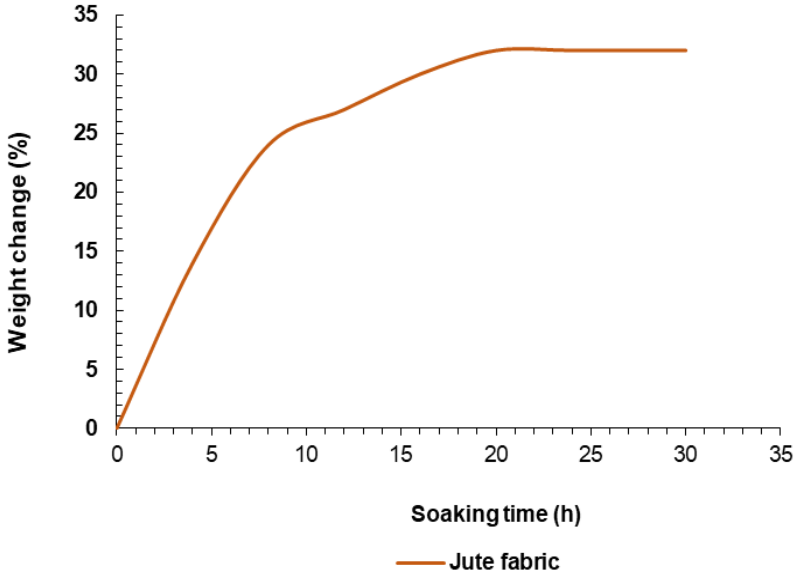


Figure 3. 12. The Water Uptake of Jute

It has been observed that with an increase in the percentage of jute fibers in the composite, the water absorption ratio increases. The highest water absorption of 11.17% is for 60/40 % weight fraction of untreated jute-fibers (Fig.3.11.). Because of the hydrophobic nature of PLA, the main factor causing increased water absorption in composites is jute fibers [210]. Therefore, jute fibers' hydrophilic nature are the cause of increased water absorption in composites.

The results of the density measurement test shows that the density increases with the increase of the polymer ratio. This is normal, especially if we know that the quantity of the polymer layer is app. 50%. The test also shows that increasing the ratio of jute in the compound has a strong effect on the density but not one way. This may be due to the fact that the polymer's ability to penetrate and enter the jute fiber, which reduces the percentage of air spaces and pockets, greatly affects the density. See Fig 3.13.

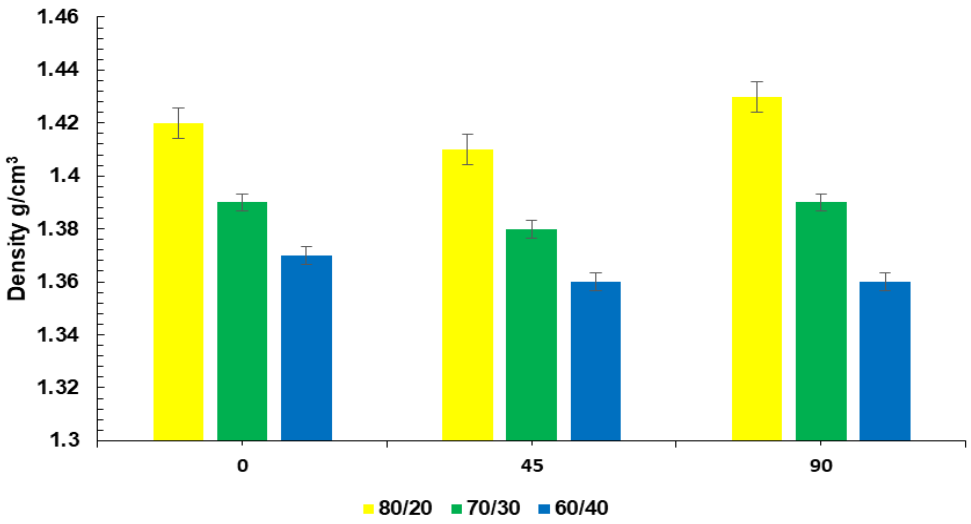


Figure 3. 13. The Density of Over-Molded PLA Composites

The flexural test is useful because it gives us a better understanding of the material that support loads without bending. The test is simple, the sample is placed on a two-support stand and the loading nose is applied at the middle of the sample. These results of the load make a three-point bending test in a fixed rate. Flexural strength is measured in terms of MPa.

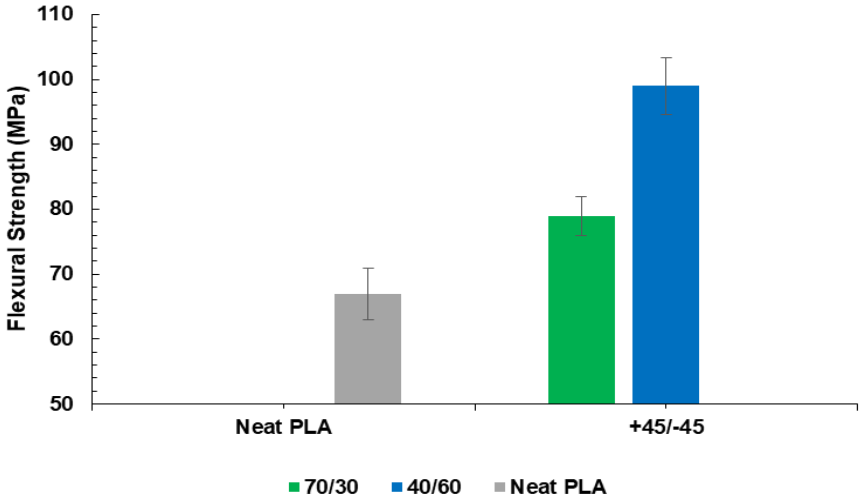


Figure 3. 14. The Flexural Strength of Over-Molded PLA/+45/ 45 ecosheet Composites

The 3-point bend test is selected to determine the flexural properties of the over-molded composites. The flexural strength of 70/30 % at 45˚ and 60/40% at 45˚ orientation is presented in Fig 3.14. In 60/40%, the flexural strength is observed to be higher (61.1 MPa). Laying the jute fiber layers at 45˚ degrees has an excellent effect on the composites; it grants compressive strength and increases the resistance of the composites. It is noted that placing the fibers at in 45˚ increases the flexural strength of the composites. As shown in the figure, the flexural strength is greatly increased in composites that contain 35% fiber weight. The reason for this noticeable improvement is the effectiveness of the interlocking between the fibers, and more importantly, the good adhesion between the fibers and the PLA matrix. With the increase in the content of fibers, it is observed that there is a need for the polymer to wet a greater portion of the fibers in order to be adhered better and to make a sufficient stress transfer [215].

We find that in the case of 70/30%, the fiber content in OM-PLA/70/30 = 20% and in 60/40%; the fiber content in OM-PLA/40/60 = 35%. Therefore, with the increase in the amount of PLA polymer that helped increase the adhesion with the fibers, an increase is observed till it reach the maximum load. A decrease in strength is observed after reaching the maximum load. Perhaps that is because the interaction of the fiber–fiber becomes the main factor more than the interaction of the fibers with the matrix. The flexural strength of the untreated jute fiber composite (Fig.3.14) at

35% fiber loading is better by 24.2% than composites with untreated 70/30 %. This is also 17.5% more than the strength of neat PLA.

As is known, the three point bend test affects the sample in two different ways, where the tensile stress is applied to the bottom of the sample and at the top of the sample (compressive stress). Most of the sample failure are at the top of the additional polymer layer. From the extrapolation of the articles, it is revealed that interaction of the fibers at an angle results in a reduction in the load carrying [218,210]. The reason for this is the presence of direct load and damage transfer mechanism. However, with the +45/-45 orientation, this is not the case because the adhesion between fiber and matrix is strong and the presence of the over-molded PLA layer is the important reason for the increase in the flexural modulus of the samples. See Fig 3.15.

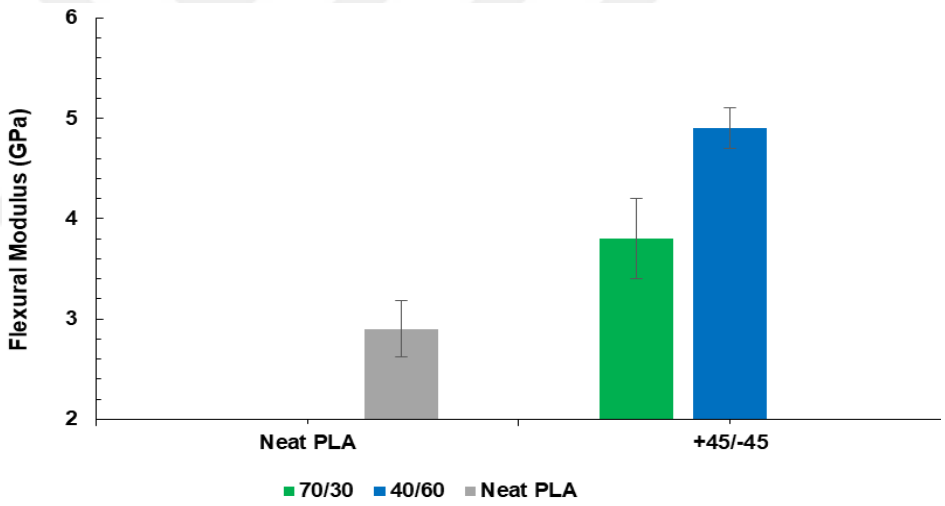


Figure 3. 15. The Flexural Modulus of Over-Molded PLA/+45/-45 Ecosheet Composites

Usually, the Izod impact test is used to study the ability of the sample to absorb shock or energy and to determine the amount of damage in the layers of the sample. In this work, all the specimens are tested in ISO 180 standard. See Fig.3.12. An unnotched specimen is used in this test. There are many factors that affect the ability of the composite to withstand impact damage, such as the strength of the fibers, the arrangement of the fibers, the thickness of the sample, and impact velocity, but the most important factor is the support conditions. For this purpose, the Izod's impact test is conducted to study the effect of the fiber layers and their ability of energy

absorption in over-molded composites and the failure types. During the test, the composite is exposed to an impact, through which, part of the energy is transferred, and this energy is responsible for elastic deformation of the composite, while the extra energy causes more damage to the fibers, or between the fibers and the matrix, or causes cracks in the sample. The amount of damage in the sample that is caused by the impact determines the magnitude of its failure. The aim of Izod test is to supply a comparative test to estimate the impact energy absorption of different composites. The results of Izod's impact test are shown in Fig.3.16. The results are averaged in terms of absorbed energy, which shows a big difference. The brittle behavior of PLA as a matrix is the reason of the reduction of energy absorption when the fiber angle increased. The results show that the failed samples take a ductile form, and also deboning and deplating of the fibers are observed.

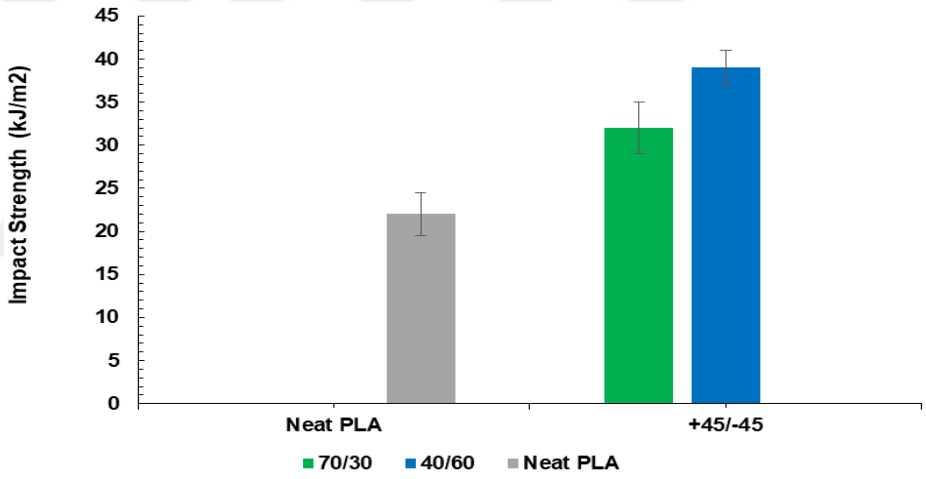


Figure 3. 16. The Impact Strength of Over-Molded PLA/+45/-45 Ecosheet Composites

In addition to cracks and debonding, the most important types of failure are the separation of the fibers from the PAL matrix, the separation among the composite layers, and this crosses with the impact energy which is similar to the strain energy release rate. In general, failure forms, which include the interphase part or fracture of the matrix, have a low fracture energies. On the other hand, failure forms that include fiber breakage outcome with greater energy dissipation [146]. As for samples with $45^{o}$, the failure form is the false ductile. This may be due to the $45^{o}$ layers shearing phenomenon. In this mode of failure, the fibers and matrix share the impact load. Because of the difference in strength between the fibers and the matrix, the failure

appears as cracks or delamination in the matrix, while the fibers remain intact. This behavior has been observed before in tensile load [147,148] . We can say that with respect to the averaged energy absorbed, the 60/40 45° samples showed the best results.

For the HDT, we can see that the over-molded PLA/jute has great heat resistance compared to neat PLA polymer. This improvement may be caused by the jute fiber reinforcement which prohibit the OM-composites. The maximum result is for OM-60/40 ecosheet at 57 C°. See figure 3.17.

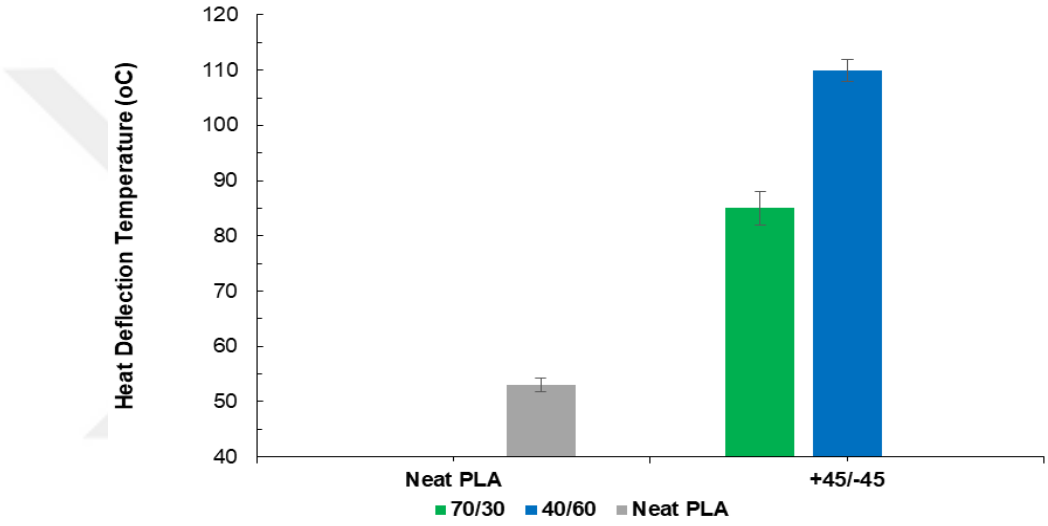


Figure 3. 17. The Heat Deflection Temperature of Over-Molded PLA/+45/-45 ecosheet Composites

DMA test is performed to determine the dynamic mechanical properties of Over-molded PLA/jute composites for all samples. Figure 3.18. Shows the storage modulus (E´) while Figure 3.19. Shows the tan δ as a function of temperature. E´ values of the PAL composite show decreases with increasing temperature. But with the stiffness of the fibers, the decrease in the matrix modulus values has been compensated. With the increase in the fibers content in the composites, an increase in the storage modulus values is observed. It is important to note that along the temperature range, a clear rise in the storage modulus in jute / PLA Over-molded composites has been observed over the values of neat PLA. This is due to the fact that the reinforced PAL matrix by the fibers increases the composites stiffness and leads to a greater transfer in the interface area of the stress transfer [144]. The values

of storage modulus of PLA/jute over-molded composites and neat PLA are shown in Table 3.2.

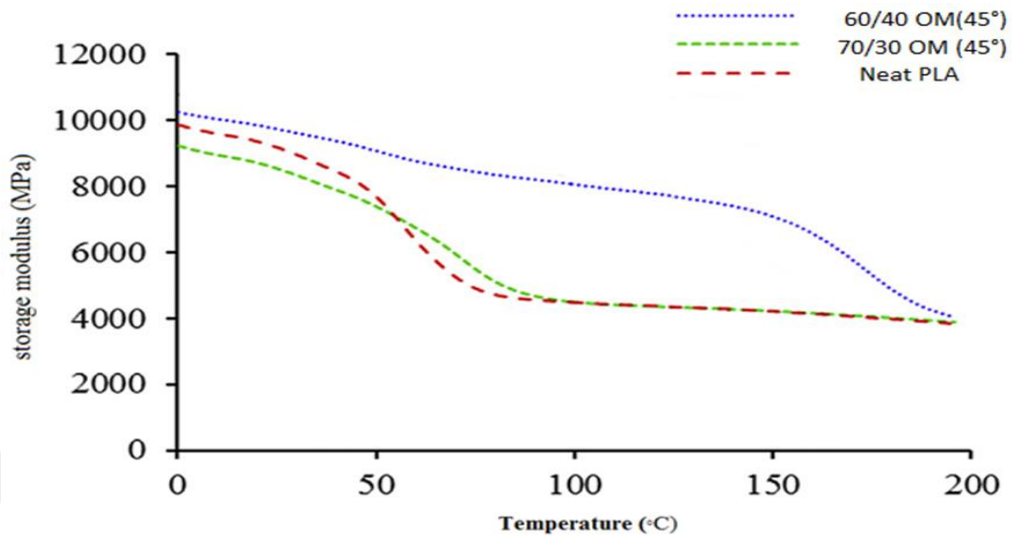


Figure 3. 18. The Storage Modulus of Over-Molded PLA/+45/-45 Ecosheet Composites

A significant increase in E′ values is observed in the area under glass transition region (from 0 to 50 °C) for composites with 35 wt% fiber content (45°) round 27% at 0 °C. The same samples show the highest values of E′ above the Tg. See Fig. 3.18. And Table 3.2. It has been observed that with increasing temperature, the storage modulus decreases and this decrease is accompanied by a significant decrease in the area between 60 and 80 °C. This decrease in the modulus is lower in 70/30% and 60/40 % composites compared to the neat PLA. This decrease is considered a transition from the glass state to the rubbery state. That's because the hydrodynamic effect of the fibers in the viscoelastic matrix. Add to that the mechanical resistance of the fibers, which impedes the movement of the matrix and reduces its deformability [45].

Tan δ is the loss modulus to storage modulus ratio, which shows the damping properties of the composites. The temperature of the tan δ peak in Fig.3.19. Is not affected by 70/30 % and neat PLA incorporation which is around 75 °C. It is observed that with an increase in the fibers content, the size of the tan δ peak decreases. The tan δ of pure PLA in glass transition area is less than the over-molded composites.

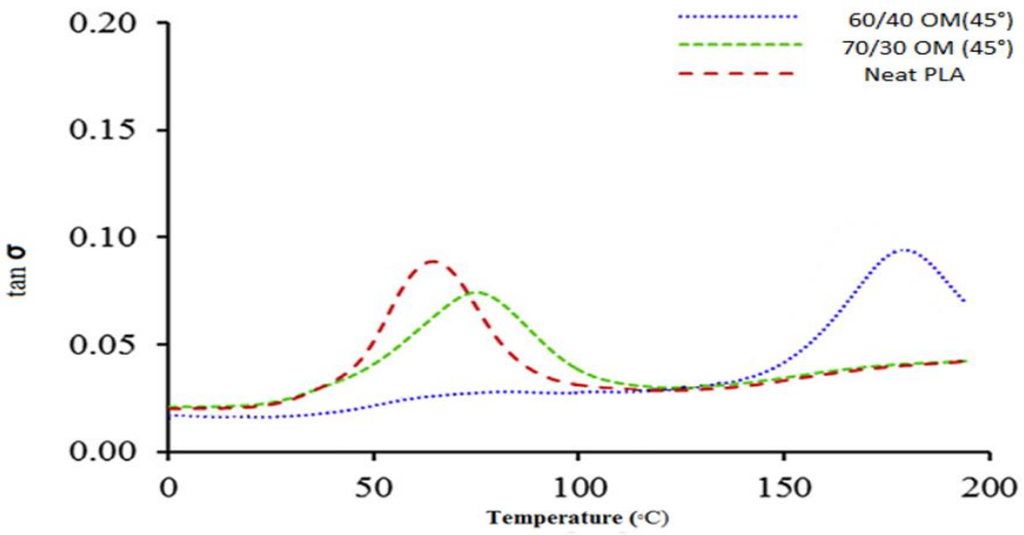


Figure 3. 19. The Tan of Over-Molded PLA/+45/-45 Ecoheet Composites

We can refer this to the same reason as previously mentioned, which is the restriction of jute fibers to the movement of the PLA matrix, which decreases viscosity and increases the storage modulus values between stress and strain [46]. Accordingly, the values of the net PAL are equal to the values of tan δ of 60/40 and less in composite of 70/30. Increasing the size of the matrix which is caused even by a minimum vibratory energy may be a second reason [147].

Table 3. 2. Storage Modulus (At 0 and 200 ◦C) and Tg Values of Jute/PLA Composites

| sample | | PLA/Jute 45◦ | PLA/Jute 0◦ | PLA/Jute 90◦ |
|---|---|---|---|---|
| Storage | 0 ◦C | 2300 | 2325 | 2251 |
| modulus (MPa) | 200 ◦C | 12 | 8 | 10 |
| Tg (◦C) | | 179 | 75 | 65 |

The SEM sample is selected from three point bending test samples. The part subjected to the test is the fractured surface part and, as shown in Figure 4.20. On the left side, we can notice the presence of cracks in the matrix; this may be due to the brittle failure behavior of the PLA and the cross loading. On the right side of Fig.3.20. We notice the uniformly woven jute fiber and a kind alignment. Fig. 3.21. (Left) shows the presence of good fibers adhering well with the PAL matrix which proves PAL well penetration of the fibers. Likewise, Figure 3.21. (Right) shows that there are no spaces between the jute fibers and the matrix, and even the broken fibers are not deboned but are covered with the matrix. This proves the strength and quality of adhesion between the matrix and the fibers. But for the more over-molded

composite, especially in the area of connection between the ecosheet and the over-molded layer, they result in less flexural strength than expected due to the speed of separation between the two layers which take lower load (Fig.3.20.). However, in many samples, the cracks are invisible and this demonstrates the brittle behavior of the composites.

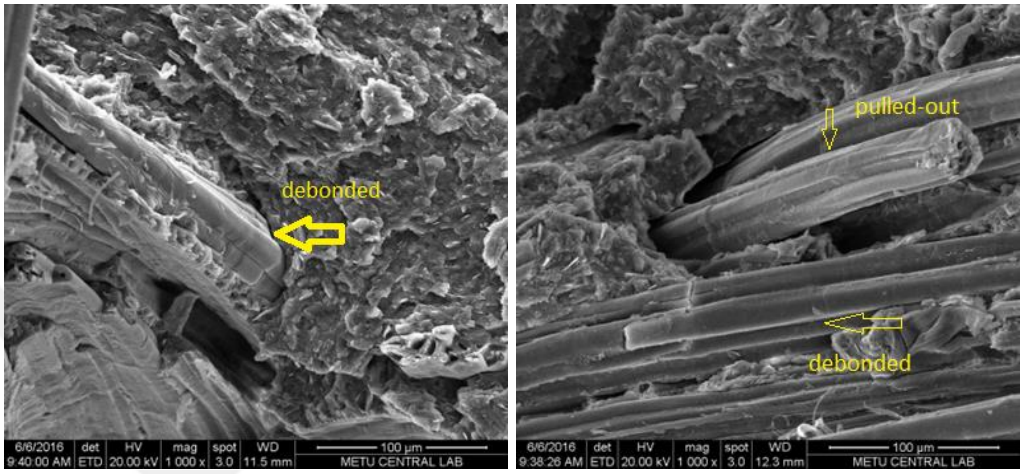


a) b)

Figure 3. 20. The flexural-fractured surface of over-molded PLA/+45/-45 ecosheet composites (a) debonded (b) pulled out

The Thermogravimetric Analysis curves for Jute, over-molded 70/30% jute/PLA 80/20 % and 60/40% with weight fraction (15%), (20%) and (35%) composites are shown in the Fig 3.22. The first degradation happen at 358 $^{o}$C for jute. In the range of 340-440 $^{o}$C, a big amount of degradation happens.

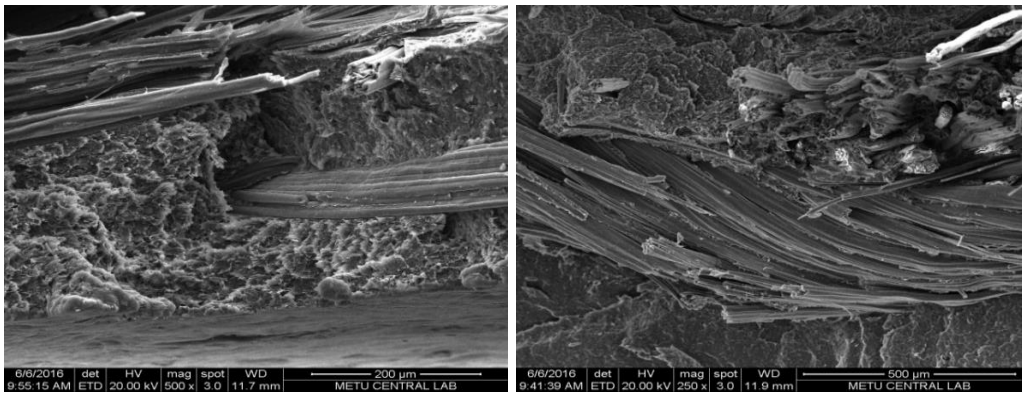


a) b)

Figure 3. 21. The tensile-fractured surface of over-molded PLA/+45/-45 ecosheet composites (a) debonded (b) pulled out

By the end of the test, the residue percentage is 8.3%. In over-molded composites, especially in 80/20 jute/PLA, the results show a significant change in the values of thermal degradation, and this proves the big effect of the over-molded layer on the composites. For 70/30% jute/PLA composite, the first degradation temperature is 380.5 °C that is higher by 17.85% compared to jute. The reason for this is the low molecular mass of jute fibers [20, 30]. In addition, the fiber orientation has an impact on the thermal degradation of composites. When we compare 60/40 % and 70/30% composites we see a decrease in the degradation temperature by 17% for 60/40 %. But by comparring to 80/20 %, the 60/40 % and 70/30% jute/PLA composites show greater and better thermal stability.

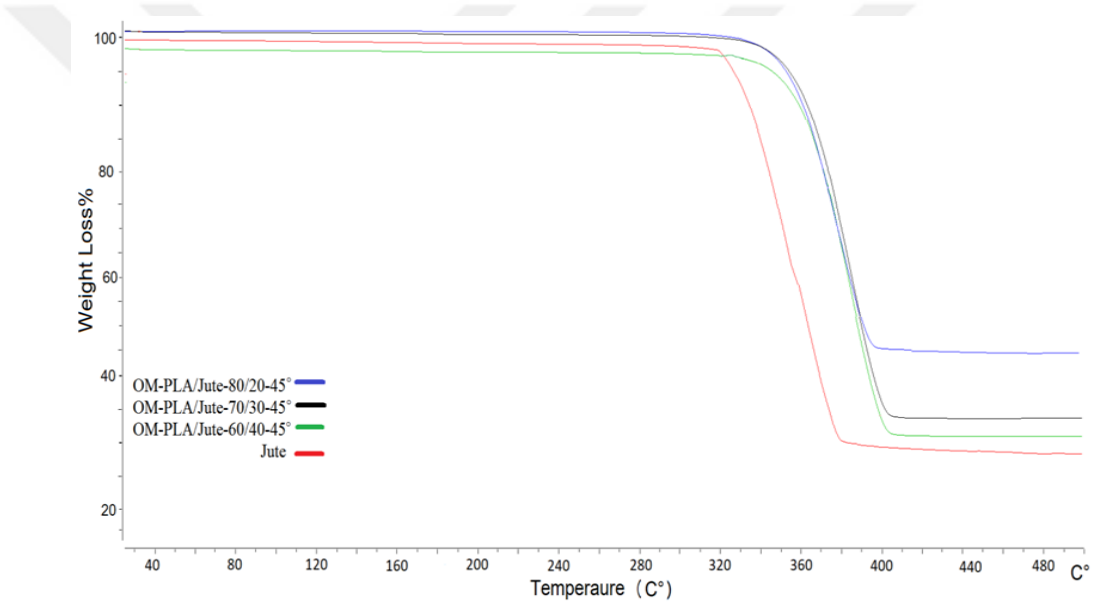


Figure 3. 22. The TGA of Jute and Over-Molded PLA/+45/-45 Ecosheet Composites

### 3.3. Chemical Treatment of Ecosheet

Cellulose is the prime component in jute as all of the natural fibers. On the other hand, hemicellulose and lignin make up the rest of the components besides other components. These components are called noncellulosic components. Hemicellulose and lignin play a big part of the fibers characteristic properties. As for the hemicellulose in the jute, it is made of polyuronide and hexosan. Hexosan has a sensitivity for the alkaline solution. On the other hand, α-cellulose and lignin have slight sensitivity for the alkaline solution. In this work, the technique we use is 1, 5 and 10% NaOH solution as alkaline solution. The NaOH solution is at the room

temperature, and the time is 2, 4, 6 and 8 hours. In the second stage, 10% NaOH + Silane (1, 1.5 and 3% Silane with 6 hours) is used as a treatments for the jute fibers. The mechanical and thermal properties of the jute and OM-composites; and the chemical treatments effects are characterized by bending 3 points: DMA, DSC, and SEM. By using the FTIR, the chemical composition of the functional groups of fibers is determined before and after the chemical treatment process and the effect of this treatment on the fibers is analyzed. At this stage, improving the thermal and mechanical properties of the ecosheet is the goal.

As mentioned in the literature, the effect of the alkaline solution on jute fibers has the greatest effect on the density of these fibers, so it is expected that the density of the jute fibers will decrease after the treatment. This can be explained by removing part of the noncellulosic compounds such as lignin and hemicellulose. However, this matter is different for silane, where the effect of the coupling agent on the surface of the fibers is different. Therefore, we expect density values close to each other [173].

Table 3. 3. Name and Code of Chemical Treatment of Ecosheet

| Name | Code |
|---|---|
| Untreated Jute | UJ |
| 1% NaOH | 1NO |
| 5% NaOH | 5NO |
| 10% NaOH | 10N |
| NaOH10%+silane1 % | 10N1S |
| NaOH10%+silane1,5 % | 10N1.5S |
| NaOH10%+silane3 % | 10N3S |

A decrease in the density and weight of the fibers is observed after the chemical treatment, especially after 2 hours of the experiment. The reason is due to the loss of hemicellulose as mentioned previously. In the period between 2 to 8 hours, there is a significant decrease in density values, gaps appeared in the fibers and became dispersed and separated. Accordingly, fibers have become brittle and stiff, compared to their extensibility and great strength previously [211].

By measuring the weight loss (%), we can determine the effect of the treatment on the fibers, and this is done according to [174,175]. An increase in fiber weight loss is observed with an increase in the time of treatment with NaOH and its concentrations, as shown in Table 3.4. The reason is the loss of hemicellulose and lignin.

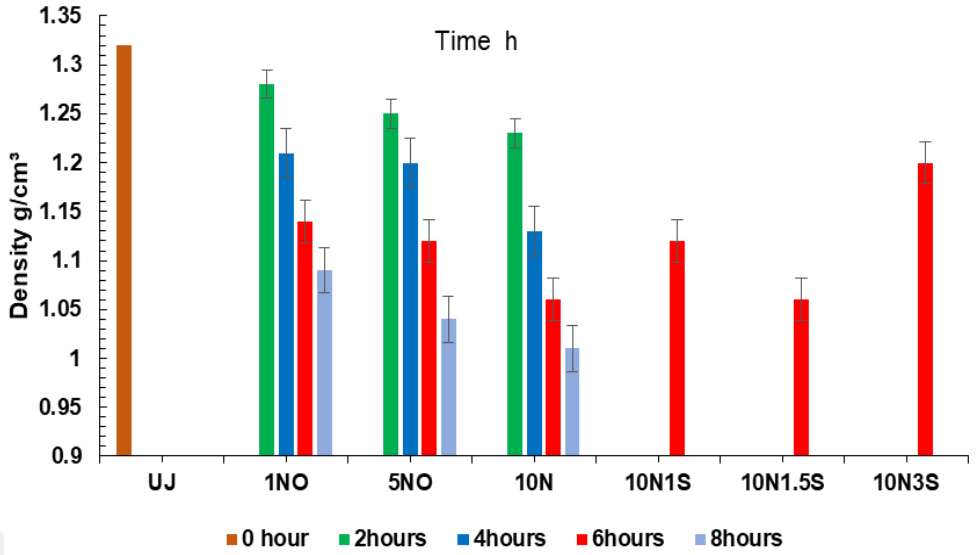


Figure 3. 23. The Densities of the Untreated and the Treated Jute Fibers

The reason for the loss of the non-cellulose compounds is due to the breaking bonds of the hydroxyl groups (–OH) and the hydrogen bonds due to the alkali attack. The defibrillation and loss of these compounds causes the fibers to shrink to smaller fibers, but at the same time increases the volume of the effective surface [176].

Table 3. 4. The Weight Loss of Jute Fiber with NaOH Treatment

| NaOH (wt. %) | 2 h | 4 h | 6 h | 8 h |
|---|---|---|---|---|
| 1 | 5.6±1.6 | 6.2±3.2 | 6.5±2.5 | 8.4±1.1 |
| 5 | 9.42±2.6 | 10.78±2.3 | 10.98±3.1 | 11.89±2.3 |
| 10 | 14.68±3.2 | 16.1±2.4 | 17.21±2.6 | 18.32±3.2 |

Because PLA can absorb very little amount of water, jute fiber content will be the major factor affecting the water absorption of the composites [119]. Jute fiber is hydrophilic because it contains an abundance of hydroxyl groups. The Water absorption of jute fiber increases as the concentration of alkaline treatment increases (Table 3.5). Water absorption of untreated jute fiber is 11.17% but is reduced to 9.76% after 5% alkaline treatment for 24 h. Because of the presence of a hydroxyl groups in jute fibers, it is the primary responsible for absorbing water in the composites, especially since PAL is a hydrophobic polymer, which is what makes fibers the main responsible for any increase in water absorption[119]. With the

increased concentration of alkaline treatment, the Water absorption of jute fiber decreased (Table 3.5). For the untreated jute fiber, the Water absorption is 11.17% but after 24 h with 5% alkali treatment, it becomes 9.76%. The top decrease in water absorption (7.08%) is for the jute fibers after the treatment with 10% NaOH + Silane 1.5 % for 30 h. An amount of 10.85, 9.76, and 8.75% of absorption is gained in fibers with 1%, 5%, and 10% of NaOH treatment for 30 h. At higher NaOH concentration, the water absorption becomes slow. But when Silane is used, the water absorption decreases significantly for the fibers.

Table 3. 5. The Water absorption of Untreated, Treated Jute Fiber and Overmolded Composite

| Soakig time (h) | Jute fabric | 1%NaOH | 5%NaOH | 10%NaOH | 1%silane | 1,5 %silane | 3%silane |
|---|---|---|---|---|---|---|---|
| 0 | 7.33±0.2 | 6.31±0.4 | 5.02±0.3 | 4.34±0.4 | 2.98±0.6 | 2.08±0.5 | 2.13 ±0.2 |
| 4 | 7.58 ±0.3 | 6.89±0.3 | 5.62±0.3 | 4.98±0.3 | 3.02±0.5 | 2.35±0.6 | 2.74 ±0.6 |
| 8 | 8.24±0.3 | 7.02±0.4 | 6.95±0.4 | 5.56±0.3 | 3.67±0.5 | 3.12±0.4 | 3.12 ±0.6 |
| 12 | 9.12±0.2 | 8.75±0.3 | 7.34±0.2 | 6.01±0.4 | 3.93±0.3 | 3.42±0.3 | 4.51 ±0.2 |
| 16 | 9.52±0.3 | 9.23±0.3 | 8.03±0.6 | 6.98±0.3 | 4.64±0.4 | 4.72±0.4 | 4.83 ±0.3 |
| 20 | 10.08±0.3 | 9.62±0.4 | 8.44±0.4 | 7.33±0.5 | 5.23±0.4 | 4.97±0.4 | 5.21 ±0.4 |
| 24 | 10.56±0.2 | 10.01±0.4 | 8.89±0.4 | 8.12±0.3 | 6.12±0.6 | 5.86±0.6 | 6.86 ±0.6 |
| 28 | 10.95±0.3 | 10.11±0.2 | 9.14±0.3 | 8.46±0.3 | 7.02±0.5 | 6.35±0.6 | 7.34 ±0.6 |
| 30 | 11.17±0.2 | 10.85±0.4 | 9.76±0.3 | 8.75±0.4 | 7.96±0.6 | 7.08±0.5 | 8.13 ±0.2 |

For the OM-Jute/PLA, water absorption after alkaline treatments is shown in Table 3.6. In the neat PLA, even after 30 hours, the water absorption is around 0.86%, which proves its hydrophobic behavior. By the increased content of the fiber in the composites, it is clear that the water absorption value increases. The results show that the NaOH treatment partially removes the hemicellulose, lignin and other surface impurities which causes a big decrease to the fibers water absorption [77]. There is a negative effect of the reaction of the alcohol groups in cellulose with NaOH. This effect is on the ability to absorb water in fibers. This can be explained by the fact that the oxidation reaction minimize the total number of hydroxide groups in the fibers [78]. We can understand that silane treatment after the NaOH treatment minimizes

the water absorption of OM- Jute /PLA. The advantage of using silane after NaOH is that the active groups of silane form an isolated layer on the surface of the fibers by forming hydrogen bonds with the hydroxyl groups. Accordingly, a decrease in the water absorption values of the OM-Jute/PLA composites are observed [79].

Table 3. 6. The Water absorption of Treated Over-molded Composite

| | | | OM-70/30 | | | OM-60/40 | |
|---|---|---|---|---|---|---|---|
| Soaking time (h) | Neat PLA | 1%NaOH | 5%NaOH | 10%NaOH | 1%NaOH | 5%NaOH | 10%NaOH |
| 0 | 0 | 0 | 0 | 0 | 0 | 0 | 0 |
| 4 | 1,5±0,5 | 3,2±0.2 | 2,9±0.4 | 2,3±0,4 | 3,8±0,9 | 3,1±0,8 | 2,6 ±0.2 |
| 8 | 1,7±0,3 | 3,7±0,5 | 3,1±0,8 | 2,5±0,7 | 4,1±0.3 | 3,6±0,4 | 2,9 ±0,6 |
| 12 | 1,7±0,4 | 3,8±0,6 | 3,6±0,4 | 2,8±0,6 | 4,6±0.4 | 3,9±0,4 | 3,4 ±0,4 |
| 16 | 1,7±0,3 | 4,3±0,4 | 4,2±0,5 | 3,2±0.4 | 4,9±0,5 | 4,3±0.4 | 3,8 ±0.2 |
| 20 | 1,74±0,3 | 4,7±0.2 | 4,6±0.3 | 3,6±0.3 | 5,1±0.3 | 4,8±0.2 | 4,2 ±0.3 |
| 24 | 1,73±0,5 | 5,2±0,4 | 5,1±0.2 | 3,9±0.2 | 5,2±0.4 | 4,9±0.3 | 4,5 ±0,6 |
| 28 | 1,75±0,4 | 5,4±0.4 | 5,3±0.2 | 4,2±0.3 | 5,4±0,5 | 4,9±0.4 | 4,5 ±0,4 |
| 30 | 1,74±0,2 | 5,4±0,9 | 5,3±0.3 | 4,2±0,4 | 5,6±0,5 | 4,9±0.2 | 4,5 ±0.4 |
| | | | OM-70/30 | | | OM-60/40 | |
| Soaking time (h) | Neat PLA | 1%silane | 1,5%silane | 3%silane | 1%silane | 1,5 %silane | 3%silane |
| 4 | 1,5±0,5 | 2,5±0.2 | 1,9±0.3 | 1,2±0,8 | 2,4±0.5 | 1,8±0,5 | 1,2 ±0,4 |
| 8 | 1,7±0,3 | 2,7±0,5 | 2,1±0.4 | 1,6±0,2 | 2,6±0.4 | 1,9±0,2 | 1,3 ±0,6 |
| 12 | 1,7±0,4 | 3,1±0.5 | 2,3±0.3 | 2,1±0.5 | 2,9±0.3 | 2,1±0,6 | 1,3 ±0,7 |
| 16 | 1,7±0,3 | 3,4±0.3 | 2,5±0.4 | 2,4±0,3 | 3,2±0,4 | 2,4±0,4 | 1,6 ±0.5 |
| 20 | 1,74±0,3 | 3,6±0.2 | 2,8±0.2 | 2,6±0.5 | 3,7±0.4 | 2,8±0,2 | 1,8 ±0.3 |
| 24 | 1,73±0,5 | 3,6±0,8 | 3,3±0,4 | 2,6±0.4 | 3,9±0.5 | 3,3±0,2 | 1,9 ±0.4 |
| 28 | 1,75±0,4 | 3,6±0,4 | 3,3±0,5 | 2,6±0,2 | 4,1±0,7 | 3,6±0.3 | 2,3 ±0,3 |
| 30 | 1,74±0,2 | 3,6±0.4 | 3,3±0,2 | 2,8±0,2 | 4,1±0,3 | 3,9±0.3 | 2,5 ±0,4 |

In this study, when treating fibers by NaOH and with 3-(trimethoxysilyl) -propylmethacrylate (silane), the monomer concentrations are 25% in Methanol (MeOH) and the treatment time is 6 hours for silane. As expected, the chemical treatment of fibers has an effect on the mechanical properties of the composites, and

this effect varies with a different concentration of NaOH. We can limit the damage resulting from the treatment of the fiber-reinforced composite to the damage of the fibers, like fiber fracture; or in the matrix, like cracks; or in the matrix -fibers area which is in the form of delamination or debonding [79]. There are three signs that indicate the effect of NaOH which are: time, temperature and NaOH concentration, but the most important one is the shrinkage of fibers which has the most influence on mechanical properties. The results for OM-Composites's 3-point bend test are given in Table 3.7. Five samples are tested for each data point.

Table 3. 7. The Flexural Strength of Treated OM-Composites

| composite | 70/30 | | | 60/40 | | |
|---|---|---|---|---|---|---|
| Time | 1%NaOH | 5%NaOH | 10%NaOH | 1%NaOH | 5%NaOH | 10%NaOH |
| 2hours | 69,4 | 73,5 | 76,8 | 66,4 | 69,4 | 76,8 |
| 4hours | 70,1 | 76,8 | 81,5 | 68,5 | 73,1 | 79,3 |
| 6hours | 73,8 | 81,2 | 89,8 | 69,5 | 78,4 | 84,6 |
| 8hours | 71,1 | 77,6 | 83,6 | 67,2 | 74,6 | 79,8 |

The mechanical properties of 6 h treated fibers composites are of ultimate improvements. By the comparison between untreated fiber composites with treated fiber composites, the Flexural Strength is 89.8 MPa and 73.2 MPa in favor of treated composites such as OM (60/40%), with an improvement of 18.56%. At 4 h, the improvement is 6.4%; and at 8 h, it is 12.14%. The composites with 8 h alkaline treatment have a lower strength values. For our study, the best results are for composites with 6 h fibers treatment. This improvement is due to that the fibers have become brittle and rigid due to crystallinity and less extensibility which make high strength [21]. As for the best concentration for NaOH in alkali-treated composites, 10% NaOH gives the best mechanical properties results. The reason for this is that the higher the alkyl concentration is, the more hemocellulose is removed from the fibers. After the removing of hemocellulose, fibers have a greater ability to rearrange themselves under tensile deformation due to the presence of voids which make it less rigid and dense. The same behavior has been observed in flax [80]. It is observed that the strength of composites with treated fibers is raised when NaOH increases by 18

%. However, this is not the case for flexural and tensile modulus as they show similar values for untreated composites. Accordingly, the best results are for the compounds treated with 10 % of NaOH, and for this reason it is chosen for the next stages.

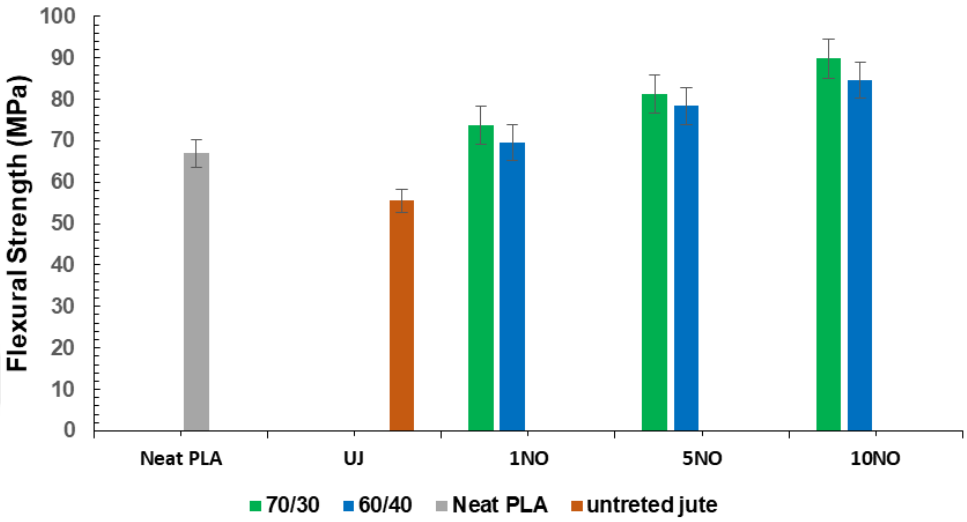


Figure 3. 24. The Flexural Strength of Treated OM-Composites

An increase in the tensile strength and tensile modulus values of the composite are observed as they are 13% and 40%, respectively. This is due to the excellent penetration of the PLA into the jute fibers, which allows a good distribution of tensile energy. Even if simple cracks appear, they will not affect the sample strength. An improvement is also observed in the flexural strength values for OM-alkali-treated jute/PLA composite as well. NaOH treatment of jute fibers make a rough surface which causes a better adhesion in matrix-fiber area because of the anchoring sites [23]. As for treated composites, the flexural properties increases due to the strong interfacial bonding between PLA and treated jute.

If we want to compare the results with neat PLA, the general rule will be that as the percentage of fibers in composites increases up to 35 wt. %, the mechanical properties will increase, like when flexural strength has increased to 23.3%, compared to neat PLA. This is a clear example of the effect of fiber reinforcement, as the composite has the ability to distribute stress energy between the matrix and fibers equally.

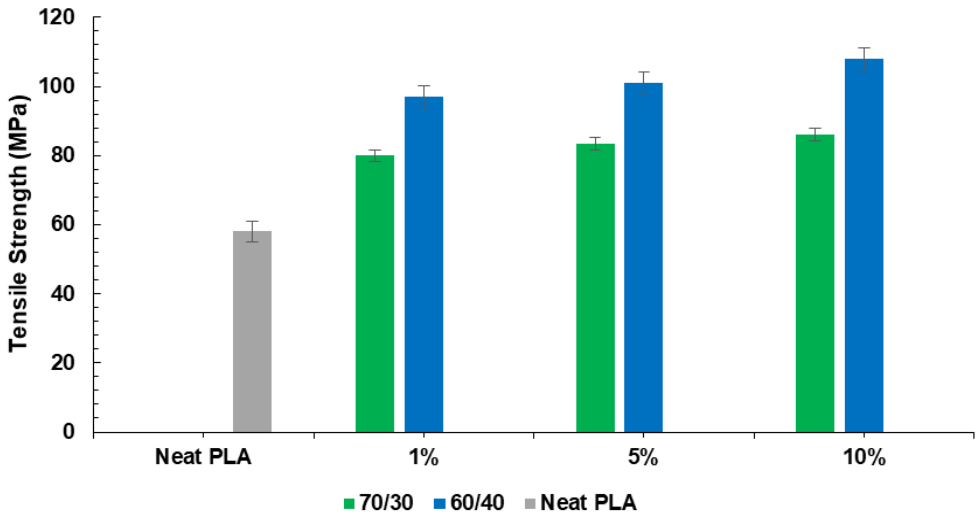


Figure 3. 25. The Tensile Strength of NaOH Treated OM-Composites

However, with 40 wt. % fiber, all the mechanical properties decrease. So it is true that everything declines after reaching its peak. The explanation for this is that the PAL matrix is not able to penetrate sufficiently into all fibers, this causes voids and an imbalance in stress distribution and is followed by failure [81].

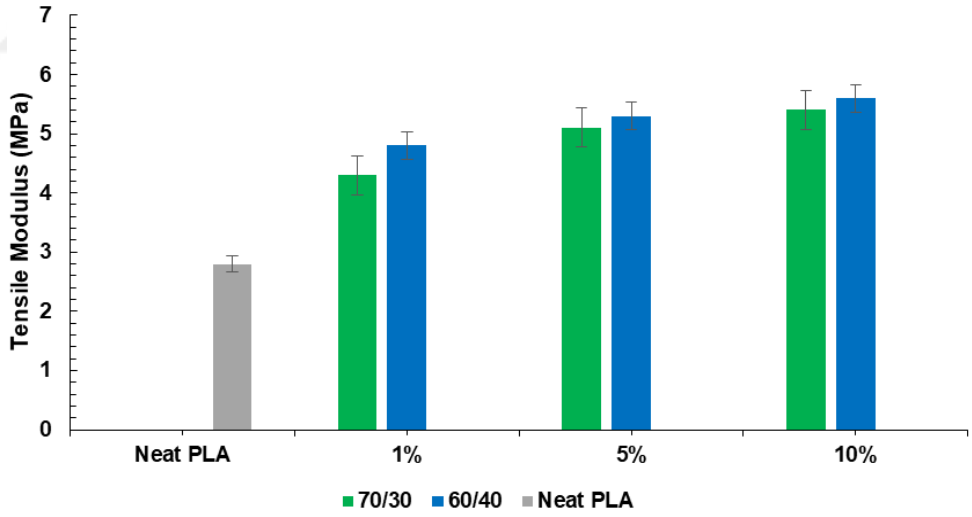


Figure 3. 26. The Tensile Modulus of NaOH Treated OM-Composites

However, it can be noted that the ratio of fiber in the compound has shown improvement in some properties but not in all the mechanical properties. Tensile and flexural modulus of the PLA/jute (60/40%) shows superiority on the ratio (70/30%) which is the opposite of what has been observed in flexural strength. See Fig 3.27.

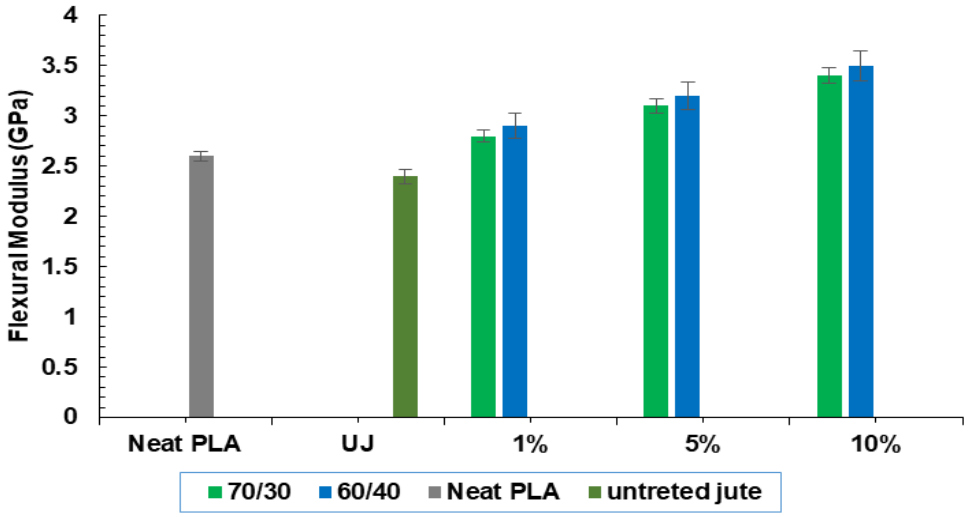


Figure 3. 27. The flexural modulus of NaOH treated om-composites

After chemical treatment, the fibers become smaller and more able to rearrange, and the surface area interacting with the matrix increases. This leads to an improvement in the mechanical properties. Chemical treatment improves the surface quality of the fibers by removing impurities, dust and wax as well [84].

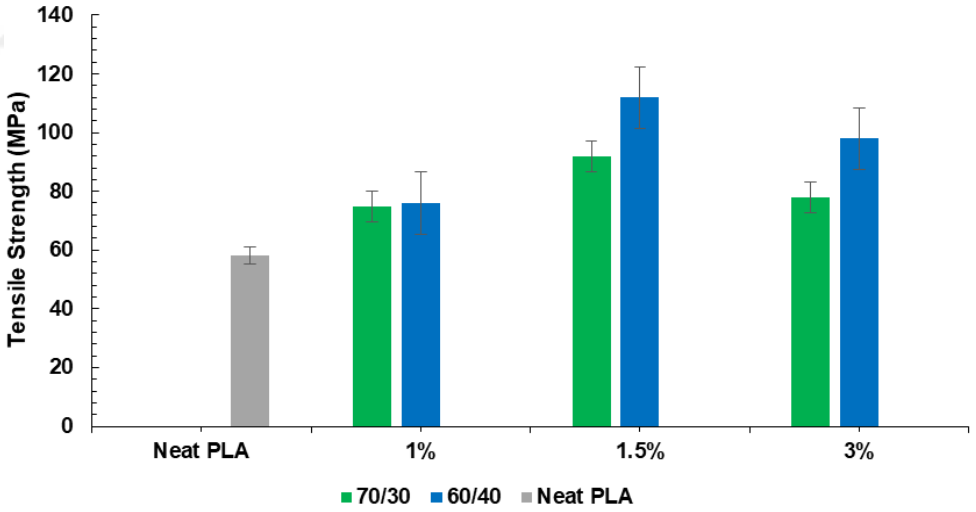


Figure 3. 28. The tensile strength of NaOH +Silane treated om-composites

The conclusion of tensile strength of the NaOH treated composite increases. The effective surface and the ability to readjust is the most important results that alkaline treatment do to the composites. [85]. Thus, the mechanical properties of chemically treated composites are much better than untreated composites. The excellent

interaction between the matrix and the fibers after treatment is what made this increase possible [86].

The goal of silane fiber treatment is to reduce the hydrophilic behavior of the fibers. Silane is applied to change the structure of jute surface to provide a stable bond between the jute fabric and incompatible PLA matrix. The Silane acts as a bridge between the fibers and the matrix where the functional groups of the Silane act as a coupling agent. By using dilute silane solution in treating jute fibers, we allow silane to better penetrate and interact within the fiber walls. Silane has been successfully interacted with jute fibers where the functional groups of Silane interact to form an –Si–O–Si– bonds. This bond acts as an adhesion promoter and also creates hydrogen bonds with hydroxyl groups in the fibers [26–28].

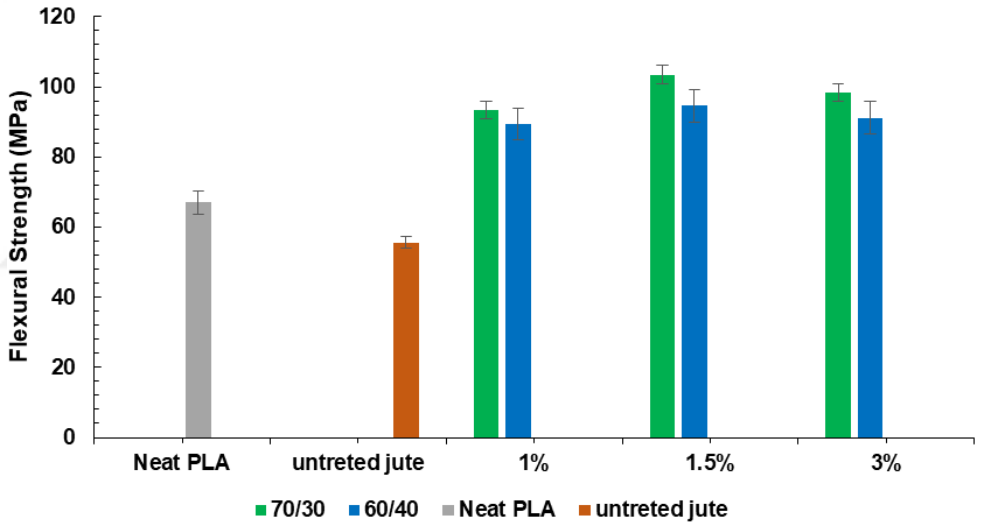


Figure 3. 29. The flexural strength of NaOH +Silane treated om-composites

The silanol makes a protective layer on the surface of the fibers called polysiloxane. Polysiloxane makes the interfacial adhesion increase by bridging the gap between the matrix and the fibers chemically [29]. This characteristic of silane gives a noticeable improvement in the mechanical properties of the composite. For example, the tensile and flexural strength of the composites improve by 43.5% and 65.2% respectively when compared to neat PLA. From understanding the definition of the flexural strength, we can say that the higher the resistance of the composite to deformation in the bending test is, the greater flexural strength this composite has. This is resulted because flexural strength increases the strain on the surface of the sample rather than

on the center or inside of the sample. Accordingly, the most important factor controlling the flexural strength is the outer layers of the reinforcement sample. In flexural test, Composite up-surface will be under compressive fracture but the bottom-surface will be under tensile fracture [29].

Because the fibers have an unclean or untreated surface, the treated composites are much better than untreated composites. That's because chemical treatment gives better adhesion and better energy distribution which make more strength. The treatment of fibers with alkali+ silane treatment increases the interfacial bonding, which reduces the opportunity of fibers pull out and increases the freedom to rearrange. It is interesting to note that there is a difference between the behavior of the tensile strength and flexural strength when the fibers content increase in the composites. Furthermore there is an increase in tensile modulus by 23.5% for (60/40%) and 25.36% for (70/30%), and in flexural modulus by 15.1%for (60/40%) and 19.9% for (70/30%), respectively. The flexural and tensile modulus of jute/PLA composites usually achieve a maximum values at a certain fiber content. At the best fiber content, the reinforced fibers are mixed homogeneously within the matrix resulting in greater wetting, thereby stress is uniformly distributed among the fibers leading to maximal properties of the composites. Several researches have reported the optimum fiber content of jute-reinforced polymer composites. [11, 30, 31]

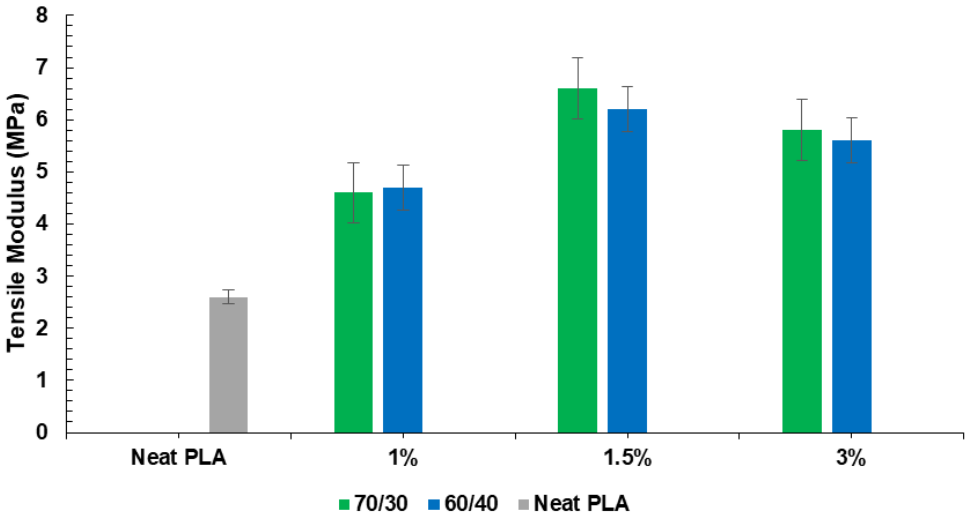


Figure 3. 30. The tensile modulus of NaOH +Silane treated om-composites

After extrapolating the results, we have demonstrated the importance of fibers content used for the reinforcement of PLA composites and their effect on mechanical properties, where it is found that the best results are due to the 20% of fibers content, as this ratio achieved the best internal adhesion between the matrix and fibers in the composites. A covalent bond is formed in the case of OM-jute/PLA (NaOH 10%+silane 1.5%) between fibers and silane after silane coupling agent. [29]. The surface of jute is covered by an adhesion promoter as thin layer which makes a good interfacial adhesion with PLA polymer.

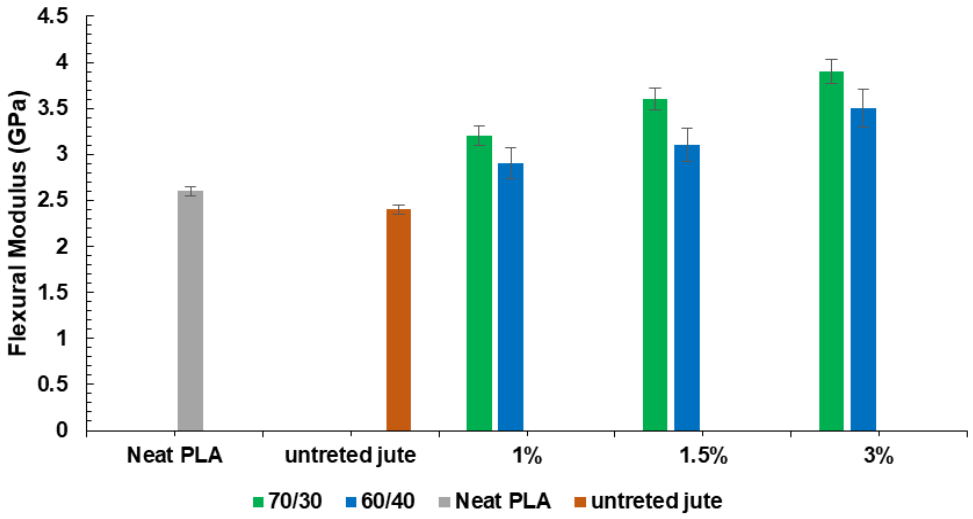


Figure 3. 31. The flexural modulus of NaOH +Silane treated om-composites

In the three-point bending test, the upper layer is exposed to the highest compression by the load member while the lower layer is exposed to the highest tension, and the inner layers remain with minimal stress. There are three factors that control the outcome for composites. The first factor is the strength of the fibers, as the strength and hardness of the fibers carry the greatest amount of stress before failure. The second factor is the treatment of fibers with silane, as the silane provides a more effective and more adherent surface to the matrix, which increases the properties remarkably [20]. The third factor is the top surface of the composite, so in the ecosheet composites, the fibers on the surface excellently immersed in the matrix, but in the over-molded composites, the fibers are presented under a layer of the PLA, and this creates a fast failure in the compression area.

Table 3. 8. The elongation of break of treated om-composites

| Composite | | NaOH Treatment | | | NaOH10%+ Silane | | |
|---|---|---|---|---|---|---|---|
| | Neat PLA | 1% | 5% | 10% | 1% | 1.5% | 3% |
| 70/30 | | 3,6 | 4,1 | 4,6 | 3,1 | 3,2 | 3,8 |
| 60/40 | | 2,8 | 4,3 | 4,1 | 2,6 | 2,8 | 3,1 |
| Neat PLA | 4,5 | | | | | | |

So in short, increasing the wettability of the fibers and the formed chemical bonds improved the interaction between the matrix and the fibers, resulting in a significant increase in the mechanical properties. Therefore, bypassing the defects of the fibers (high water absorption, lack of adhesion to the hydrophobic matrix , weak wettability) is possible and the solution lies in the chemical treatment of fibers, as this treatment will give a more effective, more adherent and less absorbent surface. These factors greatly improve the mechanical properties and longer shelf life of the composite.

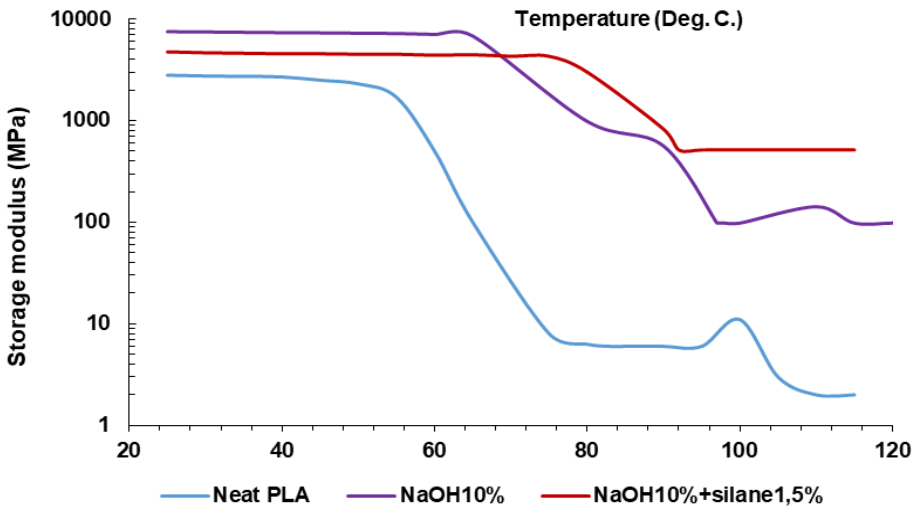


Figure 3. 32. The storage modulus of treated om-Jute/PLA (70/30%) composites

As for thermodynamic properties, there are 3 important properties that can be extracted from a DAM test: storage modulus (E'), loss modulus (E"), and damping parameter (tan δ). All these properties are done on the basis of temperature. As for

the Tg point, it can be obtained from the peak of the tan δ. For OM-Jute/PLA (70/30%) with NaOH treatment (10%) and NaOH10% +silane1.5%, the curves are shown in Fig 4.32. For the neat PLA, the Tg is 63°C, which is near to the storage modulus plot i.e. 59°C.

As for the storage modulus of PAL, it goes through two phases; at 30°C it is equal to 2750 MPa, then there is a drop due to the increase in temperature, where the E' reaches 500 MPa at a 60°C, with 97% drop. As for OM-Jute/PLA (60/40%) treated with NaOH10%, the highest levels of storage modulus are portend, it is equal to 4700 MPa compared to other composites. For the composites with NaOH10%+silane1.5% treatment, it is higher than NaOH10% composites and neat PLA. This proves the good adhesion between the fibers and the PLA polymer.

According to the known division of the curve, there is a stage above and a stage below the Tg point. Under Tg is called (glassy plateau region) and the one above it, is called (rubbery plateau region). Usually the degree of operation is less than the Tg of composite. The flatter section above Tg indicates the rubbery region of the composites. The storage modulus is increased slightly with NaOH treatment in the rubbery plateau region.

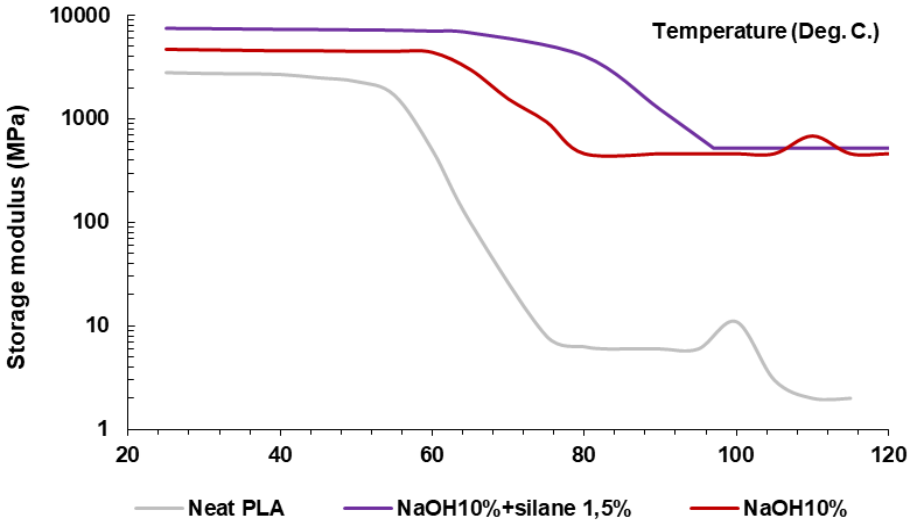


Figure 3. 33. The storage modulus of treated om-Jute/PLA (60/40%) composites

Generally, for composites at room temperature, the storage modulus is high then it decreases with the increase of temperature. The treated composites with NaOH

10%+silane 1.5% shows an improvement by 18% compared to the non-treated composites. There is a similar pattern between thermal and mechanical properties in relation to NaOH treatment composites, where a raise of 13% is observed at 10 % NaOH concentration. However, as shown in Figure 4.34. The tan δ has an inverse relationship with NaOH, as it reaches the lowest value for (70/30%) samples with a treating by 10% of NaOH. The advantage of tan δ is that it provides important information about the energy dissipated during the test [32]. Accordingly, an increase in the value of tan δ in neat PAL composites is noted, and this may be due to the greater dissipation of energy in the matrix-fibers area due to poor adhesion. Because the loss modulus correlates with the polymer's molecular chain mobility, with the increasing in crystalline structures, the storage modulus increases, and the loss modulus decreases. The storage modulus plots for jute-PLA (60/40) composites show a 4 °C shift in Tg compared to treated OM-Jute/PLA (70/30%), but for jute-PLA composite treated by silane, the Tg is 84.57 °C. In jute-PLA treated by alkali composite, it is 76.43°C. This is due to the fibers restricting the movement of molecular chains in PLA matrix.

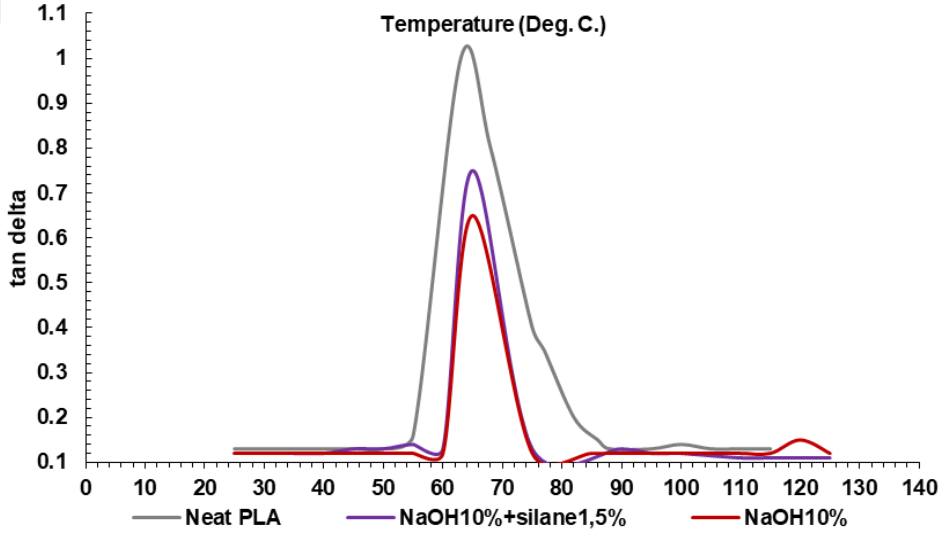


Figure 3. 34. The tan delta of treated om-Jute/PLA (70/30%) composites

In comparison with the neat PLA, a decrease in the width and height of tan δ peak is observed in OM-jute-PLA composites (see Figure 3.35). The factor responsible for this decrease is the damping capacity. As the damping capacity appears in the area

under the curve, when tan δ peak decreases, this shows a lower ability to damping impact; this can be seen in the neat PLA.

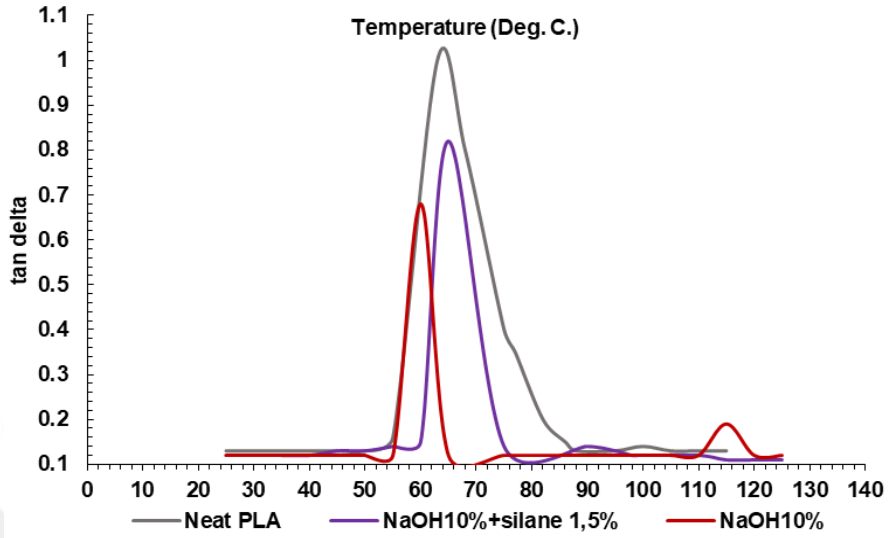


Figure 3. 35. The tan delta of treated om-Jute/PLA (60/40%) composites

To study how fibers interact with chemical treatment materials, FTIR analysis is used. For jute fibers, the O–H group is determined at 3325 cm-1 as stretching vibrations [89]. After using NaOH, a peak of O–H stretching is shifted to 3327 cm-1. After using silane, it shifts to 3446 cm-1. A decrease in the peaks intensities is observed after NaOH and silane treatments. This shift is accompanied by a rise in the peaks intensity in 2921 cm−1 that they belong to CH2 and CH3 vibrations. For the carbonyl group (C=O) in untreated jute fibers, it is determined at 1,735 cm-1[90]. After NaOH (10%-8h), there is a shift to 1,738. The same thing happens after silane (3%-6h) treatment, where the shift is to 1,744 cm-1. A sharp decrease in C=O peak is observed for untreated fiber after NaOH treatment until it is no longer seen. The reason for this disappearance is the removal of the compounds responsible for it by NaOH treatment. However, after silane treatment, an increase is observed to the intensity of the carbonyl group [91]. The peaks which belong to the absorbed water in crystalline cellulose in the region between 1,600 –1,620 cm-1 are determined [91]. In order to prove the presence of a real change after the chemical treatment, the peaks that belong to non cellulose compounds such as hemicellulose and lignin are studied. Several peaks are identified in the untreated jute fibers. After identifying these peaks, the chemical treatment is performed and then the experiment is repeated.

The results confirm that most hemicellulose and lignin peaks disappears, and this proves the effectiveness of chemical treatment. The peak at 1506 cm-1 belongs to lignin's aromatic rings [91,92]. This peak disappears after NaOH treatment [93]. The peaks that belong to hemicellulose and lignin C–H bending at 1,380–1,368 cm-1 olso disappear after NaOH treatment [93]. The peak at 1239 cm−1 is for axial asymmetric strain of = C-O-C groups. These functional groups are found in esters and ethers such as those that can be found or formed by hemicellulose and lignin. These peaks also disappear after treatment [93]. The peak of the cyclic alcohol groups in untreated jute fibers is found at 1,030 cm-1. This peak diminishes considerably after NaOH treatments, which is an indication of alcohol group's oxidation [94].

For the peaks of cellulose (C-O stretching), they are located in the fingerprint area at 1040~1060 cm-1. As for the Aegean, the aromatic skeleton vibration can be found at 1550~1650 cm-1[10,11]. These peaks remain in place after the chemical treatment, but there is a significant change in the intensities of these peaks. An increase in the ratio between the peaks of 1040~1060 cm-1 and 1550~1650 cm-1 demonstrates a decrease in the content of lignin and an increase in the cellulose content. This is exactly what happens when natural fibers are chemically treated, where the content of cellulose increases and the content of other compounds such as lignin decreases.

The FTIR results for composites treated with NaOH and composites treated with (NaOH +Silane) can be seen in Figure 4.37. With the silane treatment, on Jute/PLA, the intensity of the hydroxyl peak (3325 cm-1) is shrinking. A new peak at 1596 cm-1 belong to N-H bending appears. This can be explained by the reaction of silane with reactive hydroxyl groups on surfaces of Jute fibers [12]. Silane can undergo hydrolysis and form the silanol groups which forms with hydroxyl groups a new bond on the fibers surfaces, thereby leading to the reduction in the peak intensity at 3325 cm-1 (-OH stretching).

The presence of the 1596 cm-1 peak (N-H bending) corresponds to amine groups of silane, in the spectrum of silane treated jute/PLA. The -Si O-Si- peak is identified at 722 cm-1 as symmetric stretching, as well as -Si-C- peak is identified at 842 cm-1 as symmetric stretching. As shown, here are two peaks indicating for two reactions on the surface of jute fibers due to chemical treatment.

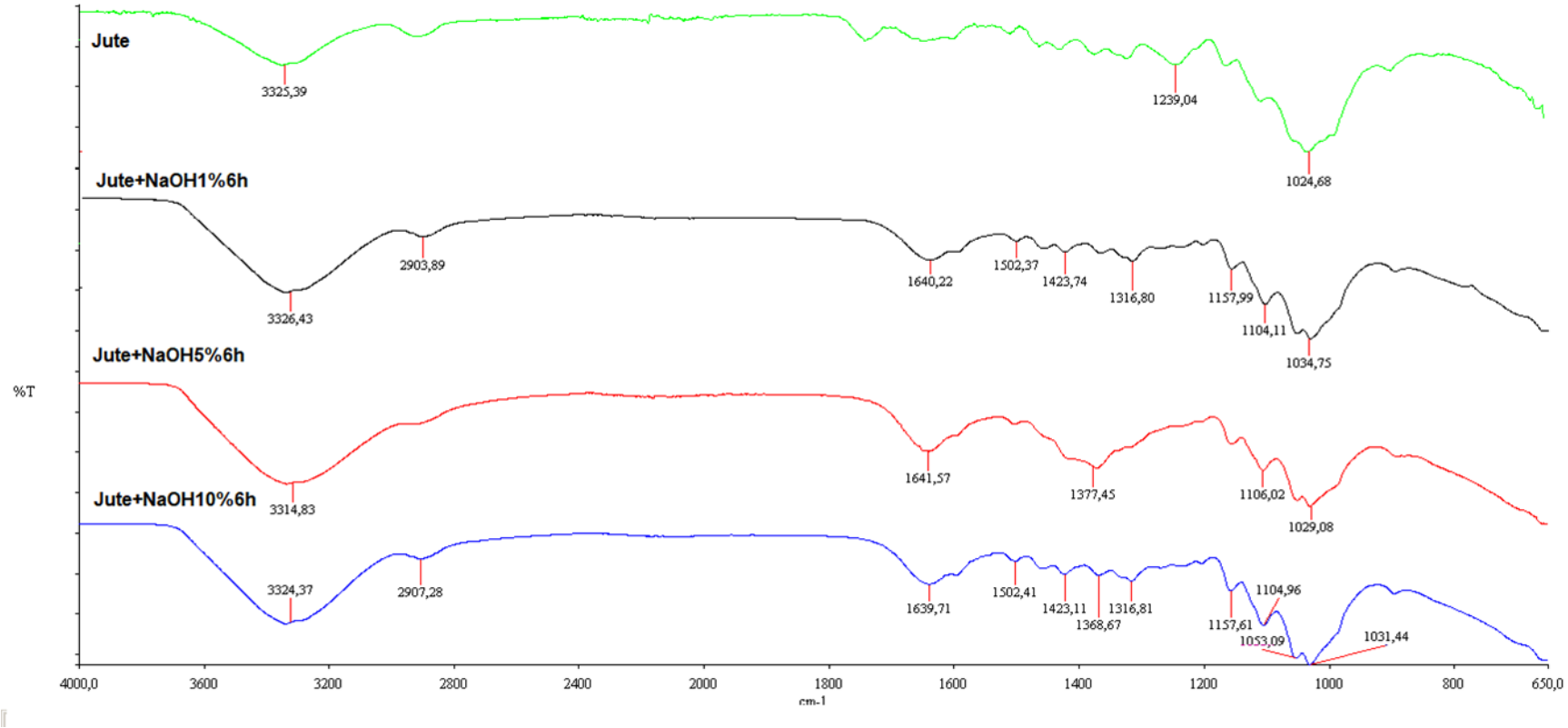


Figure 3. 36. The FTIR of Jute and NaOH Treated Jute

Table 3. 9. The characteristic peaks of jute and NaOH treated jute

| Untreated jute | NaOH Trated | | | Assignment |
|---|---|---|---|---|
| peak wave no(cm-1) | NaOH treated 2h | NaOH treated 6h | NaOH treated 8h | |
| 3325 | 3326 | 3326 | 3327 | OH stretch, Hydrogen bonded |
| 2921 | 2919 | 2920 | 2922 | C–H stretch in cellulose and hemicellulose |
| 1735-1715 | | | | C=O stretching of carboxylic acid or ester |
| 1650 | 1639 | 1640 | 1641 | Aromatic C=C stretching |
| 1600 | | | | Absorbed water |
| 1593,21 | 1593,35 | 1593,68 | 1594,12 | Lignin deformation |
| 1506 | | | | C–C stretching in lignin |
| 1440 | | | | CH2 bending in lignin |
| 1423,19 | 1423,17 | 1423,32 | 1423,74 | C–C stretch |
| 1410 | | | | CH2 and CH3 bending |
| 1380 | | | | C-H bending |
| 1326-1358 | | | | O-H in-plane bending |
| 1317 | 1316 | 1317 | 1316 | C–O stretch |
| 1234 | 1234 | 1235 | 1236 | CH2 Vibrations; HCH and OCH in plane bending; intermolecular hydrogen bonds bending |
| 1160 | | | | Ant symmetric bridge C-O-C stretching |
| 1157 | 1157 | 1155 | 1154 | C–O stretch |
| 1030 | 1029 | 1034 | 1033 | –C–O–C– stretching of side substituents of xylan and lignin aromatic C–O stretching |
| 890 | 889 | 887 | 888 | β-Glucosidic linkage |
| 675 | | | | Out-of-place bending vibration of intermolecular H bonded O-H group |

The first reaction is the deposition of siloxane on the fibers surface. It is determined at 722 cm-1, while the second reaction is the silane condensation on the fibers and it is determined at 842 cm-1. Evidence of the interaction of hydrolyzed silane with -OH groups on the surface of the fibers is the formation of a -Si-O-C- bonds that can be recognized from the peak at 1210 cm-1 [37, 38].

These changes are in fact expected to develop the fiber/matrix's interfacial adhesion to PLA/jute composites by the polar-polar bond that is resulted from an interaction between silane's amine groups (-NH2) of treated jute and PLA's ester groups (-COO-); and that explains that with the use of silane the tensile properties of jute/PLA increased. This is explained by the fact that not only the silanol groups of APTES but also the amine functionality can interact with hydroxyl groups on surfaces of the jute fibers, due to the high polarity of amine groups (-NH2) of APTES which can lead to a formation of hydrogen bonding with hydroxyl groups of jute fibers [13]. Since the surface characteristics of jute and flax fibers are similar in term of hydroxyl rich surfaces, the mechanism of silane on jute fibers is expected to be similar to that of flax fibers. This, therefore, leads to a proposed configuration of silane treated jute fibers where both the silanol and amine groups of silane interact towards the reactive hydroxyl groups of jute fibers. But due to NaOH treatment, the mechanism is different which leads to a decrease in the hydrophobic character of the silane treated jute fibers in comparison to the untreated jute [12]. As a result of the decrease in the hydrophobicity, the compatibility toward PLA matrix of silane treated jute is therefore increased and results in an increase in the fiber/matrix interfacial adhesion of the silane treated jute/PLA in comparison to the untreated jute.

SEM's device is characterized by its high resolution and great accuracy, and that's why it is chosen to analyze the samples resulting from the three point bending test (fractured surface) in order to demonstrate the effectiveness of chemical treatment of jute fibers and Jute/PLA composites in improving the quality and adhesion strength of the matrix-fiber region. Because of the reduction of density of jute fibers in composites after chemical treatment, the mechanical properties of the treated composites are significantly improved.

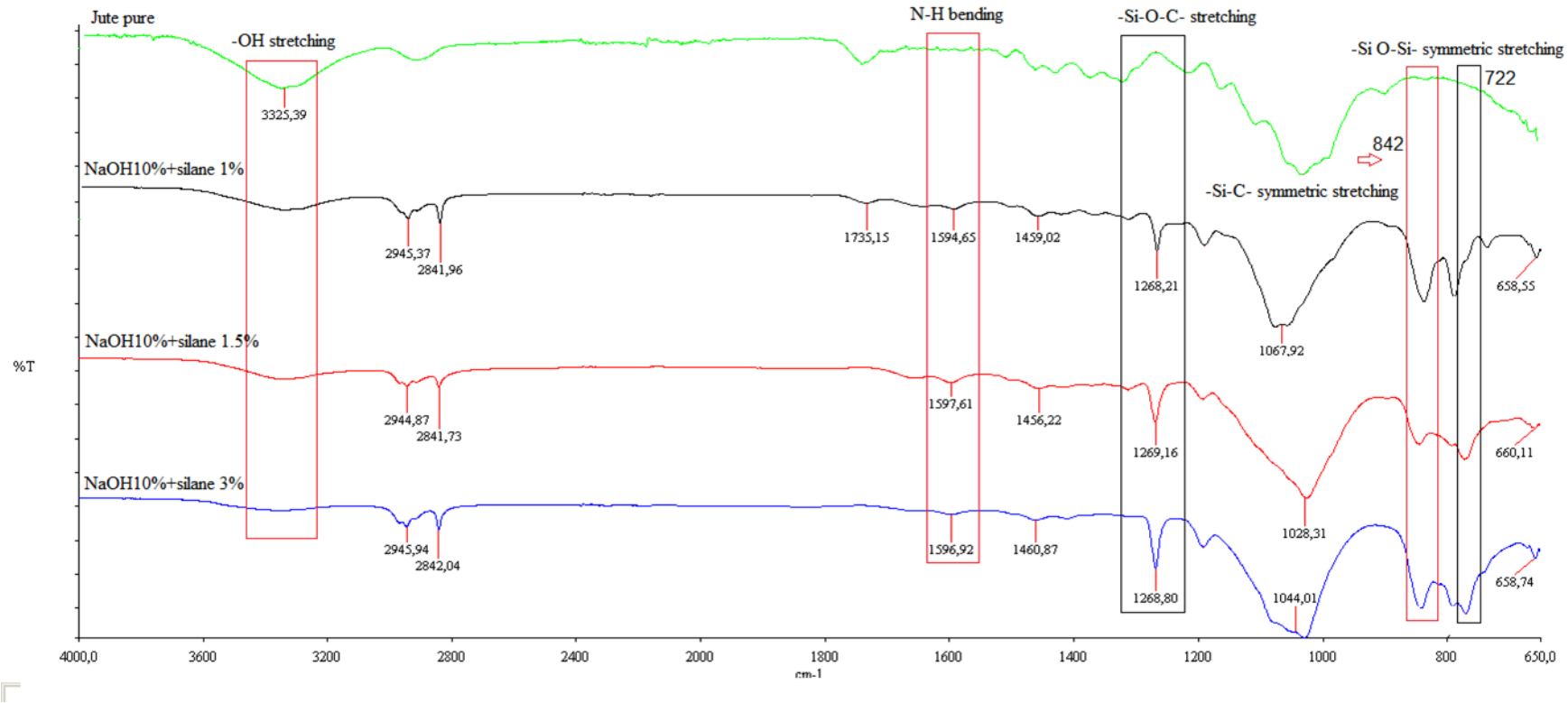


Figure 3. 37. The FT-IR spectra of NaOH and (NaOH +Silane) treated jute fiber

As seen in SEM, spacing in fibers is noticed as it becomes smaller and thinner. The responsible for this is the loss of hemicellulose due to chemical treatment, as hemicellulose is the cement of fibers.

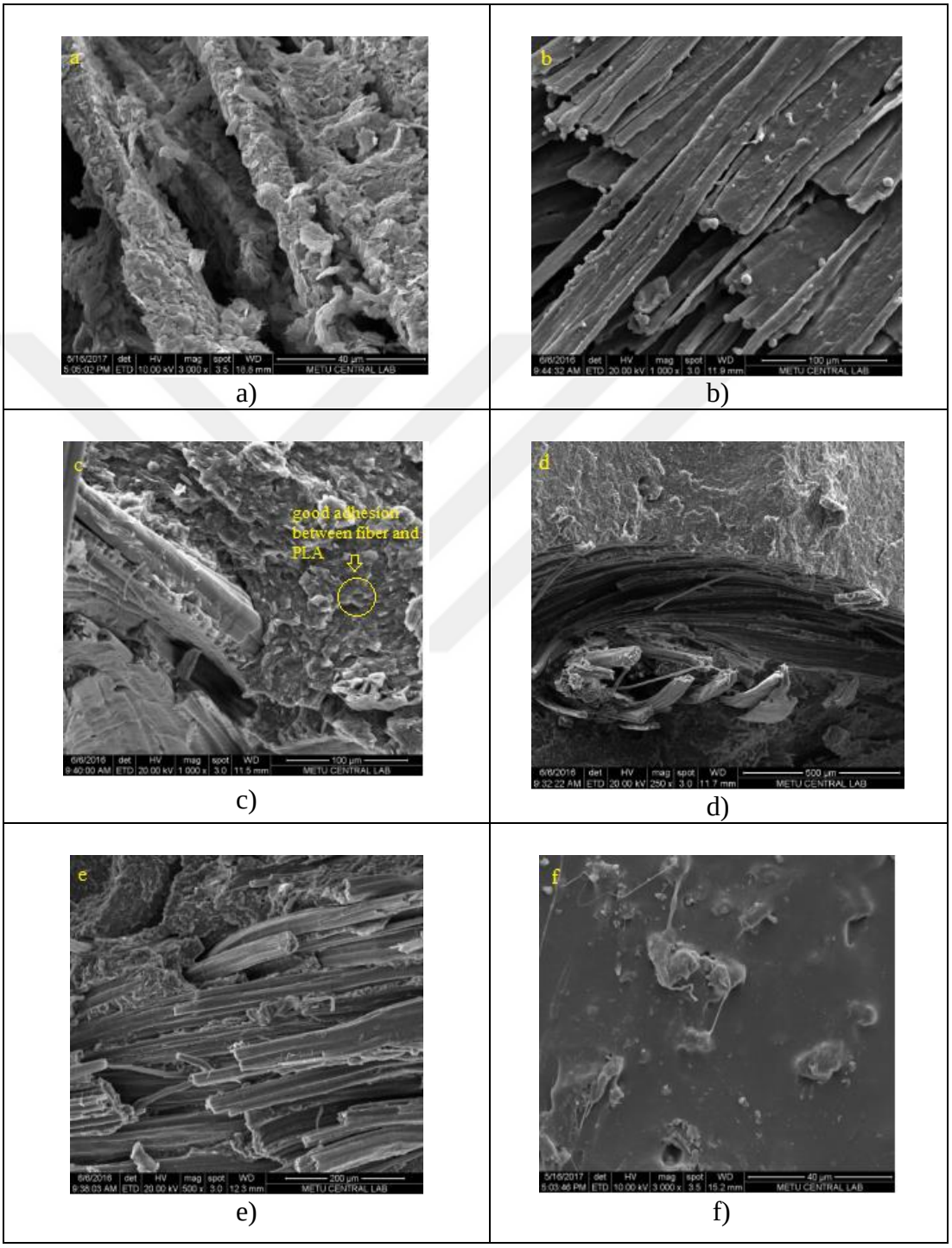


Figure 3. 38. The flexural-fractured surface of NaOH treated over-molded composites (a) NaOH1%-jute (b) NaOH 3%-Jute (c) poll out NaOH 3%-Jute (d) deboned ecosheet (e) NaOH+Saılen 1,5% (f) NaOH+Saılen 3%

Fiber breakage in untreated composites is the primary cause of the failure and the week strength of the composites as described in 3.38(a). A big amount of wax and oily substances is observed as impurities in the untreated fibers composites. From the extrapolation of the literature, it is noted that the reason for the poor adhesion between the fibers and the polymer may be due to the impurities that cover the cellulosic hydroxyl groups and thus constitute an obstacle to the interaction of these groups with the polymer matrix of the fibers in the reinforced composites [16, 35]. As previously mentioned [29, 37], jute fibers surfaces have been observed to be cleaner after NaOH (5% 6h) treatment and after being free of impurities; see picture Figure 3.36(b). After treating the jute fibers with NaOH (10% 2h), Figure 3.36. (c) Shows the surface of the jute fibers, smooth surface and clearly visible fibers. This is also due to the removal of impurities and hemicellulose where the individual cellulose fibers remain notable. But this is not the case for NaOH (10% 4h) composites, as Figure 3.36. (d) Shows a few fibers pullout. In the matrix-fiber region, some discontinuity is observed. Cracks in the matrix and pull out-fibers are observed at higher magnification levels. As for NaOH (10% 6h) composites, a respectable change in the surface of the fibers is observed. NaOH treatment improves the functionality of jute fibers surface and its wettability. That's because NaOH treatment allows the increase of the effective sites on the fibers surface that can interact with the polymer and produce stronger bonding and more adhesion composites [17]. Figure 3.36. (f) Proves that removing non-cellulosic materials and impurities by alkaline treatments cause the production of separated fibers with rough surfaces. Figure 3.36. (e) Shows the magnitude of the damage resulted in NaOH(10% 8h) treated composites, where cracks have been observed in the matrix, large amount of pullout fibers and dissociation in the fiber - matrix area. This damage can be explained by the long time of the alkaline treatment which causes the fiber surface to be significantly damaged. This may explain the weak resulted in tensile strength for treated fibers composites. Here the importance of defibrillation appears. According to the previous observations, defibrillation has the greatest effect in increasing the strength of treated composites. These results are similar to the results of NaOH treated sisal fibers in [94].

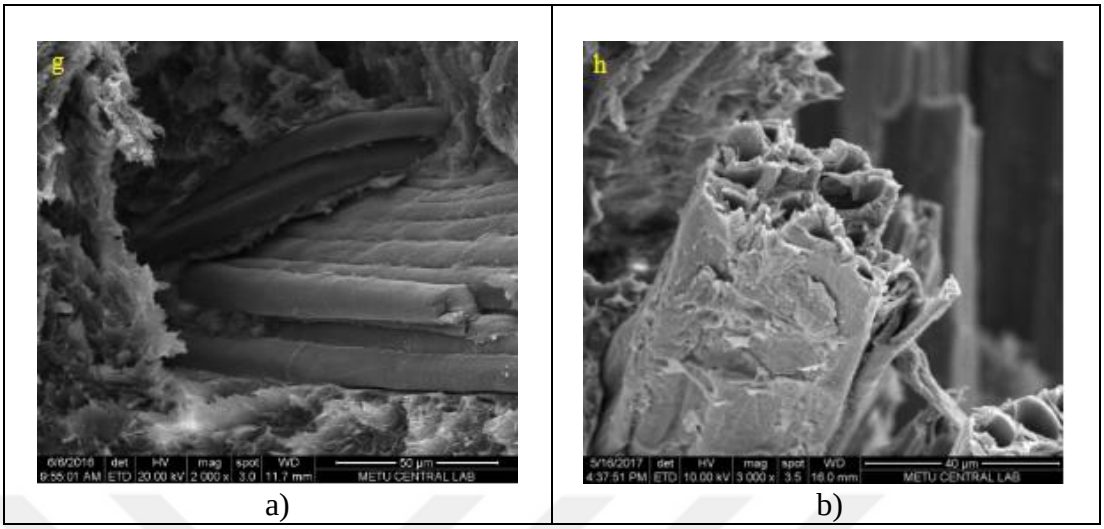


a) b)

Figure 3. 39. The flexural-fractured surface of NaOH +Silane treated over-molded composites (a) om-NaOH+Saılen 1,5% (b) om-NaOH+Saılen 3%

The change in the fibers surface results in a significant improvement in the adhesion between the matrix and the fibers in the Jute/PLA composites. With regards to the composites treated with (NaOH10%+Silane1.5%), it is observed that there is a layer on the fibers surfaces, therefore the fibers are not completely visible [39]; the coated layer is formed from siloxane deposition. See Figure 3.39. (g) and 3.39. (h).

The results show that the silane is an excellent way to improve the surface performance of the fibers; the production of interfering bonds increases the adhesion of the fibers to the matrix. An increase in the efficacy of Silane is observed after the treatment of fibers with NaOH [39].

### 3.4. The Flame Retardancy Properties of Composites

This part focuses on the physical, mechanical and thermal properties of over-molded flame retardant composites. In this work, continuous jute fiber/PLA composite layers are prepared via film stacking method in a hot press. By using injection-molding device from Xplore laboratory, the over-molded composites (OMCs) have been prepared. Prior to OMC manufacturing, PLA is compounded with a P/N based as flame retardant using an Xplore IM15. The mechanical, thermo mechanical (DMA) and morphological properties are investigated. Flame retardancy is examined via limiting oxygen index and UL 94 tests. The mechanical tests (flexural modulus and

strength) of OMCs is investigated in order to identify the most effective flame retardant for jute/PLA ecosheet and jute/PLA over-molded composites. For this reason 6 composite prepared (See table 3.10.) with different concentration.

Table 3. 10. Compositions of Different Materials

| Materials | Flame retardant (wt. %) | Jute-PLA (wt. %) | Orientation |
|---|---|---|---|
| 100Pg30-90%PLA | 100% (90/10) | 0% | - |
| 100Pg30-90%PLA+jute | 50% (90/10) | 50% (60/40) | 45 |
| 200Pg30-80%PLA | 100% (80/20) | 0% | - |
| 200Pg30-80%PLA-jute | 50% (80/20) | 50% (60/40) | 45 |
| 10APS-90%PLA | 100% (90/10) | 0% | - |
| 10APS-90%PLA-jute | 50% (90/10) | 50% (60/40) | 45 |
| 20APS-80%PLA | 100% (80/20) | 0% | - |
| 20APS-80%PLA jute | 50% (80/20) | 50% (60/40) | 45 |
| 10MPZ-90%PLA | 100% (90/10) | 0% | - |
| 10MPZ-90%PLA-jute | 50% (90/10) | 50% (60/40) | 45 |
| 20MPZ-80%PLA | 100% (80/20) | 0% | - |
| 20MPZ-80%PLA-jute | 50% (80/20) | 50% (60/40) | 45 |
| PLA100% | 0% | 0% | - |

Figure 3.40. And Fig. 3.41. Summarize the density of FR/PLA and jute/PLA composite. Neat PLA has 1.25 g/cm3 While Jute 1.46 and the materials used as anti-fire are (Ammoniumpolyphosphate with Synergists (APS) 1.6, Melamine polyphosphate and Zinc borate (MPZ) 1.6 and Aluminum diethylphosphinate (ADS) 1.35). But as is well known, after mixing the materials, these values will change. PLA and inert FR have been observed as a nucleating agent. This may be because of the inability of these substances to absorb gases. See Fig 3.40. There is a hypothesis based on the premise that at interfaces region, the decreasing of energy barrier increases the nucleation capacity of the cell compared to the neat PLA. This hypothesis is called (classical heterogeneous nucleation) [41]. A slightly increased value is observed in PLA/ADS and PLA/MPZ composite, respectively. The results of the density test confirm the nucleation hypothesis of the composite, where a big increase in the density values for PLA/APS composite is observed by about (1,52)g/cm3. In summary, the increase in volume with the decrease in density proves the formation of voids or the existence of gas bubbles, which enhances the anti-fire properties in the compound and that assures the future applications of PLA/FR.

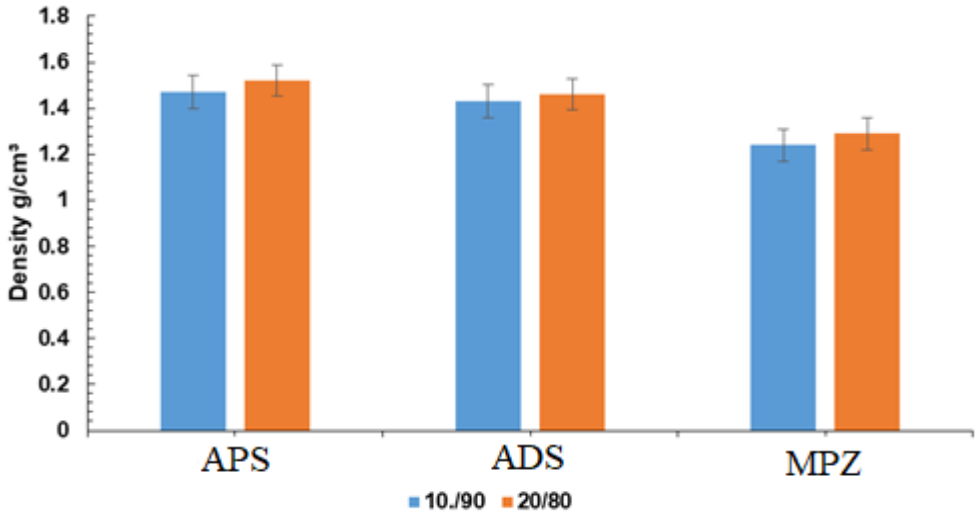


Figure 3. 40. The density of pure PLA/FR composite

In flexural mode, OM-PLA/APS (PLA/APS-jute) shows the modulus of 4.3 GPa and this is reduced with the PLA/APS to 1.7 GPa in 90/10%.

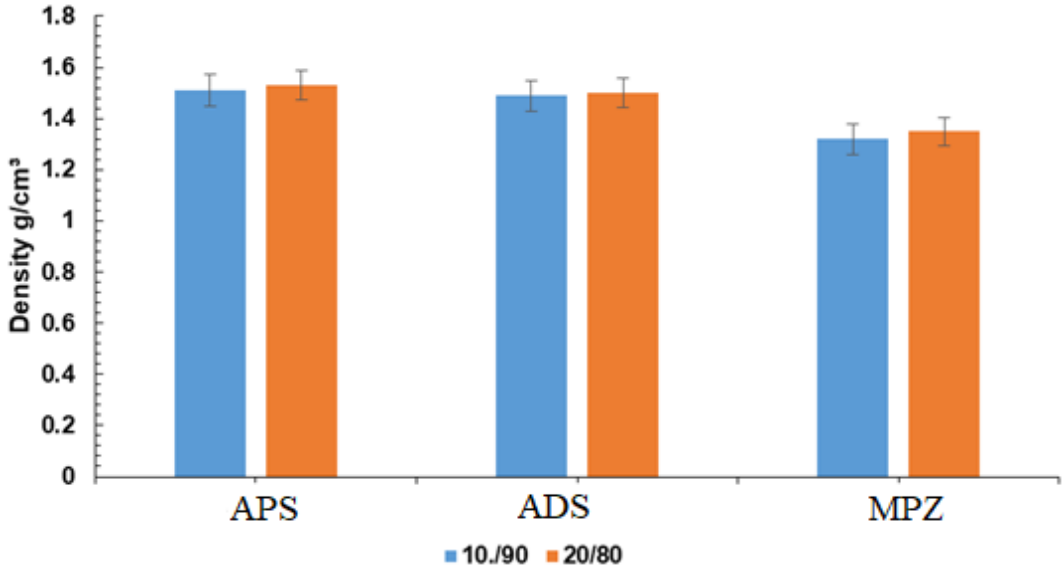


Figure 3. 41. The density of om-PLA/FR composite

In flexural mode, OM-PLA/APS (PLA/APS-jute) shows the modulus of 4.3 GPa and this is reduced with the PLA/APS to 1.7 GPa in 90/10%. That's due to the fact that flexural properties of composites are polymer matrix dependent rather than fiber reinforcement [12]; therefore, composites depending on PLA in mechanical properties will be subjected to a decrease due to interaction with APS.

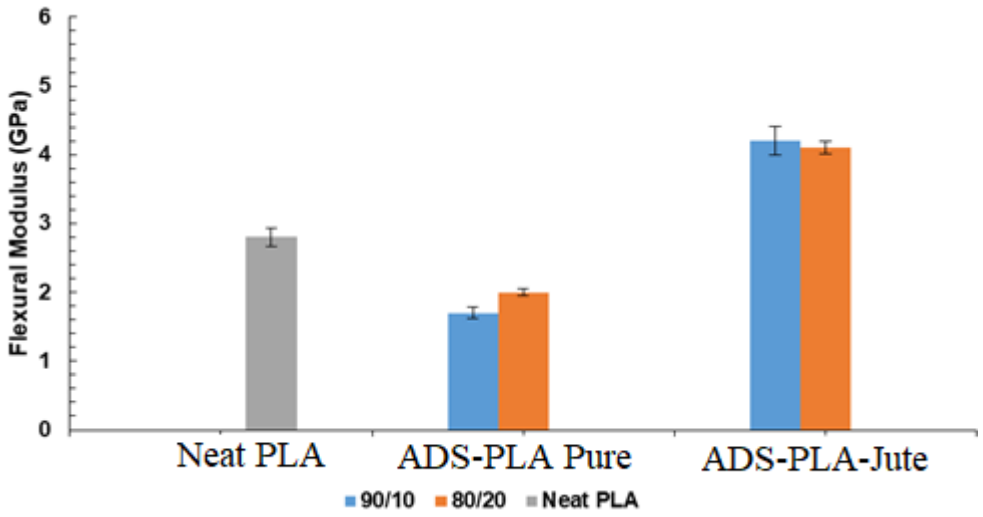


Figure 3. 42. The flexural modulus of ADS/PLA and om-ADS/PLA-Jute composite

On comparing the flexural results of PLA/MPZ with ecosheet and pure composites, ecosheet results show an increase in the flexural modulus of PLA/MPZ from 1.4 GPa in the 80/20 % to 3.8 GPa. Similar observation is also seen in the PLA/OP 30 samples. The OM-PLA/OP30 flexural modulus rise from 1.7 GPa to 4.2 GPa in 90/10%.

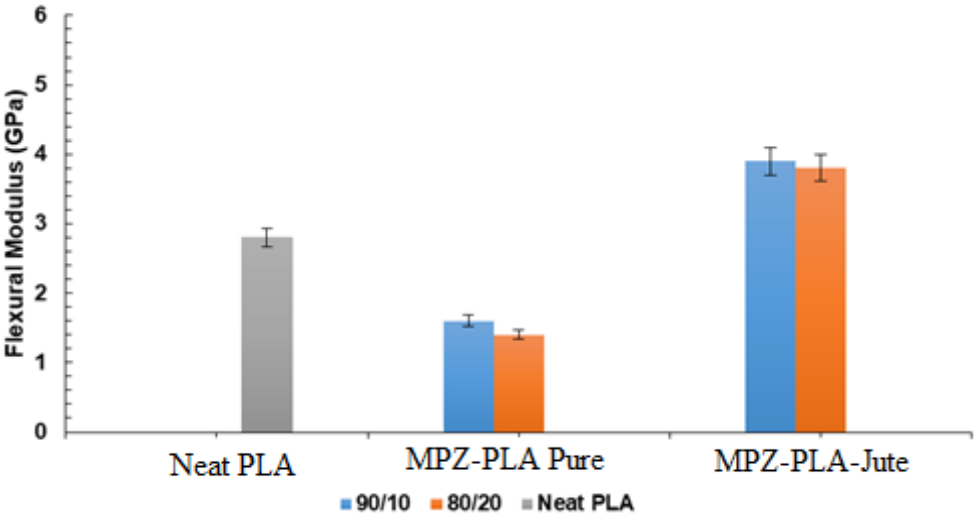


Figure 3. 43. The flexural modulus of MPZ/PLA and om-MPZ/PLA-Jute composite

The effect of ecosheet on Flexural Strength is similar to that on flexural modulus. The OM-PLA/APS composites from 80/20 % also show higher Flexural Strength than pure PLA/APS samples, Figure 3.44.

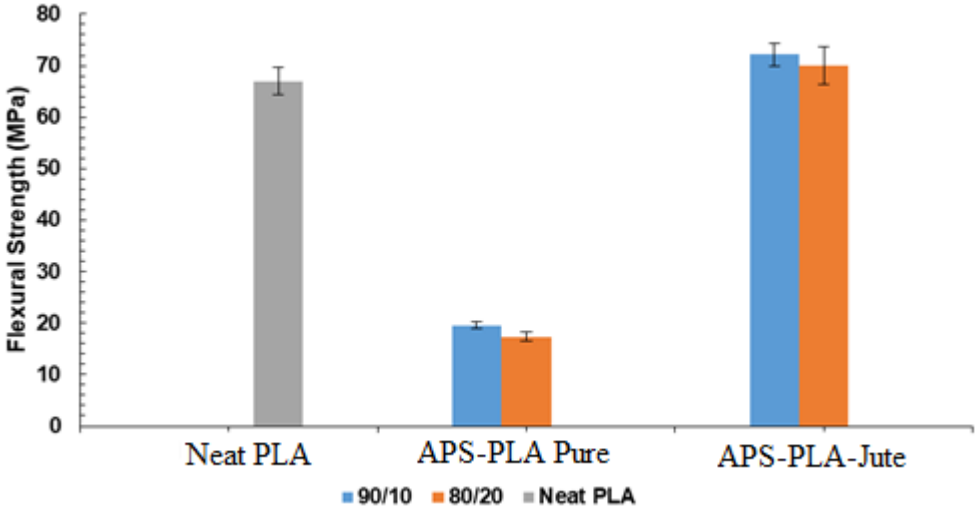


Figure 3. 44. The flexural strength of APS/PLA and om- APS/PLA-Jute composite

PLA/MPZ shows the flexural Strength of 24.1 MPa. When ecosheet is added to PLA/MPZ, the flexural modulus of increases to 73.8 MPa in 80/20%. The effect of ecosheet on flexural properties is also similar to those observed in tensile results. The flexural Strength of neat PLA and PLA/OP30 composites are lower than the OM-PLA/OP30 ones. The ecosheet increases flexural Strength of PLA/OP30 from 63.4 MPa in 90/10% sample to 96.4 Mpa.

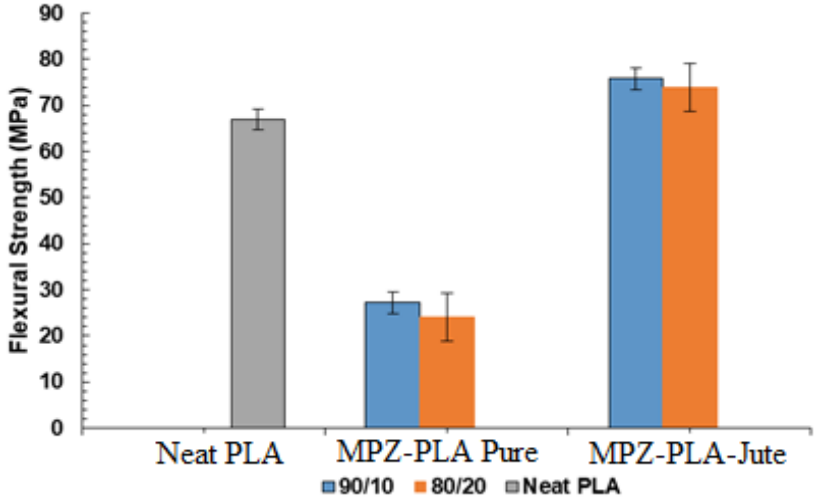


Figure 3. 45. The flexural strength of MPZ/PLA and om-MPZ/ PLA-Jute composite

The improvement in the fiber/matrix interfacial adhesion in OM samples can be explained when it's compared to the pure ones. Here the importance of interfacial

adhesion in the matrix-fiber region is worth noting, as this factor equals in its importance the factor of the dependence of flexural properties on the polymer matrix in composites. The improvement in fiber/matrix adhesion can lead to better load-transfer between fiber reinforcement and polymer matrix, and hence, results in higher flexural properties [16-18].

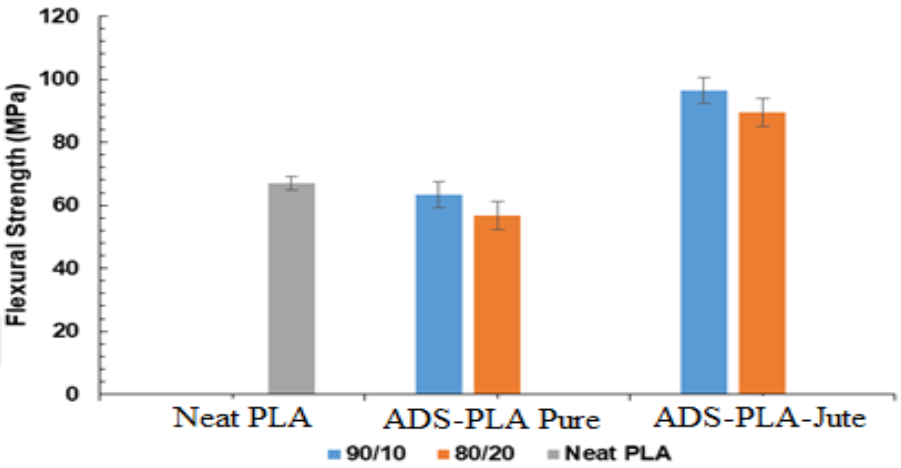


Figure 3. 46. The flexural strength of ADS/PL and om-ADS/PLA-Jute composite

The over-molded process helps in increasing the mechanical properties of PLA/APP which can be explained due to changes in the structure of PLA. Because of the interaction with the APP, the PLA surface becomes rough and the active groups interacting with the fibers increases, thereby, improves the adhesion significantly. From these results we can understand that ecosheet improves the mechanical properties of flame retarded PLA/APP composites. This increase make a better interfacial adhesion in the fiber/matrix of the composites. The increase in mechanical properties with over-molded process concludes that there is a big advantage of using an extra process during flame retardant composite preparation.

Figs 3.48, 3.50. And 3.52. Show the laboratory results of the tensile strength of the composites. As expected, neat PAL is unaffected by the extrusion and maintained high tensile strength with low ductility. An improvement in elongation at break is observed after adding Ammonium polyphosphate (APP) to PAL. At the same time, adding 10 % and 20% of APP adversely affects the tensile strength and rigidity of the composites. We expect that the addition of APP leads to a plasticizing effect on PAL

composites. From the extrapolation of the previous results, a perception is formed that the low molecular weight has a negative effect on the thermo-mechanical properties in composites. The difference in density and uptake of moisture are the most influencing factors, which can cause this results. As for moisture uptake, we face a problem that APP causes more moisture uptake in composites that contain wood [91]. This leads to a decrease in mechanical strength. In the same direction, PLA also absorbs moisture easily, which causes a hydrolytic degradation [90]. With the plasticizing effect due to increased water absorption, we notice an increase in the elongation at break and a decrease in the tensile strength [92,94]. Unfortunately, this is not the case here, because elongation at break does not increase compared to the Neat PLA, but on the contrary, it decreases .This may be due to the large amount of APP added to the polymer. Compared to neat PLA, many sources state that the intumescent formulations cause a decrease in the tensile properties of the composite and APP classifies as one of these substances [40, 42, 44, 48].

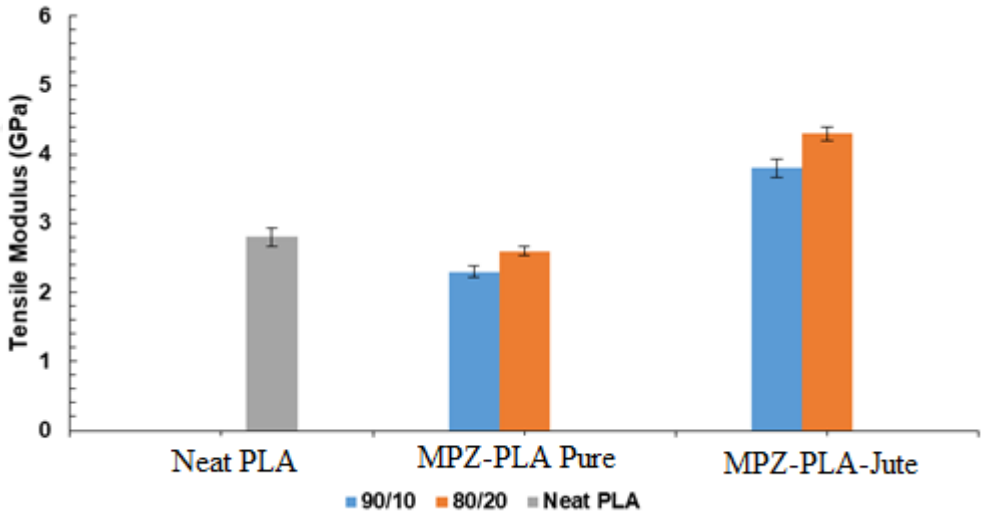


Figure 3. 47. The tensile modulus of MPZ/PLA and om-MPZ/PLA-Jute composite

Two points are observed when adding APS; molecular weight decreases (although APS dense naturally) and the samples become more brittle. APS damages the PAL network of its system, and this weakens the adhesion with jute fibers. With little APP contact with fibers, the plasticizing effect of APP remarkably decreases. The results in Fig 4.47. Show that neat PLA samples have tensile modulus of 2.8 GPa and tensile strength of 58 MPa. The addition of MPZ (20%) flame retardant reduces the tensile

modulus of PLA/MPZ (20%) to 2.6 GPa and significant reduction in tensile strength from 58 MPa to 47 MPa.

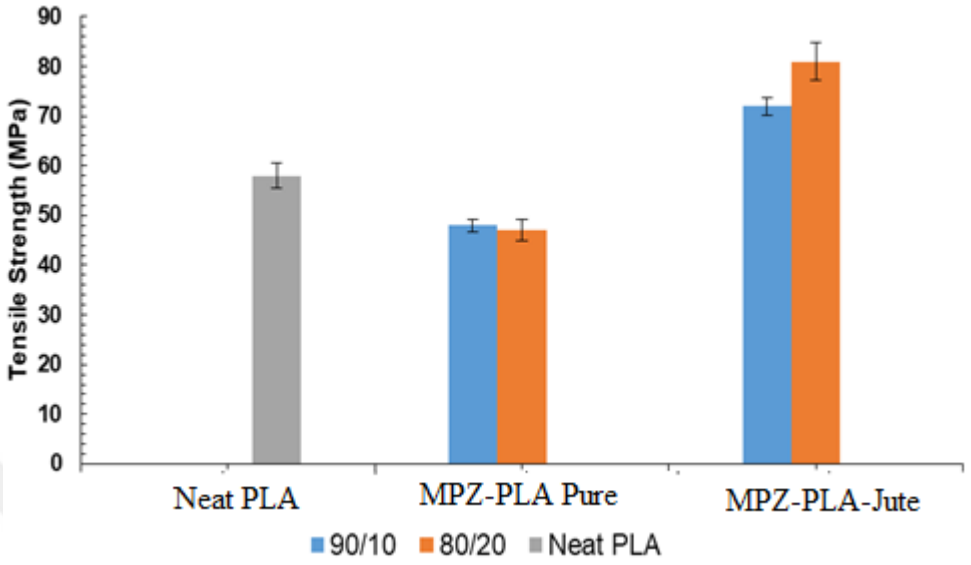


Figure 3. 48. The tensile strength of MPZ/PLA and om-MPZ/PLA-Jute composite

The significant reduction in the tensile properties of PLA/APP, particularly when compared to Neat PLA sample, can be explained by the fact that APP flame retardant produces ammonia (NH3), which can cause a degradation of PLA by hydrolysing the ester group (-COO-) in its polymeric structure, hence leading to a loss of mechanical properties of PLA and its composites [4].

On comparing the tensile results of PLA/ADS (90/10%) and PLA/ADS(80/20%), the results show that 90/10% slightly improves the tensile properties compared to 80/20 %, as shown by the increase in tensile modulus of PLA/ OP 30 from 3.7 Gpa for (80/20%) to 4.6 GPa in (90/10%). This can be attributed to the increased fraction of polymer matrix. This is due to the fact that OP30 has less tenacity than the PLA; this can be said for MPZ and APS too.

As for the results of the tensile modulus, compared to PLA/APS and PLA/MPZ, PLA/OP 30 shows a marked increase of about 50% and this is considered an important progress in this field. But we must not forget the primary goal of adding these substances, which is flame retardancy. It has been observed that MPZ and APS substances act as a filler in the composites and have close adhesion values.

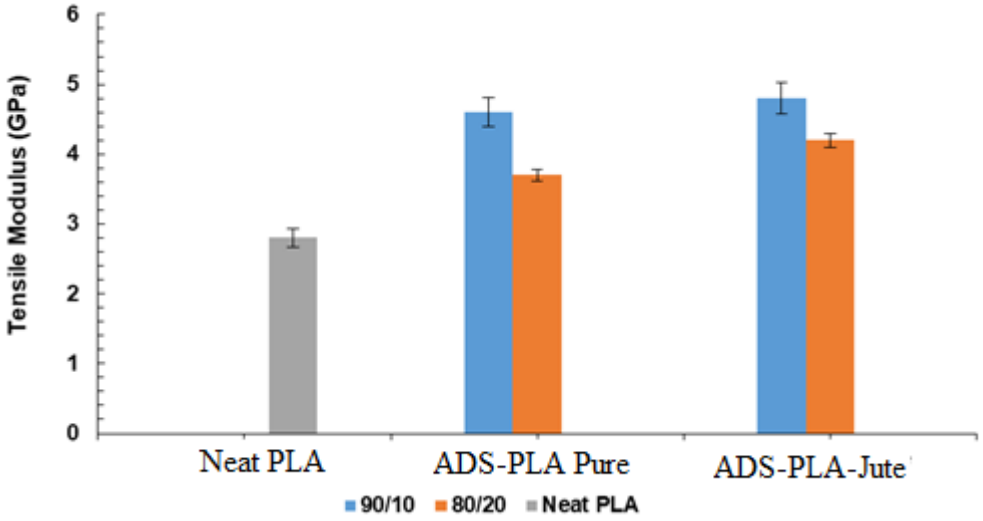


Figure 3. 49. The tensile modulus of ADS/PLA and om-ADS/PLA Jute composite

Also for comparison, the addition of 10% of APS shows a positive effect in the properties of tensile strength. The good dispersion for APS inside PLA matrix controls the tensile modulus as in 80/20 % where a decrease in the tensile modulus values is observed due to poor dispersion and the appearance of microscopic clusters that lead to an uneven distribution of the load which leads to the appearance of cracks in the matrix (Figure 3.52).

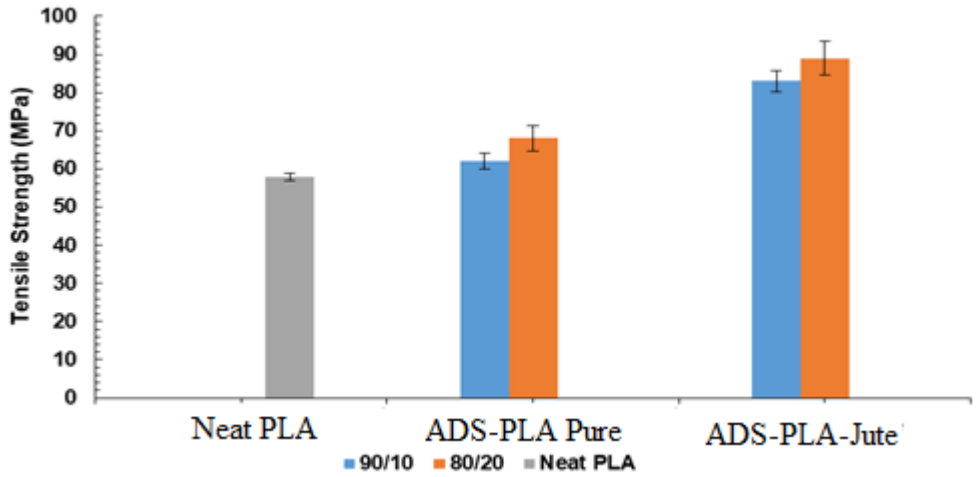


Figure 3. 50. The tensile strength of ADS/PLA and om-ADS/PLA-Jute composite

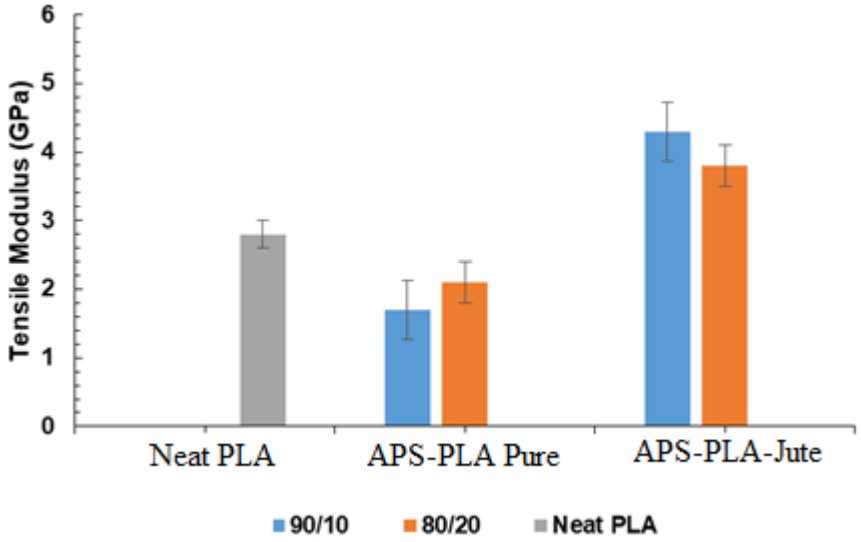


Figure 3. 51. The tensile modulus of APS/PLA and om-APS/PLA-Jute composite

APS dispersion varies with the chemical structure of the matrix. Tensile strength is severely affected by addition of APP. This effect results from reducing crystallinity of the matrix, which leads to a faster failure [50].

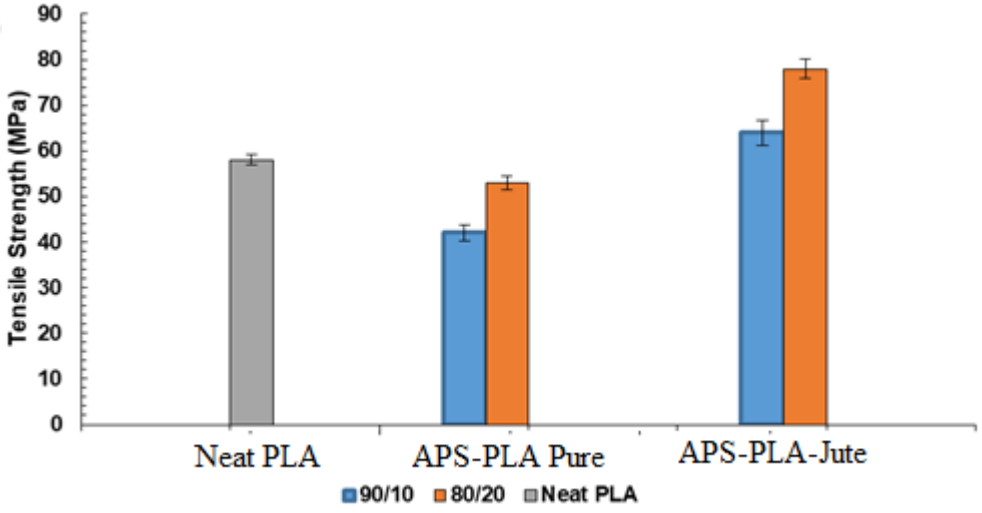


Figure 3. 52. The tensile strength of APS/PLA and om-APS/PLA-Jute composite

The introduction of jute improves the tensile strength and tensile modulus value up to 20 % due to that the treated fibers have more ability to form new bonds; these bonds increase the polymer-fibers adhesion. The hydroxyl groups in jute fibers are responsible for the new hydrogen bonds. This strong entanglement (or big

agglomerates) reduces the composite's ability to elongate; the elongation at break values decreases, and this accelerates cracking in the composites.

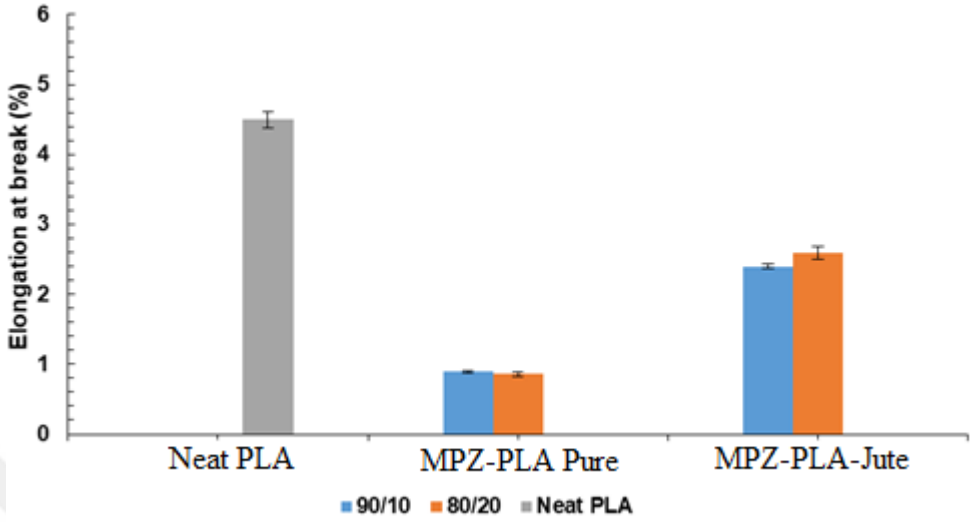


Figure 3. 53. The elongation of break of MPZ/PLA and om-MPZ/PLA-Jute composite

However, this weakness in the mechanical properties of flame retardant composite has been compensated. With the presence of the ecosheet, a significant increase in mechanical properties and high stability are observed compared with the pure materials and neat PLA. This gives these compounds a tensile strength which enables them to be used in many applications that are limited to materials with strong mechanical properties.

Phases I and II demonstrate that neat PAL has weak flame retardancy properties, on this basis a APP (as intumescent flame retardant), it was added to improve the flammability of ecosheet and composites in general. However, adding too much amount of APP to the composites may cause less tensile strength that limit applications. But the addition of jute shows enhanced mechanical properties of APP and PLA up to some extent. Figures 3.56-3.67. Show the flame-retarded PLA composites, modulus of storage, and tan δ of pure PLA. Modulus of storage associates to materials load-bearing capacity. As shown in Figure 3.56., the modulus of storage of pure PLA and the PLA /OP30 composites indicates a moderate decrease from 25 to 50°C, and then decreases speedily because of the glass transition.

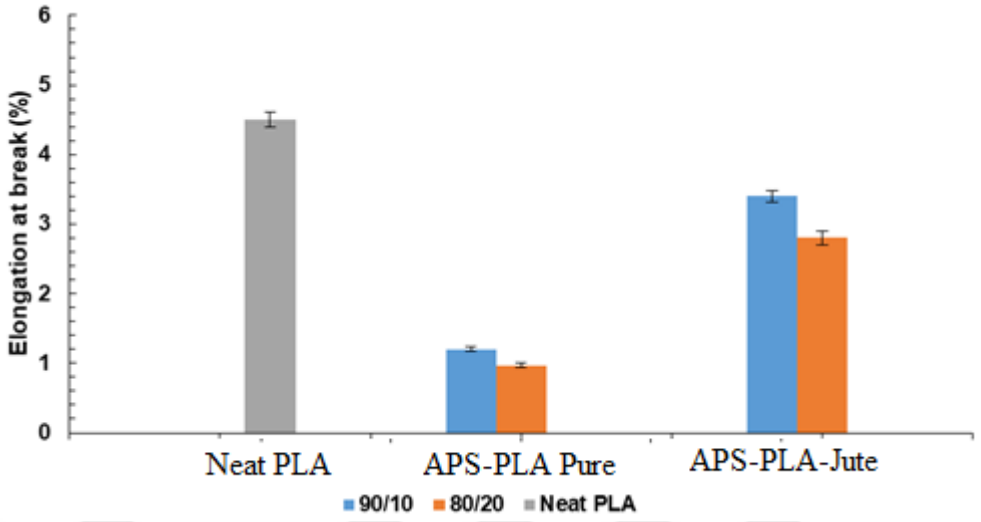


Figure 3. 54. The elongation of break of APS/PLA and om-APS/PLA-Jute composite

There is an evident increase in modulus of storage by the addition of OP30 in PLA matrix under 60 °C; for example, modulus of storage of the PLA/OP30 (80/20%) is nearly 2690 MPa, while that of pure PLA is 1855 MPa at 25°C as indicated in Fig 4.56. This increase is because of the flame-retardant effect on the crystallization behavior and the entanglement between the macromolecular flame retardant and PLA chains.

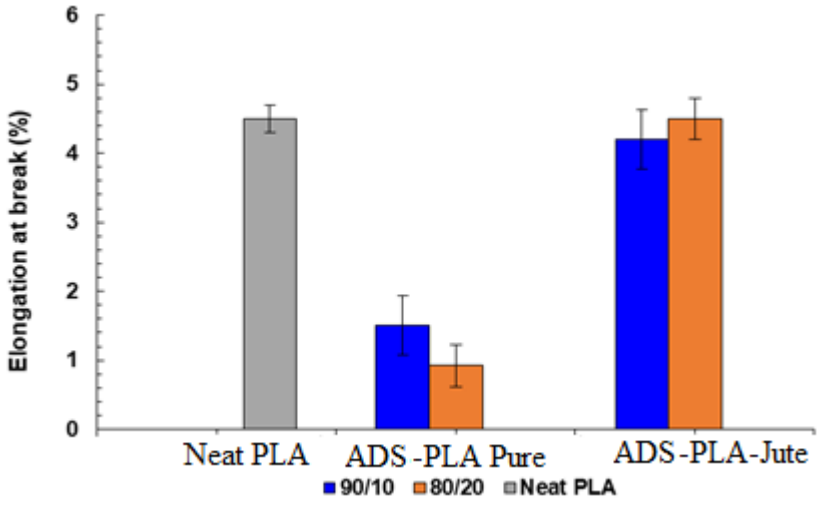


Figure 3. 55. The elongation of break of ADS/PLA and om-ADS/PLA-Jute composite

The region of glass transition for PLA and the flame-retarded PLA composites lies between 50 to 90 °C; and in this region, the modulus of storage of PLA composites is higher than that of pure PLA. For example, the modulus of storage for PLA/OP30 (90/10%) is nearly 651 MPa, while that of pure PLA is 1115 MPa at 60 °C. As seen in Figure 4.56. And in Fig 3.57., the glass transition temperature (Tg) for pure PLA is around 65 °C and the PLA/OP30 composites indicate higher peaks of temperature than that of pure PLA. The increase of modulus of storage in the glass transition state and the increase of Tg correspond that OP30 has antiplasticization effect on PLA/OP30. Furthermore, the maxima of tan δ for PLA/OP30 composites are increased compared with that of neat PLA, as shown Figure 3.57. Which shows that more polymer chains are taking part in the PLA transition composites with ADS.

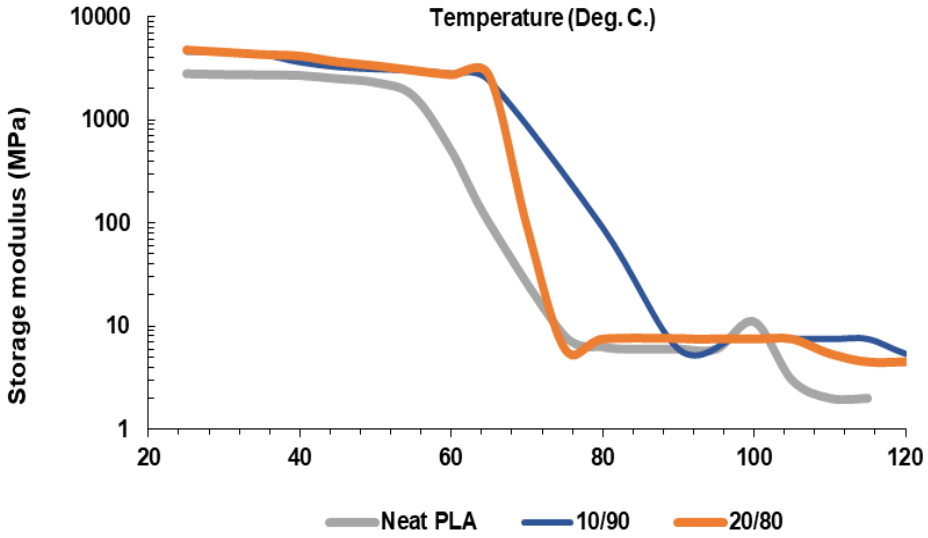


Figure 3. 56. The storage modulus of ADS/PLA composite

Dynamic mechanical analysis (DMA) for the PLA and PLA/APS acts as a function of temperature, whose curves display storage modulus (E'),and loss factor (tan δ) are recorded as shown in Figures 3.58. And 3.58. Correspondingly. Figure 4.58. Shows the storage modulus (E') which is the temperature dependence of PLA/APS with (80/20%) and (90/10%) correspondingly. The decrease of storage modulus below Tg with APS continuously enhances the mobility of polymer chains. E' curve of the blends shows a short plateau in comparison with treated PLA. Especially in (80/20%) comparing to (90/10%) which is because of a decrease in thermal mechanical stability when adding APS in PLA. The addition of APS in PLA is often reported to lower the stiffness [24].

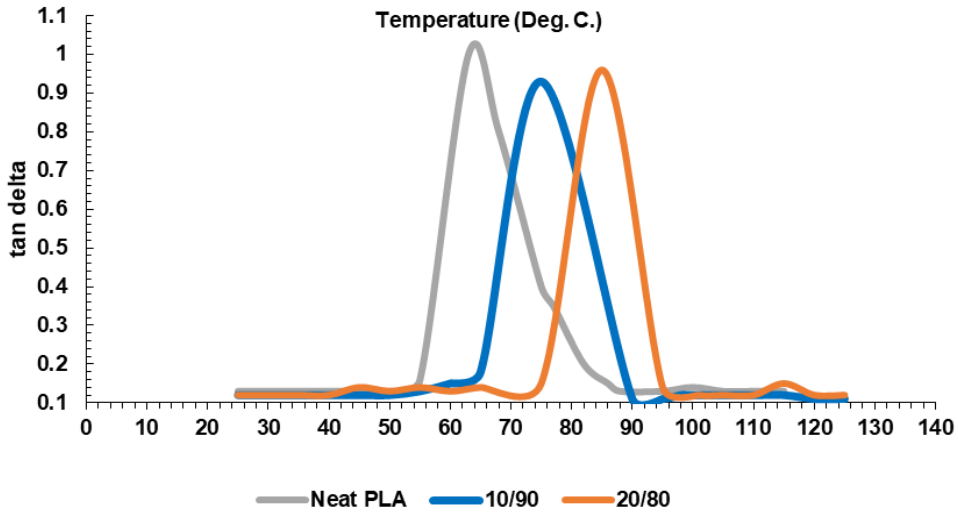


Figure 3. 57. Tan delta of ADS/PLA composite

Especially in (80/20%) comparing to (90/10%) which is because of a decrease in thermal mechanical stability when adding APS in PLA. The addition of APS in PLA is often reported to lower the stiffness [24].

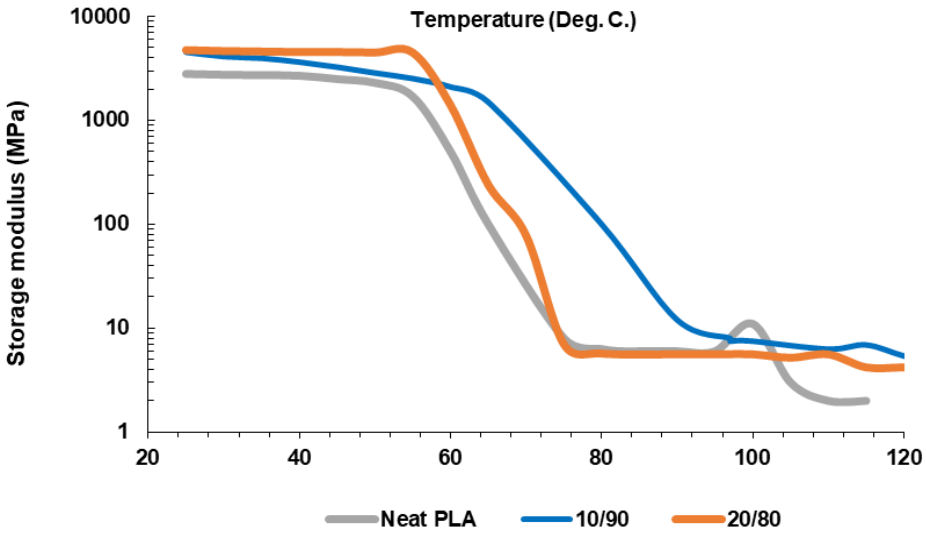


Figure 3. 58. The storage modulus of APS/PLA composite

Cold-crystallization process is the reason behind the decrease of E' with temperature and the presence of bumps in the tan δ curves after the glass transition [25]. It is also noted that the energy needed to activate molecule mobility in the material has different compositions. The increase of APS amount decreases the height of peak in tan δ curves with less displacement to a higher temperature as compares to neat PLA

.This indicates that the molecular mobility in the PLA/APS is easily activated as compares to PLA alone.

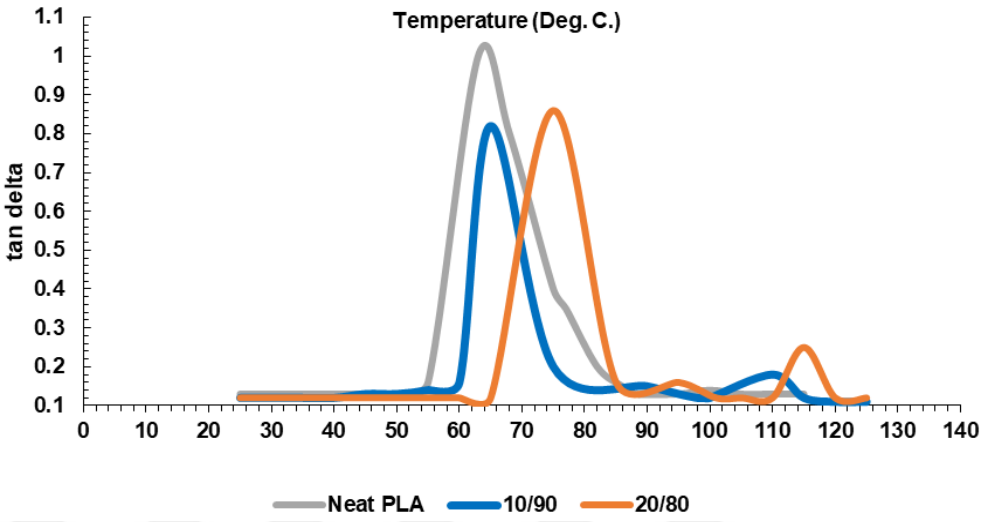


Figure 3. 59. Tan delta of APS/PLA composite

The cooperative increases with the decrease disorder; so the energy needed to initiate molecular mobility of material decreases with the increase of the disorder of any one.

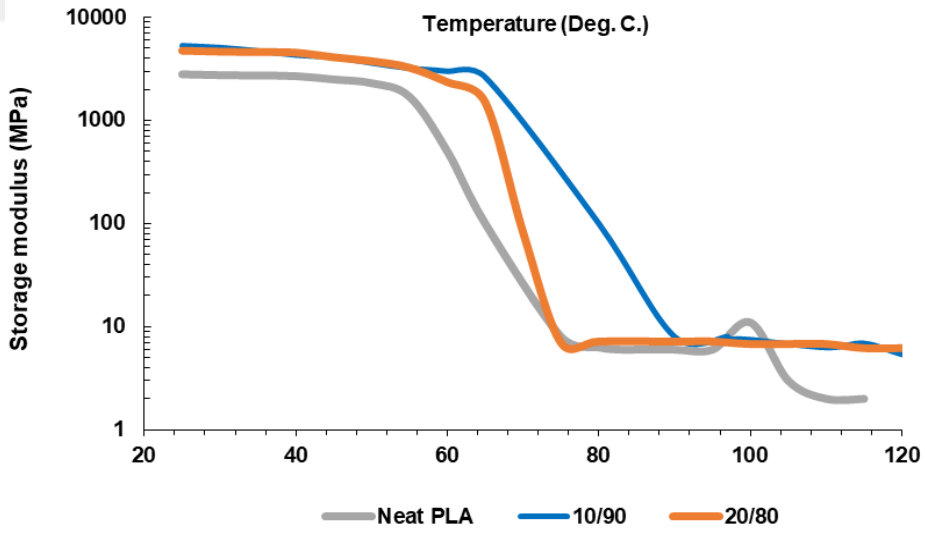


Figure 3. 60. The storage modulus of MPZ/PLA composite

As showed in Fig. 3.60., addition of the MPZ lead to a slightly increase of stiffness, a higher Tg, and a higher crystallization temperature. In these reductions, molar mass of PLA reduces in the composite. This may be due to the penetration of MPZ into a PLA chain, which has increased its adhesion and cohesion for a short period by

comparing the MPZ (80/20%) with MPZ (90/10%). (90/10%) increases the crystallization temperature and storage modulus over pure PLA.

Figure 3.61. shows the PLA/MPZ composites and tan δ vs. The temperature for the PLA Tg of pure PLA is 64°C, while the PLA/MPZ shows single peaks at 78, for (80/20%) and atg 79°C for (90/10%). The tan δ values of all PLA/MPZ composites are less in comparison to PLA.

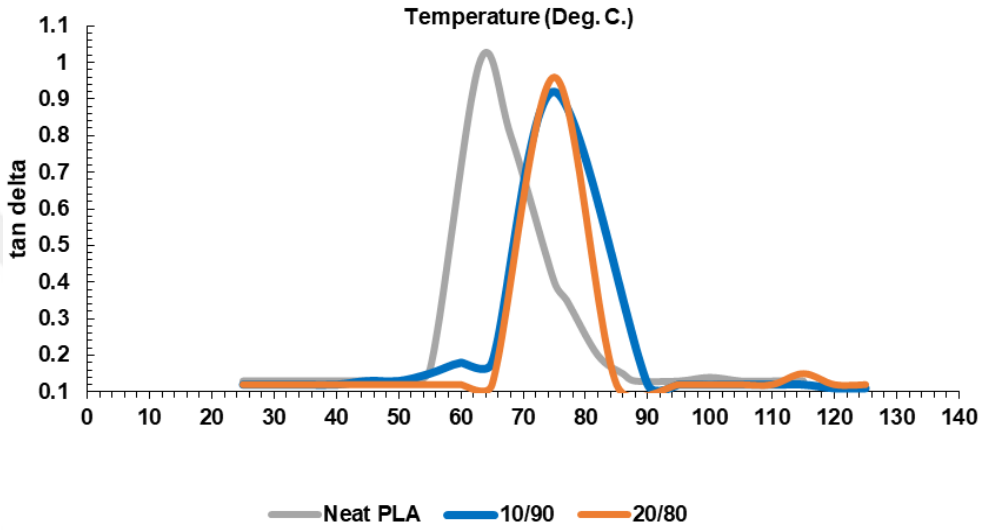


Figure 3. 61. Tan delta of ADS/PLA composite

Jute fiber composites usage has more beneficial polymer properties in comparison with based sources PLA. The most notable difference is observed in the composite viscoelasticity and properties like mechanical strength. The viscoelastic properties of solid composites are measured by a dynamic mechanical analyzer (DMA). DMA gives the information of viscoelastic polymers properties. The peak of tan δ curve is described as glass transition temperature (Tg). Load bearing capacity is intently related to storage modulus. Compared to composites whose ecosheet has been added with PLA/FR, we can clearly say that it is in PLA/FR composites. There is an obvious decrease in storage modulus after incorporating of FR into the pure PLA composites. The lack compatibility between the flame retardant and PLA lead to a decrease in modulus of storage; nevertheless, the addition of ecosheet has promising impact on the modulus of storage of PLA/FR composites. PLA/FR composites with ecosheet have higher storage modulus than the pure ones. That is possible because of the hydrogen bonding interactions between jute fibers and the PLA matrix which

increases the interfacial adhesion. In general, modulus of storage of polymer fibers relies on inorganic phase and interfacial interaction of the polymer matrix [261]. The modulus of storage of all over-molded samples somewhat decreases with an increase of temperature and has a different fall due to each type of FR material; for example, in MPZ it lies in the region between 90 to 99 °C, in OP30 it lies between 55 to 78 °C, and in APS it lies between 60 to 78 °C respectively to glass transition region of PLA/FR. Moreover, there has been another peak showed in the DMA for jute or the ecosheet in the far area (+15-20 °C) that increases the materials mechanical properties that allows the usage of the materials for applications that cannot be retrieved due to their vulnerability.

Figure 3.62. Indicates the ecosheet influence on dynamic storage modulus of the PLA/MPZ composites on various temperatures. In Figure 3.62., the E′ values of the OM-PLA/MPZ composites are greater than that of PLA/MPZ. This statement advises that the interfacial adhesion between the PLA/MPZ matrix and jute fiber is spontaneous. The E′ values decreases with an increase of temperature in all composites cases. OM-composites indicate that there is longer plateau on modulus of storage than that of neat PLA where the temperature of softening has increased from around 65°C for neat PLA and 85°C for PLA/FR. This suggests an increase in thermal stability of the neat PLA with addition of jute fiber.

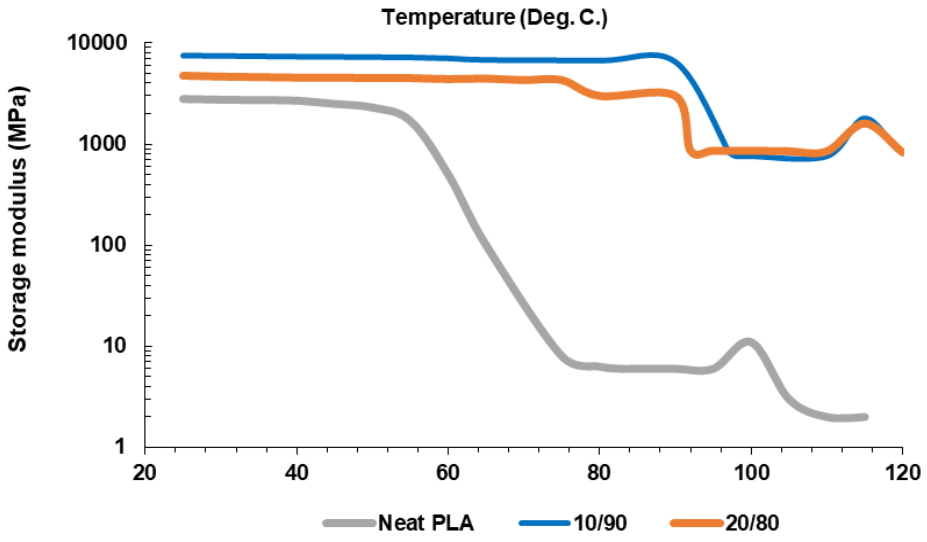


Figure 3. 62. The storage modulus of om-MPZ/PLA-Jute composite

By heating, polymer state changes from rigid to elastic by movement of molecular chains in the structure. In the fiber-reinforced PLA, damping is affected by the fibers presence. The ecosheet effect on PLA/MPZ composites is demonstrated in Figure 3.62.; it is noticeable that the magnitude of damping peaks composites increases by increase of MPZ amount. A good interface will carry greater stress and there will be less energy dissipation. Moreover, a composite material that has less interfacial bonding dissipates more energy that shows a greater magnitude damping peak as compared to a composite with a strong bonded interface [95].

Based on the current research, the verified increase of tan δ by the decrease of compatibility between jute fiber the PLA/MPZ matrix; that can be detected with SEM images that have been defined lately.

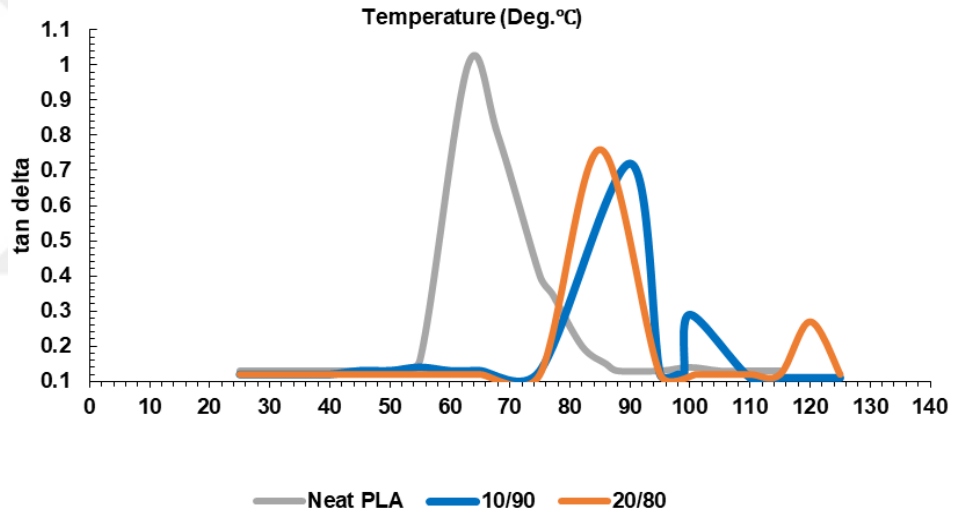


Figure 3. 63. Tan delta of om-MPZ/PLA-Jute composite

Figures 3.64. And 3.65. Show the dynamic storage modulus (E′) of OM-PLA/OP30 composites in a range of 20–140°C. The significant improvement in the E′ is shown in Figure 3.64. When ecosheet of around 2 mm in length is added to the PLA/OP30 matrix [96, 85]. An unclear drop is detected at the PLA/MPZ matrix at 58–72°C temperature that is connected with the glass transition (Tg) of PLA/OP30. After that a clear drop is detected at temperature of 85–98°C that is related Tg of ecosheet. The E′ values are continuously dropping after glass transition region. The greater E′ above Tg is accredited to inadequate thermal energy to overcome the potential barrier of rotational motions and transitional of segments of molecules of the

polymer in the glassy state, while above Tg, the thermal energy is comparable to potential energy barriers to the segmental motions.

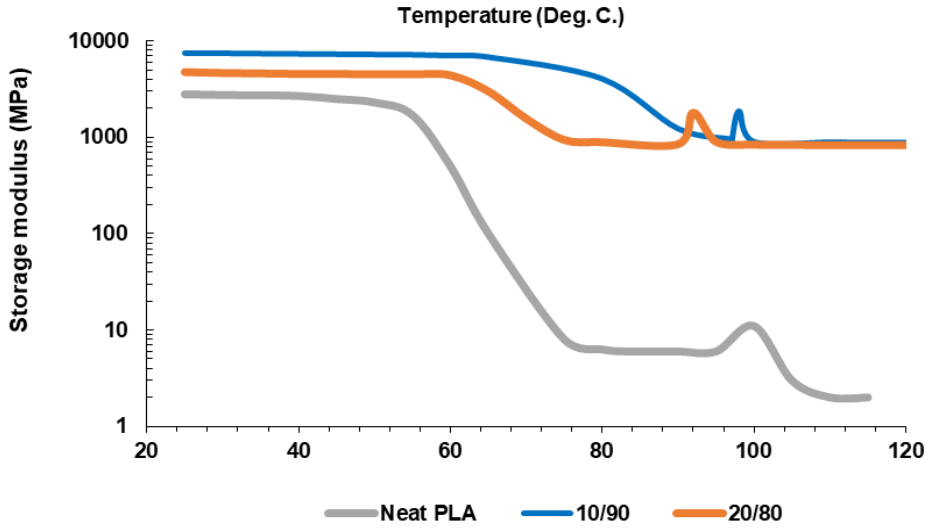


Figure 3. 64. The storage modulus of om-ADS/PLA-Jute composite

Figure 3.65. Shows the OM-PLA/OP30 and of tan δ of PLA/OP30 thermograms of tan δ. It has been noted that Tg shifts to higher temperature by adding jute. Contribution of fiber into damping is tremendously low in comparison to the PLA matrix. But the fibers of jute contributes to a flexible increase in Tg for PLA/OP30. We come to the conclusion that the PLA molecular motion at the fiber-matrix interface is usually liable by combined attenuation (damping) of jute fiber reinforced PLA composites. [87].

Figure 3.66. Indicates the additional effect of ecosheet for modulus of storage of PLA/APS composites. E′ is strictly associated to the material load-bearing capacity [86]. The value of E′ increases considerably by the addition of ecosheet to PLA/APS composites, specifically 60–85°C temperature. Moreover, more addition of APP flame-retardant in composites hinders the collaboration between PLA matrix and jute fiber that results in the decrease of E′. It is concluded that the E′ value increases because of strong interfacial adhesion and strong bond between fiber and matrix [86].

In Figure 3.67., it is obvious that OM-PLA/APS composites have lowered tan δ values in comparison to PLA/APS. This shows that all the OM-PLA/APS composites exhibit the similar order of abilities of damping. The reason of the rigid and strong

fiber-matrix interface is the better adhesion due to this molecular mobility decreases in interfacial zone.

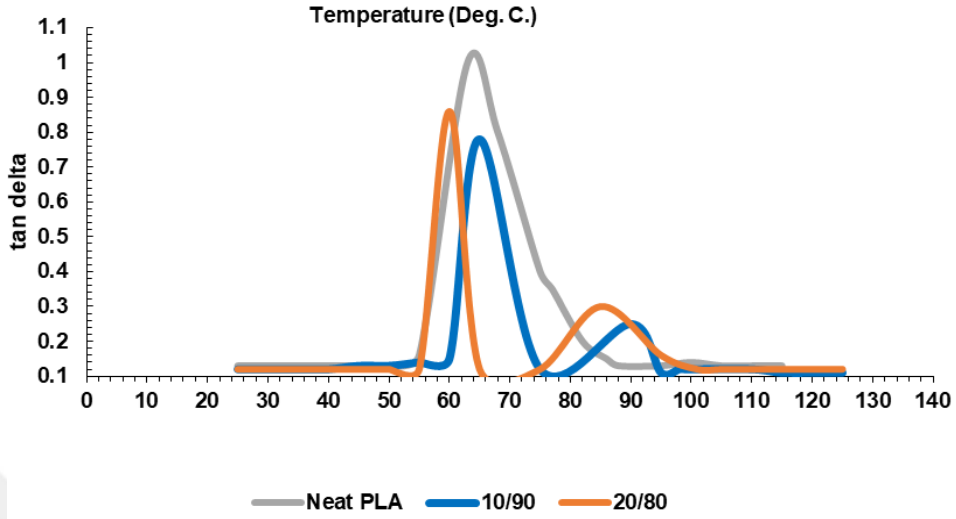


Figure 3. 65. Tan delta of om-ADS/PLA-Jute composite

In the course of the previous heating scan, the cold crystallization, glass transition, and melting temperature of the material are calculated. DSC data can be used to calculate the degree of crystallinity (Xc) as follows:

$$Xc(\%) = \frac{\Delta Hm - \Delta Hcc}{\Delta Hf \Delta XPLA} \times 100 \quad (3.2)$$

Where:

ΔHm, ΔHcc and XPLA are the enthalpy of melting, enthalpy of cold crystallization and weight fraction of PLA respectively;

ΔHf is the heat of fusion defined as the melting enthalpy of 100% crystalline PLA which is 93 J.g–1[22].

The PLA/MPZ and OM-PLA/MPZ differential scanning calorimetry (DSC) results are presented in Figure 3.68. And precised in Table4.11. The MPZ increases the glass transition temperature (Tg) of PLA from 60.42 °C to 10.29 °C and to 12.21 °C with (80/20%) correspondingly. As expected, with the increase of MPZ amount, a decrease in Tg take place, and that is accurate for MPZ.

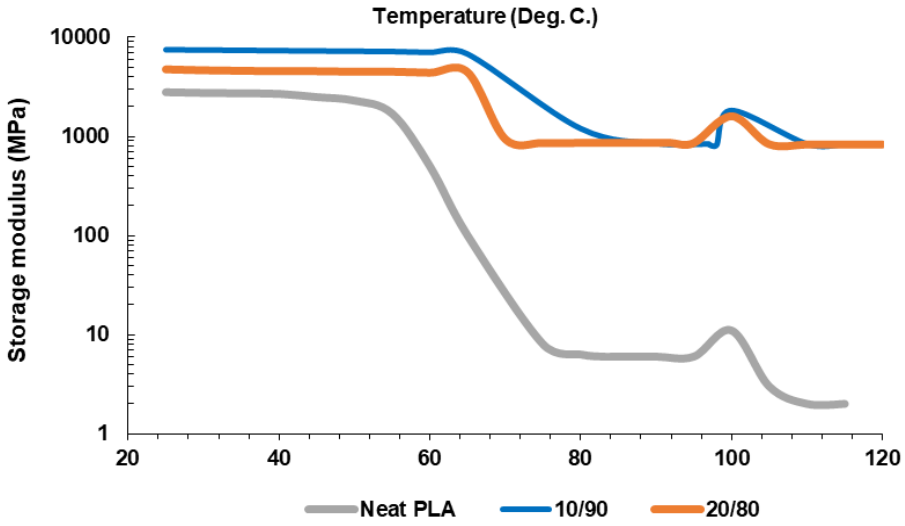


Figure 3. 66. The storage modulus of om-APS/PLA-Jute composite

The small molecular size of the FR permits it to occupy the intermolecular places among polymer chains. Decreasing the molecular motion energy leads to hydrogen bonding formation among the polymer chains; and that can increase the molecular mobility and the free volumes. By the increase of amount of the MPZ, the effectiveness of the Citrate FR to lower the Tg of the PLA is usually enriched [20].

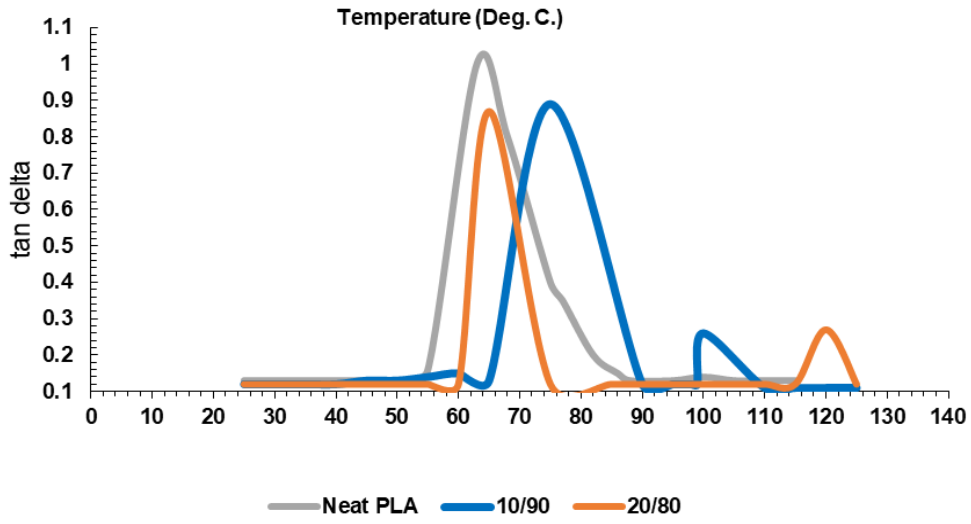


Figure 3. 67. Tan delta of om-APS/PLA-Jute composite

As for the PLA/MPZ, the addition of ecosheet disturbs the cold crystallization temperature (Tcc). The Tcc detected in PLA/MPZ at 130.94 °C is down to 71.72°C and then to 69.26 °C by the addition of (80/20%) correspondingly. The decreasing of Tg, Tcc and melting temperature (Tm) are higher with the jute fibers by the result of

improved chain mobility [23]. The rise of Tg, Tcc, Tm and also increase of degree of crystallinity as indicates in Table 4.11. Depend on the jute fibers. The crystallinity percentage of the OM-PLA/MPZ is greater in comparison with the PLA/MPZ. For the OM-PLA/MPZ, greatest crystallinity is detected by the addition of (80/20%) to a value of 8.58%, at the rate of 9.07%. The increase indicates that the PLA crystallization turn out to be hard due to chains mobility which takes place with the jute. The function of a FR is to rise the free volume and to lower the polymer chain connections that bring higher chain mobility at lesser temperature; this effect is associated with plasticization which is most probably superposed by the reduction of the glass transition temperature owing to chain mobility [19].

The PLA chain mobility becomes harder and free volume becomes lesser due to jute fibers that influence the thermal properties of PLA /MPZ positively while the relationship becomes symbiotic, giving the compound a higher ability to resist thermal effects and this is an added advantage of the over-molded process in this research.

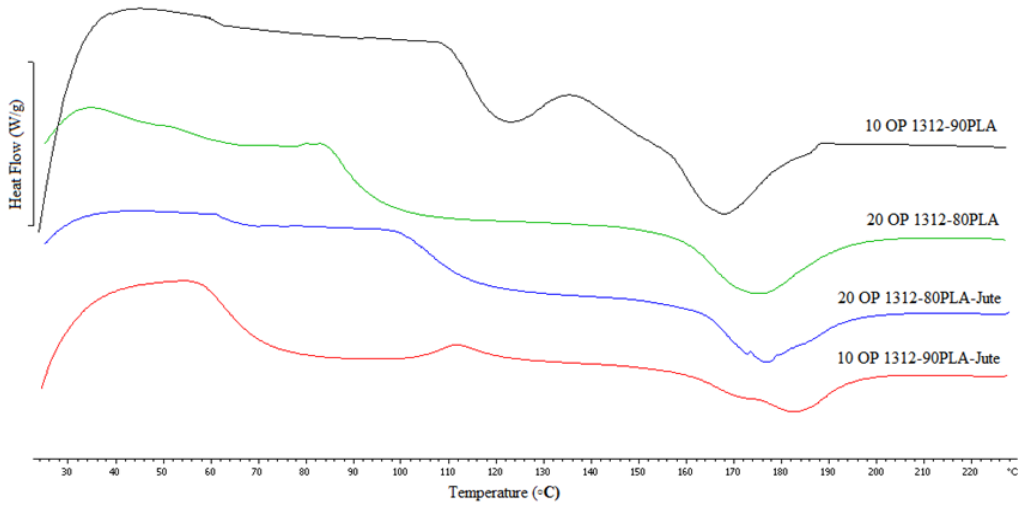


Figure 3. 68. The DSC of MPZ/PLA and om-MPZ/PLA-Jute composite

Thermal properties of PLA/APS and OM-PLA/APS are investigated by DSC. The DSC data are shown in Table 3.11. It can be seen that the glass transition temperature (Tg) of PLA/APS is lower than that of the OM-PLA/APS. [44] This may be related to the structures of APS. The basic change tendency of Tg caused by the different structures is consistent with the literature [9, 45–47]. What's more is that the Tg of

the samples of (90/10%) and (80/20%) are basically close to 60 °C and greater than neat PLA. Relatively, the regularity of different cores of PLA/APS is lesser, and all molecules have a higher rigidity, that is not valuable for the motion of molecular segment. However, the Tg of the PLA/APS is higher. The addition of jute displays two falls in the DSC curve; the mechanism of the OM-PLA/APS gives two-step thermal degradation, whereas the PLA/APS contains only one fall in the range of Tg [17]. The decomposition of composite with ecosheet is not same as of PLA/APS decomposition, that is only thermal degradation of one step [17] .In a two-step thermal degradation, the first one contains decomposition of OM-PLA/APS that is thermal decomposition of PLA/APS chain, while the second one is the residual decomposition of ecosheet containing jute. In comparison with instantaneous splitting of the whole polymeric chain in thermal decomposition of PLA/APS [17], this change exhibits that the OM-PLA/APS has more challenging to be decomposed in a conditions of common heating; it proves that APS may lead to a potential polymeric flame retardant that is useful for PLA materials also.

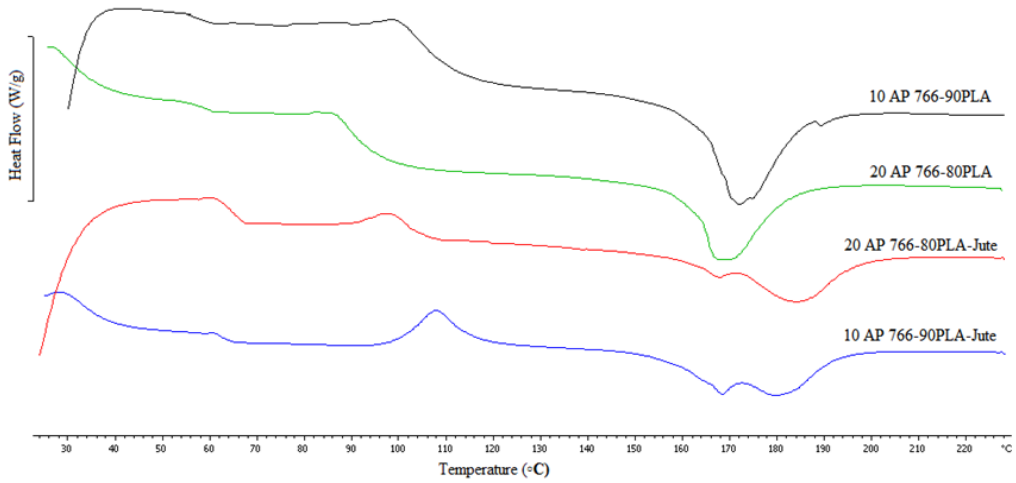


Figure 3. 69. The DSC of APS/PLA and om-APS/PLA-Jute composite

PLA/ADS thermal properties are tested by DSC, and the data of some important temperatures are shown in Fig 3.69. The results suggest that with the increase of the ADS ratio, the glass transition temperature (Tg) of PLA/ADS gradually increases due to the relatively longer PLA chain and more ADS which leads to the creation of more nuclei working to increase the interdependence which impedes the chain shift which decreases the molecular flexibility. Of course, Tg of (90/10%) is slightly

lower than that of (80/20%) as well, and the reason may be that the FR has relatively bigger distribution in PLA chains (Table 3.11); therefore, the results exhibit that the introduction of ADS into PLA chain affects the thermal properties of PLA material. More importantly, it has an important influence on the thermal decomposition temperatures which is crucial to a good flame retardant.

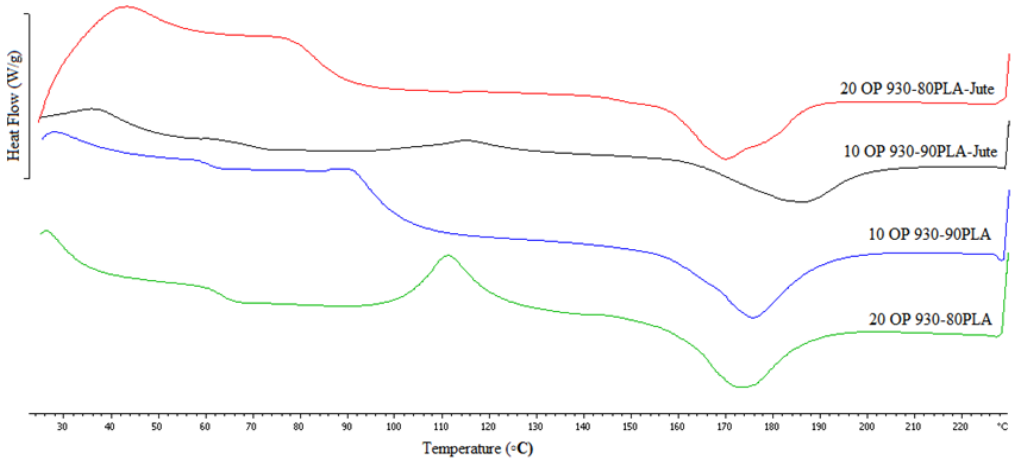


Figure 3. 70. The DSC of ADS/PLA and om-ADS/PLA-Jute composite

The UL-94 results in Table 3.12. Show that OM-PLA/ADS fails the vertical rating test. This indicates the lower flammability of OM-PLA/ADS compared to the PLA/ADS which has higher vertical rating. The inclusion of ADS in PLA composite significantly reduces the flammability of PLA/ADS and it can be seen that ADS improves the vertical rating of PLA from 'norating' in the neat PLA to V-2 rating in the PLA/ADS, Table 3.12. The Jute fabric, on the other hand, prevents the flame from completely disappearing during dripping, that is, the flame has a carrier effect and causes the material to burn up to the holder. ADS acts on both gas and solid phase in heteroatom-containing polymers such as PLA. PLA capture the hydroxyl radicals in the gas phase by increasing phosphate-based radicals in the gas phase, and to increase the drop formation and ash formation in the solid phase. The difference between ADS from (90/10%) and (80/20%) could not be identified as both samples passed V-2 rating. In summary, the UL-94 results of PLA/ADS and OM-PLA/ADS composites have shown that ecosheet has a negative effect as it slightly increases the flammability of OM-PLA/ADS composite. By adding jute, it increases the burn rate and also bring about the complete consumption of the test bars in OM-PLA/ADS.

Table 3. 11. The data of important temperatures of FR/PLA and om-FR/PLA

| name | $T_g$ (°C) | $T_m$ onset (°C) | $T_m$ midpoint (°C) | X (%) | $\Delta H$c (J/g) | Tc (°C) |
|---|---|---|---|---|---|---|
| PLA | 58.19 | | 148.60 | 39.38 | 28.17 | 110 |
| 10ADS-90%PLA | 62.28 | 163.38 | 186.33 | 33.54 | 29.54 | 117.3 |
| 10ADS-90%PLA+jute | 65.24 | 161.85 | 175.71 | 35.52 | 31.24 | 119.2 |
| 20ADS-80%PLA | 63.8 | 160.75 | 172.13 | 31.24 | 27.54 | 108.8 |
| 20ADS-80%PLA-jute | 67.12 | 161.93 | 171.24 | 33.62 | 28.36 | 110.1 |
| 10APS-90%PLA | 60.31 | 162.31 | 171.60 | 33.68 | 29.68 | 112.3 |
| 10APS-90%PLA-jute | 67.14 | 163.46 | 179.51 | 35.84 | 31.69 | 119.9 |
| 20APS-80%PLA | 61.38 | 161.75 | 168.03 | 30.62 | 27.89 | 114.5 |
| 20APS-80%PLA jute | 71.24 | 174.40 | 184.70 | 34.64 | 28.77 | 119.8 |
| 10MPZ-90%PLA | 69.24 | 155.72 | 167.63 | 33.95 | 29.81 | 118.9 |
| 10MPZ-90%PLA-jute | 72.64 | 162.23 | 182.21 | 36.14 | 31.98 | 121.5 |
| 20MPZ-80%PLA | 69.02 | 159.17 | 174.28 | 31.64 | 27.85 | 115.2 |
| 20MPZ-80%PLA-jute | 70.35 | 163.89 | 176.90 | 34.92 | 29.01 | 120.5 |

The UL-94 results in terms of vertical orientation are reported in Table 3.13. In the vertical test, the OM-PLA/MPZ and OM-PLA/APS succeed the vertical rating. The specimens are not completely burned which indicates the high fire resistance of ecosheet and PLA/FR composites.

Table 3. 12. The UL-94 results of PLA/ADS and om-PLA/ADS composites

| | First ignition time (s) | second ignition time (s) | dripping | complete burn | classification |
|---|---|---|---|---|---|
| Neat PLA | 5,8 | 13,4 | yes | yes | no rating |
| 10 ADS 90%PLA | 29 | 6,8 | yes | no | V-2 |
| 10 ADS-90% PLA +jute | 146 | 0 | yes | yes | failed |
| 20 ADS-80%PLA | 18,5 | 11,4 | yes | no | V-2 |
| 20 ADS 80% PLA +jute | 123 | 0 | yes | yes | failed |

All samples succeed the vertical rating test, except for OM-PLA/MPZ (80/20%) where V-2 rating is achieved.

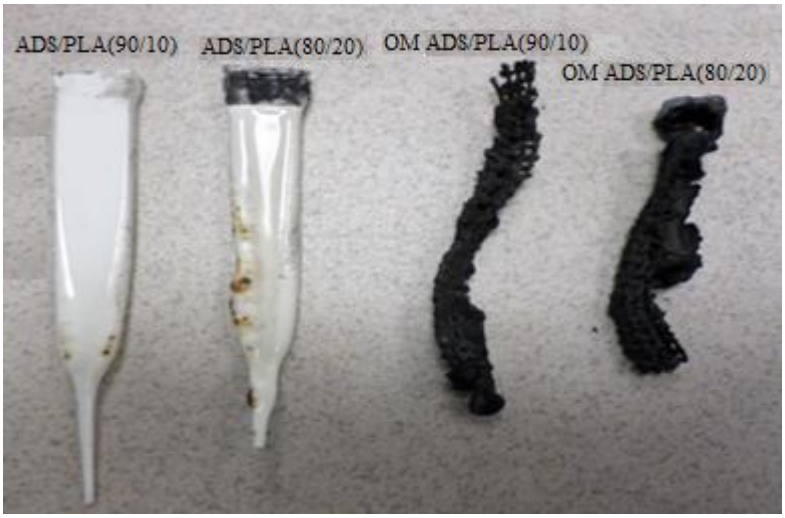


Figure 3. 71. The UL-94 of PLA/ADS and om-PLA/ADS composites

However, all other FRs significantly reduce the rates of burning of the over-molded composites, at least by 86%, in vertical orientation shown in Table 3.14. Vertical burning rate of OM-PLA is reduced with the use of APS and MPZ, and that shows better results. APS on the other hand is an APP-based flame retardant substance, forming a layer of swelling ash in the solid phase and showing a non-flammability effect. The effectiveness of this agent in the gas phase is almost negligible. As can be seen from the results, it can be concluded that APS is the most effective.

Table 3. 13. The UL-94 results of PLA/APS and om-PLA/APS composites

| | first ignition time (s) | second ignition time (s) | dripping | complete burn | classification |
|---|---|---|---|---|---|
| Neat PLA | 5,8 | 13,4 | yes | yes | no rating |
| 10APS-90% PLA | 2,5 | 4,2 | yes | no | V-0 |
| 10APS-90% PLA+ jute | 2,6 | 4,9 | yes | no | V-0 |
| 20APS-80% PLA | 2,3 | 3,6 | yes | no | V-0 |
| 20APS-80% PLA+ jute | 2,8 | 4,3 | yes | no | V-0 |

FR agents with high efficiency in solid phase are more effective in such systems. Another reason why APS is more effective is that APS changes to melt form during combustion. There is a high probability that the APS jute fibers, which goes into this

melted form, is absorbed. Since APS is an effective agent in cellulose, the flammability performance is likely to be higher in this system. It is dripping without flame even after the fire is removed. The increases of the surface area may have led to cooling the material which leads to a slight decrease in flammability.

The effect of these FRs is more obvious when being used in ecosheet, which can be due to PLA and jute being more reactive to flame retardants. All flame retardants improve the fire performance of ecosheet significantly. In PLA/APS composite, the melt appeared to be less cohesive as compared to other composites; having larger burning drips may mean that they include unmelted materials. The addition of OM-MPZ (80/20%) produces composites which extinguish in the vertical burn test once the Bunsen burner removed, but still generates burning drips through the ignition. This fact is the same as that has been stated by Bourbigot and others with a V-2 rating composite [6]. It is previously reported that during ignition, flames is extinguished only for 1 sec after the removal of ignition source by the addition of APS with ecosheet which results in composites having nonflaming drips [66]. These results show that UL-94 alone cannot identify a very clear difference between the efficiency of each FRs on fire composites performance; therefore, the fire performance of the composites is also evaluated by using LOI test and the results are discussed in the following section.

Table 3. 14. The UL-94 results of PLA/MPZ and om-PLA/MPZ composites

| | first ignition time (s) | second ignition time (s) | dripping | complete burn | classification |
|---|---|---|---|---|---|
| Neat PLA | 5,8 | 13,4 | yes | yes | no rating |
| 10MPZ-90% PLA | 1,9 | 86 | yes | no | V-0 |
| 10MPZ-90% PLA+ jute | 2,5 | 103 | yes | no | V-1 |
| 20MPZ-80% PLA | 1,5 | 22 | yes | no | V-0 |
| 20MPZ-80% PLA+ jute | 2,6 | 142 | yes | yes | V-2 |

UL94 test is a qualitative test that shows almost the same results for groups of two composites except for two cases, and this indicates that the FR amount in regard to

host polymer improves its rating. The size of the examined particles' of all the samples of APS reach V-0 class. It means fine sizes needed for the investigation for the critical specific surface area. The LOI results does not monitor the pattern of particle size. Rating of MPZ improves 10% to the rating of V-0 level. The OM-PLA/MPZ jumps to V-1 rating exceptionally. This shows the jute role in reducing the flame aggressiveness.

To see the sights of flame-retardant mechanism in UL94 test for PLA/FR, Fig. 3.71. Displays three pictures of the vertically burning test. The melt dripping occurs in virgin PLA and in flame retardant PLA composite. Therefore, the virgin PLA has droplets of fire and the absorbent cotton ignites, while the composite of 10% FR/PLA has rapid droplets with absence of the fire and the absorbent cotton held in reserve. The results suggest that FR can induce the matrix decomposes easily and generates melt dripping to excluding burning heat of the matrix. By carefully observing, it can be noted that no char is formed in the residues of APS; all samples are subsequently combusted. Consequently, the function of the PLA/APS flame-retardant depends on the flame-retardant of solid-phase. These two effects of APS not only increase the values of LOI but also enhance the rating of UL94.

The ecosheet are coated with different type of FR, such as APS, ADS and MPZ and concentration of (90/10% and 80/20%). In Figs 4.72-4.74. Results of the LOI value for both the neat PLA along with the Over-molded samples are shown. The limiting oxygen index (LOI) is to support burning the minimum amount of oxygen required in oxygen/nitrogen mixture that measures the material flammability. In an open atmosphere, material having 20 or low LOI value is easily ignitable. On the other hand, material having LOI value of >21 burns in a slow manner. When the LOI values are beyond 26, the material (polymer) can be considered as flame retardant [3]. In the current research, LOI values has been measured. The LOI value of the jute fiber is 21 which can be burned easily in an open environment. However, in every OM-FR samples, the LOI value shows significant increase. The LOI linear increases by the increase of FR added percentage. In the 20% APS sample, it increases from 21 to 26. In the OM-ADS (80/20%) sample, the LOI value reaches up to 23.4. Because of that, the ecosheet catches flame but it is burning slowly. The LOI values also support the results of the vertical burning behavior of the over-molded samples. In

the case of OM-ADS (90/10%) sample, the ecosheet displays 26 sec time for reduced flame followed by its complete burning with afterglow in 286 sec. Therefore, the total burning time is 312 sec. This burning rate reduces from 150 to 25 mm/min in the sample of neat PLA to OM-PLA/ADS (90/10%). It will continue to decrease because the percentage application of ADS increases.

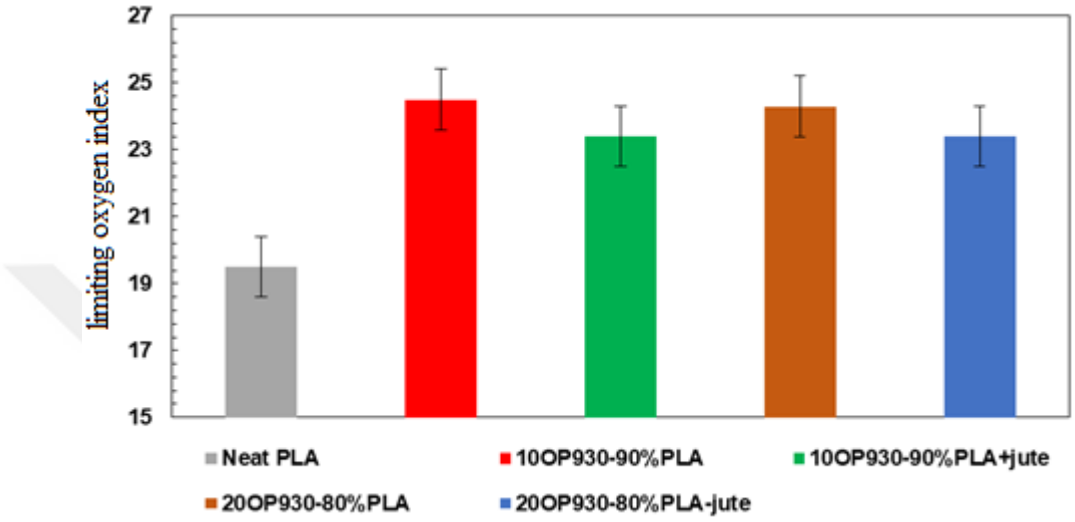


Figure 3. 72. The LIO of PLA/ADS and om-PLA/ADS composites

PLA and APS are compound into PLA/APS to increase the flame-retardant performance of ecosheet. By LOI method, the various flame retardancy samples of different ratios of PLA/APS are added into the ecosheet.

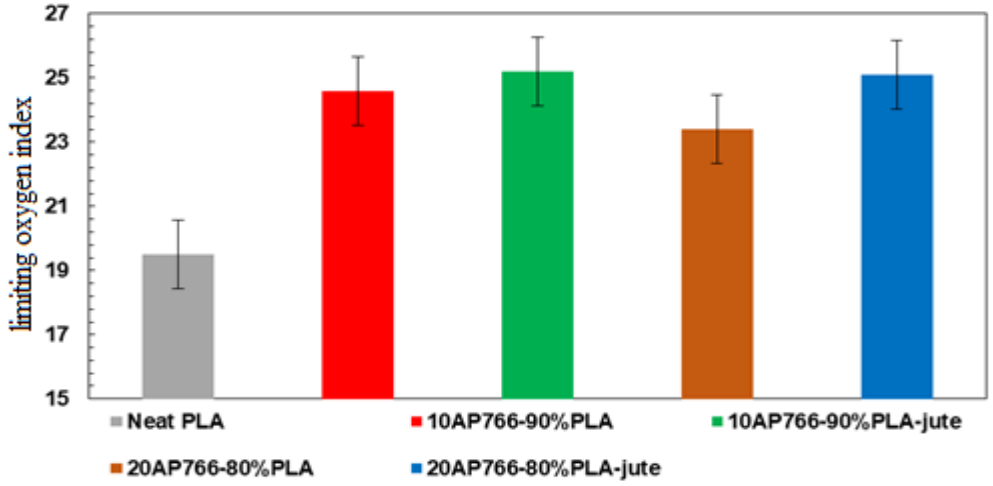


Figure 3. 73. The LIO of PLA/APS and om-PLA/APS composites

The LOI of pure PLA/APS (90/10%) and PLA/APS (80/20%) system is 24.6 % and 23.4 %, respectively. with the OM-PLA/APS (90/10%) it is 25.2 %; the LOI values of PLA/APS (80/20%); the LOI value is 25.1%. Results show that it indicates the best mass ratio of APS to PLA is 90/10 with over-mold. The values of LOI for PLA/APS system increase with ecosheet present; indicating that compounding APS and PLA can enhance performance of flame-retardant of jute and ecosheet.

The LOI results of PLA/MPZ composites with OM and without OM are listed in Fig 3.74. PLA/MPZ composites shows improved flame retardancy than ADS. The results prove that MPZ can also act as good flame retardant in jute/PLA composites. As compared to the sample of PLA/MPZ, the LOI of the OM-PLA/MPZ (90/10%) sample is higher than that of the pure PLA/MPZ (90/10%), although the amount of the MPZ in the above sample is less than the MPZ pure samples. For the OM-PLA/MPZ (80/20%) composites, LOI increases from 24.9 and does not reach to the level by containing 10% of MPZ. In case of MPZ, the composite with LOI that ranges from 24.2 to 25.3 is considered as a fire resistant material of third grade. This suggests that the flame retarding surface layer is efficient to improve the flame retardancy of the composites.

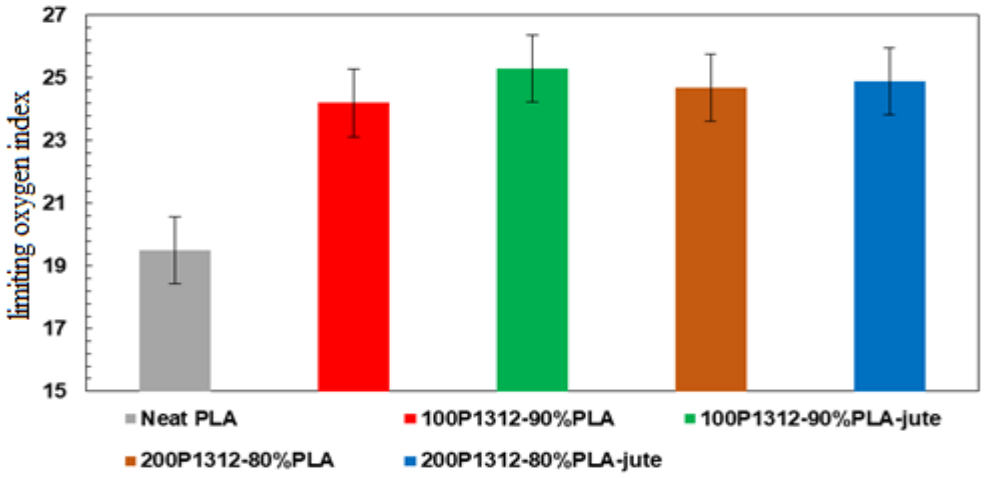


Figure 3. 74. The LIO of PLA/MPZ and om-PLA/MPZ composites

If we compare the results of LOL with UL-94 we will find similarities. The results show that the same pattern is followed in both tests, aside from the size of the particles. The reason of that is the unbalanced mixing of compound ADS. In OM composites, the FR layer protects the jute fibers from the fire, and the jute fibers also

reduce the intensity of the fire. With regard to the interaction of fibers with the polymer, there is a positive side in the composites, thanks to the increased ratios of fibers which have been able to improve the performance of the FR (LOI value increases) and remove the melt dripping in PLA. It is previously observed that the FR is unable to protect PLA from dropping in pure composites, but what can be observed now is that dropping is less and at the same time this dropping cannot ignite cotton. It is worth noting that most PLA/FR composites have drip behavior. It is also originated that OM-PLA/FR shows a better anti-dripping behavior, while the burning sample does not drip through the first test.

Due to some limitations in the complete coverage of samples by FR, the oxygen has been able to penetrate some of the weak areas causing complete burning of the samples. One of the positive sides is that adding a FR to PAL has a positive results in protecting the composites. The FR has succeed in isolating the composites from the flame, thereby making the pyrolysis zone safe and the percentage of produced gases decreases a lot. Because of the rapid destruction of the composites, oxygen index (OI) values have increased from 19 vol% (PLA) to 24.9 vol% (PLA/FR). Looking at the same composite, the UL 94 rating is changed to V-0 after it is HB.

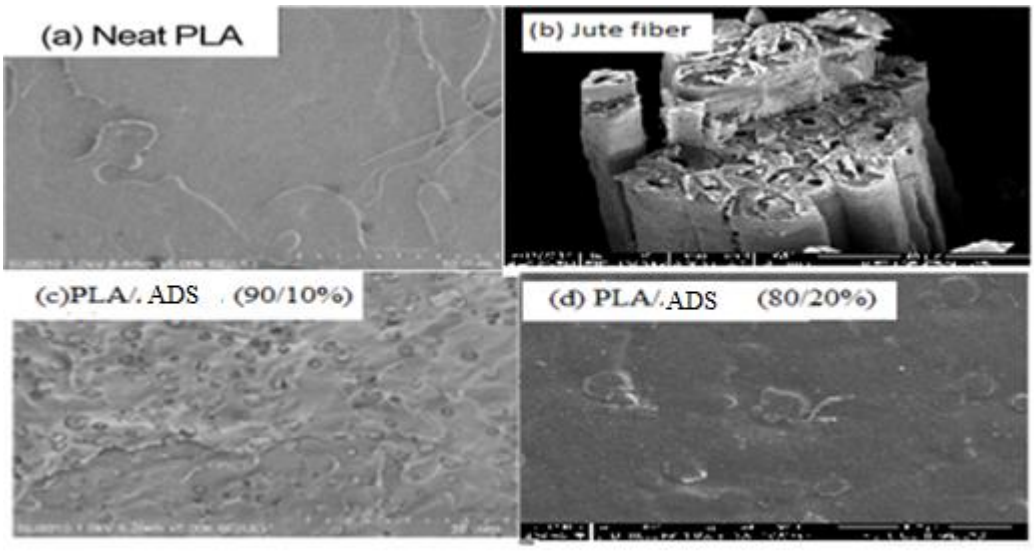


Figure 3. 75. The SEM of the char residues of PLA, Jute, PLA/ADS (80/20%) and the PLA/ADS (80/20)

SEM micrographs for PLA/FR show that fire causes a production of rough surface of jute, whereas PLA fibers seem to be less affected. This indicates that besides the

chemical effect, the FR can also increase the fiber/matrix interfacial adhesion of Jute/PLA by increasing the physical interlocking between matrix and fiber due to the production of rough surface on jute fibers.

The micrographs of SEM; the char residues of the PLA/MPZ (80/20%); and the OM-PLA/MPZ (80/20) are exposed in Fig. 4.75. All samples are combustible in air. Figure 4.75a displays the SEM (3000) of the PLA/MPZ (80/20%) that has clean surface with no gap or holes. Figure 4.75b shows the SEM (3000) of the PLA/MPZ (80/20%) after burn. It is noted that many flakes have been there on the surface. The result shows that the CO2 and NH3 from the MPZ may seal off charred layer efficiently to avoid transmission of heat. Analysis of SEM has been carried out for further characterization of the microstructure residue. In Figures 3.75c and 3.80d the residual morphology of composites is shown.

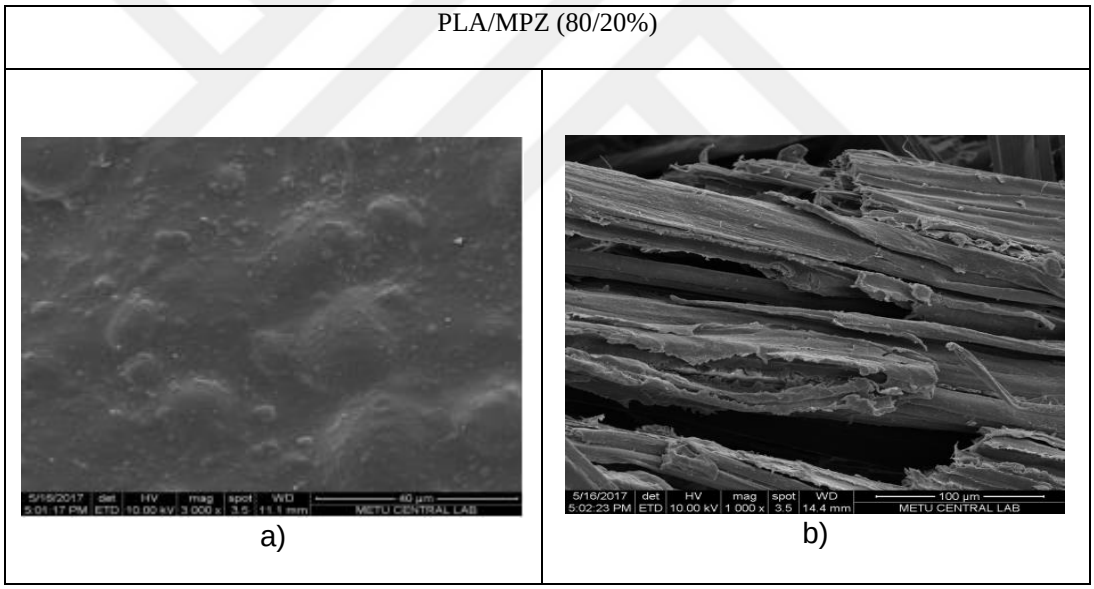


Figure 3. 76. The SEM of the char residues of (a) PLA/MPZ (80/20%) and (b) om-PLA/MPZ (80/20)

Figure 3.75d shows OM-PLA/MPZ (80/20) after burn; the residue is rambling and jute fibers are thin. When using higher resolution SEM (1000) for the OM-PLA/ MPZ (80/20), the gaps in the jute fibers become clear after the melting of PLA/ MPZ and the fibers have been covered by PLA/MPZ. See Figure 3.75d. The charred layer insulated the heat perfectly, forming a layer of gases and preventing the entry of oxygen. For J/P/A residues, the fibers have been accumulated better thanks to the APP insulation layer. Comparing these results with the results of the ecosheet and

OM-PLA/MPZ (80/20) gives us an improvement in this area. The introduction of PLA/MPZ to OM-composite acts as a layer inhibiting the combustion of composites.

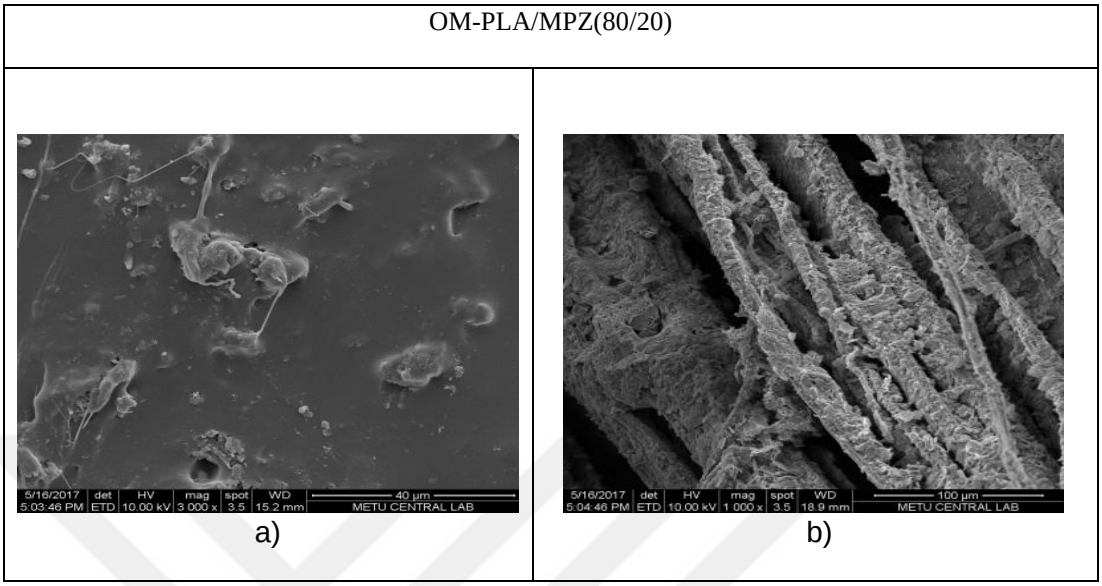


Figure 3. 77. The SEM of the char residues of the PLA/MPZ (80/20%) and the om PLA/MPZ (80/20)

Figure 3.76. Shows the remains of PLA/APS and OM-PLA/APS samples by SEM and photographs. The most important thing to be observed is the complete combustion of PAL. The increase of fibers in PLA/APS composite is accompanied by a decrease in linear burning. With the addition of 20 wt. % APS, the flame has been unable to continue after the ignition flame is withdrawn. Figure 3.74. Shows the char residues of OM-PLA/APS (80/20%) composites. The charred residue of PLA has a big porous structure appearance if we compare it to neat PLA/APS. Although the samples have been subjected to significant shrinkage during burning, the size of the carbon residue still small. The charred layer has protected the composite from melt dripping in vertical flame test, which prevents the fire from reaching the ecosheet. As for the 20 % APS, more protection has been observed for the composite and a greater amount of carbon structures has been found; and this confirms that during combustion, the cellular structures have been broken down. Figure 3.77. Shows the SEM micrograph of the pure PLA/ADS and OM-PLA/ADS. It can be seen from Figure 3.77a that it has clean and smooth surface. On the other hand, in the PLA/ADS after burn sample, the surface becomes rougher with a clear flaking in the surface (Fig. 3.77 B and E). The solid carbonization of the fabric supports the

absorption by the APS fabric. We conclude from this that the fibers (cellular structures) are thermally stable at the time of the burn which is because of the insulating layer that is dripping in the vertical burning test. This raises the anti-dripping properties of the composites. As for ADS compound, especially 10 wt %, many holes in the matrix have been seen.

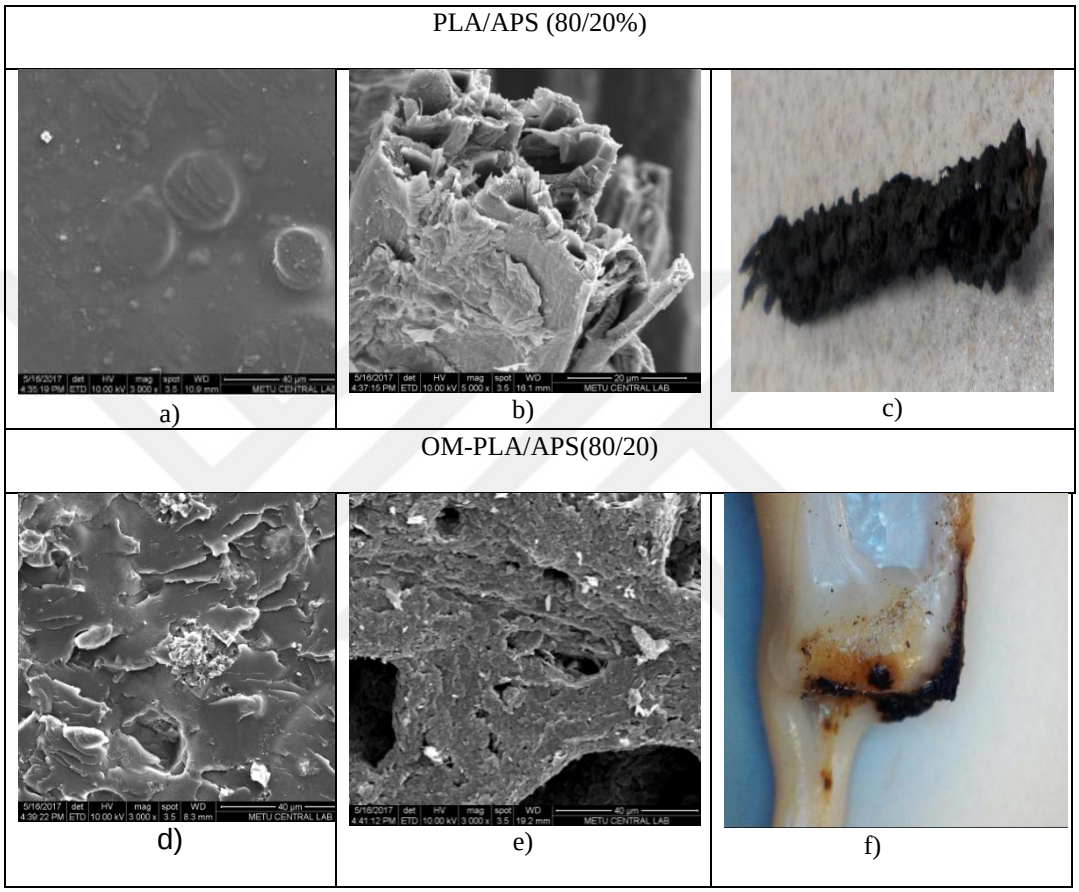


Figure 3. 78. The SEM of the Char Residues of (a) PLA/APS (80/20%) (b) Close up (c) normal photo (d) om-PLA/APS (80/20) (e) clos up (f) normal photo

ADS has a 9−14 μm and rod-like shape which is uniformly sparse in the matrix. This causes less matrix cohesion and faster failure. Although the compatibility between polymer and PLA/ADS is weak, and even with increased concentration, no significant change in properties is observed, but with regard to the melting process, it is significantly effective.

With regard to the interaction of the flame retardant with the polymer and the effect of different concentrations on the chemical composition and other properties, the FTIR spectroscopy device has been the appropriate choice for performing these tests.

The chemical components of the flame retardant substances and FR/PLA composites are identified separately and collectively. In order to determine the compatibility of the compound, interacting peaks must be found in the mixture spectrum and are different from the peaks in the two original materials [18].

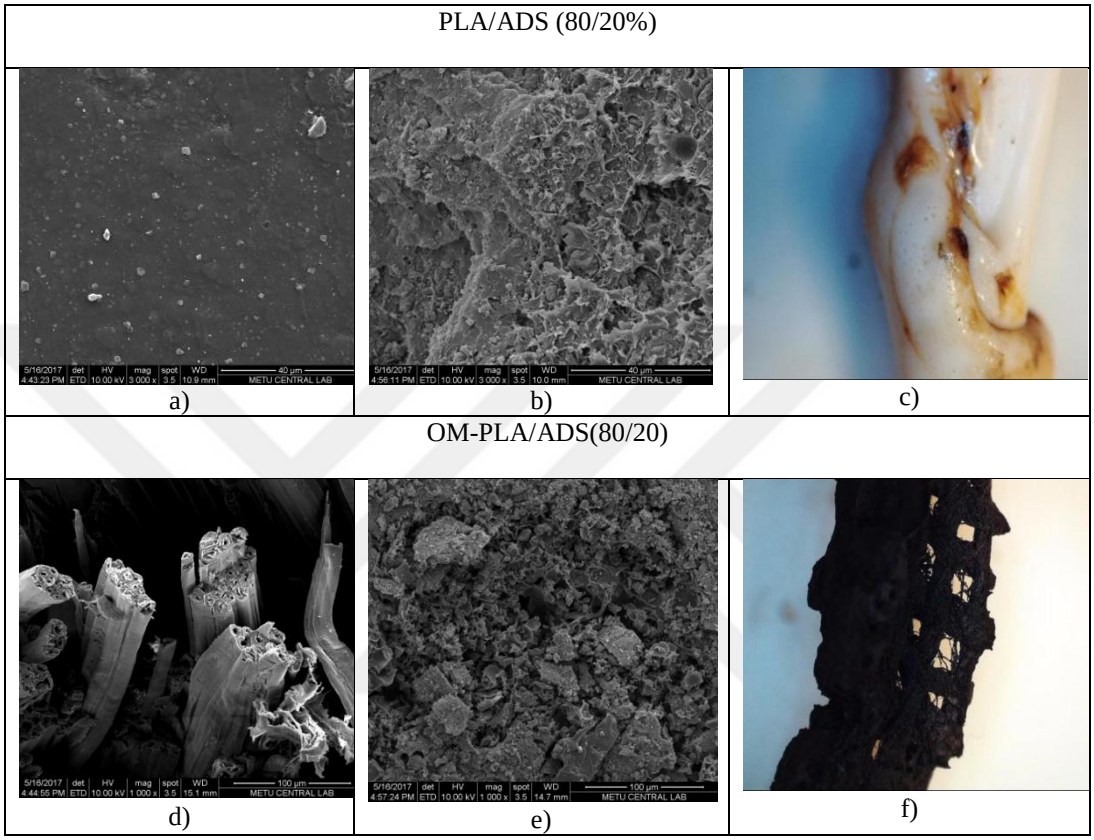


Figure 3. 79Figure 4.78. The SEM of the char residues of (a) PLA/ADS (80/20%) (b) close up (c) normal photo (d) om-PLA/ADS (80/20) (e) close up (f) normal photo

For this reason, the attenuated total reflectance (ATR) technique is being used to define these variables. This technique is popular and widely used in relation to polymers. But this technology is not without flaws. There are two drawbacks; the contact of crystal-sample area and the difficulty in controlling the pressure applied to the sample [1]. When analyzing the PLA/ADS (80/20%) pure and of PLA/ADS (80/20%) after burn sample, which showed in Figure 4.79, one of these defects appears in spectra (a). Simply, if PLA/FR blends are compatible, new peaks will emerge, or other peaks will shifts. If the change in the intensity of the peaks is significant, it is taken into consideration; if there is no compatible, the shape will be

the sum of the original spectrum for both PLA and FR. These to be added to the previous experimental error [11].

Figure 3.79. Shows PLA/ADS blend after burning. Analyzing the sample in the FTIR device will give us a greater understanding of the action mechanism of the composites and its interactions. A strong absorptions has been observed for C=O of O=C=N at 1647 cm-1. This peak has not seen before the burn. This proves an interaction between PLA and ADS. In spite of the simplicity of PLA/ADS spectra, we can notice the vibrations of P=O (skeletal vibrations) at 1112 cm-1 which occurs during PLA/ADS decomposition and –NH peak at 3435 cm-1[52]. From our results and previous studies, we have an understanding of the mechanism of interaction between PAL and ADS. The reaction mechanism is in two stages; the first stage is the reaction of ADS with PAL to form the phosphate esters. The second stage is of intermediate O=C=N compound which is produced from phosphate esters reaction [19]. This mechanism occurs in parallel with the O=C=N and O=C=N forming CO2 and C=N– reaction at 1536 cm-1. After losing NH3 we can say that the degradation of ADS begins [53, 54].

We notice from OM-PLA/ADS spectrum after burn, the disappearance of many peaks that belong to the jute fibers, and this highlights the mechanism of the decomposition of the jute fibers due to the heat. The hidden peaks are in order -OH stretching vibration (3331 cm-1), -CH stretching vibration (2922 cm-1) and -CH bending vibration (1452 cm-1 and 1382 cm-1). These results demonstrate the extraction of hydrogen from jute fibers completely. C-O (stretching) peak is identified at 1748 cm–1 which belongs to COOH and acetyl groups of jute. This is accompanied by a positive change in the intensities of C-O (vibration) peak at 1028 cm-1. This peak is directly related to the char structure.

For PAL, the characteristic peaks in PLA/APS and OM-PLA/APS composites appear in Figure 3.80 and it's as follows: C=O at 1746(stretching) asymmetric; –CH3 at 2995(stretching); –CH3 symmetric at 2946 (stretching); and C–O at 1080 cm−1. As for the Bending, two peaks found: –CH3 asymmetric; and symmetric at 1452 and 1361 cm−1respectively [3-18]. Symmetric CH2 at 1448 Cm-1(bending), and C-O at 1242 Cm-1 which belongs to lignin (stretching). [3-19].

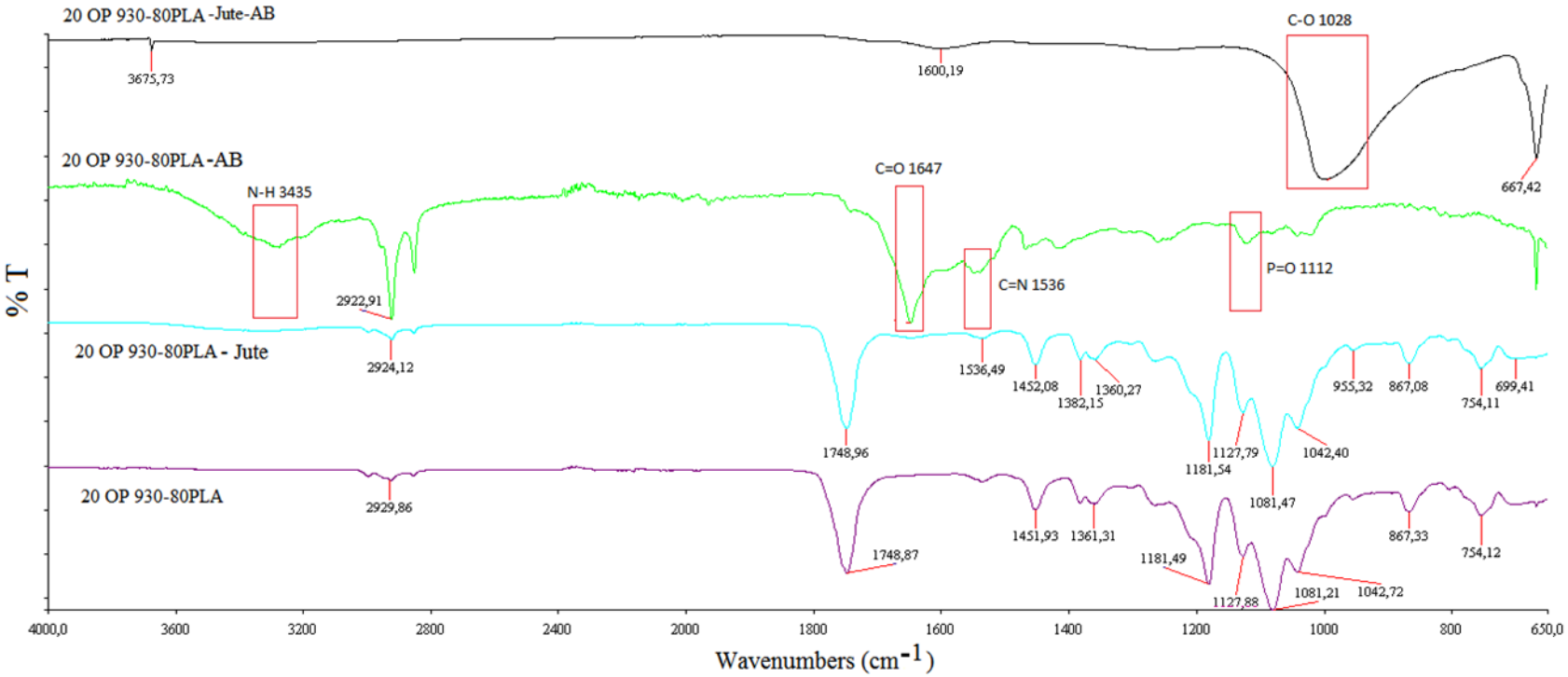


Figure 3. 80. The FTIR spectrum of PLA/ADS, om-PLA/ADS before and after burn

When comparing before and after the burn with respect to PLA/APS compound, it is found that there are no new peaks before the burn. As for the stage after the burning, the peak at 2385 Cm-1 of the P-H and the peak of N-H2 group at 3345 Cm-1 have disappeared due to the interaction with the fire. After burning, we can conclude that this kind of fire retardant is the best type because it keeps the composite intact and is able to prevent the fire from reaching the jute fiber. The peak position of some vibration bands has shifted to a higher frequency (2-3 cm-1), meanwhile the intensity of all the bands after burn has decreased.

The analysis of MPZ has been previously mentioned [45, 46]. Decomposition takes place in two steps: the condensation step, in which cross-linking or condensation of the chains of polyphosphate turns into poly (phosphoric acid); the step of releasing water and NH3 gas. Figure 4.81. Shows the first step of APP decomposition, where peaks belonging to N–H appear in three regions which are belong to NH3 at 965, 1646, and 3334 cm−1. We can track the carbonization process by studying the 850–1350 cm-1 region because the P—O bands is in this area. Moreover, the type of phosphate can be determined, and we can prove the form of new bonds such as phosphocarbonaceous. P—O—C broad peaks are identified between the 1100 and 1300 cm-1 region. This peaks belong to phosphate–carbon complexes [33]. Characteristic peaks of phosphocarbonaceous complexes are determined at 1000 cm-, these peaks belong to symmetric PO2 and PO3. We can now create a clear picture of the role of (MPZ, ADS and APS) compounds and how they work. The phosphocarbonaceous structure are considered to be the cornerstone of this understanding, which would not have been accomplished unless by using a FTIR analysis of samples after and before burning. The phosphocarbonaceous structure consists of a reaction of PAL and APP and this substance works to stabilize the blends, and this increases the properties of fire-proofing. As for pure PLA, when burned, it produces a solid substance consisting of carbon residues.

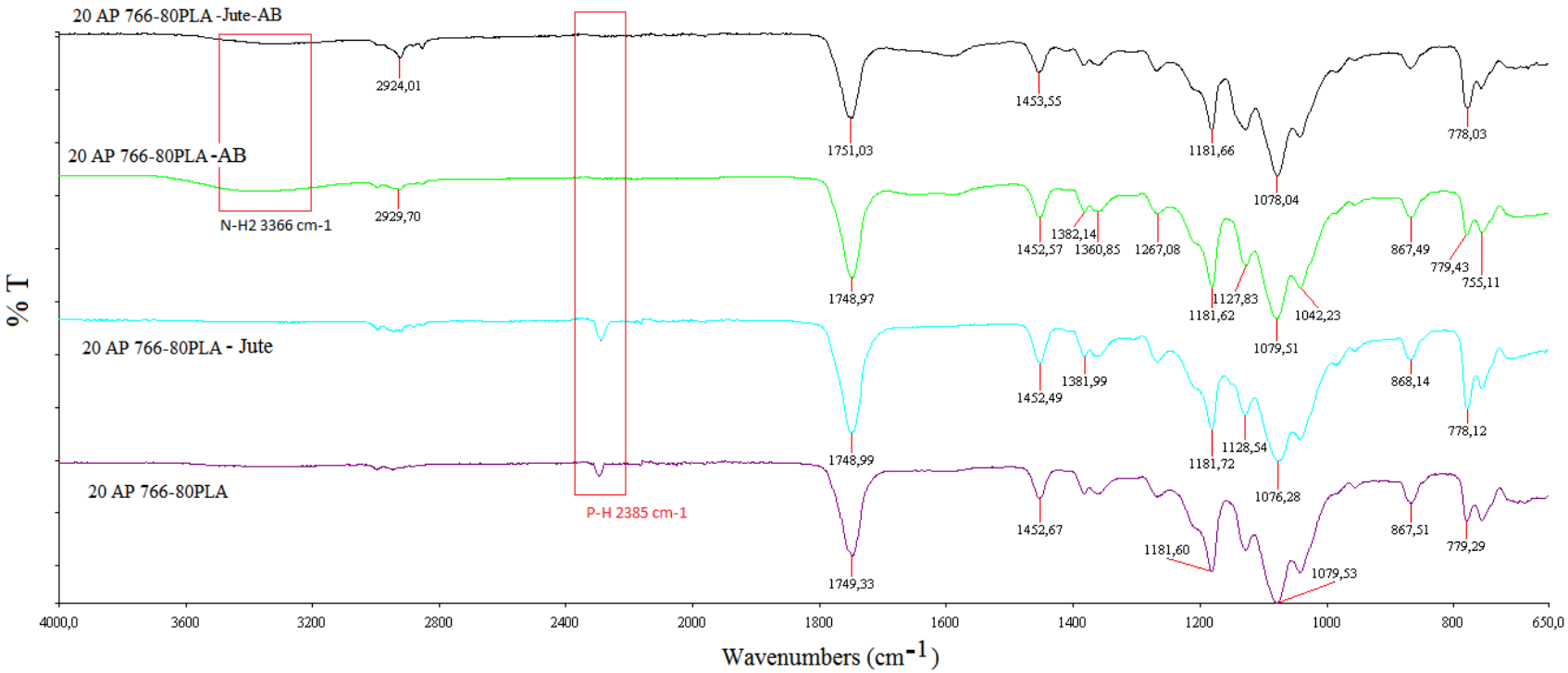


Figure 3. 81. The FTIR spectrum of PLA/APS, om-PLA/APS before and after burn

For polymers that are not treated with flame retardant materials, cracks in the polymer surface are the entry gates of the polymer in the burning time, and then it follows that internal gases result from the heat acting as a fire-stimulating fuel. As for the PLA/FR compounds, it's form a layer of P—O—C bonds at the time of fire, and this layer isolates oxygen and heat, thus, preserving the composites. This layer provides protection against crack formation and restricts the movement of internal decomposition gases. As a result of this layer, the polymer chains become able to form interstitial compounds with the phosphate group, which increases the strength of the internal mechanical properties. But the fatal defect is the melting of the APP substance, as this defect completely prevents the formation of the polycondensation reaction, and therefore, the jute fibers are exposed to fire directly.

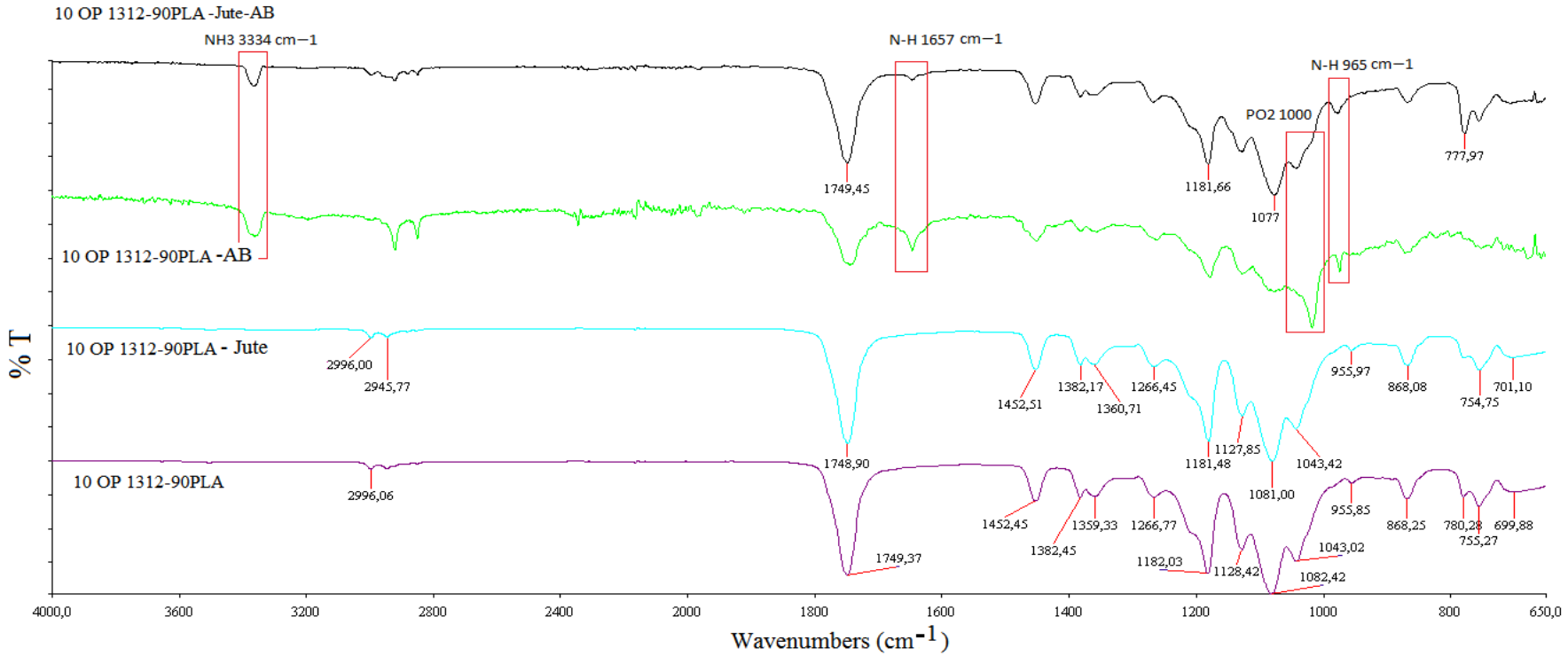


Figure 3. 82. The FTIR spectrum of PLA/MPZ and om-PLA/MPZ before and after burn

## 4. CONCLUSIONS AND RECOMMENDATIONS

With regard to the results of the study as a whole, the results will be ordered according to the stages that were conducted before. After reviewing the results, comments and recommendations were added in the light of these results. With regard to the first stage, which is the manufacturing of the ecosheet and Over-molding, whereby the best Jute/PLA ratios and the best fiber orientation were tested; then, several tests were performed. After the completion of this stage, the best composites were chosen for the second stage; then many tests were performed on them.

The results of the ecosheet manufacturing stage first can be reviewed as follows:

- For the density test, the best results were for the composite PLA/Jute 60/40 of with fiber orientation of 90° where the density reached 1.43 g/cm3.
- For the Mechanical properties (flexural strength, flexural modulus, Tensile Strength and Tensile modulus) tests, the best results were for the composite PLA/Jute 60/40 of fiber orientation of 45° where flexural strength was (168.3 MPa), flexural modulus was (8.3 GPa), Tensile Strength was (141 MPa) and Tensile modulus was (7.7 GPa).
- For the Elongation at break test, the best results were for the composite PLA/Jute 70/30 with fiber orientation of 45° where the Elongation at break reached 2.2%.
- For the Storage Modulus test, the best results were for the composite PLA/Jute 60/40 with fiber orientation of 45° where the Storage Modulus reached 4000 MPa.
- For the Tan Delta test, the best results were for the composite PLA/Jute 70/30 with fiber orientation of 45° where the Tan Delta reached 0.4 at 101C.
- For the Water Uptake test, the best results were for the composite PLA/Jute 70/30 with fiber orientation of 45° where the Water Uptake reached 11.4%.

The results of the Over-molding manufacturing stage can be reviewed as follows:

- For the density test, the best results were for the composite PLA/Jute 60/40 with fiber orientation of 45° where the density reached 1.32 g/cm

- For the Mechanical properties (Flexural Strength, flexural modulus, Tensile Strength and Tensile modulus) tests, the best results were for the composite PLA/Jute 70/30 with fiber orientation of 45° where flexural strength was ( 82 MPa), flexural modulus was (7.58 GPa), Tensile Strength was (72 MPa) and Tensile modulus was (2.01GPa).
- For the Elongation at Break test, the best results were for the composite PLA/Jute 60/40 with fiber orientation of 45° where the elongation at break reached 8.68%.
- For the Impact Strength test, the best results were for the composite PLA/Jute 60/40 with fiber orientation of 45° where the Impact Strength reached 39kJ / m2.
- For the Storage Modulus test, the best results were for the composite PLA/Jute 70/30 with fiber orientation of 90° where the Storage Modulus reached 2351 MPa.
- For the Tan Delta test, the best results were for the composite PLA/Jute 60/40 with fiber orientation of 45° where the Tan Delta reached 1.1 at 168C.
- For the Heat Deflection Temperature test, the best results were for the composite PLA/Jute 60/40 with fiber orientation of 45° where the HDT reached 110C°.
- For the Water Uptake test, the best results were for the composite PLA/Jute 70/30 with fiber orientation of 90° where the Water Uptake reached 7.26%.

The morphologies of ecosheets shows In general, good PLA penetration through the Jute fibers but poor cohesion at the interface. For the Over-molding, we can see a pseudo ductile behavior due to the shearing effect of the 45 laminate in 70/30 and 60/40 PLA/Jute composites. In addition, the failure occurred in the matrix phase, and debonding or fiber-pulling out indicated the lack of a fiber/matrix adhesion.

From this stage we can conclude that the best fibers orientation was 45 at PLA/Jute ratios 70/30 and 60/40. Therefore, these factors were chosen for the second stage composites.

In order to give a general picture of the results, the statistics program (SPSS) was used to calculate the best samples according to specific data, which are as follows:

- The samples were divided into 3 stages according to the stages of work in this research.

- Three basic standards for selection were established, which are (The preferred percentage, the mechanical and thermal efficiency).
- For each standard, the samples were studied according to each stage, then selecting the best results for each stage.
- Five factors were selected to evaluate the results descending from best to worst, and they are in order (mechanical properties, thermal properties, flame retardant properties, chemical treatment properties, and other properties such as shape).

You can see the result in Figure 4.1

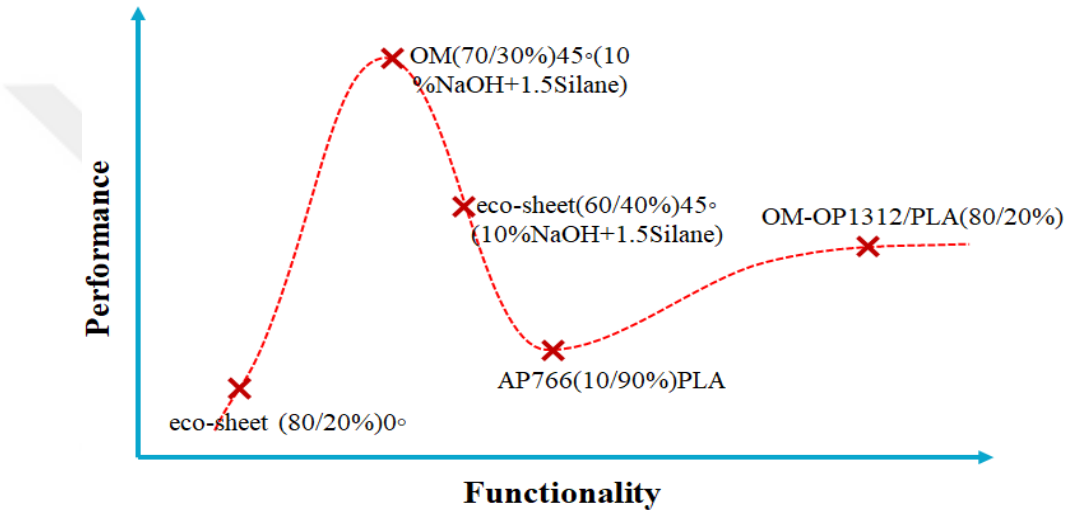


Figure 4. 1 Performance vs functionality

After reviewing the results, we can conclude the following:

The study resulted in a significant improvement in mechanical properties, especially after the introduction of overmolding and chemical treatment of the fibers, which provided excellent adhesion between the fibers and the matrix. The great improvement in mechanical properties proves the penetration of PLA polymer into the Jute fibers. The fibers and the matrix were able to distribute the load energy evenly for a long time and this is an important feature that allows these composites to be used in many industrial applications.

With regard to the thermal properties, the study proved that the resulting composites have a high heat tolerance and have high thermal stability compared to the thermal stability of neat PLA. The advantage of this improvement is the possibility of using these composites in high temperatures places. Due to the addition of flame retardant

materials, the composites could be used in many industrial applications. These composites became safe against fire, and this characteristic is added to other good thermal properties.

In general, the results of this study show that the resulting composites have a great advantage with respect to strength and weight ratio. These composites are characterized, especially after the chemical treatment and overmolding stage, with great mechanical strength in addition to being light in weight, which makes these composites strongly candidate materials for replacing industrial plastic compounds.

As all the results are considered, it is depicted that the overmolding technology with PLA applied to continuous jute mat composites, or named as ecosheets, is a promising technology to produce biodegradable polymer materials having heat resistant, low water uptake, and improved mechanical properties at a level of engineering plastics. This kind of materials can be candidates to be used in automotive, mainly under hood and inner-trim applications. This is a small step on the road to the future.

Based on the above, we recommend the following:

- Converting this research into a product in the automotive field.
- Benefiting from this research in the field of building or manufacturing prefabricated houses.
- Using the product in the third stage as an insulating material in buildings or in cars.
- Benefiting from this research in developing new types of flame retardants.
- Focus in the future on improving the performance and efficiency of PLA.
- 6- Focusing on the future on mechanically improving the performance of the third stage products

## REFERENCES


[1] McDaniels., K Downs., High strength-to-weight ratio non-woven technical fabrics for aerospace applications, *Cubic Tech Corp*, 2009, **14**(3), 1–9.

[2] Munikenche., G.T Naidu., Some mechanical properties of untreated jute fabric reinforced polyester composite, *Composites Part A*, 1999, **30** (3), 277–284.

[3] Wong K.J., Nirmal, U., Impact behavior of short and continuous fiber-reinforced polyester composites, *Reinf. Plast. Compos*, 2010, **29** (23), 3463–3474.

[4] S.O Han., M. Karevan., Int *J Polym Sci*, London, 2012.

[5] Morioka K., Tomita Y., Effect of lay-up sequences on mechan-ical properties and fracture behavior of CFRP laminate composite, *Material Characterization*, London, 2000.

[6] Y.U. Tao., L I. Yan, and R E N Jie., Mechanical, thermal and interfacial properties of jute fabric-reinforced polypropylene composites, *Trans. Nonferrous Met*, Washton 1996.

[8] Yokozeki T., Aoki T., Ogasawara T., Effect of layup angle and ply thickness on matrix crack interaction in contiguous plies of composite laminates, *Composites: Part A*, 2005, **36**, 1229–35.

[9] D Ray., N R Bose., Modification of the dynamic damping behaviour of jute/vinylester composites with latex interlayer, *Composites Part B*, 2007, **38,** 380–385.

[10] Hsen Anuar., A. Zuraida., J.G. Kovacs., Mechanical, thermal and interfacial properties of jute fabric-reinforced polypropylene composites, *Thermoplast Compos*, Mater, 2012.

[11] D Ray., B K Sarkar., S Das., Dynamic mechanical and thermal analysis of vinylester–resin–matrix composites reinforced with untreated and alkali-treated jute fibres, *Compos. Sci. Technol*, 2002, **62**, 911–917.

[12] Ray D., Sarkar B.K., Characterization of alkali-treated jute fibres for physical and mechanical properties, *J. Appl. Polym. Sci*, 2001, **80**, 1013–1020.

[13] Singsoha S., Rjs,out S.K., Influence of fisbre-surface treatment on structural, thermal and mechanical properties of jute, *J. Mater. Sci*, 2008, **43**, 2590–2601.

[14] Makambo L.Y., Ansell M.P., Modification of Hemp, Sisal, Jute, and Kapok fibres by alkalization, *J. Appl. Polym. Sci*, 2002, **84**, 2222–2234

[15] Chacsssthtjrff RP., Thermoplastic polymersin: Turi EA editor, Thermal characterization of polymeric materials, *Elsever wotson*, Press, 1997.

[16] H. Anuar., A. Zuraida J.G., Thermoplas Compos of PLA and jute composits, Mater, pares, 2011.

[17] Mylsamy K., and I Rajendran., Investigation on physicochemical and mechanical properties of raw and alkali treated agave-americana fiber, *Journal of Reinforced Plastics and Composites*, 2010, **29**, 2925–2935.

[18] M L Costa., S F Muller., Investigation on physicochemical PLA sheet, *Rezende, Amer Inst, Astron. J*, 2005, **43** (6), 1336-1345.

[19] M Jawaid., HPS A Khalil., A Bakar., Composite Mater Dynamic mechanical and thermal analysis, *Journal of Reinforced Plastics and Composites*, 2012, **1**, 263-369.

[20] M Boopalan., M J Umapathy., PLA chractrasition for thermal study and Silicon, 2005, **4**, 145-156.

[21] Swaminathan G., Shivakumar K., A Re-examination of DMA testing of polymer matrix composites, *J Reinf Plast Compos*, 2009, **28**, 979-994.

[22] Afendi M., Three-Point Bending Fracture Test of Epoxy Adhesive-bonded Dissimilar Materials, Yüksek Lisans Tezi, University of Tsukuba, Graduate School of Systems and Information Engineering, Tsukuba, Japonya, 2008.

[23] F Jacquemin., Y Abou Msallem., N Boyard., Thermally conductive polymer compounds for injection moulding, *Composites: Part A*, 2010, **41**, 108-121.

[24] Khan JA, Khan MA, Islam R, Gafur A, Mechanical, thermal and interfacial properties of jute fabric-reinforced polypropylene composites: effect of potassium dichromate, *Mater Sci Appl*, 2010, **1**(6), 350–357.

[25] Rauwendaal C., *Encyclopedia of polymer science and technology*, 2nd ed., John Wiley & Sons, Inc; 2005.

[26] Nam T H., S Ogiharaa., H Nakatania., Mechanical and thermal properties and water absorption of jute fiber reinforced poly (butylene succinate) biodegradable composites, *Advanced Composite Materials*, 2012, **21**(3), 241–258.

[27] Mishranfdr S., Misra M., Tripathy., Copolymerization of acrylonitrile on chemically modified sisal fibers, *Macromolecular Materials and Engineering*, 2001, **268**, 107–113.

[28] Shah V., *Handbook of Plastics Testing and Failure Analysis*, 3rd ed., John Wiley & Sons Inc, New Jersey, 2007.

[29] Sreivasan S., Iyder P B., Influence of delignification and on the fine structure of coir fibers (Cocos nucifera), *J. Mat. Sci*, 1996, **31**(3), 721-726.

[30] Brodfrtwn R., *Handbook of Polymer Testing - Short-Term Mechanical Tests*, Rapra Technology Limited, Shawbury, 2002.

[31] Khan G M A., Shsktams M S A., Infsluence of chemical treatment on the properties of banana stem fiber and banana stem fiber/coir hybrid fiber reinforced maleic anhydride grafted polypropylene/low-density polyethylene composites, *J. Appl. Polym. Sci*, 2013, **128**, 020- 1029.

[32] Mukherjee A., Ganguly P K., Structural mechanics of jute: The effects of hemicellulose or lignin removal, *J. Text. INS*, 1993, **84**(3), 348-353.

[33] Saheb D, Jog J. Natural fiber polymer composites: a review, *Adv Polym Technol*, 1999, **18**(4), 351–63.

[34] Auras R., Harte B., Selke S., An overview of polylactides as packaging materials, *Macromol Biosci*, 2004, **4**, 835–864.

[35] Murali B., Chandra mohan D., Nagoor vali S K., Mechanical behavior of chemically treated jute/polymer composites, *Carbon – Sci. Technol*, 2014, **6**(1), 330-335.

[36] Meinander K., Niemi M., Hakola J. S., Selin J. F., Polylactides-degradable polymers for fibers and films, *Macromol. Symp.*, 1997, **123**, 147-153

[37] Pillin I., Montrelay N., Grohens Y., Thermo-mechanical characterization of plasticized PLA: Is the miscibility the only significant factor, *Polymer*, 2006, **47**, 4676-4682.

[38] Xertgie Y., Hill CAS., Xia Z Militz., Silane coupling agents used for natural fiber/ polymer composites: a review, *Composites Part A*, 2010, **41**, 806–819.

[39] Gassan J., & Bledzki A., The influence of fibersurface treatment on the mechanical properties of jutepolypropylene composites, *Composites Part A: Applied Science and Manufacturing*, 1997, **28**, 1001–1005.

[40] Nam TH., Ogihara S., Nakatani H,, Mechanical and thermal properties and water absorption of jute fiber reinforced poly (butylene succinate) biodegradable composites, *Adv. Compos. Mater*, 2012, **16**, 241–258.

[41] Mohanty AK., Khsan MA., Hinsrichsen G., Influence of chemical surface modification on the properties of biodegradable jute fabrics–polyester amide composites, *Composites Part A*, 2000, **31**, 143–150.

[42] Rdesrtroe PJ., Antresell MP., Jute-reinforced polyester composites, *J. Mater. Sci*, 1985, **12**(2), 4015–4020.

[43] Marega C., Marigo A., Di Noto V., Zannetti R., Martorana A., Paganetto G., Structure and crystallization kinetics of poly(L-lactic acid), *Macromol Chem. Phys.*, 1992, **193**, 1599-1606.

[44] J George., S S Bhagawan., S Thomas., Thermogravimetric and dynamic mechanical thermal analysis of pineapple fibre reinforced polyethylene composites, *J. Therm. Anal*, 1996, **47**, 1121–1140.

[45] Hdersu Y., Hveu Y. AS., Topolkaraev V., Hiltner A., Baer E., Crystallization and phase seperation in blends of high stereoregular poly(lactide) with poly(ethylene glycol), *Polymer*, 2003, **44**, 5681-5689.

[46] Cantwell Wj., Morton J., The impact resistance of composite materials – a review, *Composites*, 1991, **14**, 347–62.

[47] Shdah V., *Handbook of Plastics Testing and Failure Analysis*, 3rd ed., John Wiley & Sons Inc, New Jersey, 2007.

[48] Hgretu Y., Rogunova M., Topolkaraev V., Hiltner A., Baer E., Aging of poly(lactide)/poly(ethylene glycol) blends. Part 1. Poly(lactide) with low stereoregularity, *Polymer*, 2003, **44**, 5701-5710.

[49] Seki, Y., M. Sarıkanat, K. Sever, and C. Durmu¸skahya. Extraction and properties of Ferula communis fibers as novel reinforcement for composites materials. Composites: Part B 44, 2013, 517–523.

[50] Jabasingh S A., and C V Nachiyar., Process optimization for the biopolishing of jute fibers with celluloses from aspergillus nidulans, *International Journal of Bioscience and Biochemistry and Bioinformatics*, 2012, **2**(1), 12–15.

[51] Bulut Y., and A Ak sit., A comparative study on chemical treatment of jute fiber: potassium dichromate, potassium permanganate and sodium perborate trihydrate, *Cellulose*, 2013, **20**, 3155–3164.

[52] Sdreki Y., Innovative multifunctional siloxane treatment of jute fiber surface and its effect on the mechanical properties of jute/thermoset composites, *Mater Sci Eng*, 2009, **A508**, 247–252.

[53] Sehdrki Y., Sarirrdkanat M., Sedrver K., Extraction and properties of Ferula communis (chakdgtshir) fibers as novel reinforcement for composites materials, *Compos Part B*, 2013, **44**, 517–523.

[54] Hu Y., Hu Y. S., Topolkaraev V., Hiltner A., Baer E., Aging of poly(lactide)/poly(ethylene glycol) blends. Part 2. Poly(lactide) with low stereoregularity, *Polymer*, 2003, **44**, 5711-5720.

[55] Mwaimbo LY., Ansell MP., Chemical modification of hemp, sisal, jute, and kapok fibers by alkalization, *J Appl Polym Sci*, 2002, **84**(12), 2222–2234.

[56] Bsfaiardo M., Frisoni G., Scandalo M., Rimelen M., Lips D., Ruffieux K., Wintermantel E., Thermal and mechanical properties of plasticized poly(L-

lactic acid), *J. Appl. Polym. Sci.*, 2003, **90**, 1731-1738.

[57] Siqueira, G., J. Bras, and A. Dufresne. Luffa cylindrica as a lignocellulosic source of fiber, microfibrillated cellulose and cellulose nanocrystals. Bioreources 5(2), 2010, 727–740.

[58] Brown Radoler vesl., *Handbook of Polymer Testing - Short-Term Mechanical Tests*, Rapra Technology Limited, Shawbury, 2002.

[59] Ozkoc G., Kemaloglu S., Morphology, Biodegradability, Mechanical, and Thermal Properties of Nanocomposite Films Based on PLA and Plasticized PLA, *J. Appl. Polym. Sci.*, 2009, **114**, 2481–2487.

[60] McGonigle E. A., Daly J. H., Jenkins S. D., Liggat J. J., Pethrick R. A., Influence of physical aging on the molecular motion and structural relaxation in poly(ethylene terephtalate) and related polyesters, *Macromol*, 2000, **33**, 480-489.

[61] Zdhu L., Ferng Y., Yde X., Zhvou Z., Tundning wettability and getting superhydrophobic surface by controlling surface roughness with well-designed microstructures, *Sensors and Actuators A*, 2006, **130-131**, 595-600.

[62] Hartmann M. H., High molecular weight polylactic acid polymers, Editörler: Kaplan D. L., *Biopolymers from renewable resources*, 2nd ed., Springer-Verlag, Berlin, 367-411, 1998.

[63] C H Chiang., H Ishida., JL Koenig., The structure of γ-aminopropyltriethoxysilane on glass surfaces, *J. Colloid Interface Sci*, 1980, **12**, 396-404.

[64] Jedlinski Z., Walach W., Kurcok P., Adamus G., Polymerization of lactones, 12. Polymerization of L-dilactide and L,D-dilactide in the presence of potassium methoxide, *Die Makromol. Chem.*, 1991, **192**, 2051-2057.

[65] Kurcok P., Matuszowicz Z., Jedlinski Z., Kricheldorf H., R., Dubois P., Jerome R., Substituent effect in anionic polymerization of β-lactones initiated by alkali metal alkoxides, *Macromol. Rapid Comm.*, 1995, **1**6, 513-519.

[66] Kricheldorf H., R., Kreiser-Saunders I., Polylactones, 19. Anionic polymerization of L-lactide in solution, *Die Makromol. Chem.*, 1990, **191**, 1057-1066.

[67] Kricheldorf H., R., Boettcher C., Polylactones, 25. Polymerizations of racemic-and meso-D,L-lactide with zinc, lead, antimony, and bismuth salts-stereochemical aspects, *J. Macromol. Sci. Pure Appl. Chem.*, 1993, **A30**, 441-448.

[68] Kricheldorf H., R., Serra A., Polylactones, 6. Influence of various metal salts on the optical purity of poly(L-lactide), *Polym. Bull.*, 1985, **14**, 497-502.

[69] Kleine J., Kleine H., Über hochmolekulare, insbesondere optisch active

polyester der milchsaure, ein beitrag zur stereochemie makromolekularer verbindungen, *Die Makromol. Chem.*, 1959, **30**, 23-38.

[70] Kricheldorf H., R., Boettcher C., Polylactones, 27. Anionic polymerization of L-lactide. Variation of endgroups and synthesis of block copolymers with poly(ethylene oxide), *Die Makromol. Chem. Macromol. Symp.*, 1993, **73**, 47-64.

[71] Dunsing R., Kricheldorf H., R., Polylactones, 5. Polymerization of L,L-Lactide by means of magnesium salts, *Polym. Bull.*, 1985, **14**, 491-495.

[72] Kricheldorf H., R., Kreiser-Saunders I., Scharnagl N., Anionic and pseudoanionic polymerization of lactones-a comparison, *Die Makromol. Chem. Macromol. Symp.*, 1990, **32**, 285-298.

[73] Dahlmann J., Rafler G., Fechner K., Mehlis B., Synthesis and properties of biodegradable aliphatic polyesters, *Brit. Polym. J.*, 1990, **23**, 235-240.

[74] Lim L. T., Auras R., Rubino M., Processing technologies for poly(lactic acid), *Prog. Polym. Sci.*, 2008, **33**, 820-852.

[75] Henton D. E., Gruber P., Lunt J., Randall J., Polylactic acid technology, Editors: Mohanty A. K., Misra M., Drzal L. T., *Natural fibers, biopolymers, and biocomposites*, 1st ed., Taylor and Francis, Boca Raton, 527-577, 2005.

[76] Dorgan J., R., Jansen J., Clayton M., P., Melt rheology of variable L-content poly(lactic acid), *J. Rheology*, 2005, **49**, 607-619.

[77] Celli A., Scandola M., Thermal properties and physical ageing of poly(L-lactic acid), *Polymer*, 1992, **33**, 2699-2703.

[78] Cai H., Dave V., Gross R. A., McCarthy P., Effects of physical aging, crystallinity, and orientation on the enzymatic degradation of poly(lactic acid), *J. Polym. Sci.*, 1996, **B34**, 2701-2708.

[79] Bigg D., M., Effect of copolymer ratio on the crystallinity and properties of polylacitc acid copolymers, *J. Eng. Appl. Sci.*, 1996, **2**, 2028-2039.

[80] Sarasua J. R., Arraiza A. L., Balerdi P., Maiza I., Crystallinity and mechanical properties of optically pure polylactides and their blends, *Polym. Eng. Sci.*, 2005, **45**, 745-753.

[81] Pyda M., Bopp R. C., Wunderlich B., Heat capacity of poly(lactic acid), *The J. Chem. Thermodyn.*, 2004, **36**, 731-742.

[82] Kolstad J. J., Crystallization kinetics of poly(L-lactide-co-meso-lactide), *J. Appl. Polym. Sci.*, 1996, **62**, 1079-1091.

[83] Drumright R. E., Gruber P. R., Henton D., E., Polylactic acid technology, *Adv. Mater.*, 2000, **12**, 1841-1846.

[84] Ou X., Cakmak M., X-ray studies of structural development during sequential and simultaneous biaxial of polylactic acid film, *ANTEC*, Nashville, A.B.D, 4-8 Mayıs 2003.

[85] Lee J. K., Lee K. H., Jin B. S., Structural development and biodegradability of uniaxially stretched poly(L-lactide), *Eur. Polym. J.*, 2001, **37**, 907-914.

[86] Yong X., Songmin S., Jian H., Sinchi W., Two-stage crystallization kinetics equation and nonisothermal crystallization analyses for PTEG and filled PTEG, *J. Mater. Sci.*, 2011, **46**, 4085-4091.

[87] Avrami M., Granulation, Phase change, and microstructure kinetics of phase change. III, *J. Chem. Phys.*, 1941, **9**, 177-185.

[88] Maldelkern L., Quinn F. A., Flory P. I., Crystallization kinetics in high polymers, *J. Appl. Phys.*, 1954, **25**, 830-839.

[89] Verhoyen O., Dupret F., Legras R., Isothermal and non-isothermal crystallization kinetics of polyethylene terephthalate: Mathematical modelling and experimental measurements, *Polym. Eng. Sci.*, 1998, **38**, 1594-1610.

[90] Bhdmann C., Ladfnger S., Filsinger J., Drechsler K., Analysis of the removal of peel ply from CFRP surfaces, *Compos Part B Eng*, 2016, **89**, 352-361.

[91] Deng S., Djukic L., Paton R., Ye L., Thermoplastic-epoxy interactions and their potential applications in joining composite structures - A review, *Compos Part A Appl Sci Manuf*, 2015, **68**, 121-132.

[92] Neto J. A. B. P., Campilho R. D. S. G., Da Silva L. F. M., Parametric study of adhesive joints with composites, *Int J Adhes Adhes*, 2012, **37**, 96-101.

[93] Banea M. D., Da Silva L. F. M., Adhesively bonded joints in composite materials: An overview, *Proc. IMechE Part L J Materials Design and Applications*, 2009, **223**, 1-18.

[94] Jölly I., Schlögl S., Wolfahrt M., Pinter G., Fleischmann M., Kern W., Chemical functionalization of composite surfaces for improved structural bonded repairs. *Compos Part B Eng*, 2015, **69**, 296-303.

[95] Tao R., Alfano M., Lubineau G., In situ analysis of interfacial damage in adhesively bonded composite joints subjected to various surface pretreatments, *Compos Part A Appl Sci Manuf*, 2019, **116**, 216-223.

[96] Tao R., Alfano M., Lubineau G., Laser-based surface patterning of composite plates for improved secondary adhesive bonding, *Compos Part A Appl Sci Manuf*, 2018, **109**, 84-94.

[97] Martínez-Landeros V. H., Vargas-Islas S. Y., Cruz-González C. E., Barrera S., Mourtazov K., Ramírez-Bon R., Studies on the influence of surface treatment type, in the effectiveness of structural adhesive bonding, for carbon fiber reinforced composites, *J Manuf Process*, 2019, **39**, 160-166.

[98] Budhe S., Banea M. D., de Barros S., da Silva L. F. M., An updated review of adhesively bonded joints in composite materials, *Int J Adhes Adhes*, 2017, **72**, 30-42.

[99] Song M. G., Kweon J. H., Choi J. H., Byun J. H., Song M. H., Shin S. J., Effect of manufacturing methods on the shear strength of composite single-lap bonded joints, *Compos Struct*, 2010, **92**, 2194-2202.

[100] Araújo H. A. M., Machado J. J. M., Marques E. A. S., da Silva L. F. M., Dynamic behaviour of composite adhesive joints for the automotive industry, *Compos Struct*, 2017, **171**, 549-561.

[101] Ebnesajjad S., *Handbook of Adhesives and Surface Preparation*, 1st ed., Elsevier Inc., USA, 2011.

[102] Hou M., Thermoplastic Adhesive for Thermosetting Composites, *Mater Sci Forum*, 2012, **706**, 2968-2973.

[103] Rudawska A., *Surface Treatment in Bonding Technology*, 1st ed., Academic Press; USA, 2019.

[104] Davis M., Bond D., Principles and practices of adhesive bonded structural joints and repairs, *Int J Adhes Adhes*, 1999, **19**, 91-105.

[105] DeVries K. L., Adams D. O., Mechanical Testing of Adhesive Joints, Editors: Dillard D. A., Pocius A. V., *Adhes. Sci. Eng.*, Elsevier, Netherlands, 193-234, 2002.

[106] Pisanu L., Santiago L. C., Barbosa J. D. V., Beal V. E., Nascimento M. L. F., Strength shear test for adhesive joints between dissimilar materials obtained by multicomponent injection, *Int J Adhes Adhes*, 2018, **86**, 22-28.

[107] Huang C., Chen M., Yang W., Chang K., Tseng S., Investigation on warpage and its behavior in sequential overmolding, *ANTEC 2007 Plastics: Annual Technical Conference*, Cincinnati, Ohio, USA, 2007.

[108] Kanerva M., Sarlin E., Hoikkanen M., Rämö K., Saarela O., Vuorinen J., Interface modification of glass fibre-polyester composite-composite joints using peel plies, *Int J Adhes Adhes*, 2015, **59**, 40-52.

[109] Millot C., Fillot L. A., Lame O., Sotta P., Seguela R., Assessment of polyamide-6 crystallinity by DSC: Temperature dependence of the melting enthalpy, *J Therm Anal Calorim*, 2015, **122**, 307-314.

[110] Mullin J. W., *Crystallization*, Fourth Ed., Butterworth-Heinemann, Oxford, 2001.

[111] Kulifohsnski Z., Piorkowska E., Crystallization, structure and properties of plasticized poly(L-lactide), *Polymer*, 2005, **46**, 10290-10300.

[112] Ljungberg N., Colombini D., Wesslen B., Plasticization of poly(lactic acid) with oligomeric esteramides: Dynamic mechanical and thermal film properties, *J. Appl. Polym. Sci.*, 2005, **96**, 992-1002.

[113] Ljungberg N., Wesslen B., Preparation and properties of plasticized poly(lactic acid) films, *Biomacromolecules*, 2005, **6**, 1789-1796.

[114] Ljungberg N., Wesslen B., Thermomechanical film properties and aging of blends of poly(lactic acid) and malonate oligomers, *J. Appl. Polym. Sci.*, 2004, **94**, 2140-2149.

[115] Bikiaris D. N., Nanocomposites of aliphatic polyesters: An overview of the effect of different nanofillers on enzymatic hydrolysis and biodegradation of polyesters, *Polym. Degrad. Stabil.*, 2013, **98**, 1908-1928.

[116] Ferrato F., Carriere F., Sarda L., Verger R., A critical reevaluation of the phenomenon of interfacial activation, *Methods Enzymol*, 1997, **286**, 327-347.

[117] Hakkarainen M., Aliphatic polyesters: abiotic and biotic degradation and degradation products, *Adv. Polym. Sci.*, 2002, **157**, 113-138.

[118] Jamshidian M., Tenrany E. A., Imran M., Jacquot M., Desobry S., Poly-lactic acid: Production, applications, nanocomposites, and release studies, *Compr. Rev. Food Sci. F.*, 2010, **9**, 552-571.

[119] Harada M., Ohya T., Iida K., Hayashi H., Hirano K., Fukuda H., Increased impact strength of biodegradable poly(lactic acid)/poly(butylene succinate) blend composites by using isocyanate as a reactive processing agent, *J. Appl. Polym. Sci.*, 2007, **106**, 1813-1820.

[120] Labrecque L. V., Kumar R. A., Dave V., Gross R. A., McCarthy S. P., Citrate esters as plasticizers for poly(lactic acid), *J. Appl. Polym. Sci.*, 1997, **66**, 1507-1513.

[121] Li B. H., Yang M. C., Improvement of thermal and mechanical properties of poly(L-lactic acid) with 4,4-methyelene diphenyl diisocynate, *Polym. Adv. Technol.*, 2006, **17**, 439-443.

[122] Li H., Huneault M. A., Effect of nucleation and plasticization on the crystallization of poly(lactic acid), *Polymer*, 2007, **48**, 6855-6866.

[123] Uyama H., Ueda H., Doi M., Takase Y., Okubo T., Plasticization of poly(lactic acid) by bio-based resin modifiers, *Polym. Preprints Jpn.*, 2006, **55**, 5595-5598.

[124] Jing F., Hillmyer M. A., A bifunctional monomer derived from lactide for toughening polylactide, *J. Am. Chem. SocPolym. Composite.*, 2008, **130**, 13826-13827.

[125] Wang N., Zhang X., Yu J., Fang J., Study of the properties of plasticized poly(lactic acid) with poly(1,3-butylene adipate), *Polym. Composite*, 2008, **16**, 597-604.

[126] Yang L., Chen X., Jing X., Stabilization of poly(lactic acid) by polycarbodiimide, *Polym. Degrad. Stabil.*, 2008, **93**, 1923-1929.

[127] Gajria A. M., Dave V., Gross R. A., McCarthy S. P., Miscibility and biodegradability of blends of poly(lactic acid) and poly(vinyl acetate), *Polymer*, 1996, **37**, 437-444.

[128] Nijenhuis A. J., Colstee E., Grijpma D. W., Pennings A. J., High-molecular-weight poly(L-lactide) and poly(ethylene oxide) blends: thermal characterization and physical properties, *Polymer*, 1996, **37**, 5849-5857.

[129] Tsuji H., Ikada Y., Blends of aliphatic polyesters. I. Physical properties and morphologies of solution-cast blends from poly(DL-lactide) and poly(ϵ-caprolactone), *J. Appl. Polym. Sci.*, 1996, **60**, 2367-2375.

[130] Sheth M., Kumar R. A., Dave V., Gross R. A., McCarthy S. P., Biodegradable polymer blends of poly(lactic acid) and poly(ethylene glycol), *J. Appl. Polym. Sci.*, 1997, **66**, 1495-1505.

[131] Ke T., Sun S. X., Seib P., Blending of poly(lactic acid) and starches containing varying amylose content, *J. Appl. Polym. Sci.*, 2003, **89**, 3639-3646.

[132] Ke T., Sun X., Thermal and mechanical properties of poly(lactic acid) and starch blends with various plasticizers, *T. Am. Soc. Agr. Eng.*, 2001, **44**, 945-953.

[133] Lee C. M., Kim E. S., Yoon J. S., Reactive blending of poly(L-lactic acid) with poly(ethylene-co-vinyl alcohol), *J. Appl. Polym. Sci.*, 2005, **98**, 886-890.

[134] Wang S., Tao J., Guo T., Fu T., Yuan X., Zheng J., Song C., Thermal characteristics, mechanical properties and biodegradability of polycarbonates/poly(lactic acid) (PPC/PLA) blends, *Lizi Jiaohuan Yu Xifu/Ion Exchange and Adsorption*, 2007, **23**, 1-9.

[135] Oyama H. T., Super-tough poly(lactic acid) materials: reactive blending with ethylene copolymer, *Polymer*, 2009, **50**, 747-751.

[136] Kylma J., Harkönen M., Seppala J. V., The modification of lactic acid-based poly(ester-urethane) by copolymerization, *J. Appl. Polym. Sci.*, 1997, **63**, 1865-1872.

[137] Park S., Chang Y., Cho J. H., Noh I., Kim C., Kim S. H., Kim Y. H., Synthesis and thermal properties of copolymers of L-lactic acid and ϵ-caprolactone, *Polymer*, 1998, **22**, 1-5.

[138] Park S. D., Todo M., Arakawa K., Effect of annealing on fracture mechanism

of biodegradable poly(lactic acid), *Key Eng. Mat.*, 2004, **263**, 105-110.

[139] Todo M., Effect of unidirectional drawing process on fracture behavior of poly(l-lactide), *J. Mat. Sci.*, 2007, **42**, 1393-1396.

[140] Lu D., Zhang X., Zhou T., Ren Z., Wang S., Lei Z., Biodegradable poly (lactic acid) copolymers, *Prog. Chem.*, 2008, **20**, 339–350.

[141] Li Y., Shimizu H., Improvement in toughness of poly(l-lactide) (PLLA) through reactive blending with acrylonitrile-butadiene-styrene copolymer (ABS): Morphology and properties, *J. Eur. Polym.*, 2009, **45**, 738–746.

[142] Lim J. Y., Kim S. H., Lim S., Kim Y. H., Improvement of flexural strengths of poly(L-lactic acid) by solid-state extrusion, *Macromol. Chem. Phys.*, 2001, **202**, 2447–2453.

[143] Grijpma D. W., Altpeter H., Bevis M. J., Feijen J., Improvement of the mechanical properties of poly(D,L-lactide) by orientation, *Polym. Int.*, 2002, **51**, 845–851.

[144] Quan D., Liao K., Zhao J., Effects of physical aging on glass transition behavior of poly(lactic acid)s, *Acta Polym. Sin.*, 2004, **5**, 726–730.

[145] Li Y., Wang Y., Liu L., Han L., Xiang F., Zhou Z., Crystallization improvement of poly(L-lactide) induced by functionalized multiwalled carbon nanotubes, *J. Polym. Sci. Polym. Chem.*, 2009, **47**, 326-339.

[146] Vink E. T. H., Rajbago K. R., Glassner D. A., Springs B., O'Connor R. P., Kolstad J., Gruber P. R., The sustainability of Nature Works polylactide polymers and ingeo polylactide fibers: an update of the future, *Macromol. Biosci.*, 2004, **4**, 551-564.

[147] Wolf O., Techno-economic feasibility of large-scale production of bio-based polymers in Europe, *Institute for Prospective Technological Studies, Spain: European Communities*, 2005, 50-64.

[148] Platt K., The global biodegradable polymers market. In: Biodegradable polymers, 1st ed., *Smithers Rapra Technology Limited*, Shawbury, UK, 2006, 31-48.

[149] Lim J. Y, Kim S. H., Lim S., Kim Y. H., Improvement of flexural strengths of poly(L-lactic acid) by solid-state extrusion, 2: extrusion through rectangular die. *Macromol. Mater. Eng.*, 2003, **288**, 50–57.

[150] Furukawa T., Sato H., Murakami R., Zhang J., Duan Y. X., Noda I., Ochiai S., Ozaki Y., Structure, dispersibility, and crystallinity of poly(hydroxybutyrate)/poly(L-lactic acid) blends studied by FT-IR microspectroscopy and differential scanning calorimetry, *Macromol*, 2005, **38**, 6445–6454.

[151] Mills C. A., Navarro M., Engel E., Martinez E., Ginebra M. P., Planell J.,

Errachid A., Samitier J., Transparent micro- and nanopatterned poly(lactic acid) for biomedical applications, *J. Biomed. Mater. Res.*, 2006, **76**, 781–787.

[152] Gatcher R., Müller H., *Plastic Additives Handbook*, 4th ed., Hanser Gardner Publications, München, 1993.

[153] Grijpma D. W., Zondervan G. J., Pennings A. J., High molecular weight copolymers of L-lactide and ϵ-caprolactone as biodegradable elastomeric implant materials, *Polym. Bull.*, 1991, **25**, 327-333.

[154] Perego G., Vercellio T., Balbontin G., Copolymers of L- and D,L-lactide with 6-caprolactone: synthesis and characterization, *Macromol. Chem. Phys.*, 1993, **194**, 2463–2469.

[155] Gumus S., Ozkoc G., Aytac A., Plasticized and Unplasticized PLA/Organoclay Nanocomposites: Short and Lonf-Term Thermal Properties, Morphology, and Nonisothermal Crystallization Behavior, *J. Appl. Polym .Sci.*, 2012, **123**, 2837-48.

[156] URL-1: http://en.wikipedia.org/wiki/Polyethylene_glycol, (Ziyaret tarihi: 12 Mart 2014).

[157] French A. C., Thompson A. L., Davis B. G., High-purity discrete PEG-oligomer crystals allow steuctural insight, *Angewandte Chem.*, 2009, **48**, 1248-1252.

[158] URL-2: http://www.hybridplastics.com/, (Ziyaret tarihi: 13 Mayıs 2012).

[159] Feher F. J., Luecke S., Schwab J. J., Lichtenhan J. D., Phillips S. H., Lee A., Hybrid materials from epoxide-substituted POSS frameworks, *Abst. Pap. Am. Chem. Soc.*, 2000, **219**, U362-U362.

[160] Zeng J., Kumar S., Iyer S., Schiraldi D. A., Gonzalez R. I., Reinforcement of poly(ethylene terephthalate) fibers with polyhedral oligomeric silsesquioxanes (POSS), *High Perform. Polym.*, 2005, **17**, 403-424.

[161] Zheng L., Kasi R. M., Farris R. J., Coughlin E. B., Synthesis and thermal properties of hybrid copolymers of syndiotactic polystyrene and polyhedral oligomeric sissesquioxane, *J. Polym. Sci. Polym. Chem.*, 2002, **40**, 885-891.

[162] Zheng L., Waddon A. J., Farris R. J., Coughlin E. B., X-ray Characterizations of Polyethylene Polyhedral Oligomeric Silsesquioxane Copolymers, *Macromolecules*, 2002, **35**, 2375-2379.

[163] Zheng L., Farris R. J., Coughlin E. B., Novel polyolefin nanocomposites: synthesis and characterizations of metallocene-catalyzed polyolefin polyhedral oligomeric silsesquioxane copolymers, *Macromolecules*, 2001, **34**, 8034-8039.

[164] Fu B. X., Yang L., Somani R. H., Zong S. X., Hsiao B. S., Phillips S., Blanski R., Ruth P., Crystallization studies of isotactic polypropylene containing

nanostructured polyhedral oligomeric silsesquioxane molecules under quiescent and shear conditions, *J. Polym. Sci. Polym. Phys.*, 2001, **39**, 2727-2739.

[165] Li G., Wang L., Ni H., Pittman C. U., Polyhedral Oligomeric Silsesquioxanes (POSS) polymers and copolymers: A review, *J. Inorg. Organomet. Polym.*, 2001, **11**, 123-154.

[166] Kodal M., Ozkoc G., Micro and nanofillers in rubbers, Editors: Visakh P. M., Thomas S., Chandra A. K., Mathew A. P., *Advances in elastomers I: blends and interpenetrating networks*, 1st ed., Springer-Verlag, Berlin, 318-319, 2013.

[167] Harrison P. G., Silicate cages: precursors to new materials, *J. Organomet. Chem.*, 1997, **542**, 141-183.

[168] Goffreda F., Griff A., Livinghouse T., Walsh T., Scuralli J., *Tool and Manufacturing Engineers Handbook: Plastic part manufacturing*, 5th ed., Society of Manufacturing Engineers, New York, 1998.

[169] Rauwendaal C., *Polymer Extrusion*, 4th ed., Hanser Gardner Publications, Munchen, 2011.

[170] Zeng R., Tanner R. I., Fan X. J., *Injection molding-interaction theory and modelling methods*, 1st ed., Springer-Verlag, Berlin, 2011.

[171] Karagöz S., Poli(laktik asit)/modifiye termoplastik nişasta karışımları, Yüksek lisans tezi, Kocaeli Üniversitesi, Fen Bilimleri Enstitüsü, Kocaeli, 2012, 301647.

[172] Nielsen L. E., Landel R. F., *Mechanical properties of polymers and composites*, 2nd ed., Marcel Dekker Publishing, New York, 1994.

[173] URL-3: http://www.engineeringarchives.com, (Ziyaret tarihi: 22 Mart 2014).

[174] Pişkin E., *Polimer Teknolojisine Giriş*, 2. Baskı, İnkilap Kitabevi, Ankara, 1987.

[175] Campo E. A., *Selection of Polymeric Materials*, 1st ed., William Andrew Inc., Norwich, 2008.

[176] Scheirs J., *Compositional and Failure Analysis of Polymers-A Practical Approach*, 2nd ed., John Wiley and Sons Inc., New York, 2000.

[177] Halary J. L., Laupretre F., Monnerie L., *Polymer Materials: Macroscopic properties and molecular interpretations*, John Wiley and Sons Inc., New York, 2008.

[178] Höhne G. W. H., Hemminger W. F., Flammersheim H. J., *Diffrential Scanning Calorimetry*, 2nd ed., Springer-Verlag, Berlin, 2003.

[179] Stuart B. H., *Polymer Analysis Diffrential Scanning Calorimetry*, 1st ed., John Wiley and Sons Inc., New York, 2003.

[180] Boudenne A., Ibos L., Candau Y., Thomas S., *Handbook of Multiphase Polymer Systems*, 1st ed., John Wiley and Sons Inc., New York, 2011.

[181] Doğan gazeer M., Production and characterization of boron containing flame retardant polyamide-6 and polypropylene composites and fibers, Doktora tezi, Orta Doğu Teknik Üniversitesi, Fen Bilimleri Enstitüsü, Ankara, 2011, 285608.

[182] Laoutid F., Bonnaud L., Alexandre M., Lopez-Cuesta J. M., Dubois Ph., New Nanocomposites, *Mater. Sci. Eng.: Rep.*, 2009, **63**, 100-125,

[183] Kiliaris P., Papaspyrides C. D., "Polymer/Layered Silicate (Clay) Nanocomposites: An Overview of Flame Retardancy", *Prog. Polym. Sci.*, 2010, **35**, 902- 958.

[184] Karak N., *Fundamentals of polymers: raw materials to finish products*, 1st ed., PHI Publishing, New Delhi, 2009.

[185] Menard K. P., *Dynamic Mechanical Analysis-A Practical Introduction*, 2nd ed., CRC Press-Taylor and Francis Group, Boca Raton, 2008.

[186] Stuart B., *Infrared Spectroscopy: Fundamentals and Applications*, 1st ed., John Wiley and Sons Inc., New York, 2004

[187] Gündüz T., *İnstrümental Analiz*, 5. baskı, Gazi Kitabevi, Ankara, 1999.

[188] Reimer L., *Scanning electron microscopy: Physics of image formation and microanalysis*, 2nd ed., Springer-Verlag, Berlin, 1998.

[189] URL-4: http://www.purdue.edu/rem/rs/sem.htm, (Ziyaret tarihi: 24 Mart 2014).

[190] Byorge R., Scanning transmission electron microscopy studies of precipitation in Al-Mg-Ge alloys, Doktora tezi, Norwegian University of Science and Technology, Faculty of Natural Sciences and Technology Department of Physics, Trondheim, 2011, ISBN 978-82-471-3029-2.

[191] Williams D. B., Carter C. B., *The transmission electron microscope*, 1st ed., Springer-Verlag, Berlin, 1996.

[192] URL-5: http://www.microscopyu.com/articles/polarized/polarizedintro.html, (Ziyaret tarihi: 6 Nisan 2014).

[193] Amin M., Akbar M., Amin S., Hydrophobicity of silicone rubber used for outdoor insulation, *Rev. Adv. Mater. Sci.*, 2007, **16**, 10-26.

[194] Yuan Y., Lee T. R., Contact angle and wetting properties, Editors: Bracco G., Holts B., *Surface Science Techniques*, 1st ed., Springer-Verlag, Berlin, 1-34,

2013.

[195] Qiu P., Pan H., Preparation, crystallization and hydrolitic degradation of biodegradable poly(L-lactide)/polyhedral oligomeric silsesquioxanes nanocomposite, *Compos. Sci. Technol.*, 2010, **70**, 1089-1094.

[196] Pramoda K. P., Koh C. B., Hazrat H., He C. B., Performance enhancement of polylactide by nanoblending with POSS and graphene oxide, *Polym. Compos.*, 2014, **35**, 118-126.

[197] Song L., Xuan S., Wang X., Hu Y., Flame retardancy and thermal degradation behaviors of phosphate in combination with POSS in polylactide composites, *Thermochim. Acta*, 2012, **527**, 1-7.

[198] Wang X., Xuan S., Song L., Yang H., Lu H., Hu Y., Synergistic effect of POSS on mechanical properties, flammability, and thermal degradation of intumescent flame retardant polylactide composites, *J. Macromol. Sci. Phys.*, DOI: 10.1080/00222348.2011.585334.

[199] Wang R., Wang S., Zhang Y., Morphology, rheological behavior, and thermal stability of PLA/PBSA/POSS composites, *J. Appl. Polym. Sci.*, 2009, **113**, 3095–3102.

[200] Lee J. H., Jeong Y. G., Preparation and characterization of nanocomposites based on polylactides tethered with polyhedral oligomeric silsesquioxanes, *J. Appl. Polym. Sci.*, 2010, **115**, 1039-1046.

[201] Fina A., Tabuani D., Frache A., Camino G., Polypropylene- polyhedral oligomeric silsesquioxanes (POSS) nanocomposites, *Polymer*, 2005, **46**, 7855-7866.

[202] Zhang Y., Lee S., Yoonessi M., Liang K., Pittman C. U., Phenolic resin-trisilanolphenyl polyhedral oligomeric silsesquioxane (POSS) hybrid nanocomposites: Structure and properties, *Polyme*r, 2006, **47**, 2984-2996.

[203] Kim H. U., Bang Y. H., Choi S. M., Yoon K. H., Morphology and mechanical properties of PET by incorporation of amine-polyhedral oligomeric silsesquioxane, *Compos. Sci. Technol.*, 2008, **68**, 2739-2747.

[204] Buong Woei C., Nor Azowa I., Wan Md Zin Wan Y., Mohd Zobir H., Plasticized poly(lactic acid) with low molecular weight poly(ethylene glycol): Mechanical, thermal and morphological properties, *J. Appl. Polym. Sci.*, 2013, **130**, 4576-4580.

[205] Buong Woei C., Nor Azowa I., Wan Md Zin Wan Y., Mohd Zobir H., Poly(lactic acid)/poly(ethylene glycol) polymer nanocomposites: Effects of grapheme nanoplatelets, *Polymers*, 2014, **6**, 93-104.

[206] Courgneau C., Domenek S., Guinault A., Averous L., Ducruet V., Analysis of the structure-properties relationships of different multiphase systems based on plasticized poly(lactic acid), *J. Polym. Environ.*, 2011, **19**, 362-371.

[207] Rodriguez-Llmazares S., Rivas B. L., Perez M., Perrin-Sarazin F., Poly(ethylene glycol) as a compatibilizer and plasticizer of poly(lactic aicd)/clay nanocomposites, *High Perform. Polym.*, 2012, **24**, 254-261.

[208] Nekhamanurak B., Patanathabutr P., Hongsriphan N., Thermal-mechanical property and fracture behavior of plasticized PLA-$CaCO_3$ nanocomposite, *Plast. Rubber Compos.*, 2012, **4**1, 175-179.

[209] Paul M. A., Alexandre M., Degee P., Henrist C., Rulmont A., Dubois P., New nanocomposite materials based on plasticized poly(L-lactide) and organo-modified montmorillonites: thermal and morphological study, *Polymer*, 2003, **44**, 443-450.

[210] Pluta M., Paul M. A., Alexandre M., Dubois P., Plasticized polylactide/clay nanocomposites. II. The effect of aging on structure and properties in relation to the filler content and the nature of its organo-modification, *J. Polym. Sci. Polym. Phys.*, 2006, **44**, 312-325.

[211] Lee J. H., Jeong Y. G., Preparation and crystallization behavior of polylactide nanocomposites reinforced with POSS-modified montmorillonite, *Fiber Polym.*, 2011, **12**, 180-189.

[212] Miyata T., Masuko T., Crystallization behavior of poly(L-lactide), *Polymer*, 1998, **39**, 5515-5521.

[213] Papageorgiou G. Z., Achilias D. S., Nanaki S., Beslikas T., Bikiaris D., PLA nanocomposites: Effect of filler type on non-isothermal crystallization, *Thermochim. Acta*, 2010, **511**, 129-139.

[214] Xiao H., Lu W., Yeh J. T., Effect of plasticizer on the crystallization behavior of poly(lactic acid), *J. Appl. Polym. Sci.*, 2009, **113**, 112-121.

[215] Migliaresi C., Cohn D., De Lollis A., Fambri L., Dynamic mechanical and calorimetric analysis of compression-molded PLLA of different molecular weights: Effect of thermal treatments, *J. Appl. Polym. Sci.*, 1991, **43**, 83-95.

[216] Ahmed J., Varshney S. K., Auras R., Hwang S. W., Thermal and rheological properties of L-polylactide/polyethylene glycol/silicate nanocomposites films, *J. Food Sci.*, 2010, **75**, N97-N108.

[217] Pan P., Liang Z., Zhu B., Dong T., Inoue Y., Roles of physical aging on crystallization kinetics and induction period of poly(L-lactide), *Macromolecules*, 2008, **41**, 8011-8019.

[218] Tsitsilianis C., Bokaris E. P., Enthalpy relaxation studies in isotactic polystyrene: Effects of crystalinity, *Polym. Bull.*, 1993, **30**, 609-616.

[219] Pilla S., Processing and chatacterization of novel biobased and biodegradable materilas, Doktora tezi, The University of Wisconsin, Milwauke, 2009, UMI Number 3363441.

[220] Yasuniwa M., Tsubakihara S., Sugimoto Y., Nakafuku C., Thermal analysis of the double-melting behavior of poly(L-lactic acid), *J. Polym. Sci. Polym. Phys.*, 2004, **42**, 25-32.

[221] Santhoskumar A. U., Ramkumar A., Preparation/characterization of plasticized poly(lactic acid) for packaging applications, *Turk. J. Sci. Technol.*, 2014, **9**, 73-79.

[222] Harte I., Birkinshaw C., Jones E., Kennedy J., DeBarra E., The effect of citrate esters plasticizers on the thermal and mechanical properties of poly(DL-lactide), *J. Appl. Polym. Sci.*, DOI: 10.1002/app.37600.

[223] Sungsanit K., Kao N., Bhattacharya S. N., Pivsaart S., Physical and rheological properties of plasticized linear and branched PLA, *Korea-Aust. Rheol. J.*, 2010, **22**, 187-195.

[224] Rasal R. M., Janorkar A. V., Hirt D. E., Poly(lactic acid) modifications, *Prog. Polym. Sci.*, 2010, **35**, 338-356.

[225] Signori F., Coltelli M. B., Bronco S., Thermal degradation of poly(lactic acid) (PLA) and poly(butylene adipate-co-terephthalate) (PBAT) and their blends upon melt processing, *Polym. Degrad. Stabil.*, 2009, **94**, 74-82.

[226] Romero-Guzman M., Romo-Uribe A., Zarate-Hernandez BM., Cruz-Silva R., Viscoelastic properties of POSS-styrene nanocomposite blended with polystyrene, *Rheol. Acta*, 2009, **48**, 641-652.

[227] Dorigato A., Pegoretti A., Migliaresi C., Physical properties of polyhedral oligomeric silsesquioxanes-cycloolefin copolymer nanocomposites, *J. Appl. Polym. Sci.*, 2009, **114**, 2270-2279.

[228] Zhou Z., Yin N., Zhan Y., Zhang Y., Properties of poly(butylene terephthalate) chain-extended by epoxycyclohexyl polyhedral oligomeric silsesquioxanes, *J. Appl. Polym. Sci.*, 2008, **107**, 825-830.

[229] Zhou Z., Zhang Y., Zhang Y., Yin N., Rheological behavior of polypropylene/octavinyl polyhedral oligomeric silsesquioxane composites, *J. Polym. Sci. Polym. Phys.*, 2008, **46**, 526-533.

[230] Kopesky, E. T., Haddad T. S., McKinley G. H., Cohen R. E., Miscibility and viscoelastic properties of acrylic polyhedral oligomeric silsesquioxane-poly(methyl methacrylate) blends, *Polymer*, 2005, **46**, 4743-4752.

[231] Soong S. Y., Cohen, R. E., Boyce M. C., Polyhedral Oligomeric Silsesquioxane as Novel Plasticizer for Poly(vinyl chloride), *Polymer*, 2007, **48**, 1410-1417.

[232] Soong S. Y., Mulliken A. D., Cohen R. E., Boyce M. C., Rate Dependent Deformation Behavior of POSS-Filled and Plasticized PVC, *Macromolecules*, 2006, **39**, 2900-2908.

[233] Gerds N., Katiyar V., Koch C. B., Hansen H. C. B., Plackett D., Larsen E. H., Risbo J., Degradation of L-polyactide during melt processing with layered double hydroxides, *Polym. Degrad. Stabil.*, 2012, **97**, 2002-2209.

[234] Taubner V., Shishoo R., Influence of processing parameters on the egradation of poly(L-lactide) during extrusion, *J. Appl. Polym. Sci.*, 2001, **79**, 2128-2135.

[235] Gupta M. C., Deshmukh V. G., Thermal oxidative-degradation of poly-lactic acid.1.Activation energy of thermal degradation in air, *Coll. Polym. Sci.*, 1982, **260**, 308-311.

[236] Hyon S. H., Jamshidi K., Ikada Y., Effects of residual monomer on the degradation of DL-lactide polymer, *Polym. Int.*, 1998, **46**, 196-202.

[237] Cam D., Marucci M., Influence of residual monomers and metals on poly(L-lactide) thermal stability, *Polymer*, 1997, **38**, 1879-1884.

[238] Kopinke F. D., Remmler M., Mackenzie K., Moder M., Wachsen O., Thermal decomposition of biodegradable polyesters. 2. Poly(lactic acid), *Polymer*, 1996, **53**, 329-342.

[239] Abu Bakar M. B., Leong Y. W., Ariffin A., Mohd. Ishak Z. A., Mechanical, flow and morphological properties of talc- and kaolin-filled polypropylene hybrid composites, *J. Appl. Polym. Sci.*, 2007, **104**, 434-441.

[240] Mareri P., Bastide S., Binda N., Crespy A., Mechanical behaviour of polypropylene composites containing fine mineral filler: Effect of filler surface treatment, *Compos. Sci. Technol.*, 1998, **58**, 747-752.

[241] Kim H. U., Bang Y. H., Choi S. M., Yoon K. H., Morphology and mechanical properties of PET by incorporation of amine-polyhedral oligomeric silsesquioxane, *Compos. Sci. Technol.*, 2008, **68**, 2739-2747.

# APPENDICES

## APPENDIX-A

Additive manufacturing: Katmanlı üretim
Adhesion: Adhezyon
Blow molding: Üflemeli kaplama
Braid: Örgü, lif ya da tovdan yapılan iplik örgüsü
Brittle: Gevrek
Bolt: Civata
Capillarity: Kılcallık
Carbon Fiber Reinforced Composite: Karbon elyaf takviyeli kompozit
Carbonization: Karbonlaştırma
CB: Karbon siyahı
CF: Karbon elyaf
Change of slope: Eğimin değiştiği nokta
Chopped fiber: Kırpılmış elyaf
Co-bonding: Birlikte bağlantı
Cohesion: Kohezyon
Compressin molding: Basınçla kalıplama / Hazır kalıplama
Curve: Eğri
Damping: Sönümleme
Debonding energy: Ayrılma enerjisi
Differential thermal: Diferansiyel termal (ısıl)
Dissipation: Enerji kaybı
Displacement: Yerdeğiştirme
Drawing temperature: Çekme sıcaklığı
Ductile: Sünek
Elastic trough: Elastik oluk
Extrusion: Ekstrüzyon
Fabric: Kumaş
Filament: Lif, filaman
Fixation: Kimyasal sabitleme
Flexural strength: Eğme mukavemeti
Fusion bonding: Ergitme kaynağı
Hand lay-up: Elle yatırma
Hot melt: Sıcak eriyik
Hybrid composite: Hibrit kompozit
Injection molding: Enjeksiyon kalıplama
Linear: Doğrusal
Mat: Hasır
Matrix: Matris
Mechanical fastening: Mekanik bağlantı
Milled fiber: Öğütülmüş elyaf (toz)
Modulus: Modül
Non-linear: Doğrusal olmayan
Overlap: Üst üste binme

Overmolding: Üzerine enjeksiyon
Paper: Kağıt
Particle: Parçacık
Peel stress: Soyma gerilmesi
Reversible: Tersinir
Secondary bonding: İkincil bağlantı
Single lap: Tek tesirli bindirme
Spray-up: Püskürtme
Stabilization: Dengeleme
Staple yarn: Kesikli iplik, kesik liflerden eğirilen iplik
Staple: Liflenmiş
Stiffness: Dirilik / rijitlik
Strain: Gerinim
Strand: İplik
Stress relaxation: Gerilim gevşemesi
Stress: Gerilim
Structural: Yapısal
Structure: Yapı
Surface ply fiber orientation: Yüzey kat elyafı oryantasyonu
Surface preparation: Yüzey hazırlama
Tensile Strain: Kopmada uzama
Tensile Strength: Kopma dayanımı
Tensile testing: Çekme testi
Toughness: Tokluk
Troughput: Üretim hızı
Washer: Pul
Welding: Kaynak
Woven fabric: Dokunmuş kumaş

## PERSONAL PUBLICATIONS AND WORKS


[1] Ş. Gözde İrim., **Alchekh Wis A.**, M. Aker Keskinc., Physical, mechanical and neutron shielding properties of h-BN/Gd2O3/ HDPE ternary nanocomposites, *Radiation Physics and Chemistry"Radiation Physics and Chemistry*, 2018, **144**, 434-443.

[2] Mehmet Kodal., **Alchekh Wis A.**, Guralp Ozkoc., The mechanical, thermal and morphological properties of γ-irradiated PLA/ TAIC and PLA/OvPOSS, *Radiation Physics and Chemistry*, 2018, **153**, 214-225.

[3] Oguyzhan Oguz., Kafan Bilge., Erren Simbsek., **Alchekh Wis A.**, High-Performance Green Composites of Poly (lactic acid) and Waste Cellulose Fibers Prepared by High-Shear Thermokinetic Mixing, *Industrial &Engineering Chemistry Research*, 2017, **56**, 8568−8579.

[4] Salah Eddine Hachani., **Alchekh wis A.**, Zelikha Necira, Effects of Magnesia Incorporation on Properties of Polystyrene/Magnesia Composites, *Acta Chimica Slovenica*, 2018, **65**, 125-134.

[5] Surreyya Mert Seliemoglu., Musrat Kassap., **Alchekh Wis A.**. Improved Production of Highly Active and Pure Human Creatine Kinase MB, *J Mol Microbiol Biotechnol*, 2018, **28**, 24–36.

**[6]** Kodal M., Karakaya N**.**, **Alchekh Wis A**., Özkoç Gralp., Thermal Properties (DSC, TMA, TGA, DTA) of Rubber Nanocomposites Containing Carbon Nanofillers, Editors: Yaragalla S., Kumar Mishra R., Thomas S., Kalarikkal N., Maria H. J., *Carbon-Based Nanofillers and Their Rubber Nanocomposites*, Elsevier, 325-366, 2019.

**[7]** O Baykara., **Alchekh wis A.**, G Ozkoc., Mechanical, Thermal and γ -Ray Shielding Properties of HDPE/BN/Gd2O3 Ternary: Effects of Particle Concentration, *4th International Polymeric Composites Symposium, Exhibition & Brokerage Event*, Izmir, 7-9 May 2015.

[8] M Kodal., **Alchek wis A.**, G Ozkoc., The effects of gamma irradiation on the mechanical and thermal properties of poly (lactic acid), *The 32th Annual Meeting of Polymer Processing Society (PPS-32)*, Lyon/Fransa, 25-29 Temmuz 2016.

[9] **Alcheck wis A**., Özkoç G., Overmolded Continuous Woven Jute poly (lactic acid) Eco-Composites, *AWPP-2016*, Melbourne/Australia, 2-5 November 2016.

[10] **Alchekh Wis A.**, Antoni Jose Nieto Gonzales., Güralp Özkoc., PS/PS-g-MAH/Epoksi-POSS Nanokompozitlerinin Termal ve Mekanik Özellikleri, *6 Ulusal Polimer Bilim ve Teknolojisi Kongresi*, Ankara, Eylül, 2016.

**RESUME**

Abdulmounem Alchekh Wis was born in Amman, Jordan in 1985. He took primary education in Jordan, intermediate education in Iraq, and secondary education in Yemen. The Bachelor’s degree was in Yemen at Sana'a University, College of Science, and Department of Chemistry. He graduated in 2007.

He worked in Jordan at the KHCC for two years. He worked for Total for two years in Yemen. He studied a higher diploma in Malaysia at USM. He studied Masters in Cyprus and graduated from EMU University in 2012. He worked as a professional scientific translator for 7 years.

The Ph.D. studied was at Kocaeli University in Turkey in the College of Engineering. He published 7 international articles and 8 articles in domestic and international conferences. I have two patents and a second-place prize in the SABIC competition in 2019. Married and I love playing chess and reading.